Copyright

by

Aaron Todd Wright

2006

The Dissertation Committee for Aaron Todd Wright Certifies that this is the approved version of the following dissertation:

SYNTHETIC SELECTIVE AND DIFFERENTIAL RECEPTORS FOR THE RECOGNITION OF BIOANALYTES

Committee:

Eric V. Anslyn, Supervisor

Brent L. Iverson

Michael J. Krische

John T. McDevitt

Christian Whitman

SYNTHETIC SELECTIVE AND DIFFERENTIAL RECEPTORS FOR THE RECOGNITION OF BIOANALYTES

by

AARON TODD WRIGHT, B.S.

DISSERTATION

Presented to the Faculty of the Graduate School of

The University of Texas at Austin

in Partial Fulfillment

of the Requirements

for the Degree of

DOCTOR OF PHILOSOPHY

The University of Texas at Austin

May, 2006

Dedication

To my wife, Janet, and my family and friends who have encouraged me throughout my education. Their support has been without equal.

Acknowledgements

Getting to this point in my education has been a fantastic journey, and I have received wonderful love and support from my family and friends. A love of learning was instilled in me at a young age by my parents and siblings, and I seemingly have tried to stay in school for as long as possible thanks to them!

My wife, Janet, has been a wonderful encourager and supporter throughout my graduate studies. She has seen both the best and most difficult of times, and she has stood by me and fervently prayed for me. I have been richly blessed with a loving wife, and I look forward to a lifetime of adventure and learning together.

I am indebted to, and extremely grateful for, my parents for their love, encouragement, prayer, and financial support that have helped me from preschool till now to achieve my academic goals. Both my mother and father have been excellent role models teaching me hard work and commitment to my goals. I am also thankful to my siblings, Valerie, Alene, and Andy, who have been very supportive of me. I appreciate all the tutoring in my early years, and the kind encouragement that continues to this day.

I really believe that I had the kindest, and most supportive, graduate adviser in Eric Anslyn. I have learned so much from him. I am still in awe today at his remarkable knowledge of chemistry, and his capacity to teach it so effectively and patiently. I am so grateful for the start I have received from him, and I hope that I can take the knowledge I

learned from him and make him proud during my career. I am also grateful for the encouragement and support I have received from the Anslyn group.

It is through faith and prayer that I have survived graduate school. My Lord and Savior has blessed me with an ability to understand and pursue studies in chemistry. I have learned so much about the wonder of His creation, and I look forward to pursuing it for a lifetime. It is through the strength and peace that I find in God that I can do all things.

SYNTHETIC SELECTIVE AND DIFFERENTIAL RECEPTORS FOR THE RECOGNITION OF BIOANALYTES

Publication No._____

Aaron Todd Wright, Ph.D.

The University of Texas at Austin, 2006

Supervisor: Eric V. Anslyn

This dissertation consists of five chapters. The first chapter provides an in-depth background of supramolecular chemistry and differential recognition. The first chapter also elaborates upon the necessary requirements for successful application of chemosensor assays and arrays. Additionally, sensing mechanisms and chemometric pattern recognition is described for clarification of the research conducted in chapters 2-5.

Chapter 2 discusses the synthesis and employment of a metalated receptor for the selective recognition of the tripeptide His-Lys-Lys. A receptor was synthesized with two peptide arms emanating outward from a metal ligand core using both solution and solid phase chemistry. UV/Vis titrations were used to determine binding constants for various amino acids and tripeptides to the synthetic receptor:Cu(II) complex. The receptor:Cu(II) complex was found to be selective for His-Lys-Lys over other tripeptides, amino acids, and protected amino acids.

Chapter 3 describes the synthesis and application of a fluorescent chemosensor for the recognition of unfractionated and low-molecular weight heparin. Heparin is a commonly used clinical anticoagulant for surgical situations and post-operative outpatient care. Due to the high selectivity of the receptor for heparin, studies in crude serum were attempted. It was found that the receptor was selective for heparin in serum. Therefore, fluorescent calibration charts were prepared for quantifying heparin at clinical concentrations using the synthetic receptor. This research is one of very few to be published regarding the creation of synthetic receptors with sufficient selectivity for activity in biological media.

Chapter 4 describes the combinatorial synthesis of two resin-bound receptor libraries for use in differential recognition studies. The two libraries, in conjunction with an indicator-uptake assay, were used for the detection and discrimination of three proteins and two glycoproteins as well as four tripeptides and three tripeptide mixtures using pattern recognition protocols.

Chapter 5 discusses the preparation and screening of a metalated receptor library. A colorimetric mimic of a tachykinin hormone, α-neurokinin, was created and used to screen the receptor library. Seven selective receptors were identified and subsequently sequenced to determine their molecular architecture. The receptors were resynthesized and employed in solution phase binding studies with α-neurokinin.

Table of Contents

List of Tables xiv

List of Figures xv

List of Schemes xx

Chapter 1 Introduction and Background 1

1.1 Introduction 1

1.2 Lock and Key Principle 2

1.3 Crown Ethers and Cryptands 3

1.4 Host-Guest Interactions 5

1.4.1 Electrostatics 6

1.4.2 Hydrogen-Bonding 6

1.4.3 Cation-π and π-π Interactions 7

1.4.4 Dispersion (van der Waals) Forces 7

1.5 Solvent Effects 8

1.5.1 Crude Media Detection 10

1.6 Preorganization 11

1.7 Chemosensor Development 13

1.7.1 Indicator-Displacement Assays 15

1.7.1.1 Sensing Ensemble for Aspartic Acid 17

1.7.1.2 Sensing Ensemble for Heparin 19

1.7.2 Molecular Fluorescent Sensing 20

1.8 Selective Synthetic Receptors 25

1.8.1 Synthetic Amino Acid Receptors 26

1.8.2 Synthetic Peptide Receptors 31

1.9 Combinatorial Receptor Development 39

1.9.1 Screening Peptide Libraries 41

1.9.2 Screening Receptor Libraries 43

1.9.2.1 Single-Peptide Arm Receptor Libraries 45

1.9.2.2 Two-Peptide Arm Receptor Libraries 46
1.9.2.3 Three-Armed Receptor Libraries - Molecular Bowls.....52
1.10 Multi-Analyte Sensing 53
1.10.1 Mammalian Sensory Systems - Olfaction.....56
1.10.2 Mammalian Sensory Systems - Gustation 57
1.10.3 Sensor Array Mimics of Smell and Taste 58
1.10.3.1 Synthetic Organic Differential Arrays-Electronic Tongues 61
1.10.3.2 Chemometrics 69
1.11 Summary 71
1.12 References 72

Chapter 2 Selective Tripeptide Receptor.....97
2.1 Introduction 97
2.2 Ligand Coordination to Divalent First Row Transition Metals 98
2.3 Amino Acid and Oligopeptide Coordination to Cu(II).....103
2.4 Synthesis of Receptor **2.1**.....106
2.5 Synthetic Difficulties 113
2.6 Binding Studies 116
2.6.1 $Cu(II)Cl_2$ Coordination 116
2.6.2 Amino Acid and Oligopeptide Binding Studies with **2.1** 118
2.7 Experimental 124
2.8 References 134

Chapter 3 A Functional Assay for Heparin in Serum 140
3.1 Introduction 140
3.2 Characteristics of Heparin.....141
3.3 Methods for Quantifying Heparin Concentration.....145
3.4 Design of Heparin Chemosensor **3.1** 147
3.4.1 Precedence for the Design of Heparin Chemosensor **3.1** 147
3.4.2 Design and Synthesis of Heparin Chemosensor **3.1**.....149
3.4.3 Original Chemosensor Design and Synthetic Trials.....153

3.5 Binding Studies with Chemosensor **3.1** and LMWH and UFH 156
3.6 Protamine Titrations 160
3.7 Dilution Studies 161
3.8 Calibration Curves 163
3.9 Summary 167
3.10 Experimental 168
3.11 References 181

Chapter 4 Differential Recognition 188
4.1 Introduction 188
4.2 Electronic Array Setup 190
4.2.1 Flow Cell Arrangement 191
4.2.2 Data Acquisition 195
4.2.3 Pattern Recognition 197
4.2.3.1 Indicator-Uptake Assay 200
4.2.3.2 Principal Component Analysis 204
4.3 Differential Recognition of Proteins and Glycoproteins 206
4.3.1 Design and Synthesis of Receptor Library **4.1** 206
4.3.2 Optimization of Array Studies 209
4.3.3 Full Array Studies with Proteins and Glycoproteins 212
4.4 Differential Recognition of Tripeptides and Tripeptide Mixtures 219
4.4.1 Design and Synthesis of Library **4.2** 219
4.4.2 Tripeptide Analytes 222
4.4.3 Optimization of Array Conditions 224
4.4.4 Full Array Study with Differential Receptor Library **4.2** 228
4.4.4.1 PCA Analysis of Pattern Responses Exhibited by a 30-Member Array of Library **4.2** to Tripeptides and Tripeptide Mixtures 231
4.4.4.2 Characterization of Receptors in the Array 234
4.5 Summary 236
4.6 Experimental 237

4.7 References 252

Chapter 5 Library Screening 258

5.1 Introduction 258

5.2 Tachykinins 259

5.3 Library Design and Screening 260

5.3.1 Synthesis of α-Neurokinin Mimic 261

5.3.2 Library Screening 263

5.4 UV/Vis Solution Studies with Resynthesized Receptor:Metal Complexes 270

5.5 Multianalyte Approach 275

5.6 Experimental 277

5.7 References 288

Vita 291

List of Tables

Table 1.1: Gutmann Donor and Acceptor Numbers and Dielectric Constants for Selected Solvents 9

Table 2.1: Formation Constants of Various Metal Complexes in Aqueous Solutions at pH 6.8 with **2.6** to **2.9** 103

Table 2.2: Formation Constants of Various Ligands With Cu(II) as Measured by Glass Electrode Potentiometry. Ionic strengths are listed in place of medium in some cases 105

Table 2.3: Association Constants (M^{-1}) of **2.1**:Cu(II) with Various Amino Acids, Protected Amino Acids, and Tripeptides (n.d. = not determined) .. 121

Table 4.1: Characteristics of Proteins and Glycoproteins Discriminated by Library **4.1** 212

Table 4.2: Sequencing Results from Edman Degradation of 7 Resin-Bound Receptors from Library **4.1** Either Significant or Insignificant to the Formation of PC Axis 1 218

Table 4.3: Sequencing Results and Factor Loading Values for the First Principal Component (PC1) 236

List of Figures

Figure 1.1: Lock and Key Principle Relating to Molecular Recognition 3

Figure 1.2: Reversible Boronic Acid / Diol Interaction.....5

Figure 1.3: (a) Cartoon Representation of FRET in the Fluorophore-Spacer-Receptor Approach when Bound and Unbound. (b) Frontier Orbital Diagram of the PET in the Fluorophore-Spacer-Receptor Approach… 22

Figure 1.4: Combinatorial Approach to Receptor Libraries - the position of the scaffold relative to the linkage to the resin can be varied, and may be determined by the number of combinatorially synthesized peptide arms 44

Figure 1.5: Lock-and-Key vs. Differential Recognition.....55

Figure 1.6: Taste Bud Location on the Human Tongue 57

Figure 1.7: Potentiometric Lipid Sensor Array Designed by Toko.....60

Figure 1.8: Red-Green-Blue Response to Ca^{2+} by Four Resin-Based Sensors ...63

Figure 1.9: An Ideal PCA Plot Showing the Clustering of Individual Analyte Score Points and Separation of Different Analytes.....70

Figure 2.1: Addition of $Cu(II)Cl_2$ to **2.1** (water/methanol, 1:1, pH 7.4).....117

Figure 2.2: Experimental Binding Curve for Cu(II) Complexation with **2.1** ...118

Figure 2.3: UV/Vis Absorbance Spectrum of Titration of L-Histidine to a Constant Concentration of **2.1**:Cu(II) in Water/Methanol (1:1) 119

Figure 2.4: Representative Experimental Binding Curves Generated From Absorbance Spectrum (314 nm) Titrations with: (a) L-Met; (b) MGG; (c) MKK; (d) HGG; (e) HKK.....123

Figure 3.1: (a) Absorbance and (b) Emission Profiles of **3.1** Demonstrating a Stokes Shift 157

Figure 3.2: Fluorescence Emission Spectra of Titration of UFH into **3.1** (1.92×10^{-6} M) 159

Figure 3.3: Binding Isotherm for Titration of UFH Into **3.1** (1.92×10^{-6} M). The orange line represents the calculated binding curve; a good fit is observed 159

Figure 3.4: Reversibility of LMWH:**3.1** Upon Titration with Protamine. Emission intensity at 357 nm; eleven 0.1 equivalent aliquots of LMWH (▲)were added followed by twelve aliquots of protamine (●) (approximately 1-2 equivalents total) 161

Figure 3.5: Dilution of (a) **3.1** (9.6×10^{-7} M,) with Water, and (b) Pyrene (2.99×10^{-6} M, 384 nm) with n-Hexanes, (c) Dilution of **3.1**, Note That the λ_{max} Does Not Shift 163

Figure 3.6: Emission Spectrum of **3.1** in Human Serum 165

Figure 3.7: Calibration Curves for (a) LMWH in Human Serum, (b) UFH in Human Serum, and (c) UFH in Equine Serum 166

Figure 4.1: Tentagel Amino Resin Beads Arrayed in a Micromachined Silicon Wafer 192

Figure 4.2: A Cross-Section Diagram of the Pyramidal Microcavities with a Resin Bead Held in the Cavity 193

Figure 4.3: Solvent Flow (arrows) and Arrangement of Wafer Within Teflon Discs and Aluminum Housing 194

Figure 4.4: Electronic Array Setup – the CCD is attached directly to the top of the stereoscope. The array is fixed to the scope stage. On the left hand side of the image is the FPLC for solution delivery 196

Figure 4.5: RGB Data is Collected From Each Bead in the Array From Video Card Captured Images. As seen the purple color of the bead actually relates to various levels of RGB pixel intensity 197

Figure 4.6: Mammalian Gustatory "Pattern" Recognition of Tastants.....198

Figure 4.7: Kinetic Responses from Two Analytes Represent the Difficulty in Visual Detection of Patterns.....200

Figure 4.8: Kinetic Indicator-Uptake Responses From Three Arrayed Receptors to a Single Analyte 203

Figure 4.9: PCA Chart Describing the Relationship of Analytes (Cases) on PC Axes Determined from Measurements from 35 Arrayed Variables.....205

Figure 4.10: Indicator Screening for Use in Electronic Array Studies with Library **4.1** 210

Figure 4.11: PCA Plot Illustrating the Recognition and Discrimination of Proteins and Glycoproteins by an Array of Library **4.1** 214

Figure 4.12: Expanded PCA Plot Demonstrating the Discrimination Capability of an Electronic Array of Library **4.1** 215

Figure 4.13: Numbering of Receptor Positions Within the Electronic Array.....218

Figure 4.14: Indicators Tested for the Optimization of Array Studies with Library **4.2** 225

Figure 4.15: PCA Plot for the First Full Array Analysis with Library **4.2**.....227

Figure 4.16: Indicator Uptake Slopes for Four Members of Library **4.2** in Response to a Single Tripeptide.....229

Figure 4.17: PCA Chart for Library **4.2** in Response to Tripeptides **4.18-4.21**..232

Figure 4.18: PCA Chart for an Electronic Array of Library **4.2** in Response to Tripeptides and Tripeptide Mixtures 234

Figure 5.1: Substance P, α-Neurokinin, and β-Neurokinin: Common Tachykinins 260

Figure 5.2: Images of Metalated Library **5.1** Following Incubation with Multiple Concentrations of α-Neurokinin Mimic **5.3**. Brightly colored beads indicate strong binding between the receptor:metal complex and **5.3**. These are close-up images that illustrate the relative binding (coloration) to the mimic.....264

Figure 5.3: Images of a Tripeptide Control Library Following Incubation with Multiple Concentrations of α-Neurokinin Mimic **5.3**. Brightly colored beads indicate strong binding between the tripeptides and **5.3**. These are wide images that illustrate the relative binding (coloration) to the mimic 266

Figure 5.4: Images of Metalated Library **5.1** Following Incubation with 70 μM α-Neurokinin Mimic **5.3**.....268

Figure 5.5: Sequencing Results for Selective Binders of **5.3** from Library **5.1** and the Tripeptide Control Library (Blue) 269

Figure 5.6: (a) 1:1 Binding Isotherm for **5.14** and Cu(II)Cl_2, (b) 2:1 Binding Isotherm for **5.14** Cu(II)trifluoromethanesulfonate.....271

Figure 5.7: Titration of **5.14**:Cu(II) Into Pyrocatechol Violet (60 μM). Note the drifting isosbestic point.....273

Figure 5.8: (a) UV/Vis Spectra of a Titration of 5.18 Into a Solution of Cu(II):5.12 (120 μM), (b) Binding Isotherm Generated from the Absorbance Spectrum at 321 nm 274

Figure 5.9: A PCA Plot Demonstrates the Discrimination Capability of the Resynthesized Receptor Array 276

List of Schemes

Scheme 1.1: Molecular Recognition Versus Chemosensing.....14

Scheme 1.2: Indicator-Displacement Assay 16

Scheme 1.3: Sensing Ensemble for Amino Acid Recognition.....18

Scheme 1.4: β-Lactamase Activity Detected by Disruption of FRET.....24

Scheme 1.5: "One-Bead-One-Compound" Split-and-Pool Combinatorial Synthesis.....41

Scheme 1.6: Synthesis of Library **1.53** for Detection of Proteins 67

Scheme 2.1: Metal-Complexation: Induced Cleft Formation 101

Scheme 2.2: Synthesis of **2.12**.....106

Scheme 2.3: Solution-Based Synthesis of Receptor Core.....107

Scheme 2.4: Synthesis of Mono-Fmoc Receptor Core for Solid Phase Incorporation.....109

Scheme 2.5: Key Steps of HOBt/TBTU Promoted Peptide Bond Formation110

Scheme 2.6: Synthesis of First Peptide Arm of Receptor **2.1** 111

Scheme 2.7: Addition of Receptor Core and Cleavage of **2.1** from the Resin112

Scheme 2.8: Failed Synthetic Strategies 115

Scheme 3.1: Inhibition of Coagulation Enzymes Factor Xa and Thrombin by UFH 144

Scheme 3.2: Synthesis of the Fluorescent Core of **3.1**.....150

Scheme 3.3: Preliminary Formation of the Binding Arms of **3.1**.....150

Scheme 3.4: Convergent Synthesis of UFH and LMWH Chemosensor **3.1**.152

Scheme 3.5: Attempted Synthesis of Sensor **3.18** 154

Scheme 3.6: Attempted Synthesis of **3.18** Via *N*-Alkylation.....156

Scheme 4.1: Electronic Array Indicator-Uptake Assay. Note: the adsorption of analyte is shown as a purple color for emphasis, but the substrates used did not have any intrinsic colorimetric properties 202
Scheme 4.2: Resin-Based Synthesis of Library **4.1**.....208
Scheme 4.3: Simplified Synthesis of Library **4.2**.....222
Scheme 5.1: Synthesis of the α-Neurokinin Mimic for Screening Studies ..262

Chapter 1: Introduction and Background

1.1 Introduction

Molecular recognition is the study of complexation events between host and guest molecules. This generally involves non-covalent interactions between two or more molecules regulated by geometrical and interactional complementarity. Biological systems are driven by supramolecular host-guest systems including enzyme/substrate recognition, antibody-antigen interactions, tertiary and quaternary protein structures, hormone and receptor interactions, and DNA base-pairing. These dynamic and complex interactions result in biological processes key to life. Therefore, it is no wonder that chemists and biologists alike have set out to explore the nature of molecular recognition and to develop intricate host-guest systems for many diverse applications.

Efforts to mimic natural systems and to develop new recognition and sensor applications have taken many forms. Early host-guest chemistry involved the development of synthetic selective receptors for single analytes. These receptors were developed in a "lock-and-key" fashion in which functional moieties on the receptor were complementary to functional moieties of the guest. The advent of combinatorial chemistry brought about the development of large libraries of receptors. The receptor libraries are screened against a particular guest to find strong binding "hits." The receptor screening method is advantageous for the identification of receptors for complex and dynamic guests for which synthetic receptors can not be readily developed.

As mentioned earlier, many supramolecular host-guest systems are developed to mimic, monitor, and control biological processes, but many biological analytes are large and complex, and it is prohibitive to synthetically develop or screen libraries of receptors for these dynamic analytes. Recent research into the recognition of larger dynamic analytes, as well as mixtures, has involved the development of arrays of receptors. In an array assay multiple receptors contribute to an overall signal that is diagnostic for the analyte. Receptor arrays can be assembled for recognition of all sorts and sizes of guests, and recent work has shown their use for mixture analysis. In this method multiple interaction events are incorporated into a single signal. Several novel assays have been developed and will be discussed further.

Clearly, several types of recognition assays exist for host-guest systems. No single assay is necessarily better than the other as different analytes may be more suitable for a particular recognition assay. All these receptor types will be discussed in-depth, and their direct applications to this dissertation research revealed.

1.2 Lock and Key Principle

Host-guest chemistry involves the investigation of reversible molecular systems in which the molecules are held together via complementary non-covalent binding moieties. Chemists have sought the development of host molecules that are both sterically and electronically complementary to their guests. With respect to geometry, consideration of the size, shape, and position of the binding sites within the host molecule is necessary for selective guest binding. Electronically, binding moieties such as ammoniums and carboxylates align in a complementary fashion. This notion of steric and electronic alignment was stylized by Emil Fischer over 100 years ago in his “lock

and key" principle.[1] In this model (depicted in Figure 1.1) the "lock" is the host, and it interacts with only a single specifically suited "key" guest in a selective binding event. These ideas were stimulated by Fischer's early theories on enzyme catalysis. From the "lock and key" principle the two main tenets of supramolecular chemistry were formed: molecular recognition and supramolecular function.[2] The tenet of molecular recognition is implicit within the "lock and key" principle and will be used most widely in this text. Supramolecular function is notable within enzyme-substrate selectivity and synthetic systems designed to mimic biological arrangement.

Figure 1.1 Lock and Key Principle Relating to Molecular Recognition.

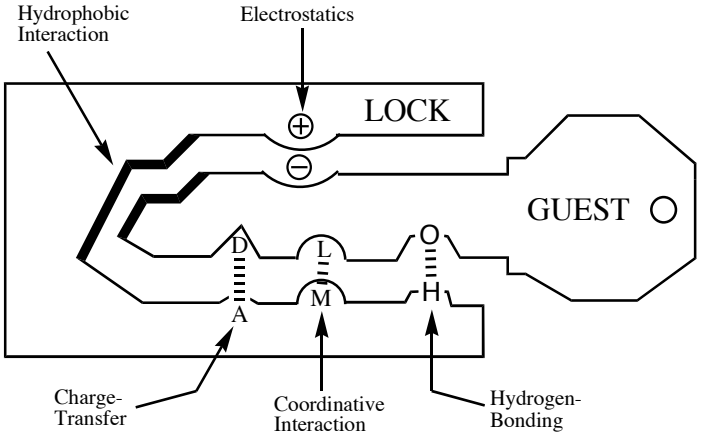

1.3 Crown Ethers and Cryptands

Crown ethers are one of the simplest macrocyclic receptors designed for the complexation of cations and neutral molecules. In 1967 Charles J. Pedersen attempted to develop bisphenol compound **1.1**, but he unexpectedly developed hexaether **1.2**. He expanded upon this discovery and went on to publish two seminal publications describing

the development of 33 cyclic polyethers derived from aromatic vicinal diols.[3] It was found that crown ethers have remarkable selectivity for spherical metal ions, and the selectivity is determined by crown ether "holes" of different sizes into which a variety of guests bind.

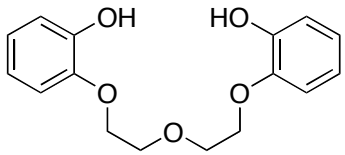

1.1

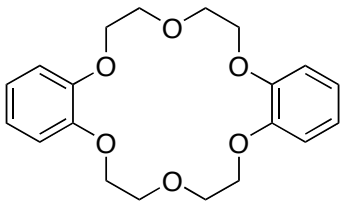

1.2

The selectivity for cations of crown ethers was enhanced through the development of bicyclic crown ether-like compounds termed cryptands. Jean-Marie Lehn first introduced these compounds that have a three-dimensional spherical shape whose size changes as the bridge-head lengths are varied.[4] The three-dimensional nature of cryptands makes them ideal for encapsulation of spherical guest molecules. A representative cryptand **1.3** is shown. Complexity and selectivity were further enhanced by Lehn and Donald J. Cram by developing more complex and rigid structures for the identification of charged and neutral metals and organic molecules. Cram, in particular, utilized molecular mechanics calculations to generate organic structures that were highly analyte specific.[5] The work of Pedersen, Cram, and Lehn earned them all a share of the 1987 Nobel Prize and set a remarkable precedent for the fields of molecular recognition, supramolecular chemistry, and chemosensing.

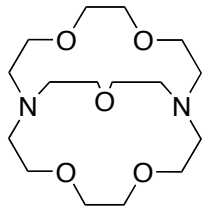

1.3

1.4 Host-Guest Interactions

A number of non-covalent interactions can be used independently or concomitantly to reversibly bind molecules. Non-covalent interactions encompass a large range of attractive and repulsive forces. These forces are mitigated by environmental parameters such as solvent and pH, and they are generally weak. The power of host-guest non-covalent interactions is found in their combination, which enhances strong and selective binding. Other reversible interactions may involve covalent or dative bonding such as metal-ligand bonding[6] and boronic acid / diol interactions (Figure 1.2).[7] The recognition assays presented later in this dissertation will utilize many of the following important host-guest interactions.

Figure 1.2 Reversible Boronic Acid / Diol Interaction.

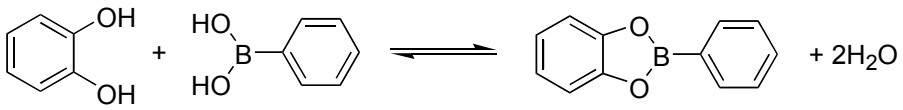

1.4.1 Electrostatics

Electrostatic interactions include ion-ion, ion-dipole, and dipole-dipole, and they are driven by the Coulombic attraction between opposite charges. Ion-ion interactions are non-directional and a favorite of supramolecular chemists for their strength of association. A simple example of an ion-ion interaction is potassium chloride. Ion-dipole interactions require suitable alignment of the dipole toward the ionic charge and are not as strong as an ion-ion interaction. Examples of this include a potassium ion encapsulated by a cryptand, and the bonding of Na^+ with a polar molecule like water. Dipole-dipole interactions are generally the weakest electrostatic interaction. They result from the attractive interaction between a single pair of poles on adjacent molecules (e.g. carbonyls) or the opposing alignment of one dipole with another. Crown ethers, cryptands, and spherands commonly exploit electrostatic interactions to form selective and strong binding interactions.[8]

1.4.2 Hydrogen-Bonding

Hydrogen bonds form when an electronegative atom A bound to H in an A-H covalent bond is sufficiently electron-withdrawing to leave the proton partially unshielded. This unshielded proton then interacts in a dipole-dipole fashion with an acceptor atom B that has available lone-pair or polarizable electrons.[9] Hydrogen bonds are directional and their strength ranges from 1-40 kcal/mol, and their length averages 1.8 Å. Base-pairing within the DNA double helix is a well-known example of hydrogen-bonding, and it is also vital to protein α-helix and β-sheet tertiary structure formation. Indeed, hydrogen-bonding is found throughout biological supramolecular interactions

and is key to the form and function of many processes. Because of their utility and the diverse functional groups that participate in hydrogen-bonding, many synthetic receptors incorporate this interaction. Later in this dissertation, recognition of amino acids, peptides, and proteins with synthetic receptors and receptor arrays that incorporate hydrogen-bonding functionalities will be discussed.

1.4.3 Cation-π and π-π Interactions

Cation-π forces arise from electronic density within olefinic bonds interacting with empty cation orbitals. These are relatively weak interactions, but they are important to biological processes. π-π stacking forces occur between molecules containing aromatic rings. Attractive interactions occur in either a face-to-face or edge-to-face manner and are likely promoted through an "electrostatic" force and/or van der Waals influences. The length of the interactions is on average 3.5 Å. π-Stacking interactions between the aryl rings of DNA base pairs help to stabilize the DNA double helix.

1.4.4 Dispersion (van der Waals) Forces

These induced dipole-dipole interactions occur via the polarization of an atom's electron cloud due to an adjacent atomic nucleus. Molecules with higher molecular weight display greater dispersion forces. However, the forces generally depend on the polarizability of the molecule; the electron cloud of a polarizable molecule is more readily distorted. Dispersion forces occur instantaneously and are generally very weak. They are difficult to design into a receptor's molecular architecture because of their

rather fleeting presence, but they have been shown to provide additional enthalpic stabilization to the coordination of a hydrophobic guest into a hydrophobic binding cavity.[10]

1.5 Solvent Effects

Host-guest interactions occur in a solvent environment that is not inert. The host-guest equilibrium may be effected if the solvent strongly solvates the host, guest, or the host-guest complex. The thermodynamic parameters of enthalpy and entropy must be considered to more fully understand the role of solvent effects.

Arguments abound for the nature of the "hydrophobic effect" since a seminal publication by Kauzman in 1959.[11] The underlying basis of the hydrophobic effect is the lack of *strong* favorable interactions between polar water molecules and non-polar molecules. The argument states that when a host-guest complex forms in an aqueous system the water mediates agglomeration of hydrophobic units to decrease the hydrocarbon-water interfacial area.[12] So upon complexation the guest sheds its hydration cover to enter the host binding cavity. Likewise, the binding cavity of the host releases water molecules back into the solvent upon guest complexation. Upon shedding and release of water molecules there is a gain in entropy; there is also an enthalpic contribution from hydrogen-bonding between solvent molecules and the host-guest complex.

The hydrophobic effect is particularly important for molecular recognition with cyclodextrin and cyclophane hosts.[13] Solvation-desolvation processes are a central factor in cyclodextrin/cyclophane-aryl guest binding resulting in highly structured complexes that can approach enzyme-substrate complexes in their stability ($K_a > 10^6$ M^{-1}).[14] The

hydrophobic effect is also a principal force in enzyme-substrate binding, protein folding, and antibody-antigen binding.[13c]

The dielectric constant of the solvent is another factor that plays an important role in mediating the strength of host-guest interactions, particularly those based on electrostatic forces. Solvents with high dipole moments interact more strongly with charged species effectively shielding host-guest complexes from forming. Therefore, a receptor system that relies on electrostatic interactions would have stronger associations in chloroform than water. Another solvent factor is its ability to donate or accept electron pairs. Donor solvents can effectively solvate cations and acceptor solvents solvate anions, thus both compete with synthetic receptors. The ability of the solvent to participate in hydrogen-bonding can also affect a host-guest system. One scale for measuring donor-acceptor values is the Gutmann donor and acceptor numbers (Table 1.1).

Table 1.1 Gutmann Donor and Acceptor Numbers and Dielectric Constants for Selected Solvents.

	Donor Number	**Acceptor Number**	**Dielectric Constant**
H_2O	33.0	54.8	80.1
CH_3SOCH_3	29.8	19.3	46.7
CH_3CN	14.1	8.9	36.0
CH_3OH	19.0	41.5	33.0
CH_3COCH_3	17.0	12.5	21.0
C_4H_8O	20.0	8.0	7.5

The role of the solvent in host-guest systems has been studied by Hamilton using bis-guanidinium receptors for the recognition of dicarboxylates.[16] He evaluated the binding of **1.4** with glutarate **1.5** in increasingly competitive solvents starting with dimethyl sulfoxide (DMSO), then methanol, and finally water. He also found that the greater the electron donor ability (hydrogen bonding) of the solvent, the weaker the interaction due to solvation of the binding partners. The K_a in DMSO was determined as 55,000 M^{-1}, but dropped off markedly in 50% water in methanol to 230 M^{-1}. It is apparent from this study and others that when designing a host-guest system the solvent for binding studies must be carefully considered.

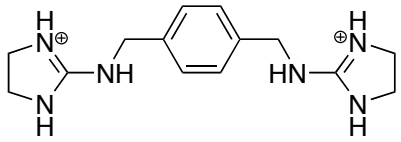

1.4

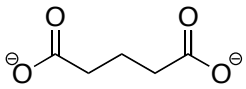

1.5

1.5.1 Crude Media Detection

A common objective when developing synthetic receptors is high binding affinity and specificity for an analyte. This is challenging when targeting a complex analyte in competitive crude media such as beverages, blood, serum, urine, or saliva. There are several competing factors in crude media including multiple other chemical compounds, pH, polarity, and dielectric constant. Minimal reports have been made in the literature regarding the use of synthetic receptors to bind analytes in crude media. The Anslyn group has made advances in this field including determination of citrate concentration in vodka,[17] phosphate concentration in serum and saliva,[18] 2,3-bisphosphoglycerate in

serum,[19] malate concentration in pinot noir,[20] gallic acid levels relating to the age of Scotch whiskeys,[21] and heparin concentration in human and equine serum.[22]

Using an indicator-displacement assay for threshold detection Anslyn monitored the maturity of pinot noir grapes using host **1.6**.[20] Gallic acid (**1.7**) is consumed for energy during maturation, therefore the levels decrease during grape maturation. Thus, determining the concentration of gallic acid in grapes may permit more precise harvest times.

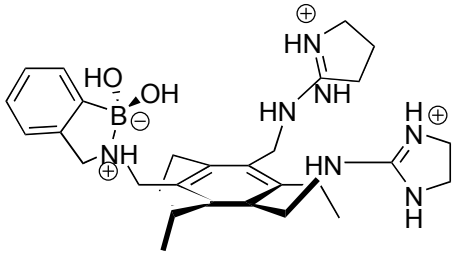

1.6

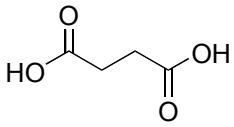

1.7

1.6 Preorganization

Earlier the notion of host-guest complementarity was discussed, as well as some of the earliest host types that led to Nobel Prizes. Cram remarked that "hosts must have binding sites which cooperatively contact and attract binding sites of guests without generating strong nonbonded repulsions."[23] However, the receptor may have the appropriate binding functionalities without having them in proper alignment, thus greatly diminishing the strength of association. The concept of preorganization involves the construction of a host molecule that has proper alignment, sterically and electronically, with a guest. The host must physically fit around the guest, and proper electrostatic and/or dipole functional matches must be made between host and guest.

Thermodynamically, the role of the solvent is critical as mentioned briefly in Solvent Effects. The host and guest both have to shed their solvent shells when aligning for complementary binding. Thus, the net free energy of complexation represents enthalpic and entropic energy gains from host-guest binding and the concomitant release of water molecules into the bulk solvent. The enthalpic loss associated with desolvation of the host/guest solvation shells and rearrangement of the host for binding must be subtracted from the net free energy. Therefore, if a host is preorganized for binding, the solvation shell is minimal about the host, and there is no entropic cost for rearrangement. This generally leads to an increase in the strength of association.[24] Kinetically, preorganization resembles transition state theory in which a reaction proceeds at a faster rate when the reactants are analogous to the transition state structures.[25]

Preorganization as a primary determinant of binding strength has been beautifully demonstrated by Cram. Receptor **1.8** was developed for binding lithium and sodium cations.[26] The six oxygens of **1.8** are octahedrally arranged with the orbitals of their unshared electron pairs forming a spherical hole. The oxygens are attached to six equatorially arranged *p*-tolyl groups and six axially arranged methyl groups, thus burying the oxygens within a hydrocarbon shell. It was stated by Cram that "no solvent can approach the six oxygens, which remain unsolvated." Receptor **1.9** differs from **1.8** in that two hydrogens replace each aryl-aryl bond. Conformationally, **1.8** is preorganized, existing in only a single conformation, but **1.9** exists in greater than 1,000 conformations. Therefore, the free energy cost of desolvating the oxygens and organizing the receptor were paid for in the synthesis of **1.8**. Receptor **1.9** has maximal conformation and rotational freedom, and the oxygens were fully solvated. The difference in binding strength to the cations by the two receptors is remarkable. There was a difference in association constant values between **1.8** and **1.9** with a lithium ion exceeding 10^{12} M^{-1} and

exceeding 10^{10} M^{-1} for a sodium ion! This beautifully demonstrates the advantage in binding strength that preorganization can impart. Hamilton has also demonstrated the positive effect of preorganization by developing a series of receptors for the barbiturate family of drugs.[28] He demonstrated that without preorganization binding events can be virtually nonexistent. Cram summarized preorganization effects by writing that "the more highly hosts and guests are organized for binding and low solvation prior to their complexation, the more stable will be their complexes."[27]

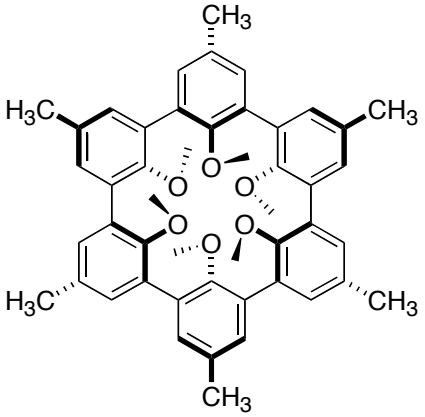

1.8

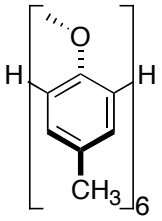

1.9

1.7 Chemosensor Development

Several fundamental aspects of molecular recognition have been discussed to this point. However, the actual transduction of a binding event into a measurable signal has not been expanded upon. A sensor is a chemical device, or simply a chemical molecule, that communicates a measurable signal that can be used for quantitative detection of analyte concentration. Czarnik has divided sensors for ion and molecule recognition into two categories: chemical sensors and chemosensors.[29] Chemical sensors are micro- or

macroscopic devices that reversibly interact with chemical analytes and provide some type of signal transduction. Chemical sensors include electrochemical, potentiometric, and amperometric sensors, mass-sensitive and thermal sensors,[30] and fiber optics.[31] Chemosensors are molecules that interact with analytes and communicate their presence to the outside of the recognition event.[7,32] The difference between the basic principle of molecular recognition and chemosensing is illustrated in Scheme 1.1. Stated again, molecular recognition involves a receptor possessing steric and electronic features complementary to a target analyte; a chemosensor requires the assembly of a receptor and a signaling unit.[33]

Scheme 1.1 Molecular Recognition Versus Chemosensing.

(a) Molecular Recognition:

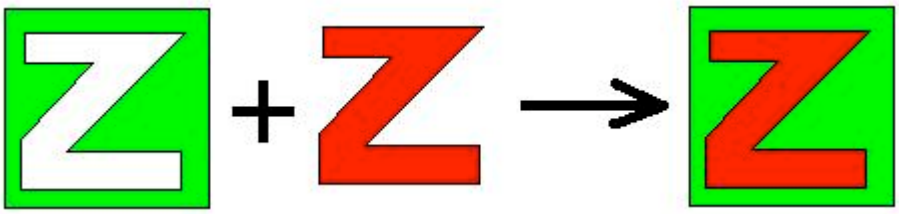

(b) Chemosensing:

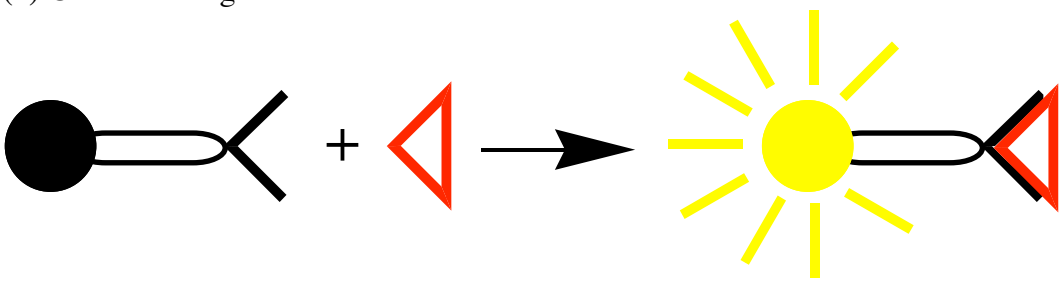

Typically, synthetic chemosensors have covalent linkages between the binding site and chromophores or fluorophores that signal analyte complexation. The analyte triggers a microenvironmental change perturbing the properties of the signaling element.

Synthetic receptors may also interact in a reversible manner with a signaling molecule. In this case a signaling molecule is initially bound to the receptor and upon introduction of an analyte the signaling molecule is displaced and its optical properties modulated. The Anslyn group has coined this as "Indicator-Displacement Assays (IDA)."[34] In both signaling methods observed spectral changes can be translated into binding stoichiometries and association constants.[35]

Signal modulations involving absorbance or fluorescent emission can arise from charge transfer, photoinduced electron transfer (PET),[36] microenvironmental changes such as pH, or fluorescence resonance energy transfer (FRET).[37] Some methods, particularly IDA and pH, are colorimetric and have the advantage of being detectable by the naked eye. These absorbance-based methods require greater receptor/analyte concentrations than fluorescence measurements, which have the advantage of enhanced sensitivity.

The following sections will discuss typical strategies for developing chemosensors using signal transduction mechanisms inherent or added to the chemical receptors. Chemosensors have been used and continue to show potential for environmental analysis, medical diagnostics, chemical and food processing, water analysis, and many other applications.

1.7.1 Indicator-Displacement Assays

Indicator-displacement assays involve a competition between an indicator and an analyte for a receptor binding pocket. An equilibrium is first established between the receptor and indicator, but analyte addition creates a competition for the receptor binding site, and indicator displacement from the binding site by the analyte is marked by signal

modulation (Scheme 1.2). pH indicators are particularly useful for IDAs as they have different protonation states when free or receptor-bound, and the protonation states vary in color. The Anslyn group has commonly employed pyrocatechol violet and fluorescein.

Several advantages exist for IDAs. First, receptor synthesis is made more facile as covalent attachment to the indicator is not required. Second, IDAs can be improved through optimization of the indicator because they are easily changed. Finally, IDAs work in both organic and aqueous solvents so they can be used in near limitless situations. Unfortunately, IDAs have not yet been shown to be acquiescent to *in vivo* studies.

Scheme 1.2 Indicator-Displacement Assay.

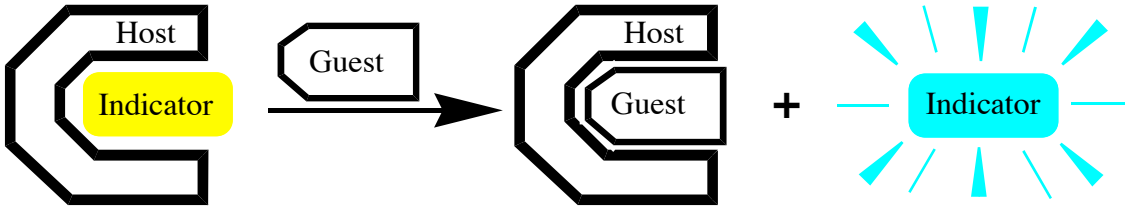

Indicator-displacement assays have been used by many research groups[34,38] including the Anslyn group. Most recently IDAs have been employed for enantioselective discrimination assays for α-amino acids,[39] α-hydroxycarboxylates and diols,[40] and α-hydroxyacids.[41] Earlier, Anslyn group IDAs were used to detect citrate[42-44] and tartrate/malate[20,45] in various beverages including scotch[21] and vodka.[17] Also, as mentioned earlier, IDAs have been used for the detection of inorganic phosphate[18] and 2,3-bisphosphoglycerate[19] in crude media. Indicator-displacement assays often require access to a fluorimeter or UV/Vis spectrophotometer. Multiple bioanalytes have been

targeted as well including inositol trisphosphate,[46] aspartic acid,[47] and heparin.[48] A recent advance was made that coated receptor and indicator on paper-based and hydrogel-based test strips for facile and naked-eye detection of analyte presence.[49] Clearly, the range of detectable analytes is very large, and only Anslyn group progress has been discussed. To clarify IDA further, the aspartic acid and heparin detection systems will be described.

1.7.1.1 Sensing Ensemble for Aspartic Acid

In a study to demonstrate large color changes observed in IDAs, and to determine the cooperativity between coordination chemistry and molecular recognition in controlling selectivity, a Zn(II) metalated 2,2':6,2''-terpyridine derivative **1.10** was used to bind multiple amino acids.[47] Metal complex **1.10** has no inherent color so it was a good choice for evaluating spectral changes with an IDA. The guanidinium groups were installed to impart selectivity for aspartate and glutamate as they are known anion ligands.[42,50] The trigonal bipyramidal geometry of Zn(II) likely aligns the guanidinium groups in the same plane making possible the hydrogen bonds shown in Scheme 1.3. Pyrocatechol violet (**1.11**) is a good metal ligand and exhibited a dynamic color change from yellow to blue when bound to **1.10** in a water/methanol mixture (1:1, buffered with HEPES, pH 7.4). When an amino acid was added the color shifted from blue back to yellow indicating that **1.11** was displaced back into the bulk solvent.

Scheme 1.3 Sensing Ensemble for Amino Acid Recognition.

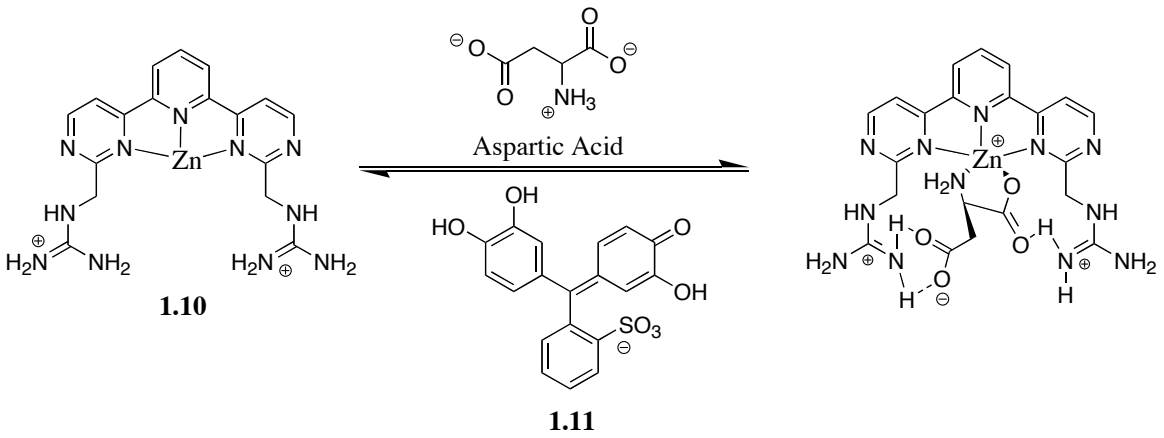

Affinities were calculated for binding between **1.10** and the hydrophobic amino acids L-valine, L-glycine, and L-phenylalanine (K_a~10^4 M^{-1} for all three) as well as the more polar L-asparagine (K_a = 2.3 × 10^4 M^{-1}). The binding constant for L-aspartic acid was 1.5 × 10^5 M^{-1}, and L-glutamic acid was 2.2 × 10^4 M^{-1}. Clearly receptor **1.10** has affinity for all the classes of amino acids. It was believed that the higher binding strength with aspartic acid was due to cooperative interactions between the guanidinium groups and the carboxylic acid of aspartic acid. This effect was not as high with glutamic acid as its side chain has two methylene units prior to the carboxylic acid and is not as well organized for binding the guanidiniums of **1.10** as aspartic acid. Therefore, this represented cooperativity between organic molecular recognition and coordination chemistry.

1.7.1.2 Sensing Ensemble for Heparin

Heparin is an anionic glycosaminoglycan biopolymer that is used therapeutically as an anticoagulant to reduce excessive blood clotting during and following surgery.[51] If not monitored properly over-administration can lead to detrimental bleeding. Though clinical methods exist for determining heparin concentration, Zhong and Anslyn postulated that a simple colorimetric test could expedite and ensure proper therapy.[48] Receptor **1.12** was used with pyrocatechol violet (**1.11**) in an IDA for heparin (**1.13**) as well as similar glycosaminoglycans chondroitin-4-sulfate and hyaluronic acid. It was expected that the boronic acids of **1.12** would form reversible cyclic esters with the saccharide groups of heparin, and the charged amines could interact with the negatively charged sulfates and carboxylates of heparin. Furthermore the hexasubstituted benzene receptor scaffold is known to have groups alternate up and down[52] creating a preorganized cavity for binding.[53]

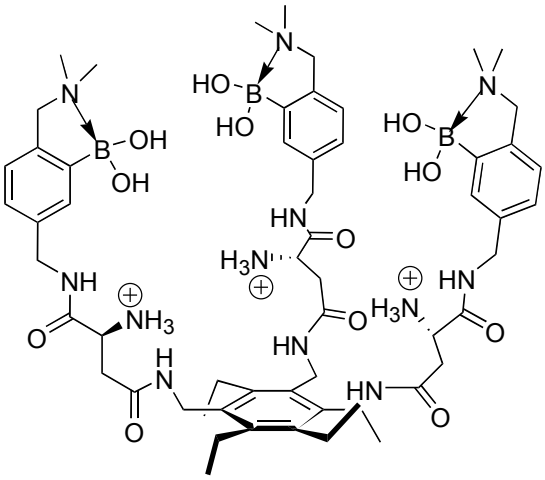

1.12

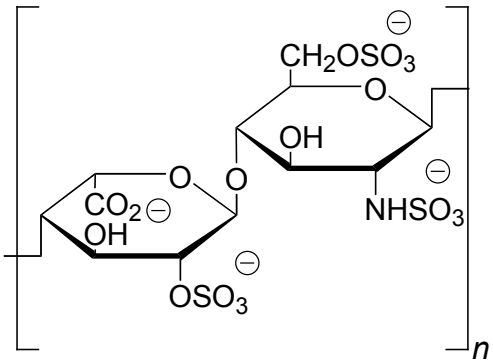

1.13
Heparin Biopolymer

Receptor **1.12** was studied using UV/Vis spectrophotometry with the various glycosaminoglycans and **1.11** in a water/methanol solution (1:1, buffered with 10 mM HEPES, pH 7.4). The binding stoichiometry between **1.11** and **1.12** was 1:1 with K_a = 7.1×10^3 M^{-1}. Following an IDA it was determined that binding between the heparin polymer (**1.13**) and **1.12** was relatively strong ($K_a = 3.8 \times 10^4$ M^{-1}). It was shown that the receptor was selective for heparin over chondroitin-4-sulfate ($K_a = 6.4 \times 10^3$ M^{-1}), and it did not bind to hyaluronic acid. This is consistent with anionic charge density trends as heparin is most anionic and hyaluronic acid the least. Interestingly, when **1.12** was tested for binding to a disaccharide variant of heparin rather than **1.13** the affinity was only slightly weakened indicating that only a modest binding affinity enhancement is due to polymerization. Unfortunately, this assay was not developed into a clinical sensor because **1.12** did not have sufficient affinity for heparin to be selective in serum.

1.7.2 Molecular Fluorescent Sensing

Molecular receptors that incorporate a binding site, fluorophore (inherent or attached), and a mechanism for communication between the binding site and fluorophore are fluorescent chemosensors.[32a] George Stokes first determined that fluorescence emission occurs at a longer wavelength than excitation. In 1852 he proposed that fluorescence could be an excellent tool for studying and detecting organic compounds.[54] Indeed, his observation was correct as fluorescence has its lowest concentration limits near 10^{-7} M, and it has been widely exploited. Fluorescence is an ideal tool for detection of analytes that exist at nM concentrations. Most fluorescent chemosensors operate via one of the following mechanisms: 1) quenching of photoinduced electron transfer (PET) or enhancement of heavy atom quenching, 2) variation of the distance between two

fluorophores to effect the efficiency of energy transfer, and 3) perturbation of the microenvironment or structure of a fluorescent sensor.[55] Sousa was one of the first to apply supramolecular receptors to fluorescence sensing. In his study naphthalene compounds **1.14** and **1.15** were perturbed by various alkali metal chloride salts causing increases and decreases in fluorescent quantum yield, phosphorescence quantum yield, and phosphorescence lifetime.[56] This study was the first study of excited states that used perturbers held noncovalently by preorganized receptors.

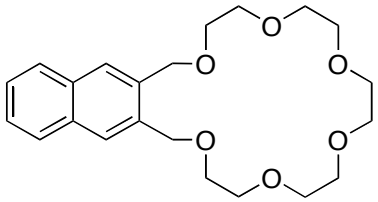

1.14

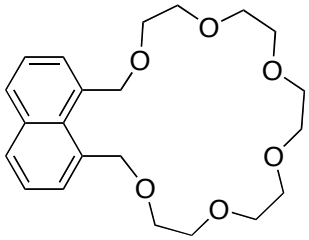

1.15

Several research groups have employed the fluorophore-spacer-receptor[57] (Figure 1.3) design for fluorescent chemosensor including Czarnik,[7a,58] Fabbrizzi,[29,32a,33,59] Tsien,[60] Shinkai,[61] de Silva and many others.[57] With the fluorophore-spacer-receptor design a PET photoelectrochemical signal modulation can be incorporated. In these systems a fluorophore is separated from the receptor by an all σ-bond spacer. In a well-designed system there is a strong long-range interaction between the nonbonding and π-electron systems such that when the fluorophore is in a photoexcited state electrons are transferred from the unbound receptor effectively quenching the fluorescence. However, when an analyte is bound the PET process is interrupted and the fluorophore emits. This process can also be reversed so that the fluorescence is switched off when the receptor is bound to

the analyte. Figure 1.3 depicts in cartoon format and in frontier orbitals the photoinduced electron transfer process.

Figure 1.3 (a) Cartoon representation of PET in the fluorophore-spacer-receptor approach when bound and unbound. (b) Frontier orbital diagram of the PET in the fluorophore-spacer receptor approach.

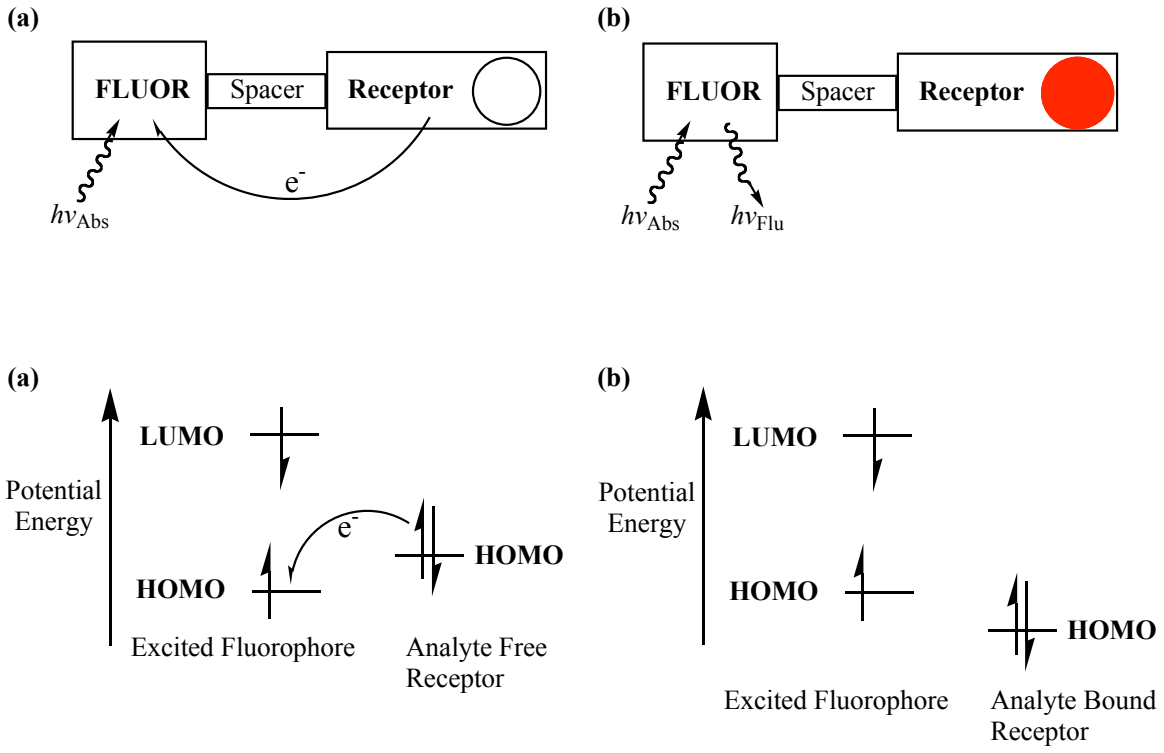

Fluorescence resonance energy transfer (FRET) is another method for fluorescent chemosensing.[62] In this signaling mechanism the distance between two fluorophores is varied to control nonradiative energy transfer between them. The two fluorophores participating in the FRET mechanism are selected according to good overlap of their excitation and emission bands for efficient energy transfer. When the first fluorophore (donor) is excited it transfers its energy to the second fluorophore (acceptor) rather than

emitting a photon. The energy accepting fluorophore subsequently emits at a longer wavelength resulting in a large shift in excitation versus emission wavelengths. The energy transfer is via a long-range dipole-dipole coupling mechanism. Therefore, spatial relationship is important as well as the relative orientation of the donor emission dipole moment and the acceptor absorption dipole moment. Common chemosensor development incorporating FRET involves the use of a receptor that has its two fluorophores too far apart to participate in energy transfer. When bound to a guest the separation distance between the two fluorophores is decreased, and the FRET process is stimulated concomitantly signaling guest binding.[63]

A nice example of FRET in a biological system has been developed by Tsien for a single-cell assay to determine the gene expression of the bacterial enzyme β-lactamase.[64] In this research fluorogenic β-lactamase substrate **1.16** was developed as a derivative of cephalosporin. β-lactamase catalyzed hydrolysis lead to the destruction of FRET between the two fluorophores, and the blue fluorescence of a single molecule **1.17** was enhanced signaling the presence and gene expression of β-lactamase with high fidelity and sensitivity.

Scheme 1.4 β-Lactamase Activity Detected by Disruption of FRET.

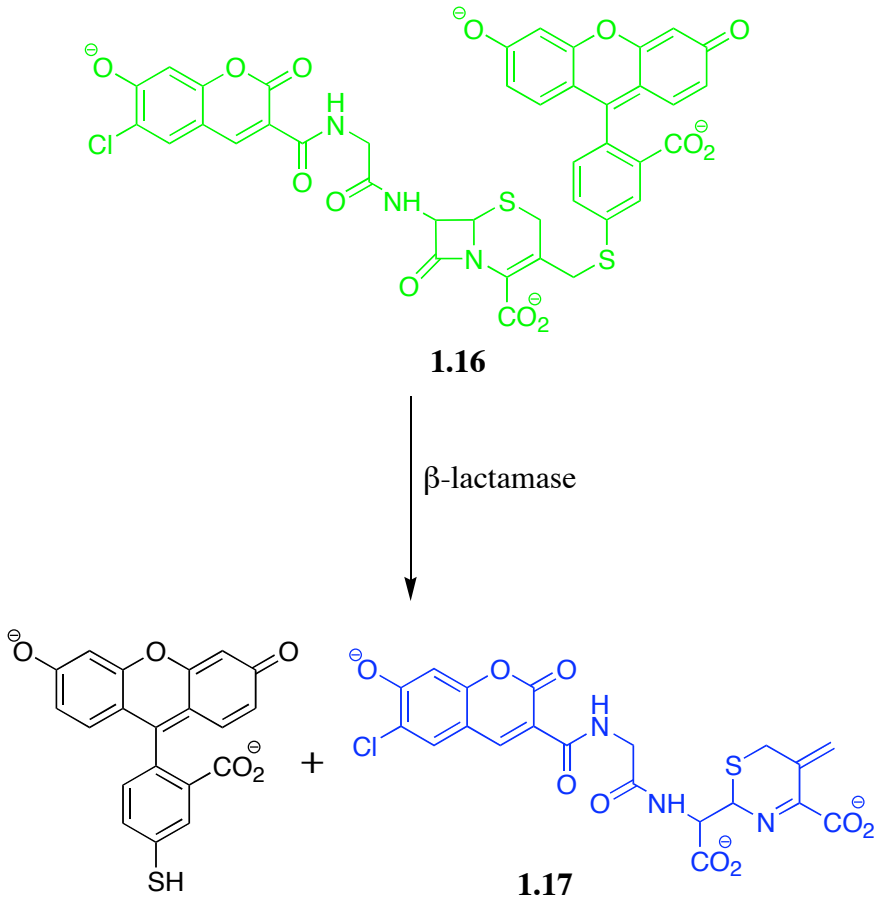

It is well established that more rigid fluorophores have enhanced fluorescence.[65] Often binding of substrates induces conformational restriction resulting in enhanced fluorescence via suppressed intersystem crossing or internal conversion. Likewise, conjugation can be disrupted by substrate binding that induces fluorescence quenching. Both mechanisms, fluorescence enhancement and quenching, have been used for chemosensing.[7,22,32,55,66] Finney has demonstrated with **1.18** an example of fluorescence enhancement via suppression of internal conversion in biaryl acetylenes due to binding of

Li^+. The addition of lithium cation lead to a small increase in the extinction coefficient and a significant increase in fluorescence. There was no change in the fluorescent response upon addition of trifluoroacetic acid indicating that the increased signal was not an electronic or charge-transfer process. Finney's observations led him to believe that signal enhancement was due to metal-binding induced conformational restriction.

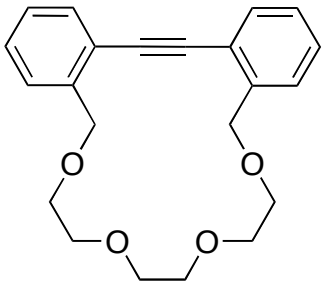

1.18

1.8 Selective Synthetic Receptors

Nature routinely demonstrates remarkable binding of highly complex molecules by natural receptors. Additionally, cells, proteins, peptides, and antibodies display high-level surface recognition via peptide interactions that commence or prevent key signaling and protection mechanisms. Chemists have attempted to mimic these binding events by synthetic development of chemosensors. Several examples exist for the recognition of biological neurotransmitters,[67] DNA/RNA,[68] anions,[69] peptides/proteins,[70] sugars,[71] biological energy sources such as ATP,[72] and metals in living cells.[68c,73] This is just a small subsection of the accomplishments made to this point, but it illustrates the diversity of compounds that have been targeted. In the next two sections an in-depth evaluation of synthetic amino acid and peptide receptors will be made.

1.8.1 Synthetic Amino Acid Receptors

Amino acids as substrates are interesting for their chemical structures and biological significance. Amino acids in peptides and proteins play a key role in many biological processes including the control of gene regulation, glycoprotein targeting, and vesicle transport. They are also found in peptide sequences important for signaling in bacterial cell wall biosynthesis and Alzheimer peptide aggregation.[74] The study of artificial receptor systems capable of selectively binding amino acids has helped scientists better understand amino acid/peptide/protein interactions.[75] A major challenge for artificial receptor systems is achieving substrate selectivity and strong binding in aqueous systems. Design of an amino acid host for target recognition in nonpolar solvents is typically straightforward because the contribution from solvation energy is significantly less than the interactions between host and guest.[76] However, strategies used for complexation in nonpolar solutions are not readily applicable to aqueous systems where polar interactions are considerably hindered by hydration.[77] Despite the difficulties in chemosensing of amino acids particularly in aqueous media, considerable gains have been made.

The molecular recognition of polar amino acids in aqueous systems has two intrinsic difficulties: a) polar amino acids are well hydrated diminishing hydrophobic effects, and b) hydrogen bonding and electrostatic interactions with polar amino acids are greatly weakened in aqueous systems when compared with nonpolar solvent systems. Kitigawa has designed a nice porphyrin system for the molecular recognition of the methyl ester of arginine in water at pH 9.[76a] In this example a series of water-soluble porphyrins with a hydrophobic binding pocket, a Lewis-acidic Zn(II) center, and multiple carboxylate groups were designed. Association constants as high as 11,000 M^{-1} were

obtained. However, this recognition system illustrates the difficulty in attaining strong and selective binding in aqueous systems. Had this same porphyrin system been used in a nonpolar solvent the strength of association likely would have been two or three-fold greater.

Classic exploitation of hydrophobic effects in aqueous systems has been shown by Morán. A receptor was designed by the combination of a crown ether and a xanthone that effectively extracted phenylalanine from water.[78] Similar studies have been conducted by Dougherty with cyclophane hosts for arginine,[79] Fabbrizzi using a Zn(II) tris(2-aminoethyl)amine receptor platform derivatized with anthracene and benzyl groups for detection of phenylalanine and tryptophan,[80] and Rebek employed receptor **1.19** developed from Kemp's triacid and acridine for the extraction of phenylalanine and tryptophan from water. The lipophilicity of receptor **1.19** was only secondary in binding importance as leucine, isoleucine, and valine did not bind demonstrating the importance of a π-stacking interaction between the aromatic amino acids and acridine. Other studies utilizing the hydrophobic effect have been done by Urbach and Nolte,[76b,82] and Niwa's use of dendrimers.[83]

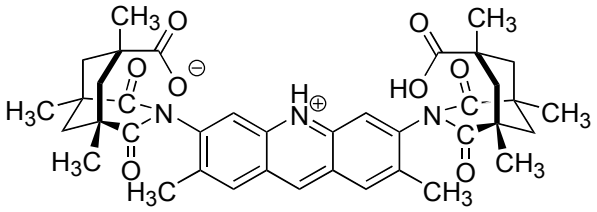

1.19

One way of increasing selectivity and binding strength in aqueous solutions is through the use of organometallic receptor complexes. The chelation of metal ions by α-amino acids through the amino and carboxyl groups gives five-membered metallocycles.

The two coordination sites on Cu(II) receptors are expected to display rapid and reversible ligand exchange to give chelates with α-amino acids in aqueous solutions. The Anslyn group has utilized both Zn(II) and Cu(II)-bound receptor ligands for recognition of aspartic and glutamic acid,[47] histidine and cysteine,[87] and enantioselective recognition of valine, leucine, phenylalanine and tryptophan using an "operationally general and simple" colorimetric technique.[39] Fabbrizzi's group has demonstrated selective binding of histidine with a Zn(II) cryptate[88] and with a fluorescent Cu(II) chemosensing ensemble.[89]

Fabbrizzi's "chemosensing ensemble" approach involved the use of receptor **1.20** noncovalently bound to a fluorophore for the selective binding of histidine.[89] In this fluorescent indicator-displacement assay the fluorophore is quenched when bound to **1.20**, but upon introduction of an analyte the fluorescence emission is restored when the fluorophore is displaced from the binding cavity. Within their research report they also demonstrated how crucial the choice of indicator is to achieve selectivity in chemosensing. Selectivity for histidine required a receptor selective for the imidazole group of His rather than the carboxyl group which is common to all amino acids. Imidazole is a weak acid and when positioned between the two Cu(II) centers as shown in **1.20** it is deprotonated and bridges the metal centers. In the ternary complex shown in **1.20** each Cu(II) center is four coordinate with a square planar geometry. Three different fluorophores were tested with the receptor: coumarin, fluorescein, and eosin Y (log K_a values of 4.5, 5.9, and 7.2 respectively).

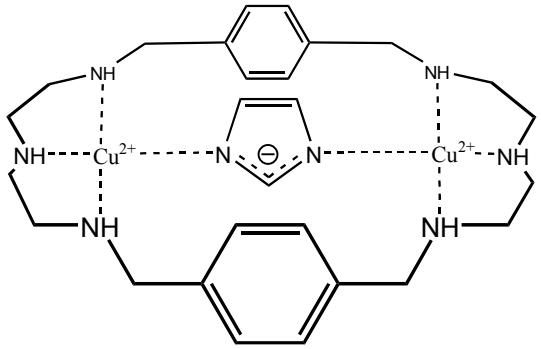

1.20

After obtaining the characteristics of binding between **1.20** and the three fluorophores, several amino acids were tested at pH 7 with the indicator concentration at 10^{-6} M and the receptor concentration suitably high enough to completely quench fluorescence. Depending on the receptor/fluorophore combination, several of the amino acids including His, Ala, Phe, Leu, Pro, Val, and Gly were able to restore the fluorescence to some degree. It was determined that the highest sensitivity was displayed with the receptor/eosin Y chemosensing ensemble. In this case only His could dislodge the covalently held eosin Y from the binding site. This is due to His being the only amino acid with the imidazole R-group for highest affinity to the dicopper ligand. A pattern of His>Gly>Ala>Phe>Val>Leu>Pro was observed for binding affinity. This observed stability trend favors amino acids with less repulsive steric effects. So proper binding geometry was required for full fluorophore displacement. If the analyte had a binding affinity similar to the fluorophore affinity then it participated in competitive displacement. However, if the fluorophore affinity was considerably stronger the equilibrium then favored the fluorophore. They concluded that a receptor with two transition metals prepositioned at a correct distance for binding an imidazole group

provided selective recognition of the ambidentate imidazole group of His over the carboxylate groups of the other amino acids.

A number of groups have explored the chemosensing of arginine which has a guanidinium handle for binding.[90] Biologically, individual arginine residues are critical to the function of many nucleotide-binding proteins that mediate a wide range of biological processes.[91] Highly conserved Arg residues bind through electrostatic contacts with phosphate groups in the polyribonucleotide backbone. For an Arg receptor to be useful it must be soluble in water and have high affinity for the N-alkylguanidinium moiety and demonstrate selectivity over other cations, specifically the ammonium side chain of lysine. An early example of Arg binding with a synthetic receptor comes from Bell's laboratory in which **1.21** (shown below bound to Arg) bound Arg selectivity in water (K_d = 34 μM).[91] Binding was determined by following the change in the UV absorption spectrum of **1.21**.

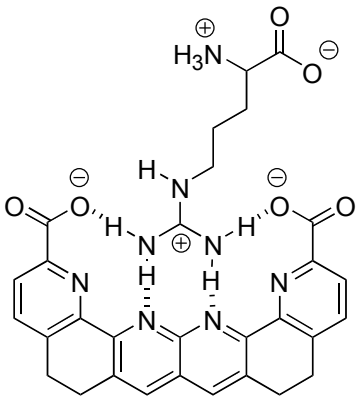

1.21

Schrader has investigated water-based recognition of Arg and Lys using a number of different biomimetic molecular tweezer receptors.[92] In a very recent example a new molecular tweezer (**1.22** – the red portion binds to the Lys ammonium, and the black

portions fold down to form a tweezer-like cavity with the blue portion at the top) for Arg and Lys was developed featuring an electron-rich torus-shaped cavity derivatized with two peripheral phosphonate groups.[74] A rather high affinity in neutral buffered water of $K_a \sim 5000\ M^{-1}$ was achieved for lysine. They also demonstrated that the receptor had some affinity for arginine, minimal affinity to histidine, and no affinity to any other amino acid. Protection of the N- and C-terminus of lysine resulted in a 10-fold increase in the binding affinity for Lys.

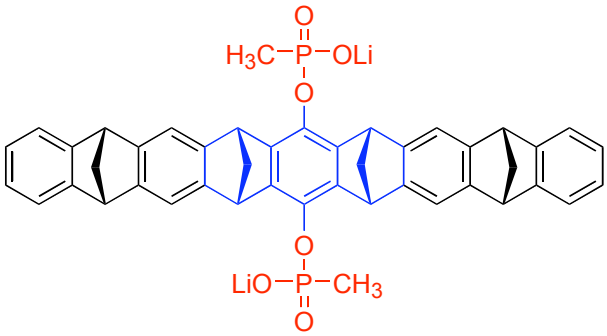

1.22

Other synthetic receptors have been developed for valine[93] and alanine,[94] aspartic and glutamic acid,[38e,48] and enantioselective synthetic receptors have been described for N-protected glutamic and aspartic acid carboxylate salts.[95] Clearly, research to this point has included the synthetic development of receptors for all classes of amino acids.

1.8.2 Synthetic Peptide Receptors

The completion of the Human Genome Project has spurred an intense area of research concerning the abundance and activity of proteins *in vivo*. Knowledge about the translational consequence of gene sequences and subsequent protein activity in normal

and disease states has been absorbed under the broad heading of proteomics.[96] One well understood tenet of proteomics is that biological interactions are often controlled by specific peptide recognition events. Therefore, scientists have pursued peptides as substrates for two key reasons – biological significance and structural complexity.[70a] First, many biochemical processes including enzymatic activity, cell-signaling, bacterial infections, and disease pathogenesis involve peptide recognition by either cell surfaces, proteins, or antibodies.[97] Therefore, creating artificial systems that mimic biological systems may enhance the overall understanding of nature's processes. Second, peptides contain a great deal of functional diversity to target with a synthetic receptor. Structural complexity and conformational flexibility of peptides also makes them interesting and highly challenging targets that a synthetic chemist can employ his entire chemical toolbox to bind.[98] The real challenge is to translate the structural features of a peptidic substrate into a complementary synthetic receptor with appropriate binding sites.[75,99]

Synthetic receptors for oligopeptides represent an intermediate step toward the recognition of proteins and protein surfaces, but peptides are important as molecular recognition targets due to their biological activity as signaling units, hormones (corticotropin, vasopressin), neurotransmitters (chemical messengers such as the tachykinins), and antibiotics (gramicidins). Some of the early work in this field by Still,[100] and later by Kilburn,[101] involved the design of synthetic peptide receptors for recognition in organic solvents. As nice and instructional as this work was, the focus of this section will be on the aqueous (or competitive solvent mixture) recognition of peptides as it is more complementary to a biological system.

One of the earliest reports of peptide recognition in water was from the Sasaki laboratory in which a 14-residue peptide was synthesized to study the interactions between polypeptides and biological polyamines such as spermine.[102] Four glutamic

acids were placed in the synthetic peptide to induce α-helical formation upon substrate binding. It was determined that the α-helicity of the synthetic peptide increased from 19% to 38% when bound to spermine at pH 7. If the pH deviated from neutral the strength of the 1:1 complex and the α-helicity diminished.

Other reports in the mid-1990s came from the laboratories of Hamilton,[103] Kelly,[104] and Still.[105] Kelly developed a synthetic peptidomimetic host that bound a tetrapeptide guest to give a host-guest complex that subsequently self-associated into a high molecular weight β-sheet. Host **1.23** was composed of alternating cationic and hydrophobic amino acid residues and was selective for anionic guests having an amphiphilic periodicity of 2.[104] Host **1.23** had a dibenzofuran diacid residue which separated the two attached peptide strands and allowed a guest to bind to form an antiparallel β-sheet (**1.24**). The three-stranded β-sheet complex **1.24** was amphiphilic and dimerized in a face-to-face fashion through hydrophobic interfacial interactions. Since this early report on developing synthetic β-sheet structures several groups including Nowick,[99b,106] Schrader,[107] König,[108] and Anslyn[87] have accomplished research in this area.

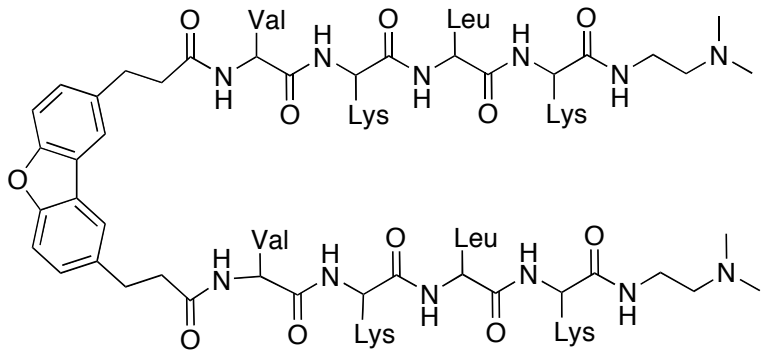

1.23

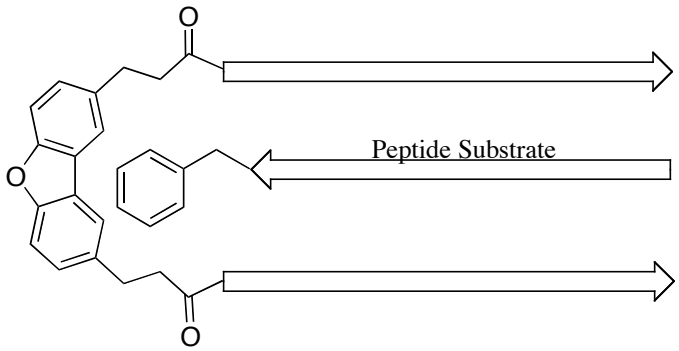

1.24 - Antiparallel Beta-Sheet

Research in the Breslow laboratory has made use of β-cyclodextrins for sequence-selective binding of peptides containing phenylalanine residues in aqueous solution.[109] Dimerization of β-cyclodextrins through the secondary face via direct alkylation was designed to enhance cooperativity in the binding of various hydrophobic acyclic or cyclic peptides of two to six amino acid residues and varying stereochemistry. Binding studies using isothermal titration calorimetry at room temperature determined that the association constants were as high as 1120 M^{-1} for acyclic peptides and 2590 M^{-1} for cyclic peptides. This was contrary to modeling studies that predicted stronger binding with the acyclic peptide variants. The researchers hypothesized that the irregularities between the experimental and modeling studies was due to an energetic penalty of unfolding the Phe

associated peptide prior to binding the β-cyclodextrins. Breslow's work was the first example in which the double binding of hydrophobic side chains was used to chelate a receptor to a peptide.

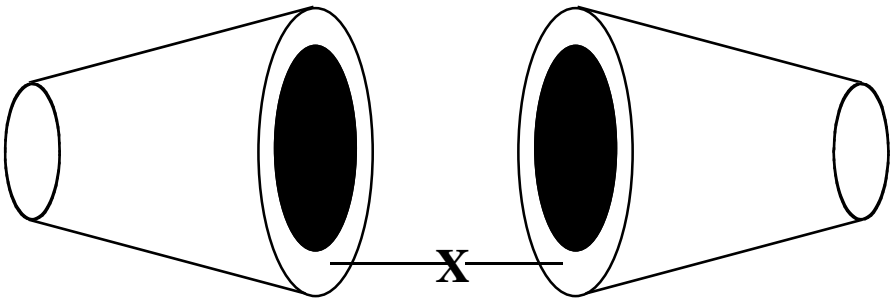

X = 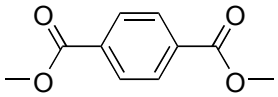

1.25

In the same year that Breslow's research was published, an elegant tripeptide receptor was designed by Schneider.[110] Receptors **1.26** and **1.27** incorporated functionality that would complement both the side chain residues of tripeptides as well as their C- and N-termini. In this way the receptors would provide directional alignment with the peptidyl substrates. It was expected that zwitterionic peptides would associate well as the 18-crown-6 unit of the receptors would interact with the N-termini, and the peralkylammonium group would interact with the C-termini. Introduction of the dansyl subunit into **1.27** increased lipophilic interactions such as π-stacking, and it permitted fluorescent studies in lieu of NMR experiments. Binding with **1.26** to Gly-Gly-Gly had the highest affinity (200 M^{-1} in water, 13000 M^{-1} in methanol), and **1.27** showed the highest affinity for Gly-Trp-Gly (2150 M^{-1} in water) and Gly-Phe-Gly (1700 M^{-1} in

water) as was expected. This work demonstrated that peptide receptors can be developed that suitably differentiate peptides according to length, amino acid composition, sequence, and if chiral elements are introduced into the receptor, configuration.

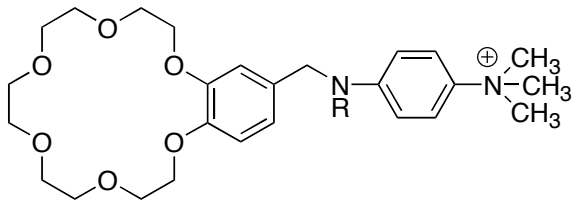

1.26 R = H

1.27 R = 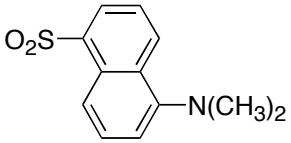

An interesting molecularly imprinted polymer (MIP) receptor for aqueous recognition of peptides was detailed by Hart and Shea in 2001.[111] Molecular imprinting creates macromolecular receptors for small peptides, and both polymerization and recognition are carried out in an aqueous environment. Two recognition sites were incorporated into their MIP receptors: a Ni(II) cation for strong binding of N-terminal histidine, and multiple weaker interactions between the imprinted peptide molecule and the polymeric receptor. In MIP a template molecule (peptide) is added during the receptor polymerization process. The polymeric receptor then forms around the templating molecule creating a lock-and-key type receptor. The binding strength in MIP systems is related to the capacity of the polymer. If an analyte "fills" the capacity of the polymer to an appreciable extent then binding is considered good. The significance of Ni(II) to binding was determined by comparing the binding capacity of a His-Ala templated polymer with and without the metal cation. When Ni(II) was added the

binding capacity of His-Ala to the templated polymer was 37 μmol/g, but when Ni(II) was removed the binding capacity dropped to 10-20 μmol/g.

Hamachi has described a series of novel fluorescent chemosensors for recognition of phosphorylated peptides.[70b,112] Phosphorylation represents a critical post-translational modification of native proteins that regulates their biological function. Phosphorylation commonly occurs on either tyrosine, serine, or threonine, and is represented shorthand by a "p" (e.g. pTyr). The sensing capability of receptor **1.28** was examined by evaluating binding with three peptides (**1.29**, **1.30**, **1.31**) that are consensus sequences modified by distinct kinases (v-Src, Bck-1, and EGFR phosphorylating domain, respectively). In addition, binding to the nonphosphorylated peptide **1.32** was evaluated. Receptor **1.28** is composed of an anthracene derivatized with dipicolylamine (Dpa) Zn(II) complexes. Binding of peptides induced a strong fluorescent emission.

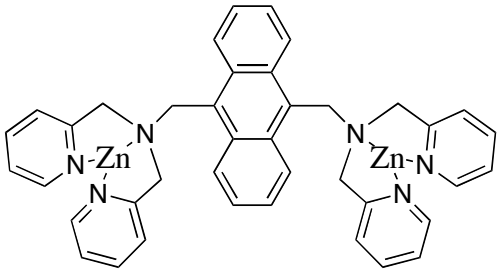

1.28

Peptide 1.29: Glu-Glu-Glu-Ile-pTyr-Glu-Glu-Phe-Asp

Peptide 1.30: Arg-Arg-Phe-Gly-pSer-Ile-Arg-Arg-Phe

Peptide 1.31: Lys-Ser-Gly-pTyr-Leu-Ser-Ser-Glu

Peptide 1.32: Glu-Glu-Glu-Ile-Tyr-Glu-Glu-Phe-Asp

Addition of less than 1 μM of **1.29** to **1.28** in water resulted in a considerable increase in the fluorescent spectrum of **1.28**. The binding affinity of the metalloreceptor

for **1.29** was determined as 10^7 M^{-1}, a very strong affinity in water. Peptide **1.29** is a Glu-rich peptide and the dinuclear Zn(Dpa) receptor bears positive charge, therefore it was theorized that the large affinity was the result of strong electrostatic attractions. This theory was confirmed when the Arg-rich peptide **1.30** displayed no affinity for the receptor due to repulsive electrostatics. Furthermore, the neutral peptide **1.31** only bound at concentrations greater than 10 μM. Peptide **1.32** did not bind at all demonstrating the receptor's affinity for phosphorylated peptides rich in acidic amino acid residues. The difference in fluorescence between the interaction of **1.28** to **1.29** and **1.28** to the nonphosphorylated peptide **1.32** is visible to the naked eye. This work represented the first chemosensors that could selectively bind and sense a phosphorylated peptide surface of biological importance under aqueous conditions.

There are others who have investigated selective peptide binding with synthetic receptors. Schmuck and Geiger have published work regarding dipeptide binding with guanidiniocarbonylpyrrole receptors within the last three years.[113] Severin has employed an indicator displacement assay with an organometallic cyclopentadiene rhodium (III) complex and the indicator azophloxine for the selective detection of histidine and methionine containing peptides in water at neutral pH.[114] Most recently, Fujita has reported a Pd-driven self-assembled pyramidal cage for sequence-selective binding of acetylated tripeptides in water with affinities as high as 10^6 M^{-1}.[115] This field has been well covered primarily because of the biological consequence of peptide binding. A great deal of information can be extracted for biological host-guest systems by appraisal of these artificial systems.

1.9 Combinatorial Receptor Development

Significant advances have been made in the selective recognition of peptides with synthetic receptors. Yet, a pervasive obstacle to synthetic design of receptors for peptides is the target's conformational and structural diversity. In the last section several receptors for aqueous peptide recognition were discussed, but on the whole strong affinities were only realized for host-guest systems employing transition metals. Without a metalloreceptor binding was not greater than 10^4 M^{-1}. In the last decade peptide binding research has turned toward the development of combinatorial libraries of receptors. Using a biomimetic approach, combinatorial libraries of receptors or analytes can be screened with complementary receptors or analytes to find strong binding hits.[116] This host-guest research effort employing combinatorial chemistry is inspired by nature's very own combinatorial approach demonstrated by the immune system in which a foreign antigen is rapidly screened against an organism's antibodies to find the strongest binding system for antigen expulsion.[117]

Combinatorial chemistry uses polymeric resin beads for rapid development of organic and biological compounds (peptides/peptoids). The method most commonly employed for synthesis is the split-and-pool, or one-bead-one-compound, pioneered by Lam.[118] In terms of peptide development, the resin is split into portions, one portion for each amino acid being used, and a single amino acid is coupled to each portion. The resin is then pooled back together, mixed, and then split into portions once again. A second amino acid is coupled to each portion, and again the resin is pooled and mixed. This splitting and pooling is continued until the desired number of amino acids has been coupled to the resin. At this point each bead in the library should have only a single

peptide on it, therefore "one-bead-one-compound" (Scheme 1.5). In terms of oligopeptide binding two approaches exist. In the first approach a combinatorial library of receptors is developed and screened against a particular oligopeptide. Either the receptor library or oligopeptide has a chromophore or fluorophore for detecting selective binding between receptor and analyte. In the second approach a single receptor is developed and screened against a library of oligopeptides that usually represents a certain peptide class. Again a chromophore or fluorophore is generally used for detection of selective binding events. Both of these methods will be elaborated in the following two sections.

Scheme 1.5 "One-Bead-One-Compound" Split-and-Pool Combinatorial Synthesis.

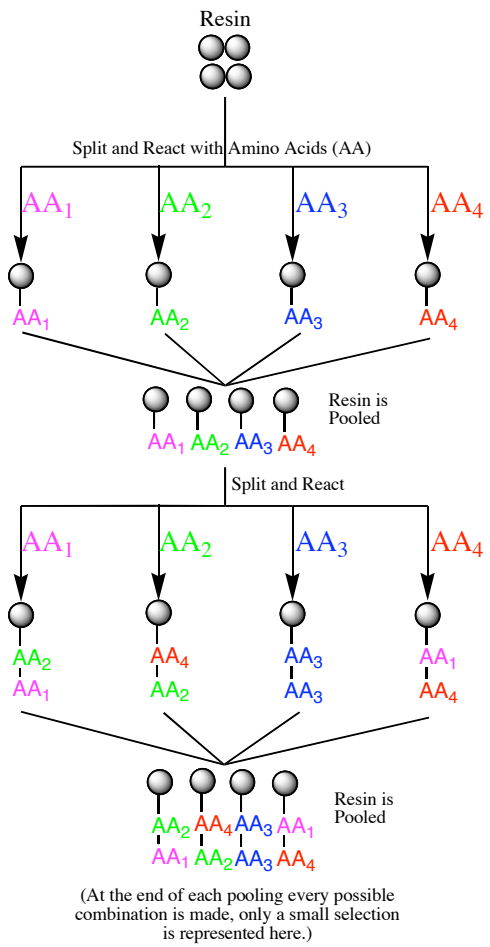

1.9.1 Screening Peptide Libraries

Far fewer studies have dealt with the screening of peptide libraries with a single receptor than the screening of receptor libraries with a single peptide. Still was the groundbreaker in this field and others have followed including Fang's work with Ru

ligands for sequence-selective binding of tripeptides.[119] In a *Science* publication in 1998, Still detailed elegant small organic receptor molecules for the sequence-selective detection of peptides from a peptide library in chloroform.[100d] Receptors **1.33** and **1.34** were synthesized with pendant fluorophores (F) and quenchers (Q) on each receptor. In both receptors F is the dansyl sulfonamide of ethanolamine and Q is a dabcyl N-hydroxysuccinimide ester. The receptors were developed from amide-linked oligomers of isophthalic acid and cyclic *trans*-1,2-diamine derivatives that are known to bind peptides well. These receptors have significant conformational restriction, a concave binding site, and hydrogen bond donors and acceptors. When not selectively bound to a peptide the fluorescence of the receptors is quenched through a fluorescence energy transfer (FET) system. Upon peptide binding the average separation between F and Q is increased resulting in a 300-500% enhancement in the fluorescent emission. With the FET system the chemosensors were sensitive enough to detect unlabeled cognate peptides both in organic solution and in the solid state at low micromolar concentrations.

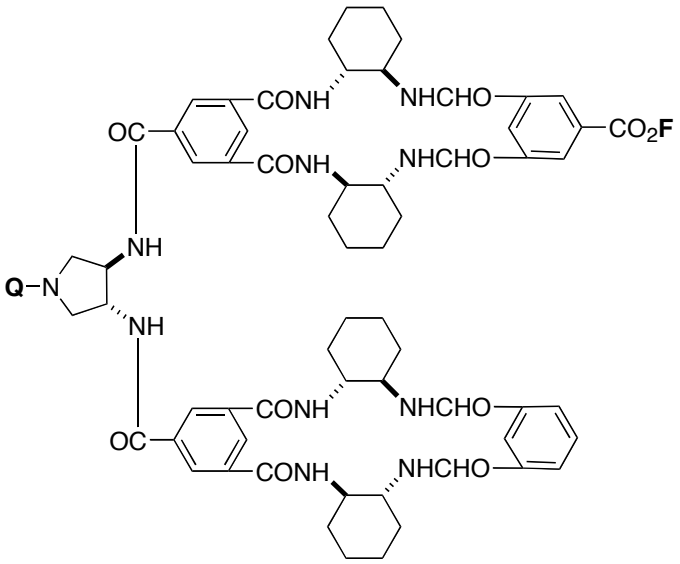

1.33

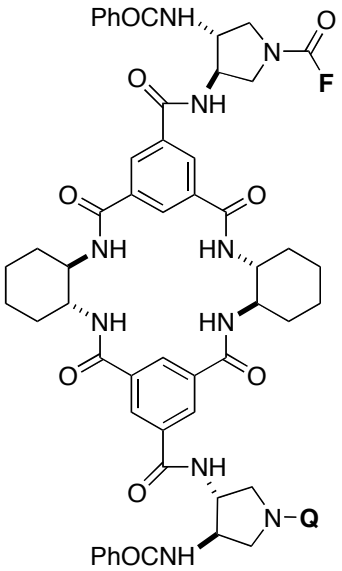

1.34

Screening a N-acetylated side-chain protected tripeptide library with 3375 members in chloroform with receptor **1.33** selectivity was found for two tripeptides: D-Pro-L-Val-L-Gln (P1) and L-Lys-L-Val-D-Pro. Therefore, **1.33** only binds one of every ~1600 sequences in the tripeptide library at a concentration of 10 μM. Receptor **1.34** was less selective binding one of every 400 sequences, but it did not bind the two sequences **1.33** was selective for, with preference for tripeptides with two L-Gln flanking a D-amino acid. Fluorescence monitored titrations of **1.33** with P1 gave an experimental K_a = 260,000 M^{-1}. Subsequent studies in the Still laboratory have expanded this research to aqueous solutions.[120]

1.9.2 Screening Receptor Libraries

Receptor libraries often have a common design that includes a scaffold or head group from which emanates multiple side-arms that are usually peptidic and generated with combinatorial synthesis (Figure 1.4). The scaffold imparts cavity preorganization, and often imparts selectivity for a certain class of peptides such as tachykinins or enkephalins. The peptidic arms are responsible for the diversity in the receptor library and are important to substrate binding. The number of peptide arms has varied from one to three, and they can be synthesized in a fashion so that each of the arms is identical, or in an orthogonal manner to create different peptide arms and greater diversity.

Figure 1.4 Combinatorial Approach to Receptor Libraries – the position of the scaffold relative to the linkage to the resin can be varied, and may be determined by the number of combinatorially synthesized peptide arms.

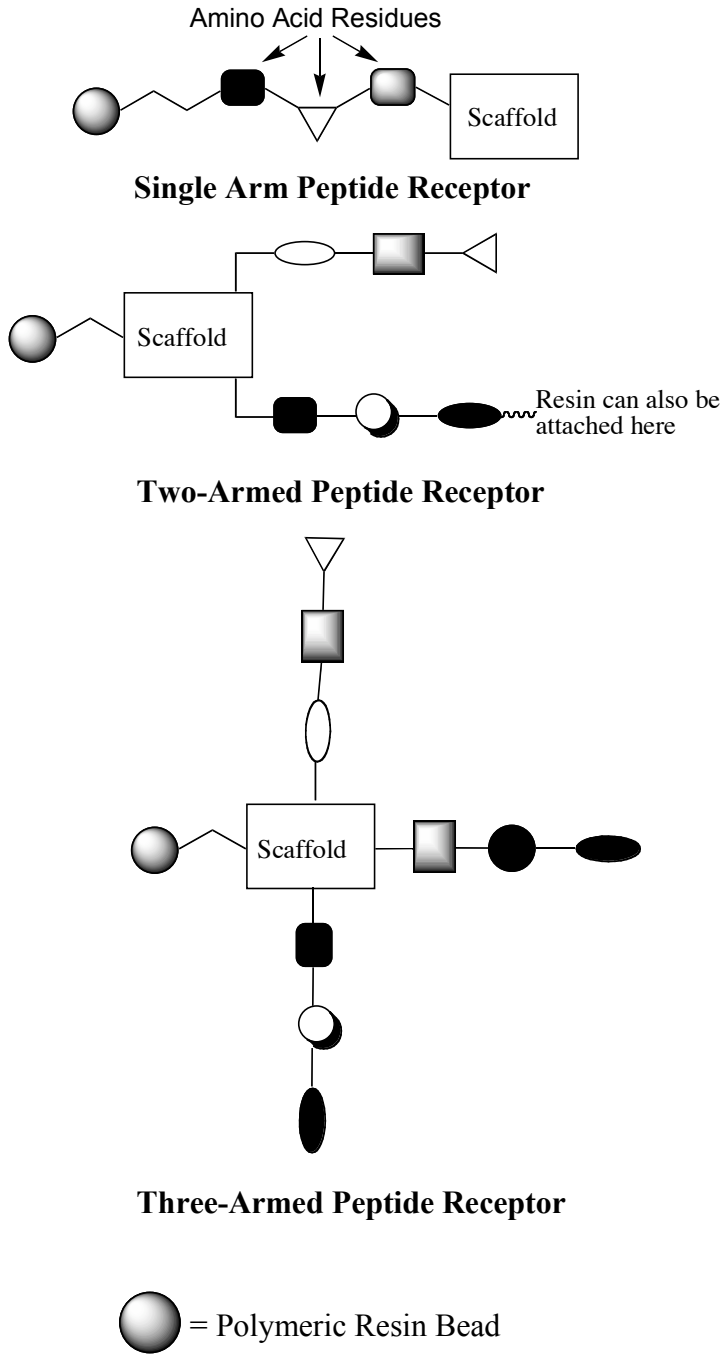

1.9.2.1 **Single-Peptide Arm Receptor Libraries**

Molecular recognition of peptides in water is considerably reduced when receptors rely on hydrogen-bonds. However, the addition of peptides to the receptor offers the advantage that several other noncovalent interactions can be exploited for substrate binding. Schmuck's research group has focused on the design of artificial receptor libraries for the hydrophobic tetrapeptide Ac-Val-Val-Ile-Ala-OH in water.[121] This tetrapeptide represents the C-terminal sequence of the amyloid β-peptide that is responsible for the formation of protein plaques within the brains of patients developing and suffering from Alzheimer's disease. These plaques are formed via self-aggregation of the amyloid β-peptide, therefore artificial receptors that bind to the tetrapeptide should promote knowledge about the molecular basis of the self-aggregation as well as the pathogenesis of Alzheimer's disease.

Employing a N-terminal dansyl derivatized variant of the amyloid β-peptide, receptor library **1.35** (512 members) was screened for a strong binding hit. The receptor has a linear tripeptide attached to a solid support resin through its C-terminus, and the N-terminus is derivatized with a cationic guanidiniocarbonylpyrrole, an excellent functional unit for complexation of carboxylates in water. It was expected that the C-termini of the tetrapeptide would complex the cationic termini of **1.35** forming an antiparallel β-sheet. Receptor library **1.35** was equilibrated with a 2.5 μM solution of the dansylated tetrapeptide and screened under UV light. The receptors selective for the tetrapeptide were clearly evident under the UV light. Association constants were determined for the tetrapeptide on-bead and were as high as 4200 M^{-1} when the residues of **1.35** were Lys(Boc)-Ser(O*t*Bu)-Phe. Several other receptors were tested for binding and solution

studies were carried out, and it was shown that association constants on-bead were similar to those in solution. This is to be expected as the polymeric resin likely has some influence on substrate binding. Furthermore, Schmuck demonstrated that single residue changes in the receptor structure lead to large changes in tetrapeptide affinity. Therefore, receptor libraries span the whole realm of possible receptors and permit the identification of the best binders.

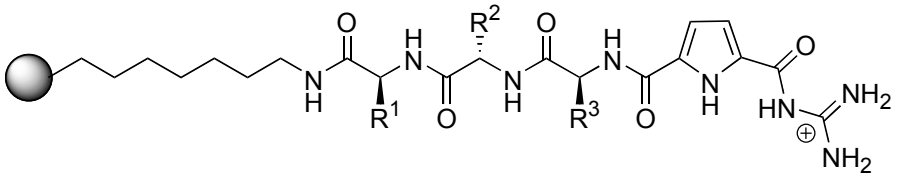

1.35

1.9.2.2 Two-Peptide Arm Receptor Libraries – Molecular Tweezers

Two-armed receptors, or molecular tweezers, are composed of two combinatorially developed peptide arms that emanate outward from a scaffold or head-group. Preorganization or arrangement of the tweezer or horseshoe shape for binding is provided by the scaffold (a.k.a. head group, core, or hinge) and may be assisted by metal complex formation. The peptide arms are generally aligned to optimize β-sheet formation through peptide bond hydrogen-bonding and noncovalent interactions between the amino acid residues. A number of research groups have experimented in this field, and their contributions continue to shape current development of synthetic hosts for bioanalytes.

The Still group has been a pioneering force in the development of two-armed peptide receptors. An early publication in 1994 described the preparation and screening

of an A,B-*cis*-cholic acid core from which two variable (combinatorial) peptide arms extended downward from the concave, α-face of the steroidal core.[122] This library was screened for binding of the N-acylated pentapeptide Leu-enkephalin using a solid-phase color assay in chloroform. It was found that only 1% of the receptor library bound tightly to the peptide substrate. This work was followed by the development of a more conformationally restricted library **1.36** built around an A,B-*trans*-steroidal core that is 3,7-axially substituted with combinatorial peptide arms.[123] Five side-chain protected amino acids of both D- and L-stereochemistry were used to develop library **1.36** with 10,000 variants. An encoding technique was used that incorporated haloaromatic tags into the peptide arms for easy identification of the composition of the peptide arms. This library was screened in chloroform for binding to a red dye labeled methyl ester Leu-enkephalin: dye-CO$(CH_2)_2$CO-(L)Tyr-Gly-Gly-(L)Phe-(L)Leu-OMe. Remarkably, only 0.1% of the library showed high affinity for the enkephalin, and even more interesting all of the binding receptors had the same amino acids in positions AA_1- AA_3: (L)Asn(*N*-trityl), (D)Asn(*N*-trityl), and (D)Phe respectively. One selective library member was selected with AA_4 as (L)Ser(*O*-tBu) and resynthesized on solid phase and used to evaluate binding strength. The absolute binding energy between the resynthesized receptor and the enkephalin was experimentally established with UV/Vis titrations in chloroform as -6.5 ± 0.1 kcal/mol. It was determined that if a single amino acid substitution was made at the N-terminal position of the enkephalin affinity was diminished by 2-3 kcal/mol. Chiral inversion or residue changes at the C-terminal position were better tolerated, but still resulted in diminished affinities of 1 kcal/mol. Molecular modeling of the targeted enkephalin with the resynthesized receptor provided evidence of eight secondary amides on the receptor available for hydrogen-bonding to the substrate. As one of the earliest

examples of molecular tweezers, remarkable peptide-binding selectivity was demonstrated with Still's steroidal host.

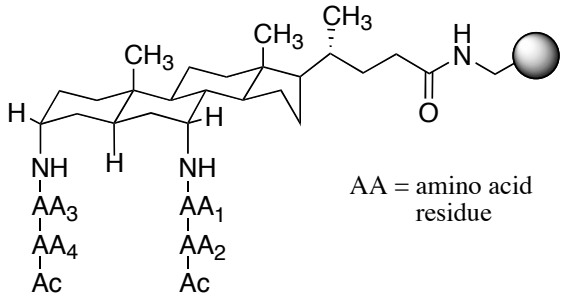

1.36

Kilburn has contributed a plethora of research to the area of molecular tweezers involving two different scaffold types: 2,6-diamidopyridine **1.38** and guanidinium-derivatized **1.39**.[116f,124] Both receptors are built from the general molecular architecture illustrated in **1.37**. A carboxy-binding site (CBS) is integrated into the head group to promote binding to the C-terminus of a peptide substrate, and the variable arms incorporate suitable functionality for binding with the backbone of the substrate. The CBS enhances the affinity above that of a β-sheet and increases the selectivity for the substrate.

Studies with receptor **1.38** involved the creation of a 2,197-member fluorenylmethoxycarbonyl (Fmoc) protected library using 13 L-amino acids as well as a 2,197-member library of receptors with free terminal amino groups.[124b] Five dansylated peptides were screened, two with protected amino acid residues and three without protection. The peptides varied in their polarity, charge, and hydrophobicity. When the protected peptides were screened against the Fmoc-protected library in chloroform, ~1%

of the receptor beads fluoresced, indicating good binding affinity. This result was the same with the free amino receptors and non-protected peptides.

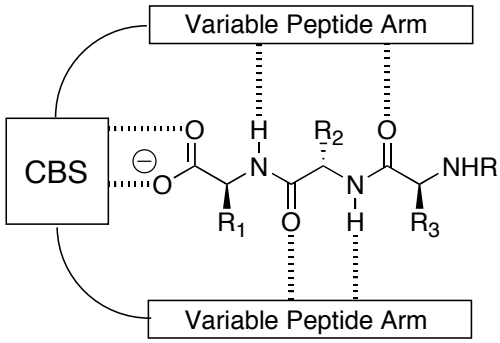

1.37

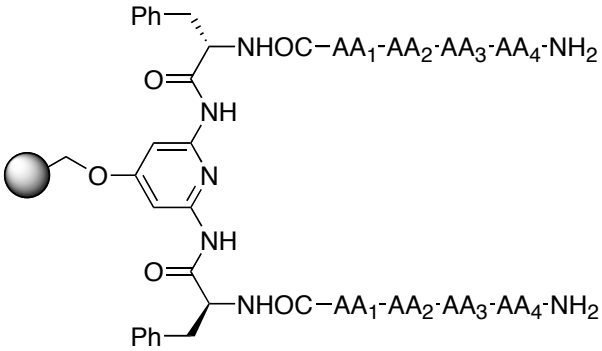

1.38

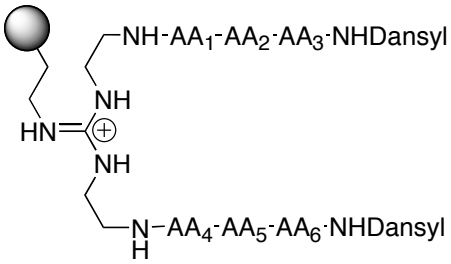

1.39

The effect of the solvent was more interesting to this study. If the solvent was changed to 10% DMSO or 10% methanol the selectivity was nearly abolished. In the case of the Fmoc-protected receptor library, selectivity was not hindered by addition of 50% acetonitrile; however, the deprotected receptor library again showed nearly no selectivity. This is to be expected though when using a library that relies heavily on hydrogen-bonding. The increased polarity of the solvent increases the solvation sphere around the peptide substrates and receptors resulting in significant loss of selectivity. A

second interesting aspect of this research was the effect of the dansyl group on the peptide substrates. Especially in the case of the Fmoc-protected receptors the dansyl group had a significant influence on binding. Therefore, this research illustrates the importance of calculating the relative contribution of all binding forces, and the difficulty in developing receptors suitable for polar or aqueous molecular recognition.

An excellent example of a synthetic chemosensor using combinatorial peptide arms for binding has been presented by the Anslyn group for the detection of adenosine triphosphate (ATP).[125] "Pinwheel" receptor **1.40** was designed to illustrate that the use of a designed core, in addition to peptide libraries and dual fluorophores to signal binding events, can produce resin-bound chemosensors with high sensitivity. The peptide arms were expected to impart selectivity for the adenine group of ATP, and the two guanidinium groups would create electrostatic attraction to the anionic phosphates.

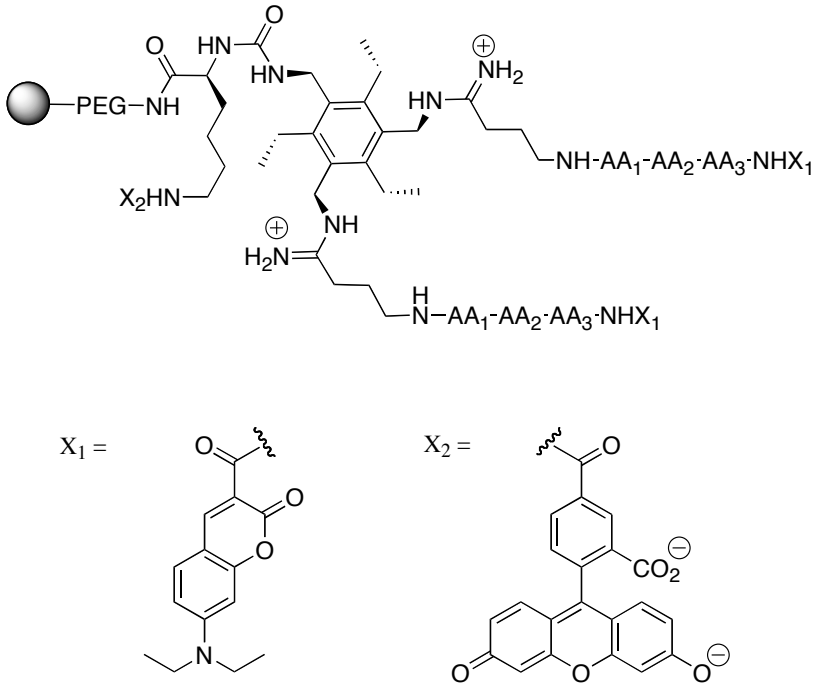

1.40

For the discovery of ATP binding receptors a fluorescently labeled N-methylanthraniloyl-ATP (MANT-ATP) was developed to screen library **1.40**. 5-Carboxyfluorescein was appended to the end of both peptide arms, and 7-diethylaminocoumarin-3-carboxylic acid was covalently fixed to the lysine group of **1.40**. It was expected that the 7-diethylaminocoumarin-3-carboxylic acid would participate in a FRET process, or serve as an internal reference. The library was equilibrated with MANT-ATP (0.25 mM) at pH 7.1 (HEPES, 10 mM) for eight hours. Upon illumination of the library resin with UV light at 366 nm ~15% of the library members were highly fluorescent. A series of the highly fluorescent beads and those that exhibited no fluorescence were characterized with Edman degradation and resynthesized. The binding of the highly fluorescent receptors with ATP was evaluated using UV studies and FRET signal transduction. Interestingly, one receptor did not show any signal modulation with ATP indicating that the MANT group may have been critical to the binding of this receptor. One receptor that had peptide arms of Ser-Tyr-Ser was found to exhibit a binding constant of 3.4×10^3 M^{-1}. This is a 10-fold increase in binding affinity over the receptor structure with guanidiniums only demonstrating a contribution in binding from the variable peptide arms. Furthermore, the Ser-Tyr-Ser receptor was tested for binding to adenosine monophosphate (AMP) and guanosine triphosphate (GTP) and no association was found. The lack of binding to AMP illustrates the necessity of triphosphates for binding to the guanidinium core of **1.40**, and the lack of binding to GTP illustrates the selective interaction of the peptide arms with adenosine.

A final example of a research group making significant contributions to this field of chemistry is Wennemers' group.[126] Diketopiperazine libraries of type **1.41** (the *trans* architecture is shown) have been screened against peptide libraries using chloroform as a

solvent. The *trans*-scaffold directs a rigid horseshoe conformation, and provides ideal separation between the two peptide arms. The *trans*-scaffold was shown to be highly selective. The *cis*-scaffold is more linear and was not as selective. An orthogonal amino-protection scheme was used when synthesizing **1.41** that permitted the development of two different peptide arms. In the studies discussed previously this method had not been employed, but it is powerful because it allows the creation of very large one-bead-one-compound receptor libraries.

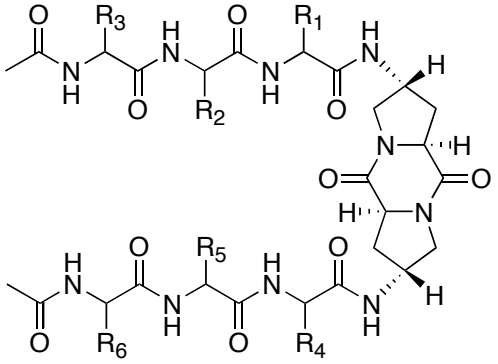

1.41

1.9.2.3 Three-Armed Receptor Libraries – Molecular Bowls

More complex "molecular bowls" developed from tripodal scaffolds increase the possible binding interactions with a given substrate. Liskamp has used triazacyclophane receptors with carboxylic acids for resin attachment to generate three-armed receptors.[127] His group has also implemented orthogonal protection schemes permitting development of receptors with three different variable binding arms (**1.42**) resulting in 46,656 possible library members. These libraries have been successfully screened to identify vancomycin-like receptors for dye-labeled D-Ala-D-Ala and D-Ala-D-Lac dipeptides in

chloroform and aqueous solutions. Other studies with the triazacyclophane receptors have identified selective Fe(III) binders.[127b]

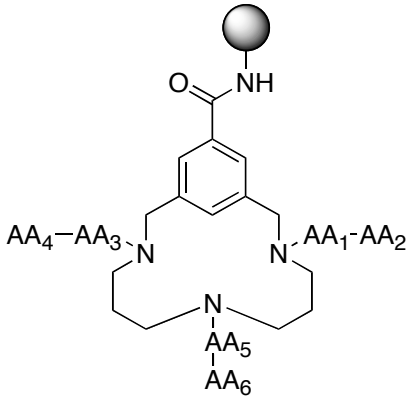

1.42

1.10 Multi-Analyte Sensing

To this point the concepts of "lock-and-key" molecular recognition and combinatorial receptor development have been discussed. In both of these cases selectivity is achieved through synthesis of a receptor, or screening of a combinatorial receptor library for identification of selective receptors. In either case the receptor is chemically complementary to the substrate. However, as the desire to sense larger and more complex analytes increases, a stumbling block is encountered because it becomes synthetically prohibitive to create synthetic receptors complementary to such complex and dynamic substrates. Furthermore, medical diagnostics, environmental monitoring, chemical warfare agent detection, and process quality assurance calls for the recognition of solutions and specific compounds in solutions. In these situations selective chemosensors have their signal transduction mechanisms muddled due to the complexity and competing nature of the solution and various chemical compounds in the solution.

Nature has supplied the field of molecular recognition with a great deal of inspiration. Molecular recognition processes continue endlessly in nature with some of the most recognizable being the extraordinary substrate selectivity of enzymes, and the antibody screening process used to identify selective binders of foreign antigens. Unfortunately, science's attempt to rival the selectivity and affinity of these recognition events has proven difficult. As indicated, large, dynamic, and complex structures such as proteins, complex carbohydrates, and DNA and RNA can not be readily bound by selective synthetic receptors. Therefore, chemists have once again turned to nature for inspiration. This stimulation has been nature's use of "differential" receptors for gustatory and olfactory sensing in which flavors and odors are detected by multiple selective and differential receptors in the nose and mouth.

Recently, arrays of synthetic receptors have been investigated for the detection of small and medium sized compounds, complex bioanalytes, and compounds in solutions as well as solution composites.[116e,128] Rather than utilizing specifically designed binding interactions, each arrayed receptor responds to a differing degree to a target substrate. These arrays do not rely on specific binding events, but multiple interactions may be pertinent as would be expected with large analytes such as proteins where several surface interactions may be relevant. Moreover, each receptor in the array is incrementally different and contributes to an array that contains as much chemical diversity as possible (Figure 1.5). These arrays use synthetic receptors that transcend the relative lack of specificity for particular substrates by organizing multiple binding events into a single substrate-selective pattern. Differentially responsive arrays take advantage of the cross-reactivity of the receptors by deliberately using the nonspecific pattern responses to discriminate analytes.

Figure 1.5 Lock-and-Key vs. Differential Recognition.[116e]

(a) Lock-and-Key – One Receptor for One Analyte

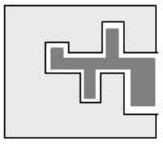

b) Differential Array of Synthetic Receptors Responding to a Single Analyte

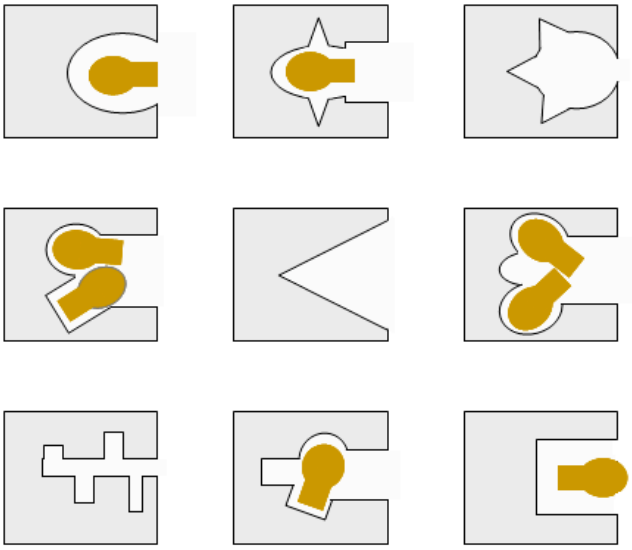

Incorporation of a signal modulating event into the array creates composite signals, or fingerprints, collected from the multiple differential binding interactions to provide a unique diagnostic pattern for a substrate or mixture of substrates. Signal transduction such as a fluorescent or colorimetric response is required as well as a method for data acquisition to obtain diagnostic patterns.[129] The patterns are obtained from equilibrium or kinetic fluorescence or chemometric responses. One difficulty is that

the patterns obtained from signal modulations are often highly convoluted; however, several chemometric tools for pattern recognition have been developed. Much research has been done to mimic the olfactory and gustatory systems; after a brief introduction to mammalian sensing, scientific models will be discussed that replicate these multivariate sensory systems.

1.10.1 Mammalian Sensory Systems - Olfaction

Olfaction and gustation are the primary sources of information collection from the environment and function by a process called chemoreception. These two forms of chemoreception can be distinguished as distant and contact, or smell and taste respectively.[130]

Sensory receptors responsible for olfaction are embedded in the olfactory epithelium at the top of the nasal passage surrounded by supporting cells. The mechanism of olfaction involves transportation of odorants across the mucus lining the surface of the nasal airway, through the mucus-air phase boundary, and to the base of the mucociliary blanket. The process of chemoreception occurs at the membrane of olfactory sensory neurons. This process involves physical interactions of the odorant with potential or actual receptor sites which can either be selective, reacting with one class of odorant, or general, reacting with multiple odorant classes to different degrees.[131] The odor of a compound is defined intrinsically by its chemical architecture, and the signaling process takes into account changes in orientation, conformation, solubility, and diffusion rate producing a diagnostic pattern "expressed as topologically defined structural features of high variability and complexity."[132] The differential response of olfaction is exquisitely sensitive with thresholds of detection in parts per billion from the general

air.[133] The brain recognizes these patterns, or categorizes them as new, and stores them for future comparison. Hence, olfaction is a powerful element of memory.

1.10.2 Mammalian Sensory Systems – Gustation

The major site of taste signaling is the surface of the tongue. The tongue has separate regions of papillae that hold clusters of taste buds. Each region of papillae is selective for a particular taste. The taste buds contain taste cells that are located within depressions in the tongue termed taste pores. The taste pores prevent diffusion of taste stimuli chemicals into the extracellular fluids and restrict recognition to the taste buds.[134]

Figure 1.6 Taste Bud Locations on the Human Tongue.

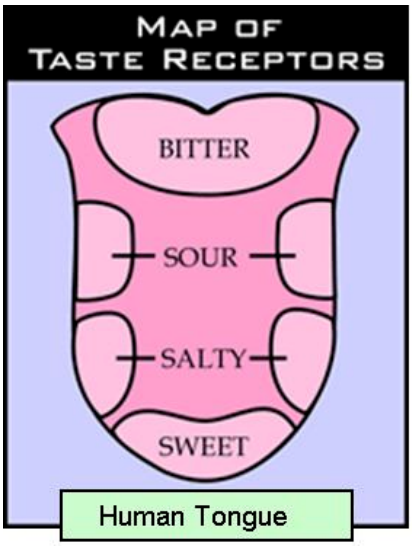

Taste has been separated into four fundamental classes: bitter, sour, salty, and sweet. A fifth taste dubbed umami has also been postulated by Japanese researchers as

relating to savory taste as found in aspartate and monosodium glutamate.[135] The tongue has been divided into regions of taste reception (Figure 1.6) in which bitter is sensed at the back of the tongue, sour on the sides of the tongue towards the back, salty on the sides toward the middle-front, and sweet at the tip of the tongue.[136]

Scientists have been inspired by the sense of taste for synthetic differential recognition because nerve fibers within taste cells in the taste buds are generally non-selective in response to multiple taste stimuli. Biological studies have uncovered multiple sweet and salty receptors, and apparently taste cells use multiple signal transduction mechanisms within a single taste class.[136] So the human brain recognizes single tastes, but the signals for these tastes are often from a cross-reactive taste cell response.

1.10.3 Sensor Array Mimics of Smell and Taste

The creation of a differential receptor system requires an inter-disciplinary approach. Arrays require receptors, a platform for holding the receptors, a signaling device, and a method for collecting and analyzing data. Lewis and Grubbs have detailed six basic criteria for developing an array: (a) using a minimum amount of hardware and energy, the sensor elements should transmit analyte presence with an easily monitored response; (b) they should display a reproducible response to an analyte; (c) the array should respond to a wide range of analytes at various concentrations in a predictable manner; (d) they should be readily fabricated from inexpensive materials that are widely available; (e) arrays should be of minimal size yet still incorporate a large number of sensors; and (f) they should be robust and stable to widely variable conditions.[137] Of course not all receptor arrays developed have followed these criteria, but these guidelines

serve as a nice foundation. Additionally, receptor arrays typically require a tandem approach involving organic, analytical, and biochemists, as well as chemical engineers and statisticians. To date, several arrays have been developed for both vapor phase (olfactory mimics) and solution phase (gustation mimics) analyte detection and recognition.

Using a large variety of "electronic nose" schemes scientists have attempted to artificially mimic the sense of smell through vapor phase analysis.[128a,138] These arrays recognize "odorous" molecules that are generally volatile organics with relative molar masses ranging from 30-300 Da. Sensors within the array are customarily non-specific but responsive to the shape, size and mass of the vapor phase analytes and respond in a relatively short time.[139] Many vapor phase sensors have been developed including those employing conducting polymers, metal oxide semiconductors, metal oxide semiconductor field effect transistors, piezoelectric, optical fluorescence, fiber optic, and amperometric gas sensors. These sensors typically operate by binding molecules to the device surface through one or more mechanisms including adsorption, absorption, chemisorption, and coordination chemistry.[138b] Persaud and Dodd first reported the design of an electronic nose using chemical sensors and pattern recognition in 1982.[140] Since this time more than 650 publications have discussed the creation of electronic noses in some format.

Electronic tongues for solution analysis have developed rapidly over the last decade. Differential sensor arrays have been formed with potentiometry, voltammetry, derivatized resin beads in silicon wafer arrays, light-addressable potentiometric sensors, and shear horizontal acoustic wave devices.[128b,141] The majority of this research has been generated in the laboratories of Toko, Gardner, and Vlasov.

The first multi-sensor system for liquid analysis using a non-specific recognition approach was a potentiometric array developed by Toko.[141b] The potentiometric

electronic tongue consisted of eight sensors with polymeric thin or thick film membranes containing PVC, a plasticizer dioctyl phenylphosphonate, and active sensor substances: lipids such as dioctyl phosphate, oleic acid, and trioctyl methyl ammonium chloride. The potentials of the sensors were measured relative to a conventional Ag/AgCl electrode, and impedance measurements were used to explore its sensitivity of the polymeric lipid membranes to various food substances (Figure 1.7).

Figure 1.7 Potentiometric Lipid Sensor Array Designed by Toko.

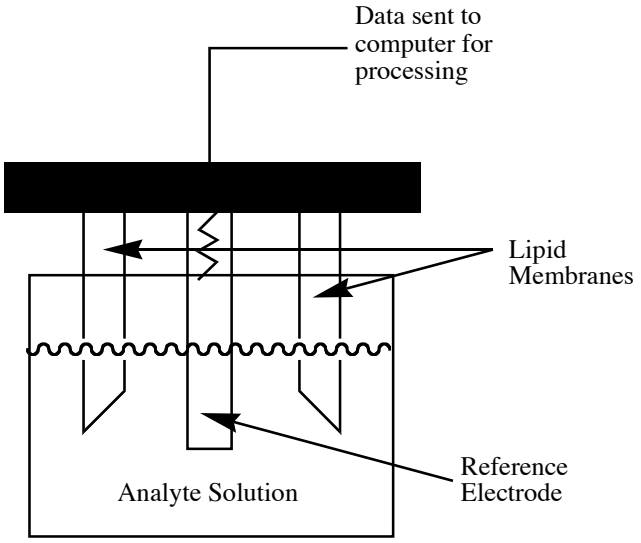

Since Toko's seminal publication in 1990, research with the potentiometric tongue has involved recognition and discrimination of 36 brands of beer, ten coffee brands from around the globe, 41 kinds of mineral water, seven milk brands, four wines, and various other substances including sake and tomato juice. Additionally, compounds known to be sweet, salty, sour, or bitter including various salts and amino acids were evaluated. After data collection and processing, principal component analysis was used

to analyze the potentiometric tongues ability to discriminate the various food substances. Clearly, the electronic tongue system designed by Toko has been absolutely amazing and widely applicable. More recent research has involved the use of synthetic organic receptor arrays. These sensor arrays permit the design of receptor substances geared towards certain classes of compounds based on molecular structure, and are therefore generally more sensitive to subtle differences in analytes such as stereochemistry or the addition of a single carbon.

1.10.3.1 Synthetic Organic Differential Arrays – Electronic Tongues

As has been discussed previously, chemists have attempted to discover the scientific basis of biological interactions by developing synthetic analogues and mimics of those processes and recognition events. Designing artificial receptors and chemosensors for biological substrates such as amino acids and oligopeptides has elucidated structural features of β-sheets and biological recognition events. Precedents have also been set for predicting the energetics and conformations of binding in aqueous systems because critical recognition events are better understood. This understanding has now translated into the development of arrays comprised of cross-reactive synthetic organic receptors created to recognize and discriminate related analytes as prior electronic tongue systems have done. Again, analytes are recognized by the array via the combination of receptor responses into diagnostic substrate-specific patterns often visualized with chemometric data translation.

Differences exist between prior potentiometric and voltammetric electronic differential arrays and synthetic differential arrays. Whereas previous electronic tongues relied on electrical signal transduction, synthetic receptor arrays generally use

colorimetric and fluorescent transduction. Prior systems generally analyzed analytes or solutions from several classes, but synthetic systems are designed to have narrow substrate class selectivity and broad intraclass selectivity. Additionally, synthetic systems are a novel test of the ability of nonspecific, and often weak, interactions between substrates and synthetic receptors to generate specific cross-reactive patterns for substrate recognition. Synthetic receptor arrays rely on all, or a large number, of recognition events common to biological systems to occur reproducibly from trial to trial. Several achievements have been made in this field recently and will be discussed here.

One of the first applications of synthetic differential receptors involved the derivatization of solid-phase resin beads with various receptors, and their incorporation into an array platform by Anslyn, McDevitt, Shear, and Neikirk.[142] The beads were positioned within micromachined pyramidal wells in Si/SiN wafers, one bead per well, to make individually addressable resin "taste buds." The signal from each bead is measured, and the combined response of all receptors provides a diagnostic analyte pattern. In an early proof-of-principle experiment, a 3×3 array of derivatized beads was created to simultaneously identify multiple analytes as a primitive simulation of mammalian tongue gustation. The array was housed within a fluidic flow cell, fixed to a stereoscope stand, and solutions were pumped through the array using a fast protein liquid chromatograph. A charge-coupled device (CCD) was fixed to the stereoscope for image capture (red, green, and blue (RGB) light density) and data acquisition. The CCD is a powerful tool allowing parallel acquisition of spectral data from multiple beads. Absorption properties of the beads are measured with the CCD, and patterns are obtained for various analytes and pH conditions by evaluation of the cumulative array response.

Figure 1.8 Red-Green-Blue Response to Ca^{2+} by Four Resin-Based Sensors.[142]

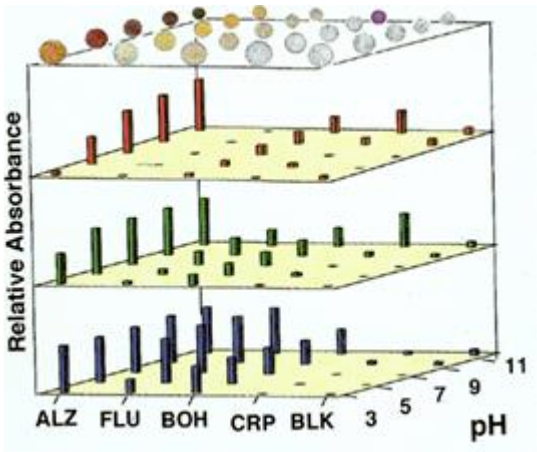

Four sensors were developed by derivatizing polymeric resins with the following: fluorescein (FLU) for pH, *o*-cresolphthalein complexone (CRP) for Ca^{2+} and pH, alizarin complexone (ALZ) for Ce^{3+}, Ca^{2+}, and pH, and a boronic ester (BOH) of resorufin-derivatized galactose for fructose and pH. Evaluation of the RGB relative absorbance values for 0.1 M solutions of the metals, as well as mixtures of the metals, at pH values of 3, 5, 7, 9, and 11, gave colorimetric patterns. This sensor array model provided rapid generation of responses, and clear, quantifiable colorimetric patterns. The responses of the derivatized resins at multiple pHs to Ca^{2+} are illustrated in Figure 1.8. As shown, the patterns are composed of various levels of RGB absorbance.

Further refinement of the array by McDevitt led to an array with enhanced concentration thresholds, reproducibility, and reversibility.[143] A video capture card was added to monitor the kinetics of binding through an indicator-displacement assay or staining (indicator-uptake) assay. The new video capture software also permitted extraction of data from each resin bead in the array. The extracted data was defined as effective absorbance ($A_R = -\log [I_R / I_B]$), in which the absorbance of a certain RGB

channel defined as "R" is obtained by measuring the –log value of the intensity of each receptor bead, divided by the intensity of an acylated blank bead. This refined system has several advantages including optical collection at multiple sites, uniform flow characteristics, real-time data acquisition, and rapid adaptation of the array for detecting different substrate classes. Indeed, the authors cite that their enhanced system can be thought of as a "programmable taste chip."[143] The Anslyn group has subsequently used this enhanced platform for pattern recognition of nucleotide phosphates,[144] proteins and glycoproteins,[145] and tripeptides and tripeptide mixtures.[146]

In the study of nucleotide phosphates: ATP, AMP, and GTP, library **1.43** was created with 4,913 receptors using combinatorial chemistry. This library is a structural variant of library **1.40**. Changes include the addition of two peptide arms that impart differential binding affinity to the receptors, and the deletion of covalently attached fluorophores. From **1.43**, 30 members were randomly selected and placed in a 7 × 5 array with 5 acetylated blanks.

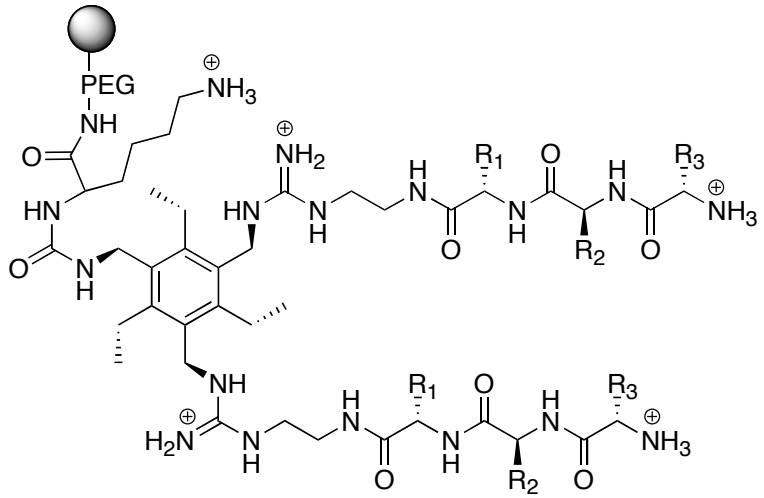

1.43

To observe binding events occurring at each receptor in the array an indicator-displacement assay was employed. Fluorescein, an anionic chromophore, was initially passed through the array resulting in receptor-indicator associations that "color" the beads. The effective absorbance values were calculated from data obtained from multiple CCD images during the displacement assay when a 2 mL injection of a 20 mM nucleotide phosphate solution was added to the array. By combining the effective absorbance values for just a single transmission (i.e. only the red channel) over the entire displacement time period, graphs were made for each receptor in the array corresponding to the rate of indicator-displacement at that site. The unique pattern for each nucleotide phosphate is composed of the cumulative collection of displacement rates from all the receptors in the array. Using principal component analysis (PCA) the three nucleotide phosphates were spatially separated indicating the ability of the array to discriminate the three analytes from one another. Sequencing of the peptide arms with Edman degradation on eight receptors important to the formation of the PCA plot revealed that several of the arms incorporated aromatic residues and serine, or the structurally similar threonine.

Principal component analysis was used to reduce the dimensionality of the data set. In this mathematical model the 30 dimension patterns are reduced to single data points on a new principal component (PC) axis. The first PC axis lies along the line of maximum variance; subsequent PC axes define diminishing levels of variance. Separation between data points on a PC plot describe how unlike they are from one another. Ideally, multiple trials of the same analyte should cluster very closely, and other analytes should be spatially separated from them.

A novel approach to differential array sensing has been the use of molecularly imprinted polymers (MIP) by Mirsky[147] and Shimizu.[148] To test a MIP array with an IDA

assay, Shimizu templated seven aryl amine analytes (**1.44**-**1.50**) and included a blank MIP sensor.[148b] For a colorimetric signal modulation, indicator **1.51** was utilized in an IDA format. Furthermore, the authors showed that a nontemplated, nonaromatic analyte, cyclohexylamine **1.52**, could be identified by the array using a pattern recognition protocol with the chemometric tool of linear discriminant analysis (LDA). Thus, the IDA strategy permitted the detection of analytes not originally used for generating the array.

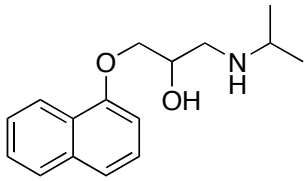

1.44

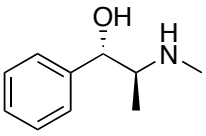

1.45

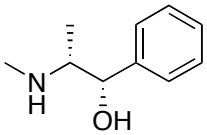

1.46

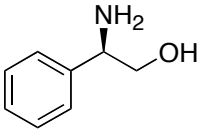

1.47

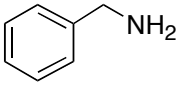

1.48

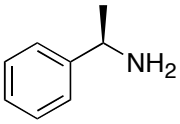

1.49

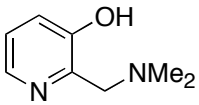

1.50

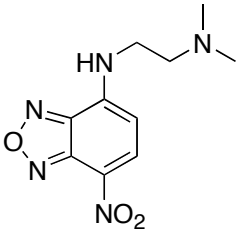

1.51

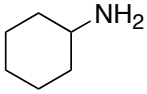

1.52

Shimizu also determined that an individual analyte would have the strongest interaction with the sensor specifically templated for that analyte. Therefore, the selectivity of the array arose from the templating process. Identification of differences in the response patterns was done using LDA where tight clustering of the analytes is indicative of both the recognition capabilities of the array and the reproducibility of the responses. Furthermore, the nontemplated analyte, **1.52**, was clearly spatially separated from the other analytes.

The use of porphyrins in synthetic sensor arrays have been evaluated by Suslick[149] and Hamilton.[150] Suslick created arrays of 36 various receptors to detect organic compounds, solvents, and mixtures such as sodas. Nice colorimetric responses were used in combination to develop diagnostic patterns for the various analytes and mixtures. Hamilton created a sensor array for the detection of multiple proteins using tetraphenylporphyrins (TPP). These porphyrins have large hydrophobic surface areas ideal for protein recognition. Derivatization of the TPP periphery with various amino acids and dipeptides resulted in library **1.53** with receptors encompassing differing charges, size, hydrophobicity, and symmetry well-suited to the recognition of proteins with various surface characteristics. The TPP derivatives also are highly fluorescent making signal detection and pattern development more facile.

Scheme 1.6 Synthesis of Library **1.53** for Detection of Proteins.

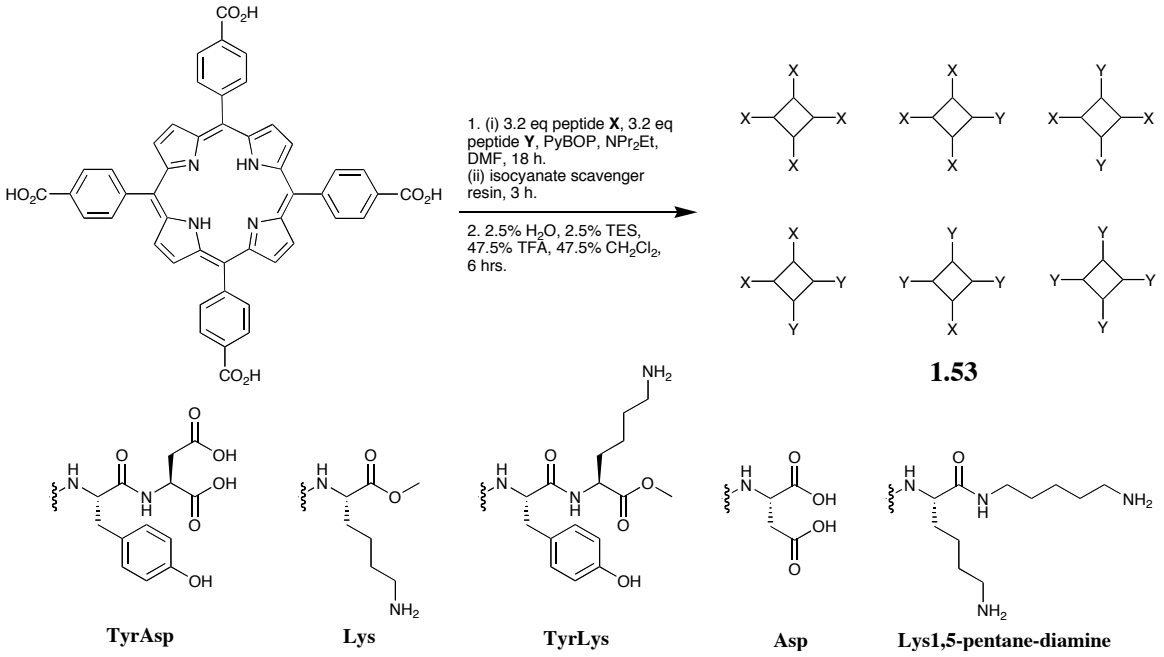

A "one-pot" synthesis (Scheme 1.6) resulted in **1.53** with 35 isolated and purified members. These 35 members were derivatized with four to eight hydrophobic groups comprising all charge combinations from +8 to -8. Eight of the TPP derivatives were arranged in 8 rows of a 96 well quartz plate. Four proteins (15 μM) with varying pIs (ferredoxin (pI 2.75), cytochrome *c*551 (pI 4.7) myoglobin (pI 6.8), and cytochrome *c* (pI 10.6)) were tested against each receptor resulting in various distinguishable quenching patterns (irradiated with UV light at 302 nm). The stronger the interaction between the receptor and protein, the greater the fluorescence quenching. However, this signal modulation could not be related to the relative binding affinities as the mechanism of quenching varied from receptor to receptor based upon the associated protein.

The response of the array was directly correlated to the charge complementarity with the proteins. The more basic receptors showed increased fluorescence quenching with the acidic protein ferredoxin, and the more acidic receptors showed increased quenching with basic cytochrome *c*. The more neutral myoglobin showed interactions with nearly every protein in the array.

Several other studies with synthetic differential receptor arrays have been done using a variety of different platforms. A platform with an ever expanding use is that of a microtiter plate (MTP) assay as demonstrated by Hamilton in the previous discussion. Wolfbeis has used MTP assays for the detection of various metal ions in water using commercially available fluorescent indicators dispersed into polymeric thin films within the wells of the MTP.[151] The Anslyn group is currently pursuing MTP technology for differential arrays as well because it offers a more universally available platform that is easy to use and relatively inexpensive.

Synthetic biomolecules have also been used for arrays. Stojanovic has developed biomolecular receptors from nucleic acid based three-way junctions for detection of

steroids and cocaine.[152] In a separate study, Basu employed colorimetric liposomes for the discrimination of various lipopolysaccharides from Gram negative bacterias.[153] In other work Severin employed a novel indicator-displacement assay with a metalloreceptor for the recognition of all 20 natural amino acids.[154] Finally, "arrays" have been formulated with the use of multiple receptors and indicators in solution. So these experiments do not rely on array platforms, but the homogenous solutions give rise to signals characteristic of particular analytes. Using two hexasubstituted benzene receptors derivatized with boronic acids and guanidiniums in addition to two indicators in solution, tartrate and malate were discriminated by pattern recognition with artificial neural networks by Anslyn.[155] Further work along these lines allowed the quantitative determination of citrate concentrations in various vodkas.[17] Suzuki has also contributed to this type of "array" sensing with his contribution of jewel-pendant ligands for UV/Vis detection of multiple metal cations.[156] Clearly differential molecular recognition with synthetic receptor arrays is gaining ground, and it is likely that sensing devices will employ this technology in the near future.

1.10.3.2 Chemometrics

Much has already been alluded to in previous sections concerning chemometric methods for pattern recognition. Pattern recognition permits the identification of a large number of chemical analytes while only using a small number of fixed receptors, e.g. differential receptor arrays.[157] Several computational techniques exist for pattern recognition including principal component analysis (PCA), linear discriminant analysis, hierarchical cluster analysis, and artificial neural networks. The focus here will be PCA because of its application to the work presented herein.

Principal component analysis is used to reduce the dimensionality of a data set by removing redundancies and providing qualitative insight into the multidimensional response from receptor combinations.[129,130] In this mathematical model the multidimensional response patterns are reduced to single data points (scores) on principal component (PC) axes. Each PC axis provides a direction in the multidimensional response space which is a linear combination of the original receptor responses. Therefore, the first PC axis lies along the line of maximum variance; subsequent PC axes define diminishing levels of variance. Thus, PC axes are weighted as to the variance they describe. Separation between scores on a PC plot describe how unlike they are from one another. Ideally, scores from multiple trials of the same analyte should cluster closely, and scores from other analytes should be spatially separated from any other analyte (Figure 1.9).

Figure 1.9 An Ideal PCA Plot Showing the Clustering of Individual Analyte Score Points and Separation of Different Analytes.

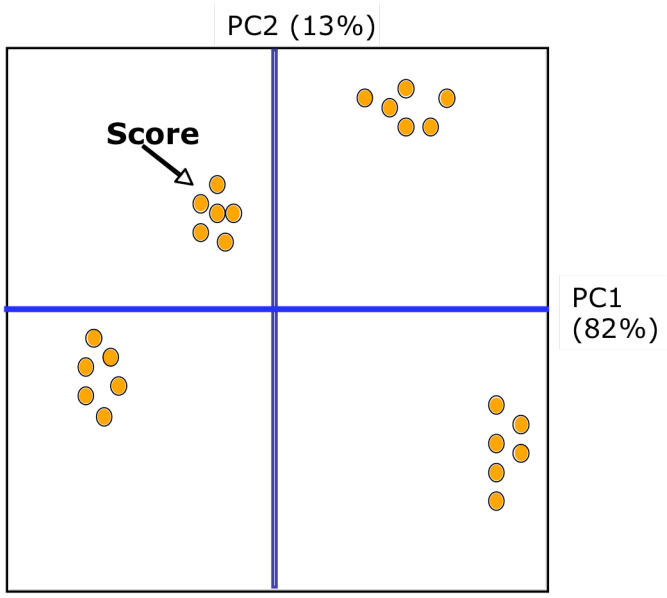

1.11 Summary

Many studies have examined the use of synthetic receptors and chemosensors for the detection of one or several analytes. Much of this work was carried out in aqueous solutions with bioanalytes and has significantly expanded our understanding of biological interactions. The longstanding tradition of biomimicry with synthetic receptors and chemosensors involved the creation of highly selective receptors for single analytes. Now a new frontier is emerging employing a combination of nonspecific receptors for identifying multiple analytes, and even analyte mixtures, with pattern recognition by exploitation of the cross-reactivity of sensor arrays.

The remaining chapters will describe work that we have completed that pertains to both the development of selective chemosensors and synthetic differential receptor arrays. A selective receptor for the tripeptide His-Lys-Lys will be described along with a fluorescent host for both low and high molecular weight heparin in aqueous solutions and human and equine serum. A combinatorial approach will also be described for detecting selective receptors for the tachykinin hormone neurokinin A. Our investigations with differential receptor arrays for the recognition and discrimination of proteins and glycoproteins, tripeptides, and tripeptide mixtures will also be discussed.

1.12 References

1) (a) Fischer, E. *Ber. Deutsch. Chem. Ges.* **1894**, *27*, 2985. (b) Behr, J. –P. *The Lock and Key Principle, The State of the Art – 100 Years On*. New York: John Wiley and Sons, 1994.

2) Desiraju, G. R. Chemistry Beyond the Molecule. *Nature* **2001**, *412*, 397-400.

3) (a) Pedersen, C. J. Cyclic Polyethers and Their Complexes With Metal Salts. *J. Am. Chem. Soc.* **1967**, *89*, 2495-2496. (b) Pedersen, C. J. Cyclic Polyethers and Their Complexes With Metal Salts. *J. Am. Chem. Soc.* **1967**, *89*, 7017-7036.

4) (a) Dietrich, B.; Lehn, J. –M.; Sauvage, J. –P. Diaza-polyoxa-macrocycles and Macrobicycles. *Tetrahedron Lett.* **1969**, *10*, 2885-2888. (b) Lehn, J. –M. Cryptates: The Chemistry of Macropolycyclic Inclusion Complexes. *Acc. Chem. Res.* **1978**, *11*, 49-57.

5) (a) Timko, J. M.; Helgeson, R. C.; Newcomb, M.; Gokel, G. W.; Cram, D. J. Structural Parameters that Control Association Constants Between Polyether Host and Alkylammonium Guest Compounds. *J. Am. Chem. Soc.* **1974**, *96*, 7097-7099. (b) Cram, D. J.; Cram, J. M. Host-Guest Chemistry. *Science* **1974**, *183*, 803-809. (c) Kyba, E. P.; Helgeson, R. C.; Madan, K.; Gokel, G. W.; Tarnowski, T. L.; Moore, S. S.; Cram, D. J. Host-guest Complexation, Concept and Illustration. *J. Am. Chem. Soc.* **1977**, *99*, 2564-2571.

6) Beer, P. D. Transition-Metal Receptor Systems for the Selective Recognition and Sensing of Anionic Guest Species. *Acc. Chem. Res.* **1998**, *31*, 71-80.

7) (a) Czarnik, A. W. Chemical Communications in Water Using Fluorescent Chemosensors. *Acc. Chem. Res.* **1994**, *27*, 302-308. (b) Wang, W.; Gao, X.;

Wang, B. Boronic Acid-Based Sensors. *Curr. Org. Chem.* **2002**, *6*, 1285-1317. (c) Zhu, L.; Zhong, Z.; Anslyn, E. V. Guidelines in Implementing Enantioselective Indicator-Displacement Assays for alpha-Hydroxycarboxylates and Diols. *J. Am. Chem. Soc.* **2005**, *127*, 4260-4269.

8) (a) Schneider, H. J.; Blatter, T.; Eliseev, A.; Ruediger, V.; Raevsky, O. A. Supramolecular Chemistry. 42. Electrostatics in Molecular Recognition. *Pure App. Chem.* **1993**, *65*, 2329-2334. (b) Verboom, W.; Cram, D.J. Spherands, Hemispherands, and Calixspherands. *Comp. Supramol. Chem.* **1996**, *1*, 213-243.

9) Jeffrey, G. A. *An Introduction to Hydrogen Bonding*. Oxford: Oxford University Press, 1997.

10) Beer, P. D.; Gale, P. A.; Smith, D. K. *Supramolecular Chemistry*. Oxford: Oxford University Press, 1999.

11) Kauzmann, W. Some Forces in the Interpretation of Protein Denaturation. *Adv. Prot. Chem.* **1959**, *14*, 1-63.

12) (a) Ben-Naim, A. *Hydrophobic Interactions*. Plenum Press: New York, 1980. (b) Tanford, C. *The Hydrophobic Effect. 2nd Ed.* Wiley: New York, 1980. (c) Lemieux, R. U. How Water Provides the Impetus for Molecular Recognition in Aqueous Solution. *Acc. Chem. Res.* **1996**, *29*, 373-380. (d) Tanford, C. How Protein Chemists Learned About the Hydrophobic Factor. *Protein Sci.* **1997**, *6*, 1358-1366.

13) (a) Ferguson, S. B.; Seward, E. M.; Sanford, E. M.; Hester, M.; Uyeki, M.; Diederich, F. Molecular Recognition by Cyclophane Hosts. *Pure & Appl. Chem.* **1989**, *61*, 1523-1528. (b) Smithrud, D. B.; Sanford, E. M.; Chao, I.; Ferguson, S. B.; Carcanague, D. R.; Evanseck, J. D.; Houk, K. N.; Diederich, F. Solvent Effects in Molecular Recognition. *Pure & Appl. Chem.* **1990**, *62*, 2227-2236. (c) Breslow, R.; Groves, K.; Mayer, M. U. The Hydrophobic Effect as a Mechanistic Tool. *Pure & Appl. Chem.* **1998**, *70*, 1933-1938. (d) Breslow, R. Hydrophobic

Effects on Simple Organic Reactions in Water. *Acc. Chem. Res.* **1991**, *24*, 159-164. (e) Easton, C. J.; Lincoln, S. F. *Modified Cyclodextrins: Scaffolds and Templates for Supramolecular Chemistry*. Imperial College Press: London, 1999.

14) Diederich, F.; Dick, K. A New Water-Soluble Macrocyclic Host of the Cyclophane Type: Host-Guest Complexation with Aromatic Guests in Aqueous Solution and Acceleration of the Transport of Arenes Through an Aqueous Phase. *J. Am. Chem. Soc.* **1984**, *106*, 8024-8036.

15) Gutmann, V. *The Donor-Acceptor Approach to Molecular Interactions*. Springer: New York, 1978.

16) Linton, B. R.; Goodman, M. S.; Fan, E.; Van Arman, S. A.; Hamilton, A. D. Thermodynamic Aspects of Dicarboxylate Recognition by Simple Artificial Receptors. *J. Org. Chem.* **2001**, *66*, 7313-7319.

17) McCleskey, S. C.; Floriano, P. N.; Wiskur, S. L.; Anslyn, E. V.; McDevitt, J. T. Citrate and Calcium Determination in Flavored Vodkas Using Artificial Neural Networks. *Tetrahedron* **2003**, *59*, 10089-10092.

18) Tobey, S. L.; Anslyn, E. V. Determination of Inorganic Phosphate in Serum and Saliva Using a Synthetic Receptor. *Org. Lett.* **2003**, *5*, 2029-2031.

19) Zhong, Z.; Anslyn, E. V. Controlling the Oxygenation Level of Hemoglobin by Using a Synthetic Receptor for 2,3-Bisphosphoglycerate. *Angew. Chem. Int. Ed.* **2003**, *42*, 3005-3008.

20) Piatek, A. M.; Bomble, Y. J.; Wiskur, S. L.; Anslyn, E. V. Threshold Detection Using Indicator-Displacement Assays: An Application in the Analysis of Malate in Pinot Noir Grapes. *J. Am. Chem. Soc.* **2004**, *126*, 6072-6077.

21) Wiskur, S. L.; Anslyn, E. V. Using a Synthetic Receptor to Create an Optical-Sensing Ensemble for a Class of Analytes: A Colorimetric Assay for the Aging of Scotch. *J. Am. Chem. Soc.* **2001**, *123*, 10109-10110.

22) Wright, A. T.; Zhong, Z.; Anslyn, E. V. A Functional Assay for Heparin in Serum Using a Designed Synthetic Receptor. *Angew. Chem. Int. Ed.* **2005**, *44*, 5679-5682.

23) Cram, D. J.; Lein, G. M. Host-Guest Complexation. 36. Spherand and Lithium and Sodium Ion Complexation Rates and Equilibria. *J. Am. Chem. Soc.* **1985**, *107*, 3657-3668.

24) (a) Cram, D. J. Preorganization – From Solvents to Spherands. *Angew. Chem. Int. Ed.* **1986**, *25*, 1039-1057. (b) Schneider, H. –J. Mechanisms of Molecular Recognition: Investigations of Organic Host-Guest Complexes. *Angew. Chem. Int. Ed.* **1991**, *30*, 1417-1436.

25) Steed, J. W.; Atwood, J. L. *Supramolecular Chemistry*. John Wiley & Sons: Chichester, 2000.

26) Cram, D. J.; Kaneda, T.; Helgeson, R. C.; Brown, S. B.; Knobler, C. B.; Maverick, E.; Trueblood, K. N. Host-Guest Complexation. 35. Spherands, the First Completely Preorganized Ligand Systems. *J. Am. Chem. Soc.* **1985**, *107*, 3645-3657.

27) Cram, D. J.; deGrandpre, M.; Knobler, C. B.; Trueblood, K. N. Host-Guest Complexation. 29. Expanded Hemispherands. *J. Am. Chem. Soc.* **1984**, *106*, 3286-3292.

28) Chang, S. –K.; Van Engen, D.; Fan, E.; Hamilton, A. D. Hydrogen Bonding and Molecular Recognition: Synthetic, Complexation, and Structural Studies on

Barbiturate Binding to an Artificial Receptor. *J. Am. Chem. Soc.* **1991**, *113*, 7640-7645.

29) Czarnik, A. W. Supramolecular Chemistry, Fluorescence, and Sensing. *Fluorescent Chemosensors for Ion and Molecule Recognition.* American Chemical Society: Washington D.C., 1993.

30) Excellent Texts Include: (a) Cattrall, R. W. *Chemical Sensors.* Oxford Science: Oxford, 1997. (b) Albery, W. J. Molecular Recognition and Molecular Sensors. *Host-Guest Interactions: From Chemistry to Biology.* John Wiley & Sons: Chichester, 1991. (c) Eggins, B. R. *Chemical Sensors and Biosensors.* John Wiley & Sons: Chichester, 2002.

31) (a) Monk, D. J.; Walt, D. R. Optical Fiber-Based Biosensors. *Anal. Bioanal. Chem.* **2004**, *379*, 931-945. (b) Brogan, K. L.; Walt, D. R. Optical Fiber-Based Sensors: Application to Chemical Biology. *Cur. Opin. Chem. Biol.* **2005**, *9*, 494-500.

32) (a) Fabbrizzi, L.; Licchelli, M.; Pallavicini, P.; Parodi, L.; Taglietti, A. Fluorescent Sensors for and With Transition Metals. *Transition Metals in Supramolecular Chemistry*; Sauvage, J. P., Ed.; John Wiley & Sons: New York, 1999. (b) Bell, T. W.; Hext, N. M. Supramolecular Optical Chemosensors for Organic Analytes. *Chem. Soc. Rev.* **2004**, *33*, 589-598.

33) Fabbrizzi, L.; Poggi, A. Sensors and Switches from Supramolecular Chemistry. *Chem. Soc. Rev.* **1995**, *24*, 197-202.

34) Wiskur, S. L.; Ait-Haddou, H.; Anslyn, E. V.; Lavigne, J. J. Teaching Old Indicators New Tricks. *Acc. Chem. Res.* **2001**, *34*, 963-972.

35) Connors, K. A. *Binding Constants, The Measurement of Molecular Stability.* John Wiley & Sons: New York, 1987.

36) Kavarnos, G. J. *Fundamentals of Photoinduced Electron Transfer*. Wiley: New York, 1993.

37) Andrews, D. L.; Demidov, A. A. *Resonance Energy Transfer*. Wiley: New York, 1999.

38) (a) Inouye, M.; Hashimoto, K.; Isagawa, K.; Nondestructive Detection of Acetylcholine in Protic Media: Artificial-Signaling Acetylcholine Receptors. *J. Am. Chem. Soc.* **1994**, *116*, 5517-5518. (b) Martinez-Manez, R.; Sancenon, F. Fluorogenic and Chromogenic Chemosensors and Reagents for Anions. *Chem. Rev.* **2003**, *103*, 4419-4476. (c) Hanshaw, R. G.; Hilkert, S. M.; Jiang, H.; Smith, B. D. An Indicator Displacement System for Fluorescent Detection of Phosphate Oxyanions Under Physiological Conditions. *Tetrahedron Lett.* **2004**, *45*, 8721-8724. (d) Jelinek, R.; Kolusheva, S. Carbohydrate Biosensors. *Chem. Rev.* **2004**, *104*, 5987-6016. (e) Schmuck, C.; Geiger, L. Efficient Complexation of N-Acetyl Amino Acid Carboxylates in Water by an Artificial Receptor: Unexpected Cooperativity in the Binding of Glutamate but not Aspartate. *J. Am. Chem. Soc.* **2005**, *127*, 10486-10487. (f) Leontiev, A. V.; Rudkevich, D. M. Revisiting Noncovalent SO_2-Amine Chemistry: An Indicator-Displacement Assay for Colorimetric Detection of SO_2. *J. Am. Chem. Soc.* **2005**, *127*, 14126-14127.

39) Folmer-Andersen, J. F.; Lynch, V. M.; Anslyn, E. V. Colorimetric Enantiodiscrimination of α-Amino Acids in Protic Media. *J. Am. Chem. Soc.* **2005**, *127*, 7986-7987.

40) Zhu, L.; Zhong, Z.; Anslyn, E. V. Guidelines in Implementing Enantioselective Indicator-Displacement Assays for α-Hydroxycarboxylates and Diols. *J. Am. Chem. Soc.* **2005**, *127*, 4260-4269.

41) Zhu, L.; Anslyn, E. V. Facile Quantification of Enantiomeric Excess and Concentration with Indicator-Displacement Assays: An Example in the Analyses of α-Hydroxyacids. *J. Am. Chem. Soc.* **2004**, *126*, 3676-3677.

42) Metzger, A.; Lynch, V. M.; Anslyn, E. V. A Synthetic Receptor Selective for Citrate. *Angew. Chem. Int. Ed.* **1997**, *36*, 862-865.

43) Metzger, A.; Anslyn, E. V. A Chemosensor for Citrate in Beverages. *Angew. Chem. Int. Ed.* **1998**, *37*, 649-652.

44) Cabell, L. A.; Anslyn, E. V. Metal Triggered Fluorescence Sensing of Citrate Using a Synthetic Receptor. *J. Chem. Soc. Perk. Trans. 2.* **2001**, 315-323.

45) Lavigne, J. J.; Anslyn, E. V. Teaching Old Indicators New Tricks: A Colorimetric Sensing Ensemble for Tartrate/Malate in Beverages. *Angew. Chem. Int. Ed.* **1999**, *38*, 3666-3669.

46) Nguyen, B. T.; Wiskur, S. L.; Anslyn, E. V. Using Indicator-Displacement Assays in Test Strips and to Follow Reaction Kinetics. *Org. Lett.* **2004**, *6*, 2499-2501.

47) Niikura, K.; Metzger, A.; Anslyn, E. V. Chemosensor Ensemble with Selectivity for Inositol-Trisphosphate. *J. Am. Chem. Soc.* **1998**, *120*, 8533-8534.

48) Ait-Haddou, H.; Wiskur, S. L.; Lynch, V. M.; Anslyn, E. V. Achieving Large Color Changes in Response to the Presence of Amino Acids: A Molecular Sensing Ensemble with Selectivity for Aspartate. *J. Am. Chem. Soc.* **2001**, *123*, 11296-11297.

49) Zhong, Z.; Anslyn, E. V. A Colorimetric Sensing Ensemble for Heparin. *J. Am. Chem. Soc.* **2002**, *124*, 9014-9015.

50) Albert, J. S.; Goodman, M.; Hamilton, A. D. Molecular Recognition of Proteins: Sequence-Selective Binding of Aspartate Pairs in Helical Peptides. *J. Am. Chem. Soc.* **1995**, *117*, 1143-1144.

51) (a) Despotis, G. J.; Gravlee, G.; Filos, K.; Levy, J. Anticoagulation Monitoring During Cardiac Surgery. *Anesthesiology* **1999**, *91*, 1122-1151. (b) Hirsh, J.; Dalen, J.; Deykin, D.; Poller, L. Heparin: Mechanism of Action, Pharmacokinetics, Dosing Considerations, Monitoring, Efficacy, and Safety. *Chest* **1992**, *102*, 337S-351S.

52) (a) Iverson, D. J.; Hunter, G.; Blount, J. F.; Damewood, J. R.; Mislow, K. Static and Dynamic Stereochemistry of Hexaethylbenzene and of its Tricarbonylchromium, Tricarbonylmolybdenum, and Dicarbonyl(triphenylphosphine)chromium Complexes. *J. Am. Chem. Soc.* **1981**, *103*, 6073-6083. (b) Kilway, K. V.; Siegel, J. S. Effect of Transition-Metal Complexation on the Stereodynamics of Persubstituted Arenes. Evidence for Steric Complementarity Between Arene and Metal Tripod. *J. Am. Chem. Soc.* **1992**, *114*, 255-261. (c) Gottlieb, H. E.; Ben-Ari, C.; Hassner, A.; Marks, V. *Tetrahedron* **1999**, *55*, 4003-4014.

53) (a) Stack, T. D. P.; Hou, Z.; Raymond, K. N. Rational Reduction of the Conformational Space of a Siderophore Analog Through Nonbonded Interactions: the Role of Entropy in Enterobactin. *J. Am. Chem. Soc.* **1993**, *115*, 6466-6467. (b) Szabo, T.; O'Leary, B. M.; Rebek, J. Self-Assembling Sieves *Angew. Chem. Int. Ed.* **1998**, *37*, 3410-3413. (c) Jon, S. Y.; Kim, J.; Kim, M.; Park, S. –H.; Jeon, W. S.; Heo, J.; Kim, K. A Rationally Designed NH4+ Receptor Based on Cation-π Interaction and Hydrogen Bonding. *Angew. Chem. Int. Ed.* **2001**, *40*, 2116-2119.

54) Stokes, G. G. On the Change of Refrangibility of Light. *Philos. Trans. R. Soc. London, A.* **1852**, *142*, 463-562.

55) McFarland, S. A.; Finney, N. S. Fluorescent Chemosensors Based on Conformational Restriction of a Biaryl Fluorophore. *J. Am. Chem. Soc.* **2001**, *123*, 1260-1261.

56) Sousa, L. R.; Larson, J. M. Crown Ether Model Systems for the Study of Photoexcited State Response to Geometrically Oriented Perturbers. The Effect of Alkali Metal Ions on Emission from Naphthalene Derivatives. *J. Am. Chem. Soc.* **1977**, *99*, 307-310.

57) (a) Bissell, R. A.; de Silva, A. P.; Guanaratne, H. Q. N.; Lynch, P. L. M.; Maguire, G. E. M.; Sandanayake, K. R. A. S. Molecular Fluorescent Signaling with 'Fluor-Spacer-Receptor' Systems: Approaches to Sensing and Switching Devices via Supramolecular Photophysics. *Chem. Soc. Rev.* **1992**, *21*, 187-195. (b) Bissell, R. A.; de Silva, A. P.; Gunaratne, H. Q. N.; Lynch, P. L. M.; Maguire, G. E. M.; McCoy, C. P.; Sandanayake, K. R. A. S. Fluorescent PET Sensors. *Top. Curr. Chem.* **1993**, *168*, 223-264. (c) de Silva, A. P.; Gunaratne, H. Q. N.; Gunnlaugsson, T.; Huxley, A. J. M.; McCoy, C. P.; Rademacher, J. T.; Rice, T. E. Supramolecular Photoionic Devices: Photoinduced Electron Transfer (PET) Systems with Switchable Luminescence Output. *Adv. Supramol. Chem.* **1997**, *4*, 1-53. (d) de Silva, A. P.; Gunaratne, H. Q. N.; Gunnlaugsson, T.; Huxley, A. J. M.; Rademacher, J. T.; Rice, T. E. Signaling Recognition Events with Fluorescent Sensors and Switches. *Chem. Rev.* **1997**, *97*, 1515-1566. (e) Amendola, V.; Fabbrizzi, L.; Licchelli, M.; Mangano, C.; Pallavicini, P.; Parodi, L.; Poggi, A. Molecular Events Switched by Transition Metals. *Coord. Chem. Rev.* **1999**, *190-192*, 649-669. (f) de Silva, A. P.; Fox, D. B.; Huxley, A. J. M.; Moody, T. M. Combining Luminescence, Coordination, and Electron Transfer for Signaling Purposes. *Coord. Chem. Rev.* **2000**, *205*, 41-57. (g) Prodi, L.; Bolletta, F.; Montalti, M.; Zaccheroni, N. *Coord. Chem. Rev.* **2000**, *205*, 59-83.

58) Czarnik, A. W. Fluorescent Chemosensors for Metal and Non-metal Ions in Aqueous Solution Based on the CHEF Paradigm. *Adv. Supramol. Chem.* **1993**, *3*, 131-157.

59) Fabbrizzi, L.; Licchelli, M.; Pallavicini, P.; Sacchi, D.; Taglietti, A. Sensing of Transition Metals Through Fluorescence Quenching or Enhancement. *Analyst* **1996**, *121*, 1763-1768.

60) Tsien, R. Y. Intracellular Signal Transduction in Four Dimensions: From Molecular Design to Physiology. *Am. J. Physiol. Cell Physiol.* **1992**, *263*, C723-C728.

61) (a) Sandanayake, K. R. A. S.; James, T. D.; Shinkai, S. Molecular Design of Sugar Recognition Systems by Sugar Diboronic Acid Macro Cyclization. *Pure & Appl. Chem.* **1996**, *68*, 1207-1213. (b) James, T. D.; Sandanayake, K. R. A. S.; Shinkai, S. Novel Photoinduced Electron Transfer Sensor for Saccharides Based on the Interaction of Boronic Acid and Amine. *Chem. Commun.* **1994**, 477-478. (c) James, T. D.; Sandanayake, K. R. A. S.; Iguchi, R.; Shinkai, S. Novel Saccharide-Induced Photoinduced Electron Transfer Sensors Based on the Interaction of Boronic Acid and Amine. *J. Am. Chem. Soc.* **1995**, *117*, 8982-8987. (d) James, T. D.; Sandanayake, K. R. A. S.; Shinkai, S. Saccharide Sensing with Molecular Receptors Based on Boronic Acid. *Angew. Chem. Int. Ed.* **1996**, *35*, 1910-1922.

62) (a) Van der meer, B. W.; Cocker, G.; Chen, S. –Y. S. *Resonance Energy Transfer: Theory and Data*. Wiley-VCH: New York, 1997. (b) Lakowicz, J. R. *Principles of Fluroescence Spectroscopy*. 2nd ed. Plenum Publishing Corporation: New York, 1998.

63) (a) Schneider, S. E.; O'Neil, S. N.; Anslyn, E. V. Coupling Rational Design with Libraries Leads to the Production of an ATP Selective Chemosensor. *J. Am. Chem. Soc.* **2000**, *122*, 542-543. (b) Takakusa, H.; Kikuchi, K.; Urano, Y.; Higuchi, T.; Nagano, T. Intramolecular Fluorescence Resonance Energy Transfer System with Coumarin Donor Included in β-Cyclodextrin. *Anal. Chem.* **2001**, *73*, 939-942. (c) Lewis, F. D.; Zhang, L.; Zuo, X. Orientation Control of Fluorescence Resonance Energy Transfer Using DNA as a Helical Scaffold. *J. Am. Chem. Soc.* **2005**, *127*, 10002-10003. (d) Sharma, B.; Deo, S. K.; Bachas, L. G.; Daunert, S. Competitive Binding Assay Using Fluorescence Resonance Energy Transfer for the Identification of Calmodulin Antagonists. *Bioconjugate Chem.* **2005**, *16*, 1257-1263.

64) (a) Zlokarnik, G.; Negulescu, P. A.; Knapp, T. E.; Mere, L.; Burres, N.; Feng, L. X.; Whitney, M.; Roemer, K.; Tsien, R. Y. Quantitation of Transcription and Clonal Selection of Single Living Cells with -Lactamase as Reporter. *Science* **1998**, *279*, 84-88. (b) for biological activity see also: de Silva, A. P.; Eilers, J.; Zlokarnik, G. Emerging Fluorescence Sensing Technologies: From Photophysical Principles to Cellular Applications. *Proc. Natl. Acad. Sci. USA* **1999**, *96*, 8336-8337.

65) Berlmann, I. *Handbook of Fluorescence Spectra of Aromatic Molecules*. Academic Press: New York, 1971.

66) (a) Fabbrizzi, L.; Francese, G.; Licchelli, M.; Pallavicini, P.; Perotti, A.; Poggi, A.; Sacchi, D.; Taglietti, A. Fluorescent Chemosensors Which Take Profit From the Metal-Ligand Interaction. *Chemosensors of Ion and Molecule Recognition*. Desvergne, J.P.; Czarnik, A. W., Eds.; Kluwer: Boston, 1997. (b) Mello, J. V.; Finney, N. S. Dual-Signaling Fluorescent Chemosensors Based on Conformational Restriction and Induced Charge Transfer. *Angew. Chem. Int. Ed.* **2001**, *40*, 1536-1538. (c) Zheng, Y.; Huo, Q.; Kele, P.; Andreopoulos, F. M.; Pham, S. M.; LeBlanc, R. M. A New Fluorescent Chemosensor for Copper Ions Based on Tripeptide Glycyl-Histidyl-Lysine (GHK). *Org. Lett.* **2001**, *3*, 3277-3280. (d) McFarland, S. A.; Finney, S. A. Fluorescent Signaling Based on Control of Excited State Dynamics. Biarylacetylene Fluorescent Chemosensors. *J. Am. Chem. Soc.* **2002**, *124*, 1178-1179.

67) (a) Webb, T. H.; Wilcox, C. S. Enantioselective and Diastereoselective Molecular Recognition of Neutral Molecules. *Chem. Soc. Rev.* **1993**, *22*, 383-395. (b) Bell, T. W.; Hou, Z.; Luo, Y.; Drew, M. G. B.; Chapoteau, E.; Czech, B. P.; Kumar, A. Detection of Creatine by a Designed Receptor. *Science* **1995**, *269*, 271-274. (c) Coskun, A.; Akkaya, E. U. Three-Point Recognition and Selective Fluorescence Sensing of L-DOPA. *Org. Lett.* **2004**, *6*, 3107-3109. (d) Secor, K. E.; Glass, T. E. Selective Amine Recognition: Development of a Chemosensor for Dopamine and Norepinephrine. *Org. Lett.* **2004**, *6*, 3727-3730.

68) (a) Zimmerman, S. C.; Zeng, Z. Improved Binding of Adenine by a Synthetic Receptor. *J. Org. Chem.* **1990**, *55*, 4789-4791. (b) Kool, E. T. Recognition of DNA, RNA, and Proteins by Circular Oligonucleotides. *Acc. Chem. Res.* **1998**, *31*, 502-510. (c) Pina, F.; Bernardo, M. A.; Garcia-Espana, E. Fluorescent Chemosensors Containing Polyamine Receptors. *Eur. J. Inorg. Chem.* **2000**, 2143-2157.

69) (a) Schmidtchen, F. P.; Berger, M. Artificial Organic Host Molecules for Anions. *Chem. Rev.* **1997**, *97*, 1669-1680. (b) Beer, P. D.; Gale, P. A. Anion Recognition and Sensing: The State of the Art and Future Perspectives. *Angew. Chem. Int. Ed.* **2001**, *40*, 486-516. (c) Descalzo, A. B.; Rurack, K.; Weisshoff, H.; Martinez-

Manez, R.; Marcos, M. D.; Amoros, P.; Hoffmann, K.; Soto, J. Rational Design of a Chromo- and Fluorogenic Hybrid Chemosensor Material for the Detection of Long-Chain Carboxylates. *J. Am. Chem. Soc.* **2005**, *127*, 184-200.

70) (a) Peczuh, M. W.; Hamilton, A. D. Peptide and Protein Recognition by Designed Molecules. *Chem. Rev.* **2000**, 2479-2494. (b) Ojida, A.; Mito-oka, Y.; Sada, K.; Hamachi, I. Molecular Recognition and Fluorescence Sensing of Monophosphorylated Peptides in Aqueous Solution by Bis(zinc(II)-dipicolylamine)-Based Artificial Receptors. *J. Am. Chem. Soc.* **2004**, *126*, 2454-2463.

71) Hamachi, I.; Nagase, T.; Shinkai, S. A General Semisynthetic Method for Fluorescent Saccharide-Biosensors Based on a Lectin. *J. Am. Chem. Soc.* **2000**, *122*, 12065-12066.

72) Kwon, J. Y.; Singh, N. J.; Kim, H. N.; Kim, S. K.; Kim, K. S.; Yoon, J. Fluorescent GTP-Sensing in Aqueous Solution of Physiological pH. *J. Am. Chem. Soc.* **2004**, *126*, 8892-8893.

73) Zeng, L.; Miller, E. W.; Pralle, A.; Isacoff, E. Y.; Chang, C. J. A Selective Turn-On Fluorescent Sensor for Imaging Copper in Living Cells. *J. Am. Chem. Soc.* **2006**, *128*, 10-11.

74) Fokkens, M.; Schrader, T.; Klarner, F. –G. A Molecular Tweezer for Lysine and Arginine. *J. Am. Chem. Soc.* **2005**, *127*, 14415-14421.

75) Schmuck, C. E.; Wienand, W.; Geiger, L. Bioorganic Receptors for Amino Acids and Peptides: Combining Rational Design with Combinatorial Chemistry. *Highlights in Bioorganic Chemistry*. Schmuck, C.; Wennemers, H., Eds.; Wiley-VCH: London, 2003; pp. 140-153.

76) (a) Mizutani, T.; Wada, K.; Kitagawa, S. Porphyrin Receptors for Amines, Amino Acids, and Oligopeptides in Water. *J. Am. Chem. Soc.* **1999**, *121*, 11425-11431. (b) Bush, M. E.; Bouley, N. D.; Urbach, A. R. Charge-Mediated Recognition of N-Terminal Tryptophan in Aqueous Solution by a Synthetic Host. *J. Am. Chem. Soc.* **2005**, *127*, 14511-14517.

77) Adrian, J. C.; Wilcox, C. S. Chemistry of Synthetic Receptors and Functional Group Arrays. 15. The Effects of Added Water on Thermodynamic Aspects of Hydrogen Bond Based Molecular Recognition in Chloroform. *J. Am. Chem. Soc.* **1991**, *113*, 678-680.

78) Hernandez, J. V.; Muñoz, F. M.; Oliva, A. I.; Simón, L.; Pérez, E.; Morán, J. R. A Xanthone-Based Neutral Receptor for Zwitterionic Amino Acids. *Tetrahedron Lett.* **2003**, *44*, 6983-6985.

79) Ngola, S. M.; Kearney, P. C.; Mecozzi, S.; Russell, K.; Dougherty, D. A. A Selective Receptor for Arginine Derivatives in Aqueous Media. Energetic Consequences of Salt Bridges That Are Highly Exposed to Water. *J. Am. Chem. Soc.* **1999**, *121*, 1192-1201.

80) Fabbrizzi, L.; Licchelli, M.; Perotti, A.; Poggi, A.; Rabaioli, G.; Sacchi, D.; Taglietti, A. Fluorescent Molecular Sensing of Amino Acids Bearing an Aromatic Residue. *Perkin Trans. 2* **2001**, 2108-2113.

81) Rebek, J. Jr.; Nemeth, D. Molecular Recognition: Three-Point Binding Leads to a Selective Receptor for Aromatic Amino Acids. *J. Am. Chem. Soc.* **1985**, *107*, 6739-6740.

82) Escuder, B.; Rowan, A. E.; Feiters, M. C.; Nolte, R. J. M. Enantioselective Binding of Amino Acids and Amino Alcohols by Self-Assembled Chiral Basket-Shaped Receptors. *Tetrahedron* **2004**, *60*, 291-300.

83) Higashi, N.; Koga, T.; Niwa, M. Enantioselective Binding and Stable Encapsulation of α-Amino Acids in a Helical Poly(L-Glutamic Acid)-Shelled Dendrimer in Aqueous Solutions. *ChemBioChem* **2002**, *3*, 448-454.

84) Severin, K.; Bergs, R.; Beck, W. Bioorganometallic Chemistry-Transition Metal Complexes with α-Amino Acids and Peptides. *Angew. Chem. Int. Ed.* **1998**, *37*, 1634-1654.

85) Laurie, S. H. *Comprehensive Coordination Chemistry*. Wilkinson, G.; Gillard, R. D.; McCleverty, J. A., Eds.; Pergamon Press: New York, 1987; Vol. 2, p. 739.

86) (a) Martell, A. E. *Metal Complexes in Aqueous Solutions*. Plenum Press: New York (1996); pp 217-230. (b) Wilkins, R. G. *Kinetics and Mechanism of Reactions of Transition Metal Complexes*. Wiley-VCH: Weinhem, Germany (1991); pp 199-227.

87) Wright, A. T.; Anslyn, E. V. Cooperative Metal-Coordination and Ion Pairing in Tripeptide Recognition. *Org. Lett.* **2004**, *6*, 1341-1344.

88) Fabbrizzi, L.; Francese, G.; Licchelli, M.; Perotti, A.; Taglietti, A. Fluorescent Sensor of Imidazole and Histidine. *Chem. Commun.* **1997**, 581-582.

89) Hortala, M. A.; Fabbrizzi, L.; Marcotte, N.; Stomeo, F.; Taglietti, A. Designing the Selectivity of the Fluorescent Detection of Amino Acids: A Chemosensing Ensemble for Histidine. *J. Am. Chem. Soc.* **2002**, *125*, 20-21.

90) (a) Lehn, J. M.; Vierling, P.; Hayward, R. C. Stable and Selective Guanidinium and Imidazolium Complexes of a Macrocyclic Receptor Molecule. *J. Chem. Soc. Chem. Commun.* **1979**, 296-298. (b) Schrader, T. Strong Binding of Alkylguanidinium Ions by Molecular Tweezers: An Artificial Selective Arginine Receptor Molecule with a Biomimetic Recognition Pattern. *Chem. Eur. J.* **1997**,

3, 1537-1541. (c) Eliseev, A. V.; Nelen, M. I. Use of Molecular Recognition to Drive Chemical Evolution. 1. Controlling the Composition of an Equilibrating Mixture of Simple Arginine Receptors. *J. Am. Chem. Soc.* **1997**, *119*, 1147-1148.

91) Bell, T. W.; Khasanov, A. B.; Drew, M. G. B.; Filikov, A.; James, T. L. A Small-Molecule Guanidinium Receptor: The Arginine Cork. *Angew. Chem. Int. Ed.* **1999**, *38*, 2543-2547.

92) (a) Rensing, S.; Arendt, M.; Springer, A.; Grawe, T.; Schrader, T. Optimization of a Synthetic Arginine Receptor. Systematic Tuning of Noncovalent Interactions. *J. Org. Chem.* **2001**, *66*, 5814-5821. (b) Grawe, T.; Schrader, T.; Finocchiaro, P.; Consiglio, G.; Failla, S. A New Receptor Molecule for Lysine and Histidine in Water: Strong Binding of Basic Amino Acid Esters by a Macrocyclic Host. *Org. Lett.* **2001**, *3*, 1597-1600.

93) Schmuck, C.; Bickert, V. N'-Alkylated Guanidiniocarbonyl Pyrroles: New Receptors for Amino Acid Recognition in Water. *Org. Lett.* **2003**, *5*, 4579-4581.

94) Schmuck, C.; Graupner, S. Amino Acid Binding in Water by a New Guanidiniocarbonyl Pyrrole Dication: the Effect of the Experimental Conditions on Complex Stability and Stoichiometry. *Tetrahedron Lett.* **2005**, *46*, 1295-1298.

95) (a) Kyne, G. M.; Light, M. E.; Hursthouse, M. B.; de Mendoza, J.; Kilburn, J. D. Enantioselective Amino Acid Recognition Using Cyclic Thiourea Receptors. *Perkin Trans. 1* **2001**, 1258-1263. (b) Rossi, S.; Kyne, G. M.; Turner, D. L.; Wells, N. J.; Kilburn, J. D. A Highly Enantioselective Receptor for N-Protected Glutamate and Anomalous Solvent-Dependent Binding Properties. *Angew. Chem. Int. Ed.* **2002**, *41*, 4233-4236. (c) Ragusa, A.; Rossi, S.; Hayes, J. M.; Stein, M.; Kilburn, J. D. Novel Enantioselective Receptors for N-Protected Glutamate and Aspartate. *Chem. Eur. J.* **2005**, *11*, 5674-5688.

96) (a) Pandey, A.; Mann, M. Proteomics to Study Genes and Genomes. *Nature* **2000**, *405*, 837-846. (b) Kodadek, T. Protein Microarrays: Prospects and Problems.

Chem. Biol. **2001**, *8*, 105-115. (c) Gerlt, J. A. "Fishing" for the Functional Proteome. *Nat. Biotech.* **2002**, *20*, 786-787. (d) *Protein Arrays, Biochips, and Proteomics.* Albala, J. S.; Humphrey-Smith, I.; Eds., Marcel Dekker Inc.: New York (2003). (e) Speers, A. E.; Cravatt, B. F. Chemical Strategies for Activity-Based Proteomics. *Chem. Biochem.* **2004**, *5*, 41-47.

97) Hirschmann, R. Medicinal Chemistry in the Golden Age of Biology: Lessons From Steroid and Peptide Research. *Angew. Chem. Int. Ed.* **1991**, *30*, 1278-1301.

98) (a) Carrell, R. W.; Lomas, D. A. Conformational Disease. *Lancet* **1997**, *350*, 134-138. (b) Schneider, H. –J.; Eblinger, F.; Sirish, M. Synthetic Peptide Receptors: Noncovalent Interactions Involving Peptides. *Advances in Supramolecular Chemistry*. Gokel, G. W., Ed.; JAI Press: Stamford, CT, 2000; V. 6, pp. 185-216.

99) (a) Schneider, J. P.; Kelly, J. W. Templates That Induce alpha-Helical, beta-Sheet, and Loop Conformations. *Chem. Rev.* **1995**, *95*, 2169-2187. (b) Nowick, J. S. Chemical Models of Protein β-Sheets. *Acc. Chem. Res.* **1999**, *32*, 287-296.

100) (a) Yoon, S. S.; Still, W. C. An Exceptional Synthetic Receptor for Peptides. *J. Am. Chem. Soc.* **1993**, *115*, 823-824. (b) Yoon, S. S.; Still, W. C. Synthesis and Properties of A4B6 Cyclooligomeric Receptors. *Tetrahedron Lett.* **1994**, *35*, 2117-2120. (c) Yoon, S. S.; Still, W. C. Cyclooligomeric Receptors for the Sequence Selective Binding of Peptides. A Tetrahedral Receptor from Trimesic Acid and 1,2-Diamines. *Tetrahedron Lett.* **1994**, *35*, 8557-8560. (d) Yoon, S. S.; Still, W. C. Sequence-Selective Peptide Binding with a Synthetic Receptor. *Tetrahedron* **1995**, *51*, 567-578. (d) Chen, C. –T.; Wagner, H.; Still, W. C. Fluorescent, Sequence Selective Peptide Detection by Synthetic Small Molecules. *Science* **1998**, *279*, 851-853.

101) Henley, P. D.; Kilburn, J. D. A Synthetic Receptor for the Cbz-L-Ala-L-Ala-OH Dipeptide Sequence. *Chem. Commun.* **1999**, 1335-1336.

102) Tabet, M.; Labroo, V.; Sheppard, P.; Sasaki, T. Spermine-Induced Conformational Changes of a Synthetic Peptide. *J. Am. Chem. Soc.* **1993**, *115*, 3866-3868.

103) Albert, J. S.; Goodman, M. S.; Hamilton, A. D. Molecular Recognition of Proteins: Sequence-Selective Binding of Aspartate Pairs in Helical Peptides. *J. Am. Chem. Soc.* **1995**, *117*, 1143-1144.

104) LaBrenz, S. R.; Kelly, J. W. Peptidomimetic Host that Binds a Peptide Guest Affording a β-Sheet Structure that Subsequently Self-Assembles. A Simple Receptor Mimic. *J. Am. Chem. Soc.* **1995**, *117*, 1655-1656.

105) Torneiro, M.; Still, W. C. Sequence-Selective Binding of Peptides in Water by a Synthetic Receptor Molecule. *J. Am. Chem. Soc.* **1995**, *117*, 5887-5888.

106) (a) Nowick, J. S.; Chung, D. M.; Maitra, S.; Stigers, K.; Sun, Y. An Unnatural Amino Acid that Mimics a Tripeptide β-Strand and Forms β-Sheetlike Hydrogen-Bonded Dimers. *J. Am. Chem. Soc.* **2000**, *122*, 7654-7661. (b) Nowick, J. S.; Lam, K. S.; Khasanova, T. V.; Kemnitzer, W. E.; Maitra, S.; Mee, H. T.; Lui, R. An Unnatural Amino Acid that Induces β-Sheet Folding and Interaction in Peptides. *J. Am. Chem. Soc.* **2002**, *124*, 4972-4973. (c) Nowick, J. S.; Chung, D. M. Sequence-Selective Molecular Recognition Between Beta-Sheets. *Angew. Chem. Int. Ed.* **2003**, *42*, 1765-1768. (d) Chung, D. M.; Nowick, J. S. Enantioselective Molecular Recognition between β-Sheets *J. Am. Chem. Soc.* **2004**, *126*, 3062-3063.

107) (a) Rzepecki, P.; Nagel-Steger, L.; Feuerstein, S.; Linne, U.; Molt, O.; Zadmard, R.; Aschermann, K.; Wehner, M.; Schrader, T.; Riesner, D. Prevention of Alzheimer's Disease-Associated Aβ Aggregation by Rationally Designed Nonpeptidic β-Sheet Ligands. *J. Biol. Chem.* **2004**, *279*, 47497-47505. (b) Wehner, M.; Janssen, D.; Schäfer, G.; Schrader, T. Sequence-Selective Peptide Recognition with Designed Molecules. *Eur. J. Org. Chem.* **2006**, 138-153.

108) Mandl, C. P.; König, B. Luminescent Crown Ether Amino Acids: Selective Binding to N-Terminal Lysine in Peptides. *J. Org. Chem.* **2005**, *70*, 670-674.

109) Breslow, R.; Yang, Z.; Ching, R.; Trojandt, G.; Odobel, F. Sequence Selective Binding of Peptides by Artificial Receptors in Aqueous Solution. *J. Am. Chem. Soc.* **1998**, *120*, 3536-3537.

110) Hossain, M. A.; Schneider, H. –J. Sequence-Selective Evaluation of Peptide Side-Chain Interaction. New Artificial Receptors for Selective Recognition in Water. *J. Am. Chem. Soc.* **1998**, *120*, 11208-11209.

111) Hart, B. R.; Shea, K. J. Synthetic Peptide Receptors: Molecularly Imprinted Polymers for the Recognition of Peptides Using Peptide-Metal Interactions. *J. Am. Chem. Soc.* **2001**, *123*, 2072-2073.

112) Ojida, A.; Mito-oka, Y.; Inoue, M.; Hamachi, I. First Artificial Receptors and Chemosensors Toward Phosphorylated Peptide in Aqueous Solution. *J. Am. Chem. Soc.* **2002**, *124*, 6256-6258.

113) (a) Schmuck, C.; Geiger, L. Carboxylate Binding by Guanidiniocarbonyl Pyrroles: From Self-Assembly to Peptide Receptors. *Curr. Org. Chem.* **2003**, *7*, 1485-1502. (b) Schmuck, C.; Geiger, L. Dipeptide Binding in Water by a de Novo Designed Guanidiniocarbonylpyrrole Receptor. *J. Am. Chem. Soc.* **2004**, *126*, 8898-8899.

114) Buryak, A.; Severin, K. An Organometallic Chemosensor for the Sequence-Selective Detection of Histidine- and Methionine-Containing Peptides in Water at Neutral pH. *Angew. Chem. Int. Ed.* **2004**, *43*, 4771-4774.

115) Tashiro, S.; Tominaga, M.; Kawano, M.; Therrien, B.; Ozeki, T.; Fujita, M. Sequence-Selective Recognition of Peptides within the Single Binding Pocket of a Self-Assembled Coordination Cage. *J. Am. Chem. Soc.* **2005**, *127*, 4546-4547.

116) (a) Still, W. C. Discovery of Sequence-Selective Peptide Binding by Synthetic Receptors Using Encoded Combinatorial Libraries. *Acc. Chem. Res.* **1996**, *29*, 155-163. (b) Still, W. C. Combinatorial Chemistry Searching for a Winning Combination. *Curr. Opin. Chem. Biol.* **1997**, *1*, 3-4. (c) De Miguel, Y. R.; Sanders, J. K. M. Generation and Screening of Synthetic Receptor Libraries. *Curr. Opin. Chem. Biol.* **1998**, *2*, 417-421. (d) Linton, B.; Hamilton, A. D. Host-Guest Chemistry: Combinatorial Receptors. *Curr. Opin. Chem. Biol.* **1999**, *3*, 307-312. (e) Lavigne, J. J.; Anslyn, E. V. Sensing a Paradigm Shift in the Field of Molecular Recognition: From Selective to Differential Receptors. *Angew. Chem. Int. Ed.* **2001**, *40*, 3118-3130. (f) Srinivasan, N.; Kilburn, J. D. Combinatorial Approaches to Synthetic Receptors. *Curr. Opin. Chem. Biol.* **2004**, *8*, 305-310.

117) Löwik, D. W. P. M.; Weingarten, M. D.; Broekema, M.; Brouwer, A. J.; Still, W. C. Liskamp, R. M. J. Tweezers with Different Bite: Increasing the Affinity of Synthetic Receptors by Varying the Hinge Part. *Angew. Chem. Int. Ed.* **1998**, *37*, 1846-1850.

118) (a) Lam, K. S.; Salmon, S. E.; Hersch, E. M.; Hruby, V. J.; Kazmierski, W. M.; Knapp, R. J. A New Type of Synthetic Peptide Library for Identifying Ligand-Binding Activity. *Nature* **1991**, *354*, 82-84. (b) Lam, K. S.; Lebl, M.; Krchnák, V. The "One-Bead-One-Compound" Combinatorial Library Method. *Chem. Rev.* **1997**, *97*, 411-448.

119) Chang, K. –H.; Liao, J. –H.; Chen, C. –T.; Mehta, B. K.; Chou, P. –T.; Fang, J. –M. Stereoselective Recognition of Tripeptides Guided by Encoded Library Screening: Construction of Chiral Macrocyclic Tetraamide Ruthenium Receptor for Peptide Sensing. *J. Org. Chem.* **2005**, *70*, 2026-2032.

120) (a) Ryan, K.; Gershell, L. J.; Still, W. C. A Synthetic Receptor Motif Designed for Extended Peptide Conformations. *Tetrahedron* **2000**, *56*, 3309-3318. (b) Iorio, E. J.; Shao, Y.; Chen, C. –T.; Wagner, H.; Still, W. C. Sequence-Selective Peptide Detection by Small Synthetic Chemosensors Selected From an Encoded Combinatorial Chemosensor Library. *Bioorg. Med. Chem. Lett.* **2001**, *11*, 1635-1638.

121) (a) Schmuck, C.; Heil, M. Using Combinatorial Methods to Arrive at a Quantitative Structure-Stability Relationship for a New Class of One-Armed Cationic Peptide Receptors Targeting the C-Terminus of the Amyloid β-Peptide. *Org. Biomol. Chem.* **2003**, *1*, 633-636. (b) Schmuck, C.; Heil, M. Peptide Binding by One-Armed Receptors in Water: Screening of a Combinatorial Library for the Binding of Val-Val-Ile-Ala. *ChemBioChem.* **2003**, *4*, 1232-1238.

122) Boyce, R.; Li, G.; Nestler, H. P.; Suenega, T.; Still, W. C. Peptidosteroidal Receptors for Opioid Peptides. Sequence-Selective Binding Using a Synthetic Receptor Library. *J. Am. Chem. Soc.* **1994**, *116*, 7955-7956.

123) Cheng, Y.; Suenaga, T.; Still, W. C. Sequence-Selective Peptide Binding with a Peptido-A,B-*trans*-steroidal Receptor Selected from an Encoded Combinatorial Receptor Library. *J. Am. Chem. Soc.* **1996**, *118*, 1813-1814.

124) (a) Fessmann, T.; Kilburn, J. D. Identification of Sequence-Selective Receptors for Peptides with a Carboxylic Acid Terminus. *Angew. Chem. Int. Ed.* **1999**, *38*, 1993-1996. (b) Braxmeier, T.; Demarcus, M.; Fessmann, T.; McAteer, S.; Kilburn, J. D. Identification of Sequence Selective Receptors for Peptides with a Carboxylic Acid Terminus. *Chem. Eur. J.* **2001**, *7*, 1889-1898. (c) Jensen, K. B.; Braxmeier, T. M.; Demarcus, M.; Frey, J. G.; Kilburn, J. D. Synthesis of Guanidinium-Derived Receptor Libraries and Screening for Selective Peptide Receptors in Water. *Chem. Eur. J.* **2002**, 1300-1309. (d) Arienzo, R.; Kilburn, J. D. Combinatorial Libraries of Diamidopyridine-Derived 'Tweezer' Receptors and Sequence Selective Binding of Peptides. *Tetrahedron* **2002**, *58*, 711-719.

125) Schneider, S. E.; O'Neil, S. N.; Anslyn, E. V. Coupling Rational Design with Libraries Leads to the Production of an ATP Selective Chemosensor. *J. Am. Chem. Soc.* **2000**, *122*, 5542-543.

126) (a) Wennemers, H.; Conza, M.; Nold, M.; Krattiger, P. Diketopiperazine Receptors: A Novel Class of Highly Selective Receptors for Binding Small Peptides. *Chem.*

Eur. J. **2001**, *7*, 3342-3347. (b) Conza, M.; Wennemers, H. Selective Binding of Two-Armed Diketopiperazine Receptors to Side-Chain-Protected Peptides. *J. Org. Chem.* **2002**, *67*, 2696-2698. (c) Krattiger, P.; Wennemers, H. Water-Soluble Diketopiperazine Receptors – Selective Recognition of Arginine-Rich Peptides. *Synlett* **2005**, 706-708.

127) (a) Opatz, T.; Liskamp, R. M. J. A Selectively Deprotectable Triazacyclophane Scaffold for the Construction of Artificial Receptors. *Org. Lett.* **2001**, *3*, 3499-3502. (b) Opatz, T.; Liskamp, R. M. J. Synthesis and Screening of Libraries of Synthetic Tripodal Receptor Molecules with Three Different Amino Acid or Peptide Arms: Identification of Iron Binders. *J. Comb. Chem.* **2002**, *4*, 275-284. (c) Chamorro, C.; Liskamp, R. M. J. Approaches to the Solid Phase of a Cyclotriveratrylene Scaffold-Based Tripodal Library as Potential Artificial Receptors. *J. Comb. Chem.* **2003**, *5*, 794-801. (d) Chamorro, C.; Hofman, J. –W.; Liskamp, R. M. J. Combinatorial Solid-Phase Synthesis and Screening of a Diverse Tripodal Triazacyclophane (TAC)-based Synthetic Receptor Library Showing a Remarkable Selectivity Towards a D-Ala-D-Ala Containing Ligand. *Tetrahedron* **2004**, *60*, 8691-8697.

128) (a) Albert, K. J.; Lewis, N. S.; Schauer, C. L.; Sotzing, G. A.; Stitzel, S. E.; Vaid, T. P.; Walt, D. R. *Chem. Rev.* **2000**, *100*, 2595-2626. (b) Wright, A. T.; Anslyn, E. V. Differential Receptor Arrays and Assays for Solution-Based Molecular Recognition. *Chem. Soc. Rev.* **2006**, *35*, 14-28.

129) (a) Beebe, K. R.; Pell, R. J.; Seasholtz, M. B. *Chemometrics: A Practical Guide*. Wiley: New York, 1998. (b) Jurs, P. C.; Bakken, G. A.; McClelland, H. E. Computational Methods for the Analysis of Chemical Sensor Array Data from Volatile Analytes. *Chem. Rev.* **2000**, *100*, 2649-2678. (c) Brereton, R. G. *Chemometrics: Data Analysis for the Laboratory and Chemical Plant*. Wiley: Chichester, 2003.

130) Burgard, D. R.; Kuznicki, J. T. *Chemometrics: Chemical and Sensory Data*. CRC Press: Boca Raton, FL, 1991; p. 63.

131) Moulton, D. G. Structure-Activity Relations in Olfaction. *Odor Quality and Chemical Structure*. Moskowitz, H. R.; Warren, C. B., Eds.; ACS Symposium Series 148; American Chemical Society: Washington, D.C., 1981; pp. 211-230.

132) Schleppnik, A. A. Structure Recognition as a Peripheral Process in Odor Quality Control. *Odor Quality and Chemical Structure*. Moskowitz, H. R.; Warren, C. B., Eds.; ACS Symposium Series 148; American Chemical Society: Washington, D.C., 1981; pp. 161-175.

133) Furia, T. E.; Bellanca, N. *Fenaroli's Handbook of Flavor Ingredients*. CRC Press: Boca Raton, FL, 1975.

134) Miller, I. J. Jr. 23. Anatomy of the Peripheral Taste System. *Handbook of Olfaction and Gustation*. Doty, R. L., Ed.; Marcel-Dekker: New York, 1995; pp. 521-548.

135) Kawamura, Y.; Kare, M. R. *Umami: A Basic Taste*. Marcel-Dekker: New York, 1987.

136) Spielman, A. I.; Brand, J. G.; Kare, M. R. Tongue and Taste. *Encyclopedia of Human Biology*. Dulbecco, R., Ed.; Academic Press: San Diego, CA, 1991; Vol. 7, pp. 527-535.

137) Lonergan, M. C.; Freund, M. S.; Severin, E. J.; Doleman, B. J.; Grubbs, R. H.; Lewis, N. S. Array-Based Vapor Sensing Using Chemically Sensitive, Polymer Composite Resistors. *IEEE* **1997**, *3*, 583-631.

138) A number of fine reviews exist in this area: (a) Grate, J. W. Acoustic Wave Microsensor Arrays for Vapor Sensing. *Chem. Rev.* **2000**, *100*, 2627-2648. (b) James, D.; Scott, S. M.; Ali, Z.; O'Hare, W. T. Chemical Sensors for Electronic Nose Systems. *Microchim. Acta.* **2005**, *149*, 1-17.

139) Gardner, J. W.; Bartlett, P. N. *Electronic Noses – Principles and Applications*. Oxford Science Publications: Oxford, 1999, p. 67.

140) Persaud, K.; Dodd, G. Analysis of Discrimination Mechanisms in the Mammalian Olfactory System Using a Model Nose. *Nature* **1982**, *299*, 352-355.

141) A number of reviews have covered electronic tongues: (a) Vlasov, Y.; Legin, A. Non-Selective Chemical Sensors in Analytical Chemistry: from "Electronic Nose" to "Electronic Tongue." **1998**, *361*, 255-260. (b) Toko, K. Electronic Tongue. *Biosens. & Bioelec*. **1998**, *13*, 701-709. (c) Krantz-Rülcker, C.; Stenberg, M.; Winquist, F.; Lundström, I. Electronic Tongues for Environmental Monitoring Based on Sensor Arrays and Pattern Recognition: a Review. *Anal. Chim. Acta* **2001**, *426*, 217-226. (d) Vlasov, Y.; Legin, A.; Rudnitskaya, A. Electronic Tongues and Their Analytical Application. *Anal. Bioanal. Chem*. **2002**, *373*, 136-146.

142) Lavigne, J. J.; Savoy, S.; Clevenger, M. B.; Ritchie, J. E.; McDoniel, B.; Yoo, S. – J.; Anslyn, E. V.; McDevitt, J. T.; Shear, J. B.; Neikirk, D. Solution-Based Analysis of Multiple Analytes by a Sensor Array: Toward the Development of an "Electronic Tongue." *J. Am. Chem. Soc*. **1998**, *120*, 6429-6430.

143) Goodey, A.; Lavigne, J. J.; Savoy, S. S.; Rodriguez, M. D.; Curey, T.; Tsao, A.; Simmons, G.; Wright, J.; Yoo, S. –J.; Sohn, Y.; Anslyn, E. V.; Shear, J. B.; Neikirk, D. P.; McDevitt, J. T. Development of Multianalyte Sensor Arrays Composed of Chemically Derivatized Polymeric Microspheres Localized in Micromachined Cavities. *J. Am. Chem. Soc*. **2001**, *123*, 2559-2570.

144) McCleskey, S. C.; Griffin, M. J.; Schneider, S. E.; McDevitt, J. T.; Anslyn, E. V. Differential Receptors Create Patterns Diagnostic for ATP and GTP. *J. Am. Chem. Soc*. **2003**, *125*, 1114-1115.

145) Wright, A. T.; Griffin, M. J.; Zhong, Z.; McCleskey, S. C.; Anslyn, E. V.; McDevitt, J. T. Differential Receptors Create Patterns That Distinguish Various Proteins. *Angew. Chem. Int. Ed.* **2005**, *44*, 6375-6378.

146) Wright, A. T.; Anslyn, E. V.; McDevitt, J. T. A Differential Array of Metalated Synthetic Receptors for the Analysis of Tripeptide Mixtures. *J. Am. Chem. Soc.* **2005**, *127*, 17405-17411.

147) Hirsch, T.; Kettenberger, H.; Wolfbeis, O. S.; Mirsky, V. M. A Simple Strategy for Preparation of Sensor Arrays: Molecularly Structured Monolayers as Recognition Elements. *Chem. Commun.* **2003**, 432.

148) (a) Greene, N. T.; Morgan, S. L.; Shimizu, K. D. Molecularly Imprinted Polymer Sensor Arrays. *Chem. Commun.* **2004**, 1172-1173. (b) Greene, N. T.; Shimizu, K. D. Colorimetric Molecularly Imprinted Polymer Sensor Array Using Dye Displacement. *J. Am. Chem. Soc.* **2005**, *127*, 5695-5700.

149) Zhang, C.; Suslick, K. S. A Colorimetric Sensor Array for Organics in Water. *J. Am. Chem. Soc.* **2005**, *127*, 11548-11549.

150) (a) Baldini, L.; Wilson, A. J.; Hong, J.; Hamilton, A. D. Pattern-Based Detection of Different Proteins Using an Array of Fluorescent Protein Surface Receptors. *J. Am. Chem. Soc.* **2004**, *126*, 5656-5657. (b) Zhou, H.; Baldini, L.; Hong, J.; Wilson, A. J.; Hamilton, A. D. Pattern Recognition of Proteins Based on an Array of Functionalized Porphyrins. *J. Am. Chem. Soc.* **2006**, *128*, 2421-2425.

151) (a) Mayr, T.; Liebsch, G.; Klimant, I.; Wolfbeis, O. S. Multi-ion Imaging Using Fluorescent Sensors in a Microtiterplate Array Format. *Analyst* **2002**, *127*, 201-203. (b) Mayr, T.; Igel, C.; Liebsch, G.; Klimant, I.; Wolfbeis, O. S. Cross-Reactive Metal Ion Sensor Array in a Micro Titer Plate Format. *Anal. Chem.* **2003**, *75*, 4389-4396.

152) Stojanovic, M. N.; Green, E. G.; Semova, S.; Nikic, D.; Landry, D. W. Cross-Reactive Arrays Based on Three-Way Junctions. *J. Am. Chem. Soc.* **2003**, *125*, 6085-6089.

153) Rangin, M.; Basu, A. Lipopolysaccharide Identification with Functionalized Polydiacetylene Liposome Sensors. *J. Am. Chem. Soc.* **2004**, *126*, 5038-5039.

154) Buryak, A.; Severin, K. A Chemosensor for the Colorimetric Identification of 20 Natural Amino Acids. *J. Am. Chem. Soc.* **2005**, *127*, 3700-3701.

155) Wiskur, S. L.; Floriano, P. N.; Anslyn, E. V.; McDevitt, J. T. A Multicomponent Sensing Ensemble in Solution: Differentiation between Structurally Similar Analytes. *Angew. Chem. Int. Ed.* **2003**, *42*, 2070-2072.

156) Komatsu, H.; Citterio, D.; Fujiwara, Y.; Minamihashi, K.; Araki, Y.; Hagiwara, M.; Suzuki, K. Single Molecular Multianalyte Sensor: Jewel Pendant Ligand. *Org. Lett.* **2005**, *7*, 2857.

157) Osbourn, G. C.; Bartholomew, J. W.; Ricco, A. J.; Frye, G. C. Visual-Empirical Region-of-Influence Pattern Recognition Applied to Chemical Microsensor Array Selection and Chemical Analysis. *Acc. Chem. Res.* **1998**, *31*, 297-305.

Chapter 2: Selective Tripeptide Receptor

2.1 Introduction

Synthetic selective receptors designed in a "lock-and-key" fashion are inspired by nature's remarkable affinity and selectivity.[1] To this end, we have designed a Cu(II):receptor (**2.1**) complex selective for His-Lys-Lys (HKK) (**2.2**) in an aqueous media, and its binding properties to single amino acids, amino acids protected at their N- and C-termini, and tripeptides were evaluated.[2]

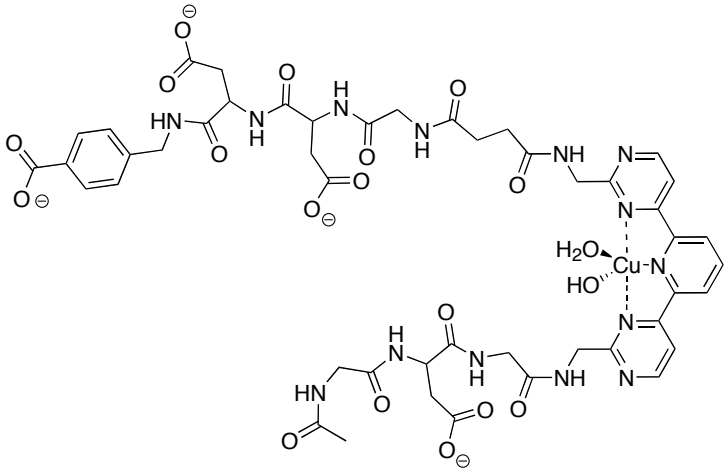

2.1:Cu(II)

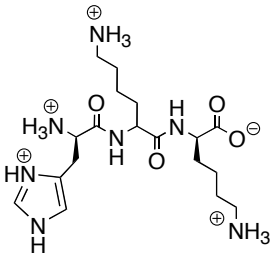

2.2

The relationship of receptor **2.1** to a previous Anslyn group study on a selective L-Asp receptor incorporating an indicator-displacement assay will be reviewed.[3] Additionally, full synthetic details of the HKK receptor will be discussed including synthetic failures and the final development of **2.1**. Metal coordination by both **2.1** and

2.2 will also be described, and binding studies will be shown. The results of this study illustrate the cooperative effect that the peptide arms and metal core of **2.1** have upon the magnitude of guest binding. We believe that the peptide arms of **2.1** form an antiparallel β-sheet when bound to **2.2**.[4]

This work sought to translate the structural features of a peptidic substrate into a complementary synthetic receptor with appropriate binding sites.[5] Peptide binding is interesting as artificial systems attempting to mimic biological systems may enhance the overall understanding of nature's processes. Additionally, peptides contain a great deal of functional diversity with which to target binding to a synthetic receptor. Structural complexity and conformational flexibility of peptides also makes them intriguing and highly challenging targets that a synthetic chemist can employ his entire chemical toolbox to bind.[6]

A number of prior reports have described the design of synthetic peptide receptors for molecular recognition in both organic[7] and aqueous solvents.[8] Using lessons learned from these prior reports, receptor **2.1** was synthesized, and the metal complex was found to have an affinity for HKK (10^6 M^{-1}) that is one of the highest reported to date in an aqueous environment at biological pH (pH 7.4). This work eventually translated into differential studies that are discussed in chapter four.

2.2 Ligand Coordination to Divalent First Row Transition Metals

The ligand coordination properties of 2,2':6,2''-terpyridines (terpyridine, or tpy) to divalent metals have been well studied. Formation constants of terpyridine in aqueous solutions with an ionic strength of 0.1 have been reported as 1.6×10^{13} M^{-1} for Cu(II) (1:1 stoichiometry), and 1.0×10^6 M^{-1} for Zn(II) (1:1 stoichiometry).[9] The much higher

stability of Cu(II) for terpyridine influenced our decision to use Cu(II) rather than Zn(II). The stability constants for divalent cations and terpyridine are consistent with the Irving-Williams series of stability of divalent first row transition-metal: Mn < Fe < Co < Ni < Cu > Zn.[10] This order of stability is irrespective of the nature of the ligand.[11]

Multiple geometries have been reported for Cu(II) when bound to terpyridine-like structures. Fabbrizzi has published crystal structures of two different ternary Cu(II) complexes, not terpyridines, one exhibiting a Jahn-Teller distorted trigonal bipyramidal[12] geometry, and the second a distorted square planar geometry[13] when bound to their respective analytes. Interestingly, the prototypical Jahn-Teller Cu(II) ion is characterized by a marked axial distortion, which typically results in a square pyramidal geometry, and by a strong preference for ligands with nitrogen donor centers.[14]

In regard to terpyridine complexes, Lehn published an elegant crystal structure of complex **2.3** in which two different ligands are wrapped in a helix around the pentacoordinate metal ions.[15] The central coordination geometry is trigonal bipyramidal and the lateral metal ions are in a square pyramidal geometry.

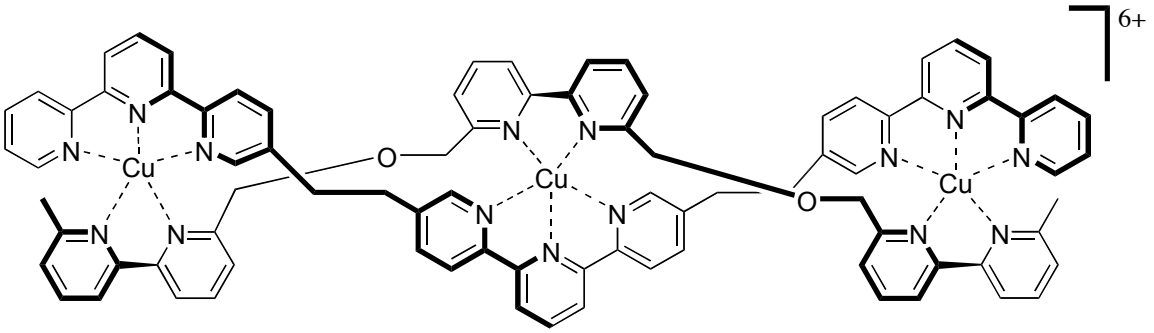

2.3

Additional crystal structures have shown a square pyramidal geometry for a tridentate terpyridine-Cu(II) complex coordinated to bidentate 1,10-phenanthroline.[16] In

this structure the bond lengths of the terpyridine coordinating nitrogens are: N(1)-Cu = 2.048 Å, N(2, center N)-Cu = 2.040 Å, N(3)-Cu = 1.987 Å. These values are on par with known values (N-Cu ≅ 2.0 Å). Another study involving two bidentate bipyridines and a chloride coordinating to Cu(II) (**2.4**) generated an X-ray structure that revealed a slightly distorted trigonal-bipyramidal coordination geometry of Cu(II); the axial ligands and the Cu(II) atom deviated slightly from linearity [N-Cu-N = 175.3°].[17] Clearly, there are a number of geometries exhibited by terpyridine complexes, some displaying significant distortion from typical metal-ligand bond lengths and metal-ligand bond angles. In our own studies with **2.1** a crystal structure was not obtained, but we believe that binding was likely through a distorted trigonal bipyramidal or square pyramidal geometry as suspected by the nature of the analyte ligand (His-Lys-Lys) and known terpyridine coordination.

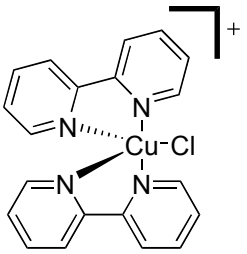

2.4

Chemosensor **2.1** employs a 2,6-di(pyrimidin-4-yl)pyridine core that is a terpyridine derivative for metal chelation. Using this 2,6-di(pyrimidin-4-yl)pyridine core rather than a terpyridine core permits ready functionalization for receptor and chemosensor development.[18] Previously, this core ligand was derivatized with auxiliary guanidinium appendages (**2.5**), and coordinated to a Zn(II) metal ion for both the promotion of RNA hydrolysis[19] and as part of a chemosensing ensemble for the selective

detection of aspartic acid[3] by the Anslyn group. Furthermore, crystal structures and formation constants in water for derivatized 2,6-di(pyrimidin-4-yl)pyridine cores have been determined by Anslyn.[20]

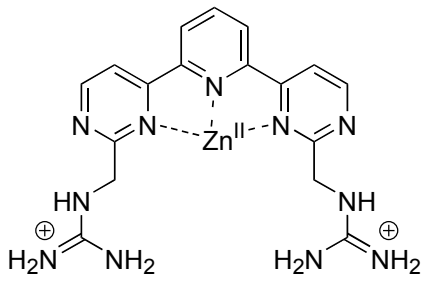

2.5

Importantly, the crystal structures demonstrate a "required" (or preorganized) horseshoe ligand conformation for metal binding, as opposed to the thermodynamically favored extended conformation (Scheme 2.1). The horseshoe ligand conformation places the variable R appendages in the proximity of the metal center. The ligand core is optimal for binding guest molecules as the divalent metal center imparts some selectivity toward the guest, and the auxiliary appendages of the cleft can be functionalized to optimize guest binding, thus enhancing the cooperativity.

Scheme 2.1 Metal-Complexation: Induced Cleft Formation.

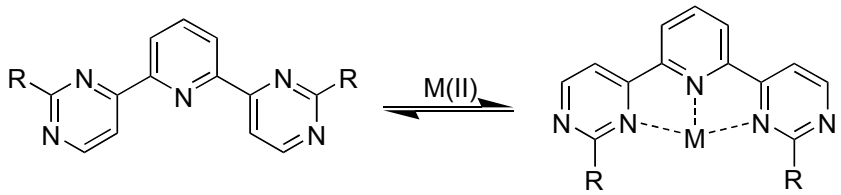

Formation constants with divalent Cu and Zn were also determined for four 2,6-di(pyrimidin-4-yl)pyridine derivatives, **2.6–2.9**.[20] UV/Vis titrations of the metals into aqueous solutions of the ligands (pH 6.8) resulted in significant modulation of the ligand absorbance spectra, and two distinct isosbestic points (265 nm and 307 nm). Formation constants were determined assuming a 1:1 stoichiometry for the metal complexes (Table 2.1).

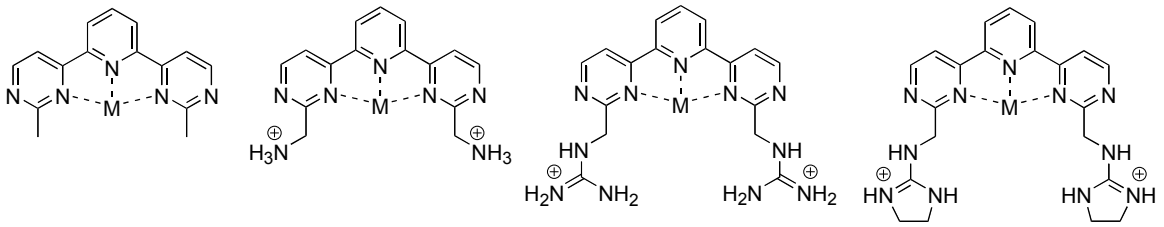

2.6 **2.7** **2.8** **2.9**

It is readily apparent from Table 2.1 that the nitrogen-containing auxiliary groups disrupt ligand binding, presumably due to electrostatic repulsions and electron-withdrawal from the ligand core. As would be expected from the Irving-Williams series, all Cu(II) complexes were stronger. Taking these studies to the drawing board influenced our design of **2.1** incorporating a Cu(II) center to enhance **2.1** core's affinity for the divalent metal. Acidic peptide arms were incorporated to increase electrostatic binding between **2.1:Cu(II)** and **2.2**.

Table 2.1 Formation Constants of Various Metal Complexes in Aqueous Solutions at pH 6.8 with **2.6** to **2.9**. (n.d. = not determined).

Ligand	Metal	Stoichiometry	K (M^{-1})
2.6	Cu(II)	1:1	1×10^6
2.6	Zn(II)	1:1	8.4×10^3
2.7	Cu(II)	Not 1:1	n.d.
2.7	Zn(II)	1:1	4.5×10^5
2.8	Cu(II)	1:1	7.8×10^4
2.8	Zn(II)	1:1	<100
2.9	Cu(II)	1:1	4.1×10^4
2.9	Zn(II)	1:1	<100

2.3 Amino Acid and Oligopeptide Coordination to Cu(II)

Metal coordination in biological systems is often mediated by histidine, which presents three potential coordination sites in aqueous solution. The carboxyl group (pK_a = 1.9), the imidazole nitrogen (pK_a = 6.1), and the amino nitrogen (pK_a = 9.1) become available for coordination as the pH of the solution increases. When His is part of a peptide, either its carboxy terminus, amino terminus, or both are tied up in amide bonds. In this case the imidazole nitrogen becomes a primary source of metal ion chelation, which is often the case in biological systems. An interesting facet of imidazole binding has been illustrated in the comparison of ammonia coordination of Cu(II) to imidazole coordination of Cu(II). Though ammonia is nearly 170 times more basic then imidazole, it is not as strong a Cu(II) ligand. Imidazole is also a stronger Cu(II) and Zn(II) ligand

than 4-methylimidazole, but it is nearly four times less basic.[21] These ligand effects are due in part to the π-acceptor properties of imidazole, which permit it to accept electronic charge from d-orbitals on the divalent metal ions.

Interesting results have shown that the Cu(II) ligand His-Gly coordinates via the amino, peptide, and carboxylate donor groups. However, it was shown that dimers form in which the Cu(II) atoms are bridged via the imidazole nitrogens.[22] In the same study it was demonstrated that if the amino group is free for binding, a very stable complex is formed. Formation constants for several amino acids, including protected forms, and oligopeptides are shown in Table 2.2. These stability constants illustrate the relative affinity of particular peptides and amino acids for Cu(II), and the protected forms illustrate the contribution of donor groups on amino acids.

Several aspects of the formation constants listed in Table 2.2 helped us in the design of receptor **2.1**. An obvious feature is the affinity of both His and Cys for Cu(II); however, these formation constants involve two ligands and one metal. A second aspect is the similarity of formation constants for Gly, Met, and Lys. This is likely due to minimal contributions from the side chains of the amino acids toward binding Cu(II), including the protonated side chain of Lys. As would be expected, ester and acyl protection of Gly and His result in reduced formation constants. More subtle conclusions can be drawn from the formation constants for dipeptides. While an N-terminal His results in a strong complex, a Lys group at the C-terminus results in enhanced coordination. However, these formation constants with dipeptides were measured without the protonation of the Lys residue.

Table 2.2 Formation Constants of Various Ligands With Cu(II) as Measured by Glass Electrode Potentiometry. Ionic strengths are listed in place of medium in some cases.[23]

Ligand	Equilibrium	Temp (°C)	Medium (M)	Log K_{eq}
Gly	[ML]/([M]+[L])	25	0.15 $NaClO_4$	8.18
His	$[M_2L]/([2M]+[L^{2-}])$	25	0.15 $NaClO_4$	14.00
Cys	$[M_2L]/([2M]+[L^{2-}])$	20	0.15 $NaClO_4$	14.00
Met	[ML]/([M]+[L])	20	0.15 $NaClO_4$	8.00
Lys	[ML]/([M]+[L])	20	0.1 KNO_3	7.56
Gly-OEt	[ML]/([M]+[L])	25	0.1 $NaClO_4$	4.04
His-OMe	[ML]/([M]+[L])	25	0.1 KCl	10.21
Acyl-His	[ML]/([M]+[L])	22	0.10	9.43
Gly-His	[ML]/([M]+[L])	25	0.16	4.38
Gly-Lys	[ML]/([M]+[L])	37	0.10	11.60
His-Gly	[ML]/([M]+[L])	25	0.16	5.89
His-Lys	[ML]/([M]+[L])	37	0.10	8.51
Gly-His-Gly	$[ML_2]/([M]+[2L])$	25	3.0	19.95
Gly-Gly-His	[ML]/([M]+[L])	25	0.16	4.63

To determine the importance of both a metal-coordinated receptor core, and the cooperative effects of pendant peptide arms, chemosensor **2.1** was designed with a terdentate Cu(II) ligand core and peptide arms. The metal center was shown to enhance selectivity for N-terminal His peptides, and peptide arms enriched in aspartic acid residues showed selectivity for basic amino acids; thus, tripeptide **2.2** was targeted. The

binding studies with **2.1:Cu(II)** were proof-of-principle experiments for future differential arrays.

2.4 Synthesis of Receptor 2.1

The synthesis of receptor **2.1** required both solution phase and solid phase synthetic approaches. The ligand core was developed using solution-based organic synthesis, but was incorporated onto solid phase for synthesis of the peptide arms. Several challenges were faced in the synthesis that will be described in greater detail in section 2.5.

Generation of the core required a convergent synthesis of two compounds for heterocycle formation. Synthesis commenced with di-*tert*-butyl dicarbonate (Boc) protection of 2-aminoacetonitrile•HCl (**2.10**) to give **2.11**. The Boc-protected aminoacetonitrile was then condensed in ammonia saturated methanol using N-acetyl-L-cysteine as a catalyst to give the carboxamidine **2.12** (Scheme 2.2).[24]

Scheme 2.2 Synthesis of **2.12**.

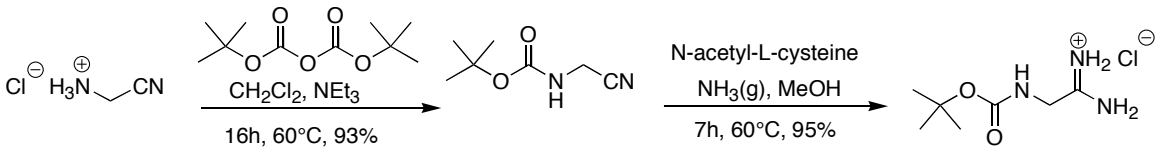

2.10 **2.11** **2.12**

Subsequent to the formation of **2.12** the bisenaminone **2.15** was generated from the reaction of bis(dimethylamino)-tert-butoxymethane (Bredereck's reagent)[25] **2.13** with

2,6-diacetylpyridine **2.14** using a catalytic amount of N,N-dimethylformamide (DMF).[26] Formation of the heterocyclic 2,6-di(pyrimidin-4-yl)pyridine diboc-protected core (**2.16**) in marginal 40% yield occurred via condensation of carboxamidine **2.12** with bisenaminone **2.15** in refluxing ethanol with a significant excess of sodium ethoxide. The Boc protecting groups were subsequently removed with trifluoroacetic acid in methylene chloride, and bisammonium **2.17** was collected via precipitation with cold ethanol from the reaction solution. This series of reactions is illustrated in Scheme 2.3. The ammonium groups of **2.17** were free-based with 1M NaOH for later use.

Scheme 2.3 Solution-Based Synthesis of Receptor Core.

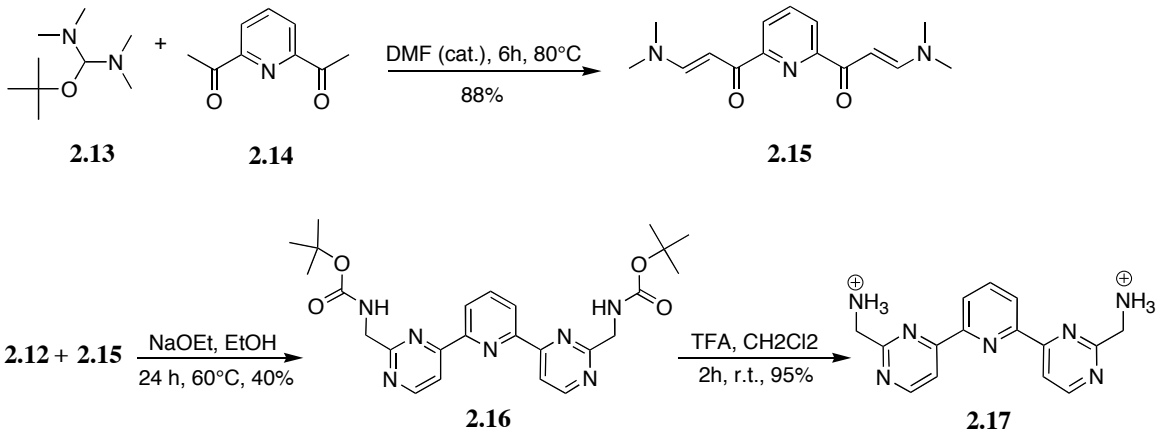

One method for solid-phase synthesis of peptides uses an amino acid protection scheme in which the N-terminus of each amino acid is protected with the base labile protecting group 9-fluorenylmethyloxycarbonyl (Fmoc). Using this protection scheme the first amino acid is attached to the resin through its carboxy terminus in a peptide-bond forming step. This is followed by deprotection of the Fmoc group with piperidine in DMF. A second Fmoc-protected amino acid is then attached to the first amino acid on

the resin through another peptide-bond forming reaction. Subsequently, the second Fmoc group is removed. The bond-forming and deprotection reactions are continued until the desired peptide is synthesized. The ability to incorporate the receptor core (**2.17**) into a growing peptide chain on solid phase was critical to our research. This required Fmoc protection of only a single amine of **2.17**.

Single Fmoc protection of diamines is not an intuitively obvious process. A statistical reaction process to form the mono-Fmoc protected **2.17** always resulted in near complete formation of bis-Fmoc protected **2.17**, or no protection at all. As puzzling as this was, conditions were never determined for a mono-Fmoc protection strategy. A successful strategy involved the statistical mono-Boc protection of **2.17**. Mono-Boc protection was followed by Fmoc protection of the remaining free amine, and subsequent deprotection of the Boc group to give the mono-Fmoc core. This was achieved by reacting free-based **2.17** with di-*tert*-butyl dicarbonate (0.3 equivalents) in water in a statistical manner. This resulted in ~33% yield of product **2.18**, a very small amount of di-Boc protected **2.17**, and ~60% yield of unreacted **2.17**. The unreacted **2.17** would be collected and reacted again with Boc until an 80% yield of **2.18** was collected. **2.18** was reacted with 9-fluorenylmethyloxycarbonyl chloride in *p*-dioxane to give orthogonally protected **2.19**. Deprotection of Boc with trifluoroacetic acid in toluene resulted in **2.20**, which was ready for incorporation into solid phase peptide chemistry as shown in Scheme 2.4.

Scheme 2.4 Synthesis of Mono-Fmoc Receptor Core for Solid Phase Incorporation.

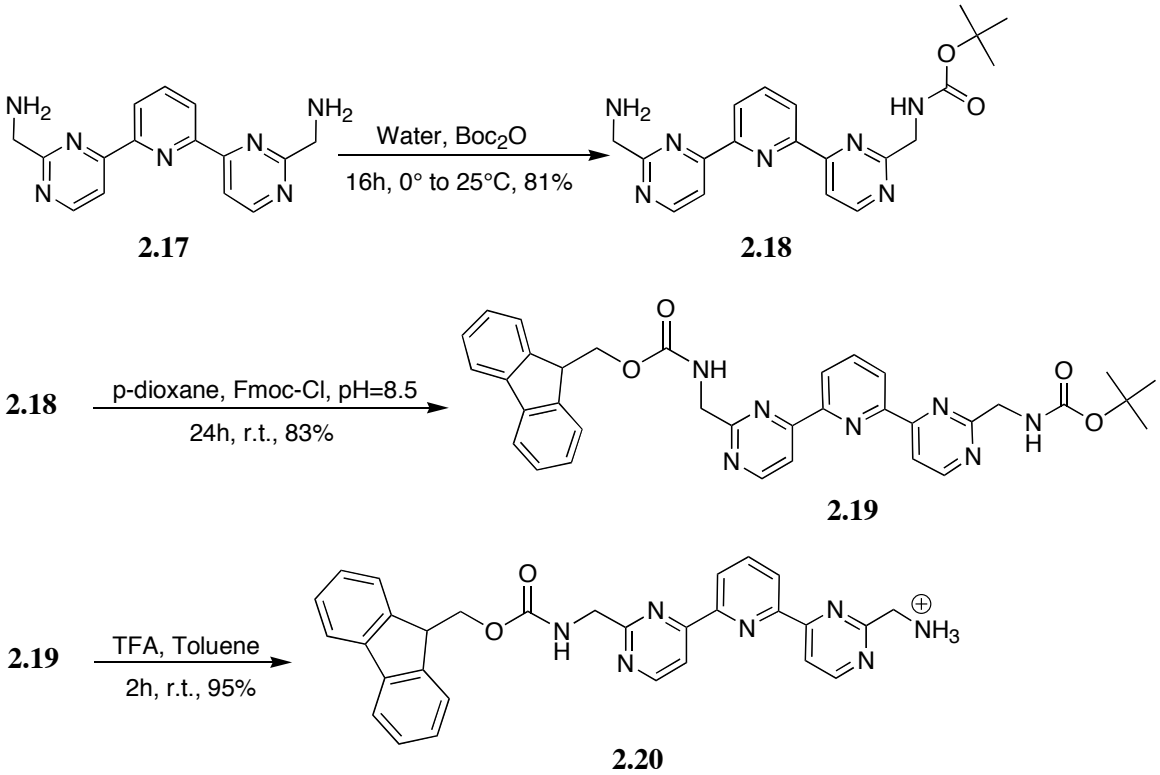

For the solid phase synthesis of **2.1**, an acid-labile resin was required to cleave the receptor for use in solution phase binding studies. 4-aminomethylbenzoyl-2-chlorotrityl resin was purchased from NovaBiochem and used for synthesis. This resin was chosen for its high lability to trifluoroacetic acid. Solid phase peptide coupling steps were completed using 1-hydroxybenzotriazole **2.21** (HOBt), 2-(1H-benzotriazole-1-yl)-1,1,3,3-tetramethyluronium tetrafluoroborate **2.22** (TBTU), and N-methylmorpholine (NMM).[27] These coupling agents were chosen for their high reactivity and prevention of amino acid epimerization during coupling steps. The mechanism involves deprotonation of the amino acid with NMM, followed by TBTU promoted amino acid ester formation with

HOBt. This activated ester facilitates rapid coupling with a second Fmoc-protected amino acid with minimal racemization (Scheme 2.5).

Scheme 2.5 Key Steps of HOBt/TBTU Promoted Peptide Bond Formation.

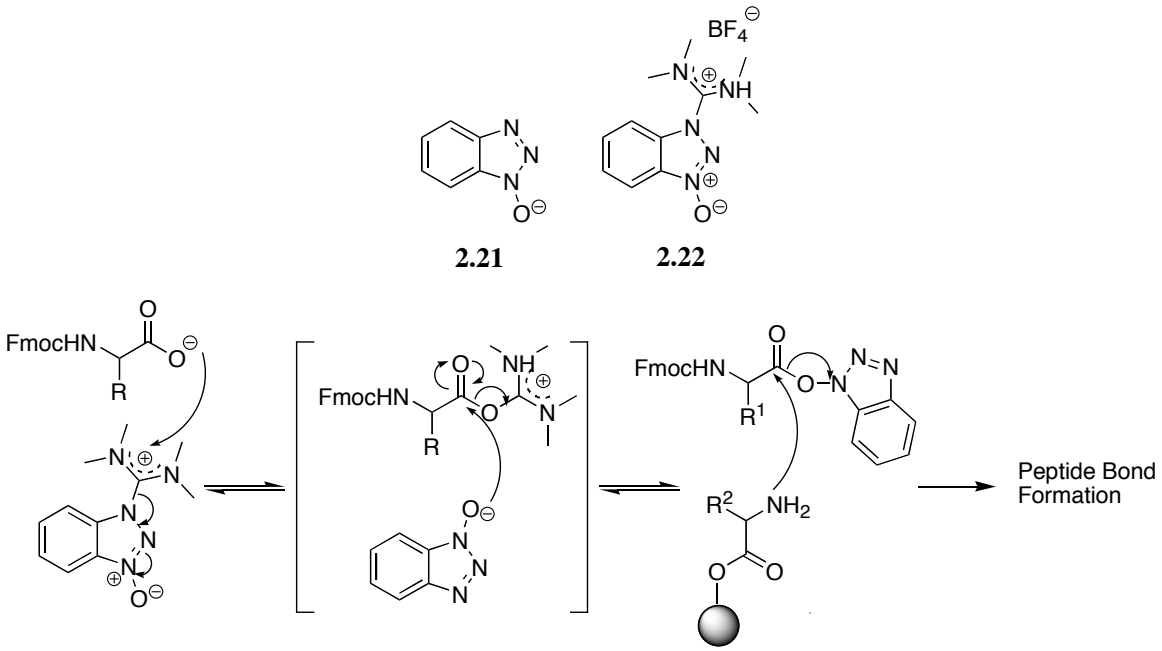

Three amino acids, Asp-Gly-Gly were placed on the resin (**2.23**) using the Fmoc protocol and reagents listed above to give **2.24**. After removal of the Fmoc group from Gly with piperidine to give **2.25**, the free N-terminus of Gly was coupled to a linker group, mono-fluorenyl methanol (Fm) protected succinic acid[28] (**2.26**), to give resin bound **2.27** (Scheme 2.6). The aspartic acid residues were protected with *t*Bu groups to prevent side peptide coupling reactions from occurring. These protecting groups were removed at the end of the synthesis concomitantly with cleavage of the receptor from the resin.

Scheme 2.6 Synthesis of the First Peptide Arm of Receptor **2.1**

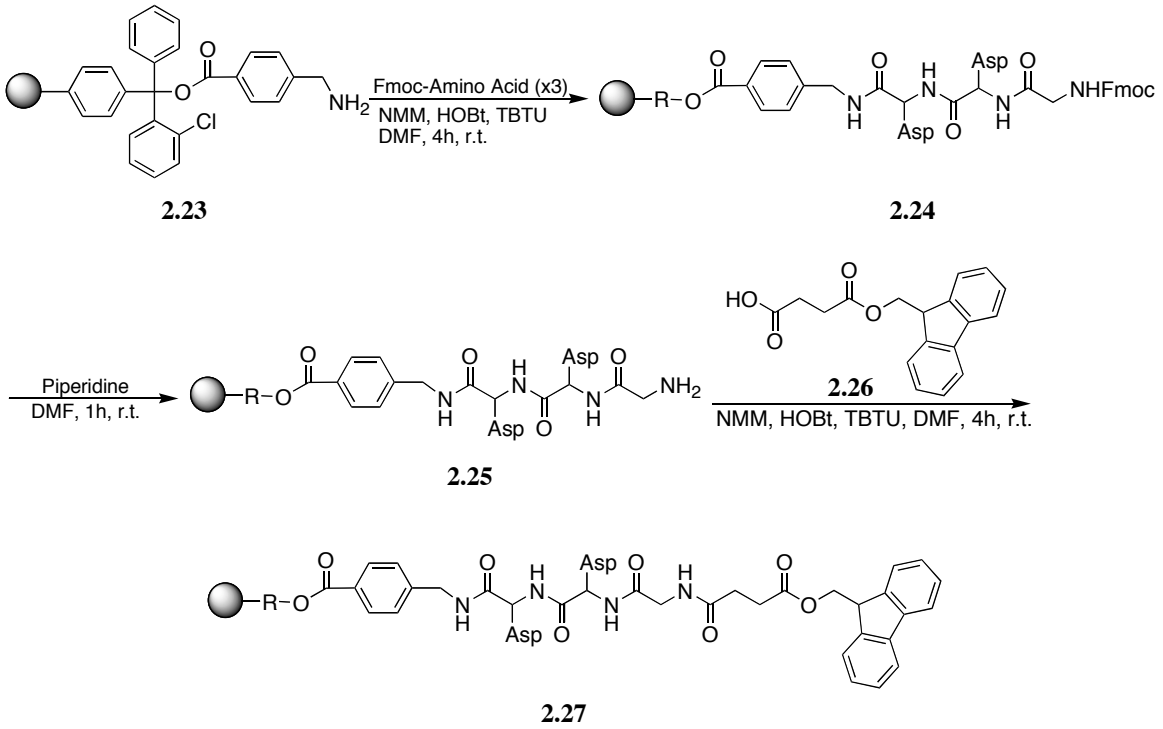

The succinic acid linker was necessary for incorporation of the diamine core because it could not be coupled directly to the amine terminus of the resin bound peptide. Incorporating the succinic acid linker allowed a standard peptide bond forming reaction to be used with the diamine core. The Fm protecting group of succinic acid was removed with 20% piperidine in DMF leaving the free carboxylate (**2.28**). Under standard coupling conditions discussed above, the mono-Fmoc diamine core **2.20** was added to the growing peptide (**2.29**). The Fmoc group was removed to give **2.30**, and subsequently three more amino acids were added: glycine, aspartic acid, and acetyl-protected glycine, yielding resin-bound **2.31**. Cleavage of the receptor from the resin was completed with trifluoroacetic acid:methylene chloride:triethylsilane (60:39:1) to give receptor **2.1** as illustrated in Scheme 2.7. Triethylsilane was added as a cation scavenger, and notably,

cleavage of the resin left a residual benzoic acid as part of **2.1**. This was viewed as advantageous as additional acidic groups should enhance electrostatic affinity for **2.2**.

Scheme 2.7 Addition of Receptor Core and Cleavage of **2.1** from the Resin.

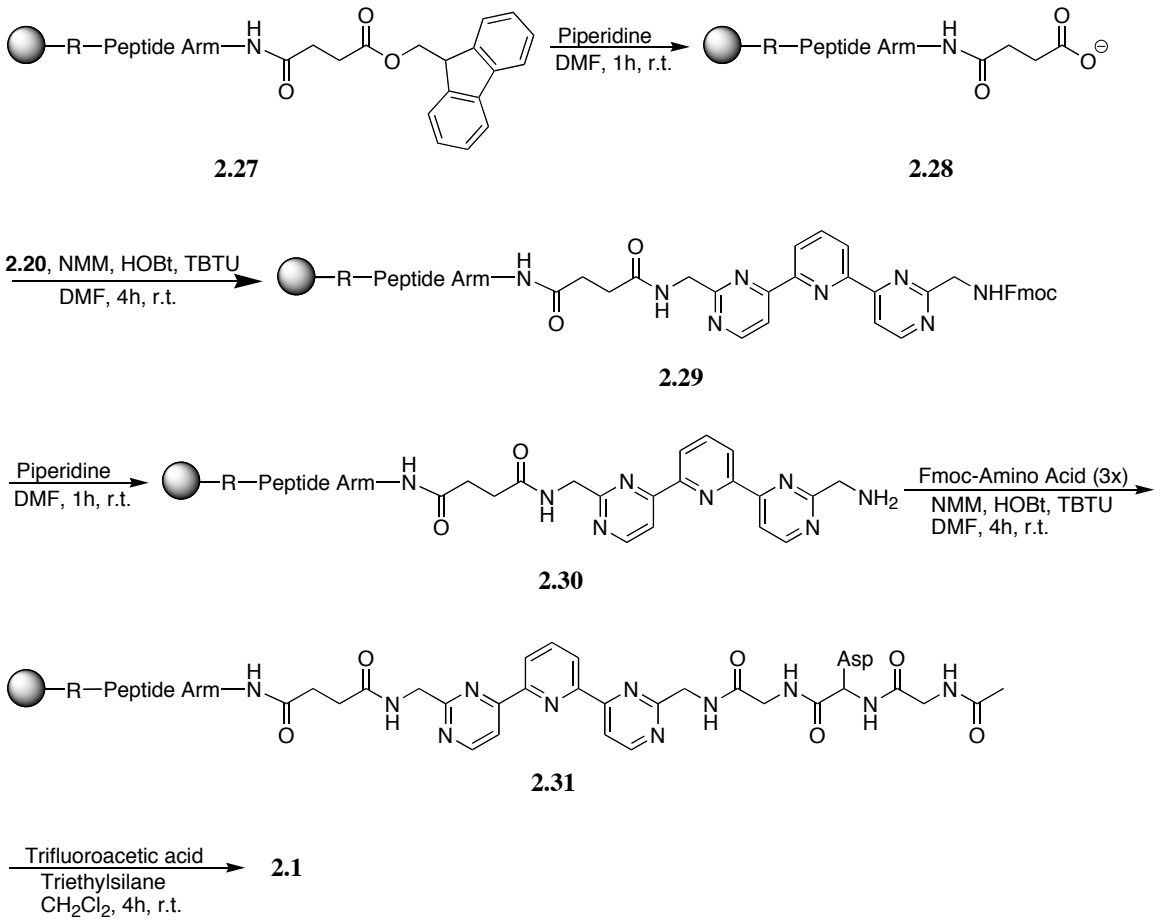

Receptor **2.1** was collected from the cleavage solution by precipitation with cold ether followed by solvation with water and lyophilization. The lyophilized product was redissolved in water and washed several times with ether and methylene chloride. It was

then lyophilized triply to give a fluffy white solid product that was characterized and used for binding studies.

2.5 Synthetic Difficulties

The initial strategy was to synthesize the core of **2.1** using synthetic organic solution-phase chemistry (Scheme 2.8). The majority of problems were encountered when attempting to add the succinic acid linker directly to the mono-Fmoc receptor core **2.20**. Initial efforts involved adding succinic anhydride (**2.32**) to **2.20** in a chloroform/ethanol mixture (50/50) with sodium carbonate as base.[29] It was expected that the free amine of **2.20** would open the anhydride and form a peptide bond. After multiple trials in varying solvent systems and temperatures, direct attachment of succinic anhydride did not work. A second anhydride strategy involved N-methylmorpholine as the base in DMF.[30] Multiple temperatures and concentrations were again attempted to no avail.

The second strategy involved HOBt/TBTU/NMM coupling of monomethylsuccinic acid (**2.33**) to **2.20** in DMF. This reaction yielded 88.4% of the purified product **2.34**. Chasing a saponification strategy found in the literature, **2.34** was dissolved in THF/methanol (3:2), heated to reflux, and LiOH was added.[31] This reaction is contradictory to chemical intuition as it seems evident that the Fmoc protecting group would be readily cleaved under these forcing conditions. It required less than five minutes to determine that indeed the Fmoc group was rapidly deprotected. Acidic saponification was also attempted using 1M HCl in THF at forcing conditions and only starting material was recovered.

A third strategy coupled mono-*tert*-butylsuccinic acid **2.35** to **2.20** yielding 85% **2.36**. We believed that the *t*Bu group would be a more labile protecting group with mild trifluoroacetic acid conditions known to effect its cleavage. Trifluoroacetic acid (TFA) with triethylsilane (TES) (4:1) was added to **2.36** in methylene chloride. After two days, using an increasing temperature gradient, a disappointing 5% yield was collected. A second attempt with acetic acid in methylene chloride yielded no product. Seeking guidance from the literature, a third attempt was made using TFA/anisole (10:1).[32] After an overnight run no product was detected. Rather than incorporating a cation scavenger a fourth attempt at *t*Bu deprotection was made with trifluoroacetic acid/methylene chloride (1:1).[33] Again, a temperature gradient was used over two days without appreciable product formation.

A fourth and final strategy involved reductive amination with **2.20** and *p*-formylbenzoic acid **2.37**. **2.20** was dissolved in a DMF/methanol (1:1) mixture with activated 3Å molecular sieves and catalytic acetic acid. Synthetic attempts were made using both $NaBH_4$ and $NaCNBH_3$ as reducing agents. Again, no product was attained.

As a qualitative assessment of the mono-*tert*-butylsuccinic acid strategy, **2.38** was synthesized. Using standard TFA/methylene chloride deprotection, **2.39** was obtained in near quantitative yield. Scheme 2.8 illustrates the myriad synthetic strategies that were attempted.

Scheme 2.8 Failed Synthetic Strategies.

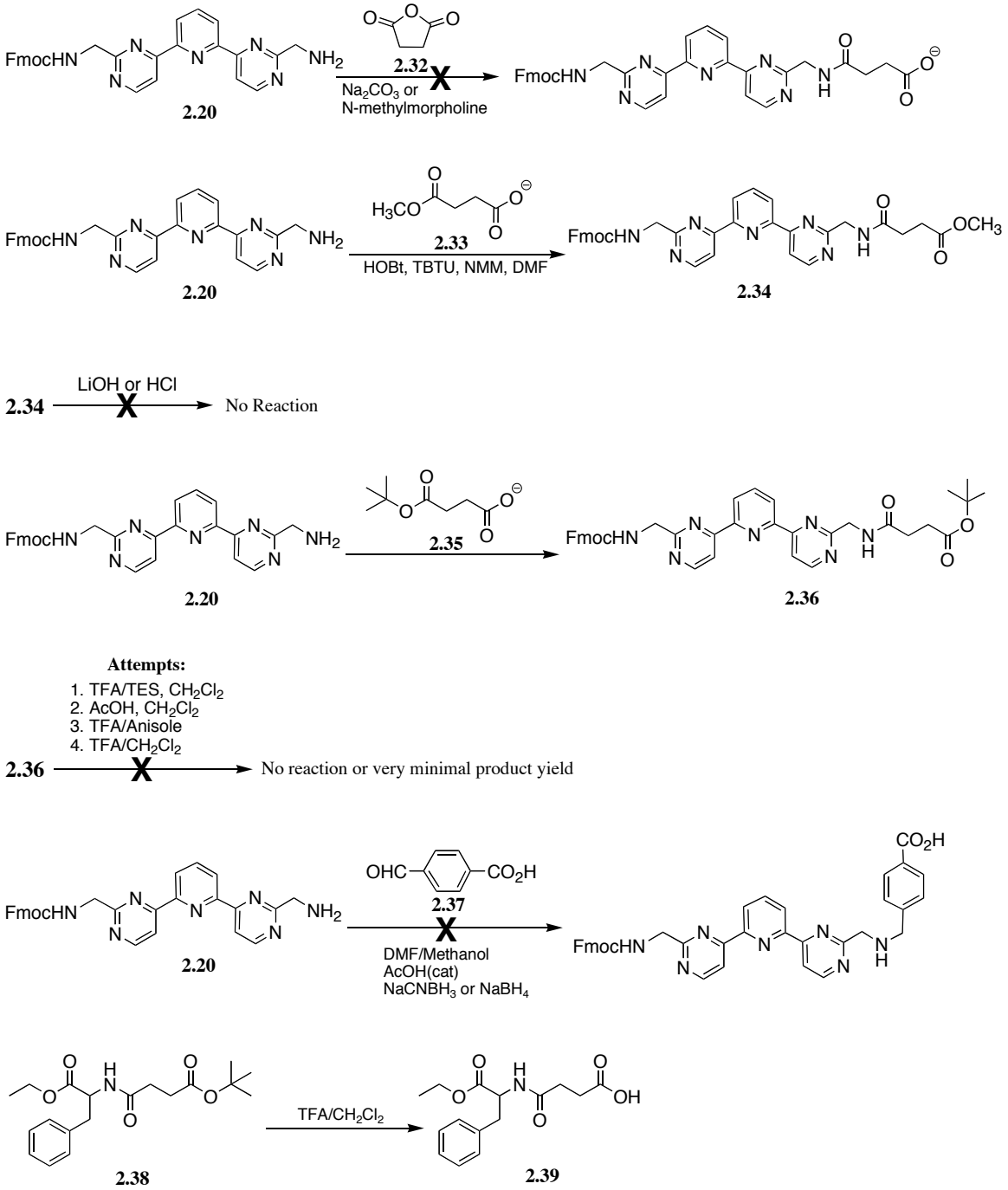

2.6 Binding Studies

2.6.1 Cu(II)Cl_2 Coordination

The absorbance spectrum of **2.1** was used to monitor binding to divalent Cu(II)Cl_2. Binding studies were carried out in a water/methanol solution (1:1, buffered with 100 mM HEPES, pH 7.4) with a constant **2.1** concentration (100 μM) using a 1.2 mL sample volume in a 3 mL quartz cuvet. Each titration of Cu(II) added was 0.2 equivalents, and the titrant solution was prepared to ensure that the concentration of buffer and ligand would not change over the course of the titration. The absorbance spectrum changed moderately upon complexation to Cu(II) as shown in Figure 2.1. Though a clear isosbestic point did not form upon chelation, the absorbance spectrum shifts to a wavelength max of 322 nm and saturates after ~1.8 equivalents of added Cu(II).

Figure 2.1 Addition of $Cu(II)Cl_2$ to **2.1** (water/methanol, 1:1, pH 7.4).

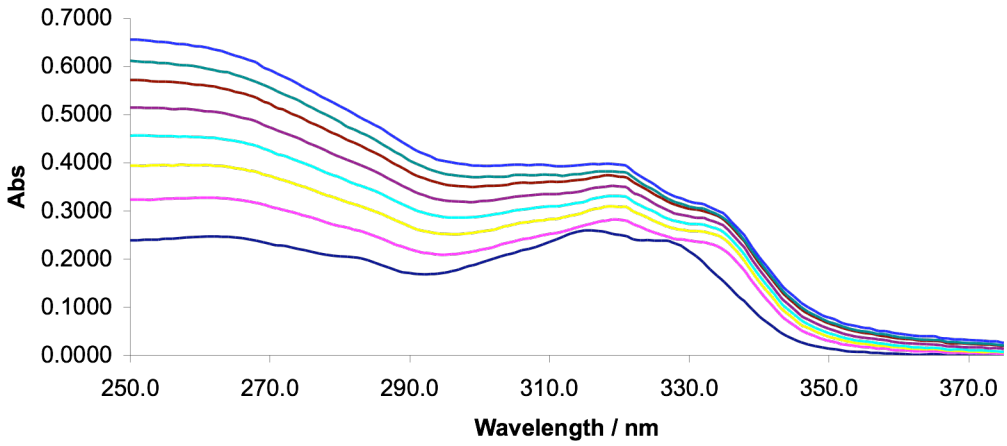

Association constants for the metal-ligand complex were determined by fitting experimental binding curves to theoretical binding curves generated using equation 1,[20,34] assuming a 1:1 stoichiometry for the equilibrium shown in equation 2. The concentration of the free metal ion [M] is related to known variables and parameters by the quadratic equation 3.

$$\Delta A = (\Delta\varepsilon K_f[M][L]_t)/(1 + K_f[M]) \qquad (1)$$

$$[M] + [L] \overset{[K_f]}{\rightleftharpoons} [ML] \qquad (2)$$

$$K_f = [ML]/([M][L]$$

$$[M] = -b + (b^2 - \{4K_f[M]_t\}^{1/2})/2K_f \qquad (3)$$

The parameters in the equations above are defined as: $\Delta\varepsilon$ = the difference in the extinction coefficient between the ligand and M:L complex; K_f = formation constant of the M:L complex; [M] = concentration of free metal; $[M]_t$ = total concentration of metal added to the solution; $[L]_t$ = total concentration of ligand **2.1** in the solution; [L] =

concentration of free ligand **2.1**; [ML] = concentration of the complex; $b = 1 - K_f[M]_t + K_f[L]_t$. An Excel spreadsheet had been generated previously by the Anslyn group that employed the above equations to create theoretical binding curves. Figure 2.2 shows the experimental binding curve for Cu(II) ligation by **2.1**. This curve is generated by plotting the absorbance of starting **2.1** and subsequent titrations at 322 nm. Using the theoretical binding equations, a formation constant for the M:L complex was determined as 7.5×10^4 M^{-1}. This is consistent with the experimentally determined M:**2.8** formation constants. Clearly, addition of the peptidic arms decreases the affinity of **2.1** for Cu(II) as compared to **2.6**.

Figure 2.2 Experimental Binding Curve for Cu(II) Complexation with **2.1**.

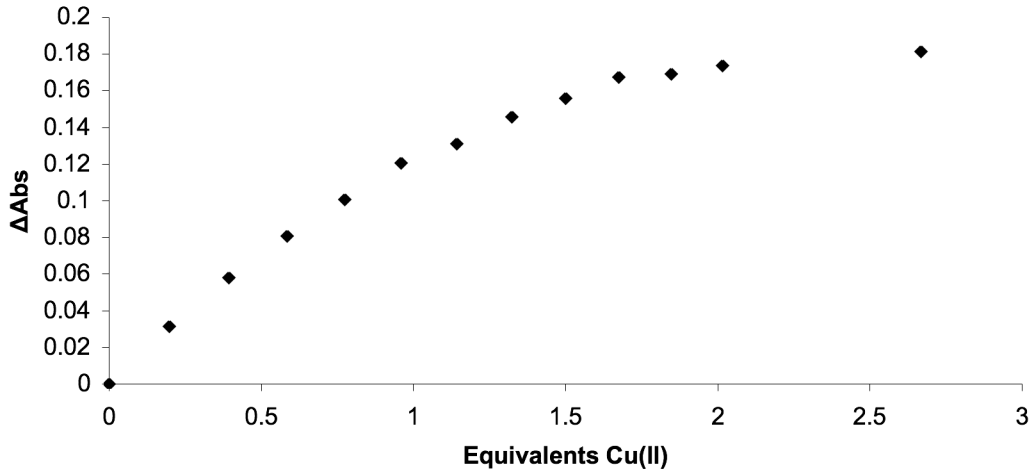

2.6.2 Amino Acid and Oligopeptide Binding Studies with 2.1

A number of amino acids, protected amino acids, and tripeptides were tested for binding to a **2.1:Cu(II)** complex (1:1) in a water/methanol solution (1:1, buffered with 100 mM HEPES, pH 7.4). Concentration of the metal-ligand complex was held constant

during titration of amino acids/tripeptides (100 μM). Upon binding any guest, there was an overall hypsochromic shift, and three isosbestic points were well defined (λ = 298, 322, and 330 nm) as seen in Figure 2.3. Using the absorption data obtained at 314 nm, binding constants were calculated using the 1:1 binding algorithm described above according to the following equilibrium:

$$[\text{M:}\mathbf{2.1}] + [\text{Amino Acid}] \underset{}{\overset{K_f}{\rightleftharpoons}} [\text{M:}\mathbf{2.1}\text{:Amino Acid}]$$

Table 2.3 shows the affinity of the metal:host complex for the various amino acids, protected amino acids, and tripeptides measured at 25 °C. Figure 2.4 shows a number of representative experimental binding curves for various analytes that were fit with theoretical algorithms to give the affinities found in Table 2.3.

Figure 2.3 UV/Vis Absorbance Spectrum of Titration of L-Histidine to a Constant Concentration of **2.1**:Cu(II) in Water/Methanol (1:1).

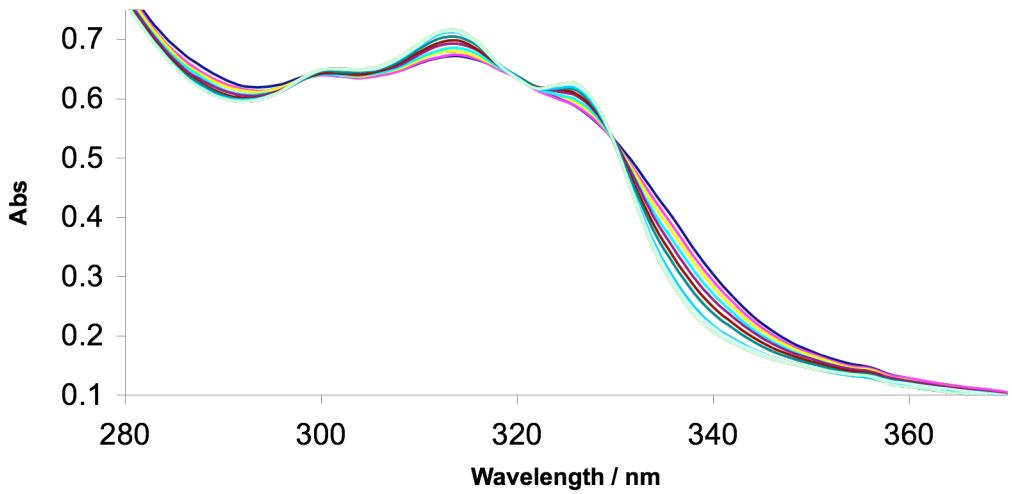

It is evident from Table 2.3 and the binding curves of Figure 2.4 that those amino acids that are good copper ligands bound well to the receptor complex. L-His, D/L-Cys, and L-Met, with their coordinating imidazole nitrogen, thiol, and thioether respectively, bound the copper complex. As would be expected, the thioether of L-Met had a reduced association constant. The association constants also fit our hypothesis that a strong metal ligand, such as L-His, with two additional amino acids (L-Lys-L-Lys) with molecular recognition sites that complement **2.1** would bind well. Further, strong association was witnessed with L-Cys and its respective L-Lys containing tripeptide. Additionally, the association constants of the protected peptides show that amino acids bound through their amino termini. When L-His was acylated at its amino terminus, no measurable binding occurred. However, the methyl ester L-His with a free amino terminus did bind. When a tripeptide terminated in the carboxyl group of L-His followed by two lysines, no binding was experimentally determined.

Table 2.3 Association Constants (M-1) of **2.1**:Cu(II) with Various Amino Acids, Protected Amino Acids, and Oligopeptides (n.d. = not determined).

Analyte	Association Constant
Ac-L-His	n.d.
L-His-OMe	1.0×10^5
L-His	$1.2 \times 10^5 – 2.55 \times 10^5$
D/L-Cys	8.0×10^4
L-Met	3.0×10^3
L-Val	n.d.
Gly	n.d.
L-His- L-Lys- L-Lys	1.0×10^6
L-His-Gly-Gly	1.5×10^4
Gly-Gly-Gly	n.d.
L-Cys- L-Lys- L-Lys	3.0×10^5
L-Cys-Gly-Gly	5.0×10^2
L-Met- L-Lys- L-Lys	1.0×10^5
L-Met-Gly-Gly	2.5×10^4

Importantly, L-His bound with an experimentally determined association constant as high as 2.55 x 10^5 M^{-1}, but the tripeptide HKK had an association constant of 10^6 M^{-1}. This illustrates the effect of the two additional residues and demonstrates the validity of our preorganized chemosensor design. Indeed, the peptide arms of **2.1** enhanced the binding event. This was verified further by noting the differences in association constants between L-Met and MKK. Methionine is not a strong metal ligand, but as a

tripeptide with complementing functionalities to the receptor, MKK bound via ion-pairing. The importance of the peptide arms was also shown through the minimal binding constants obtained when the first amino acid was followed by two glycines. In these instances, the binding event was significantly decreased or nonexistent. Therefore, the data demonstrated that both the Cu(II) and the pendant peptide arms were important for binding. There is at least a ten-fold increase in binding when multivalent binding through the side arms was exploited. In summary, a selective receptor for L-His-L-Lys-L-Lys was developed. It was demonstrated that the metal binding site and the pendant peptide arms of the receptor enhance the affinity through a cooperative effect for **2.2**.

Figure 2.4 Representative Experimental Binding Curves Generated From Absorbance Spectrum (314 nm) Titrations with: (a) L-Met; (b) MGG; (c) MKK; (d) HGG; (e) HKK.

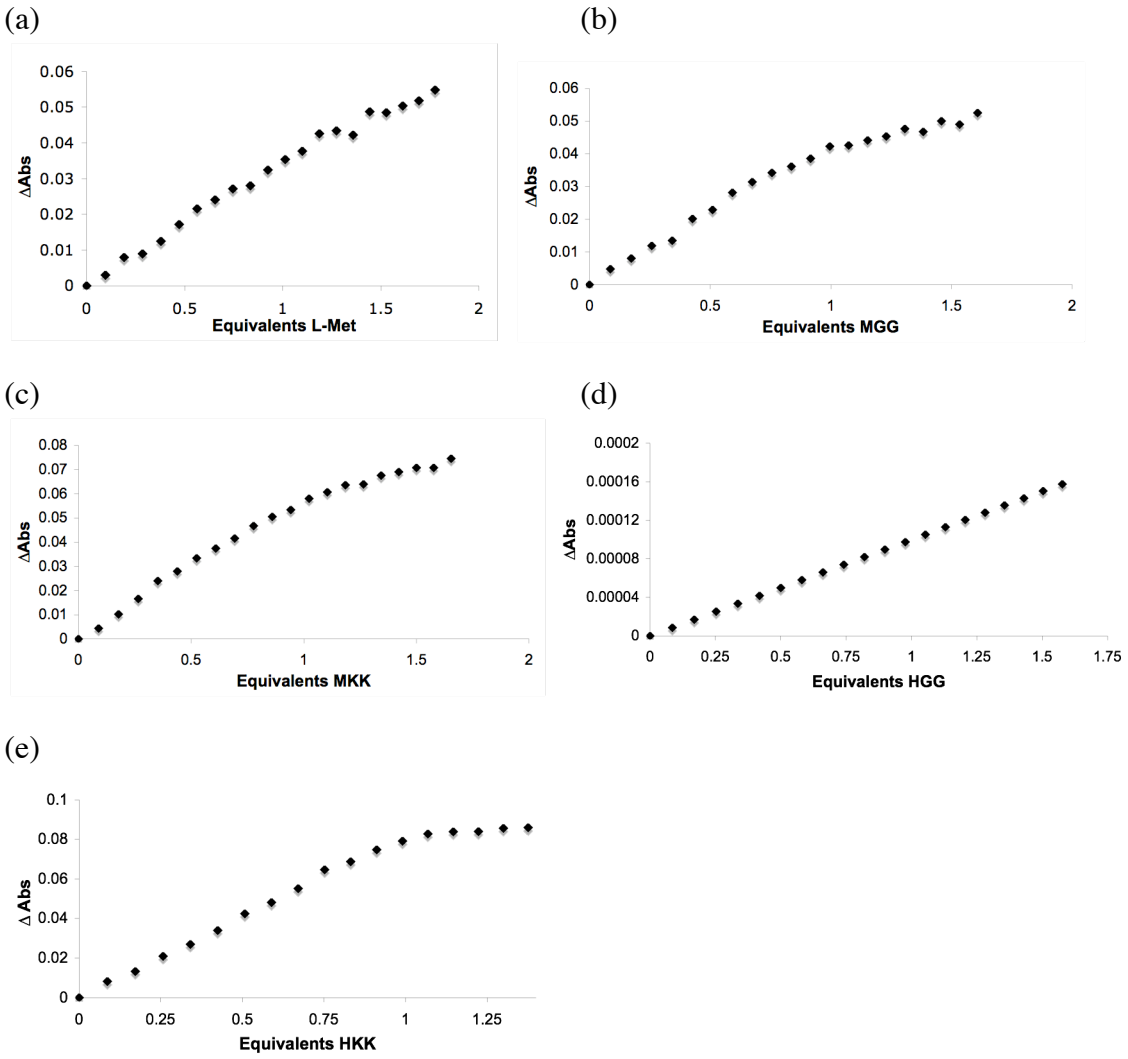

2.7 Experimental

General. Reactions were run under an atmosphere of argon unless otherwise indicated. Anhydrous solvents were transferred by an oven-dried syringe. Flasks were flame dried under a stream of argon. The chemicals were obtained from Acros Organics, Aldrich, Alfa Aesar, and NovaBiochem and were used without further purification unless otherwise noted. Methlyene chloride and triethylamine were distilled over calcium hydride. A Varian Gemini 400 MHz NMR was used to obtain ^{1}H and ^{13}C spectra. A Finnigan MAT-VSQ 700 spectrometer was used to obtain low-resolution mass spectra. Melting points were measured on a Thomas Hoover capillary melting point apparatus and are uncorrected. The UV-visible absorption measurements were recorded on a Beckman DU640 spectrometer. All products were dried for at least 6 hours prior to spectral analysis.

Procedures:

The syntheses of **2.12**, **2.15**, and **2.26** have been detailed in references 24, 26, and 28 respectively.

(4-{6-[2-(*tert*-butoxycarbonylamino-methyl)-pyrimidin-4-yl]-pyridin-2-yl}-pyrimidin-2-ylmethyl)-carbamic acid *tert*-butyl ester (2.16)

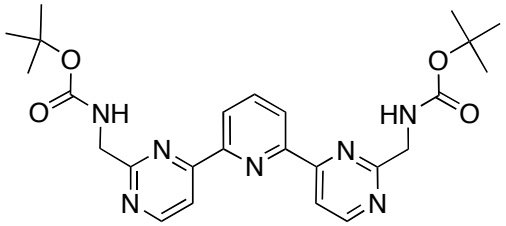

Bisenaminone **2.15** (2.77g, 10.1 mmol) and N-Boc-aminomethylcarboxamidine **2.12** (13.70 g, 50.19 mmol) were dissolved in absolute ethanol (95 ml) at 90 °C. Sodium metal (2.08 g, 90.2 mmol) was also dissolved in absolute ethanol (55 mL). The sodium ethoxide was added to the reaction that was held at 90 °C for 24 h. Within 1 h of NaOEt addition the solution turned dark purple. After 24 h the reaction was concentrated *in vacuo* and the solid residue redissolved in methylene chloride (200 mL). The organic layer was washed with water (3 x 100 mL), sat. $NaHCO_3$ (2 x 50 mL), and sat. NaCl (1 x 60 mL). The organic layer was dried over sodium sulfate and concentrated *in vacuo*. The product was purified on alumina gel chromatography (ethyl acetate as eluent) to yield an off-white solid (2.01 g, 4.08 mmol), mp: 205 ºC (decomposition). 40% yield. ^{1}H NMR ($CDCl_3$): 8.85 (d, 2H), 8.67 (d, 2H), 8.36 (d, 2H), 8.06 (t, 1H), 5.71 (b, 2H), 4.72 (d, 4H), 1.5 (s, 18H). ^{13}C NMR ($CDCl_3$): 166.9, 162.5, 159, 156.1, 153.6, 139, 123.7, 115.4, 79.6, 46.4, 28.7. MS (CI^+) *m/z* 494 $[M]^+$.

C-{4-[6-(2-aminomethyl-pyrimidin-4-yl)-pyridin-2-yl]-pyrimidin-2-yl}-methylamine (2.17)

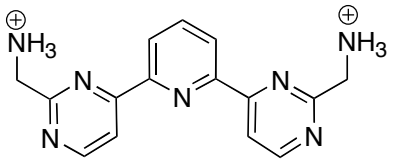

2.16 (2.01 g, 4.08 mmol) was dissolved in a 5:1 methylene chloride:trifluoroacetic acid solution (20 mL). The solution was stirred for 2 h. The product was precipitated upon addition of absolute ethanol (50 mL), washed with ether, and collected via vacuum filtration to yield **2.17** as a white solid (as TFA salt) (2.05 g, 3.88 mmol), mp: 230 ºC (decomposition). 95% yield. ^{1}H NMR (CD_3OD): 8.87 (d, 2H), 8.67 (d, 2H), 8.59 (d, 2H), 8.18 (t, 1H), 4.22 (d, 4H). ^{13}C NMR (CD_3OD): 163.7, 162.5, 159.4, 153.4, 139.9, 125, 117.7, 44.2. MS (CI^+) *m/z* 294 $[M]^+$.

{4-[6-(2-aminomethyl-pyrimidin-4-yl)-pyridin-2-yl]-pyrimidin-2-ylmethyl}-carbamic acid *tert*-butyl ester (2.18)

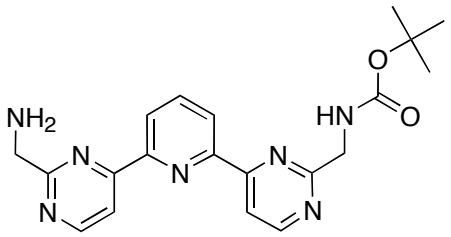

Free-based **2.17** (0.414 g, 1.41 mmol) was dissolved in deionized water (10 mL). The solution was cooled to 0 °C upon which Boc_2O (0.077 g, 0.35 mmol) in isopropanol (2 mL) was added dropwise. The reaction was warmed to room temperature and stirred for

24 hours. The solvent was removed *in vacuo* and the residue redissolved in 1M NaOH. The mono and diboc protected compounds were extracted with ethyl acetate. The aqueous layer was also extracted with methylene chloride to yield the unreacted diamine. The ethyl acetate layer was extracted with 10% citric acid, basified, and the monoboc product extracted with methylene chloride. 46% yield of monoboc (pale yellow solid), mp: 118 ºC (decomposition). Further reaction of the diamine gave an overall 81% yield of the monoboc protected heterocycle **2.18** (0.450 g). ^{1}H NMR (CD_2Cl_2): 8.65 (d, 2H), 8.33 (d, 2H), 8.1 (d, 2H), 7.79 (t, 1H), 6.31 (b, 1H), 6.08 (b, 1H), 4.53 (d, 2H), 4.06 (d, 2H), 1.46 (s, 9H). ^{13}C NMR (CD_2Cl_2): 170.4, 166.3, 161.9, 157.8, 155.5, 153.1, 137.8, 122.4, 114.7, 78.6, 48.1, 45.7, 28.0. MS (CI^+) *m/z* 394 $[M]^+$.

[4-(6-{2-[(9*H*-fluoren-9-ylmethoxycarbonylamino)-methyl]-pyrimidin-4-yl}-pyridin-2-yl)-pyrimidin-2-ylmethyl]-carbamic acid *tert*-butyl ester (2.19)

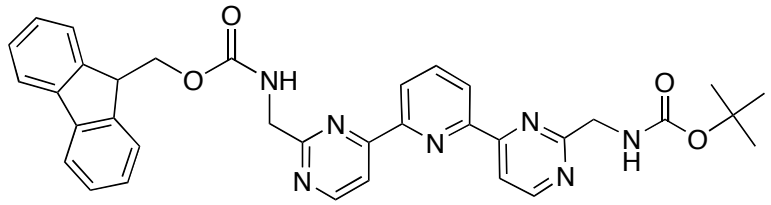

2.18 (0.058 g, 0.147 mmol) was dissolved in *p*-dioxane (8 mL). The pH was set to 8.5 with 10% $NaHCO_3$. 9-fluorenylmethoxy acid chloride (0.045 g, 0.147 mmol) in *p*-dioxane (4 mL) was added and the reaction stirred for 24 hours. Precipitation of the product occurred upon addition of deionized water (30 mL). The product was filtered and washed with water to give **2.19** as an off-white solid (0.076 g, 0.123 mmol), mp: 149 ºC (decomposition). 83% yield. ^{1}H NMR ($CDCl_3$): 8.88 (t, 2H), 8.66 (t, 2H), 8.40 (t, 2H), 8.02 (t, 2H), 7.75 (d, 2H), 7.70 (d, 2H), 7.36 (d, 2H), 7.30 (d, 2H), 6.09 (b, 1H), 5.78

(b, 1H), 4.81 (d, 2H), 4.70 (d, 2H), 4.47(d, 2H), 4.32 (t, 1H), 1.48 (s, 9H). ^{13}C NMR ($CDCl_3$): 166.4, 162.6, 162.4, 158.3, 153.9, 143.9, 141.3, 138.5, 127.7, 127, 125.1, 123.6, 120, 115.6, 79.9, 67.6, 47.2, 46.7, 28.4. MS (CI^+) *m/z* 616 $[M]^+$.

{4-[6-(2-aminomethyl-pyrimidin-4-yl)-pyridin-2-yl]-pyrimidin-2-ylmethyl}-carbamic acid 9*H*-fluoren-9-ylmethyl ester (2.20)

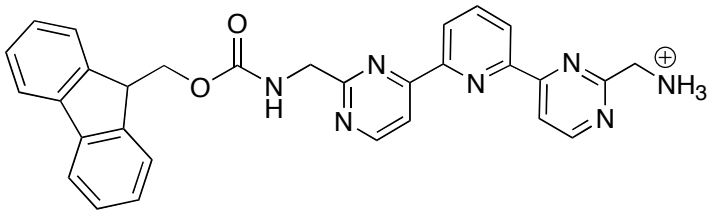

Dissolved **2.19** (0.445 g, 0.724 mmol) in a 1:1 solution of TFA:toluene (10 mL). The solution was stirred vigorously for two hours and subsequently the solvent was removed *in vacuo*. Excess TFA was azeotroped off by the addition and removal of toluene *in vacuo*. The residue was dissolved in DMF (0.6 mL) and DMF was removed under reduced pressure in the presence of silica gel (0.4 g). The compound adsorbed on silica gel was placed at the top of a silica gel chromatography column (99:1 DCM: MeOH (Sat. NH_3) as eluent). **2.20** was collected from the column as an off-white solid (0.335 g), 90% yield, mp: 126 ºC (decomposition). ^{1}H NMR (DMF): 9.03 (dd, 2H), 8.73 (dd, 2H), 8.57 (dd, 2H), 7.97 (d, 2H), 7.82 (d, 2H), 7.48 (t, 1H), 7.36 (t, 2H), 4.71 (d, 2H), 4.37 (m, 3H), 4.09 (s, 2H). ^{13}C NMR (DMF): 170.9, 167.4, 158.7, 158.4, 156.7, 153.5, 153.3, 143.9, 140.8, 138.7, 128.6, 127.3, 126.9, 126.7, 125, 122.9, 120.9, 119.7, 119.5, 115, 114.6, 108.4, 65.9, 48.3, 46.7, 46.5. MS (CI^+) *m/z* 294, 179 $[M]^+$.

Representative Solid Phase Procedure. The resin was washed for two minutes with 5 mL of each of the following prior to and after the reaction: DMF, DCM (2x), MeOH (2x), and DMF. Fmoc-protected acid (0.052 mmol), HOBt (0.212 mmol), TBTU (0.212 mmol), and N-methylmorpholine (0.848 mmol) were dissolved in DMF (4 mL). This was stirred for 15 minutes (the time necessary for activated ester formation). This solution was added to the resin (0.106 mmol) bearing a free amino group and mixed for 3-4 h followed by washing. The resin was dried under reduced pressure, and a ninhydrin test and mass spectra were obtained. Negative ninhydrin tests were associated with complete coupling of the Fmoc protected amino acids.

The resin was then washed once again, and subjected to a 20% solution of piperidine in DMF that removed the Fmoc and Fm protecting groups. This solution was mixed for 10-15 minutes. Washing of the resin followed. The resin was dried on the high vacuum, and the ninhydrin test completed. Positive ninhydrin tests were associated with protecting group removal. Upon completion of the solid phase synthesis the compound was cleaved from the resin using a 60/39/1 TFA/CH_2Cl_2/Triethylsilane solution. The product was obtained by precipitation with ether, and was subsequently dissolved in water and lyophilized multiple times to obtain solid products.

Synthesis of 2.1

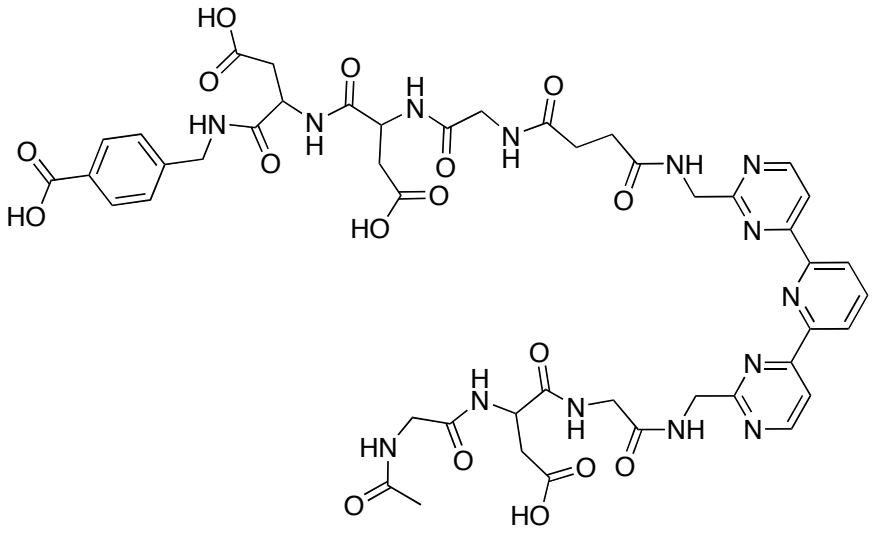

4-aminomethylbenzoyl-2-chlorotrityl resin (1.0 mmol/g loading, 0.44 g, 0.44 mmol, 1.0 eq) was washed as described above. In a separate flask Fmoc-Asp(O*t*Bu)-OH (0.208 g, 0.53 mmol, 1.2 eq), HOBt (0.124 g, 0.88 mmol, 2.0 eq), TBTU (0.288 g, 0.88 mmol, 2.0 eq), and N-methylmorpholine (NMM) (0.4 mL, 0.352 mmol, 8.0 eq) were dissolved in DMF (10 mL) and stirred for 15 minutes. Upon formation of the activated ester the solution was added to the resin and mixed for 4 h. The reaction solution was flushed from the resin and the resin was thoroughly washed. A ninhydrin test was negative indicating the desired peptide formation. To remove the Fmoc group 20% piperidine in DMF (9 mL) was added and mixed for 1 h. A ninhydrin test was positive indicating the desired free amine group. Following this first amino acid addition to the resin two more were added using the exact same conditions and reagents except for the following amino acids: Fmoc-Asp(O*t*Bu)-OH (0.208 g, 0.53 mmol, 1.2 eq) and Fmoc-Gly (0.158 g, 0.53 mmol, 1.2 eq). After addition of the third amino acid the Fmoc group was removed as before and a ninhydrin test was positive as desired. Addition of the linker **2.26** (.157 g,

0.53 mmol, 1.2 eq) was completed using the same amounts of HOBt, TBTU, and NMM, and solvent. Removal of the Fm protecting group was completed using 20% piperidine in DMF (9 mL) with a short 10 minute reaction time. Reaction times longer than 20 minutes resulted in undesirable side products, likely the succinic anhydride. A ninhydrin test at this point was positive for the free carboxy terminus. The Fmoc-protected core of the receptor **2.20** (0.109 g, 0.212 mmol, 1.2 eq) was added using the same reagents as with the amino acids. The Fmoc group was removed using 20% piperidine in DMF (12 mL) with an increased reaction time of 1.5 h. The last three amino acids were added in the same manner as those above: Fmoc-Gly (0.063 g, 0.211 mmol, 1.2 eq), Fmoc-Asp(O*t*Bu)-OH (0.0833 g, 0.211 mmol, 1.2 eq), and Acyl-Gly (.0247 g, 0.211 mmol, 1.2 eq). Upon completion of the solid phase synthesis **2.1** was cleaved from the resin using a TFA/CH_2Cl_2/Triethylsilane solution (60/39/1). The product was obtained by precipitation with ether and was subsequently dissolved in water and lyophilized multiple times to obtain a white fluffy solid (0.142 g, 74.3% yield). ^{1}H NMR (CD_3OD): 8.8 (d, 2H), 8.41 (d, 2H), 7.83 (m, 3H), 7.25 (m, 4H), 4.65 (m, 3H), 4.36 (m, 6H), 3.71 (m, 6H), 2.71 (m, 6H), 2.37 (m, 6H), 1.85 (s, 3H). MS (CI^-) *m/z* 1083.5 $[M]^-$.

Synthesis of Tripeptide Analytes. 2.2 as Example.

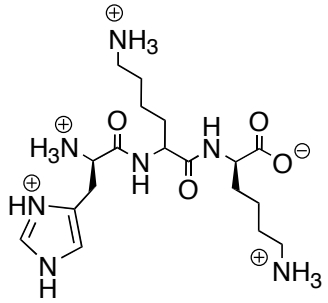

Fmoc-Lys(Boc)-OH (0.330 g, 0.704 mmol, 1.1 eq) was dissolved in methylene chloride (10 mL) and NMM was added (0.3 mL, 2.56 mmol, 4.0 eq). To this reagent solution was added 2-chlorotritylchloride resin (1.6 mmol/g loading, 0.400 g, 0.64 mmol, 1.0 eq). This reaction stirred 1 h. Unreacted resin was quenched with a 9:1 methanol:diisopropylethylamine (10 mL) solution. The resin was filtered from the reaction solution and washed in typical fashion with methylene chloride, DMF, and methanol. The Fmoc group was removed with 20% piperidine in DMF (10 mL), 1 h run time. The second amino acid, Fmoc-Lys(Boc)-OH (0.36 g, 0.77 mmol, 1.2 eq), was dissolved with HOBt (0.173 g, 1.28 mmol, 2.0 eq), TBTU (0.411 g, 1.28 mmol, 2.0 eq) and NMM (0.56 mL, 5.12 mmol, 8.0 eq) in DMF (10 mL). The solution was stirred for 15 minutes and added to the resin (1.0 eq). The Fmoc group was removed in standard fashion. Fmoc-His(Boc)-OH (0.443 g, 0.77 mmol, 1.2 eq) was added to the resin with the same reagents and times as listed before. The Fmoc group was removed in standard fashion. HKK was cleaved from the resin using methylene chloride/TFA/TES (60:39:1) (10 mL) for a 4 h run time. Precipitation and lyophilization as described in the synthesis of **2.1** was used to collect the solid HKK product (0.45 g, 85.9%). ^{1}H NMR (CD_3OD): 8.72 (s, NH), 8.25 (s, NH), 7.87 (s, NH), 7.35 (s, 1H), 7.05 (d, 1H), 4.63 (t, 1H), 4.19 (t,

1H), 3.89 (t, 1H), 3.05 (d, 2H), 2.81 (m, 4H), 1.78 (m, 4H), 1.59 (m, 4H), 1.42 (m, 4H). MS (CI^+) *m/z* 415 $[M]^+$.

UV/Vis titrations of Cu(II)Cl_2 and 2.1:

All solutions were buffered at pH 7.4 with HEPES buffer (100 mM) in 50% methanol in water (v/v). A solution of **2.1** (100 μM, 1.2 mL) was prepared in a quartz cuvette and into this was titrated a stock solution of Cu(II) (each 5 μL titration was 0.1 equivalents) keeping the buffer and host concentration constant. The data was collected at 322 nm to determine the association constant.

UV/Vis titrations of amino acids, protected amino acids, and tripeptides and 2.1:

All solutions were buffered at pH 7.4 with HEPES buffer (100 mM) in 50% methanol in water (v/v). A 1:1 complex of **2.1**:Cu(II) (100 μM) was prepared in a quartz cuvette (total volume 1.2 mL) and into this was titrated a stock solution of amino acid/protected amino acid/oligopeptide (each 5 μL titration was 0.1 equivalents) keeping the buffer and host:Cu(II) concentration constant. The data was collected at 314 nm to determine the association constant.

2.8 References

1) (a) Fischer, E. *Ber. Deutsch. Chem. Ges.* **1894**, *27*, 2985. (b) Behr, J. –P. *The Lock and Key Principle, The State of the Art – 100 Years On*. New York: John Wiley and Sons, 1994.

2) Wright, A. T.; Anslyn, E. V. Cooperative Metal-Coordination and Ion Pairing in Tripeptide Recognition. *Org. Lett.* **2004**, *6*, 1341-1344.

3) Ait-Haddou, H.; Wiskur, S. L.; Lynch, V. M.; Anslyn, E. V. Achieving Large Color Changes in Response to the Presence of Amino Acids: A Molecular Sensing Ensemble with Selectivity for Aspartate. *J. Am. Chem. Soc.* **2001**, *123*, 11296-11297.

4) (a) Nowick, J. S.; Chung, D. M.; Maitra, S.; Stigers, K.; Sun, Y. An Unnatural Amino Acid that Mimics a Tripeptide β-Strand and Forms β-Sheetlike Hydrogen-Bonded Dimers. *J. Am. Chem. Soc.* **2000**, *122*, 7654-7661. (b) Nowick, J. S.; Lam, K. S.; Khasanova, T. V.; Kemnitzer, W. E.; Maitra, S.; Mee, H. T.; Lui, R. An Unnatural Amino Acid that Induces β-Sheet Folding and Interaction in Peptides. *J. Am. Chem. Soc.* **2002**, *124*, 4972-4973. (c) Nowick, J. S.; Chung, D. M. Sequence-Selective Molecular Recognition Between Beta-Sheets. *Angew. Chem. Int. Ed.* **2003**, *42*, 1765-1768. (d) Chung, D. M.; Nowick, J. S. Enantioselective Molecular Recognition between β-Sheets *J. Am. Chem. Soc.* **2004**, *126*, 3062-3063.

5) (a) Schneider, J. P.; Kelly, J. W. Templates That Induce alpha-Helical, beta-Sheet, and Loop Conformations. *Chem. Rev.* **1995**, *95*, 2169-2187. (b) Nowick, J. S. Chemical Models of Protein β-Sheets. *Acc. Chem. Res.* **1999**, *32*, 287-296. (c) Schmuck, C. E.; Wienand, W.; Geiger, L. Bioorganic Receptors for Amino Acids and Peptides: Combining Rational Design with Combinatorial Chemistry. *Highlights in Bioorganic Chemistry*. Schmuck, C.; Wennemers, H., Eds.; Wiley-VCH: London, 2003; pp.140-153.

6) (a) Carrell, R. W.; Lomas, D. A. Conformational Disease. *Lancet* **1997**, *350*, 134-138. (b) Schneider, H. –J.; Eblinger, F.; Sirish, M. Synthetic Peptide Receptors: Noncovalent Interactions Involving Peptides. *Advances in Supramolecular Chemistry*. Gokel, G. W., Ed.; JAI Press: Stamford, CT, 2000; V. 6, pp. 185-216.

7) (a) Yoon, S. S.; Still, W. C. An Exceptional Synthetic Receptor for Peptides. *J. Am. Chem. Soc.* **1993**, *115*, 823-824. (b) Yoon, S. S.; Still, W. C. Synthesis and Properties of A4B6 Cyclooligomeric Receptors. *Tetrahedron Lett.* **1994**, *35*, 2117-2120. (c) Yoon, S. S.; Still, W. C. Cyclooligomeric Receptors for the Sequence Selective Binding of Peptides. A Tetrahedral Receptor from Trimesic Acid and 1,2-Diamines. *Tetrahedron Lett.* **1994**, *35*, 8557-8560. (d) Yoon, S. S.; Still, W. C. Sequence-Selective Peptide Binding with a Synthetic Receptor. *Tetrahedron* **1995**, *51*, 567-578. (d) Chen, C. –T.; Wagner, H.; Still, W. C. Fluorescent, Sequence Selective Peptide Detection by Synthetic Small Molecules. *Science* **1998**, *279*, 851-853. (e) Henley, P. D.; Kilburn, J. D. A Synthetic Receptor for the Cbz-L-Ala-L-Ala-OH Dipeptide Sequence. *Chem. Commun.* **1999**, 1335-1336.

8) (a) Tabet, M.; Labroo, V.; Sheppard, P.; Sasaki, T. Spermine-Induced Conformational Changes of a Synthetic Peptide. *J. Am. Chem. Soc.* **1993**, *115*, 3866-3868. (b) Albert, J. S.; Goodman, M. S.; Hamilton, A. D. Molecular Recognition of Proteins: Sequence-Selective Binding of Aspartate Pairs in Helical Peptides. *J. Am. Chem. Soc.* **1995**, *117*, 1143-1144. (c) LaBrenz, S. R.; Kelly, J. W. Peptidomimetic Host that Binds a Peptide Guest Affording a β-Sheet Structure that Subsequently Self-Assembles. A Simple Receptor Mimic. *J. Am. Chem. Soc.* **1995**, *117*, 1655-1656. (d) Torneiro, M.; Still, W. C. Sequence-Selective Binding of Peptides in Water by a Synthetic Receptor Molecule. *J. Am. Chem. Soc.* **1995**, *117*, 5887-5888. (e) Breslow, R.; Yang, Z.; Ching, R.; Trojandt, G.; Odobel, F. Sequence Selective Binding of Peptides by Artificial Receptors in Aqueous Solution. *J. Am. Chem. Soc.* **1998**, *120*, 3536-3537. (f) Hossain, M. A.; Schneider, H. –J. Sequence-Selective Evaluation of Peptide Side-Chain Interaction. New Artificial Receptors for Selective Recognition in Water. *J. Am. Chem. Soc.* **1998**, *120*, 11208-11209. (g) Hart, B. R.; Shea, K. J. Synthetic Peptide Receptors: Molecularly Imprinted Polymers for the Recognition of Peptides Using Peptide-Metal Interactions. *J. Am. Chem. Soc.* **2001**, *123*, 2072-2073. (h) Ojida, A.; Mito-oka, Y.; Inoue, M.; Hamachi, I. First Artificial Receptors and Chemosensors Toward Phosphorylated Peptide in Aqueous Solution. *J. Am. Chem. Soc.* **2002**, *124*, 6256-6258. (i) Schmuck, C.; Geiger, L. Carboxylate Binding by Guanidiniocarbonyl Pyrroles: From Self-Assembly to Peptide Receptors. *Curr.*

Org. Chem. **2003**, *7*, 1485-1502. (j) Ojida, A.; Mito-oka, Y.; Sada, K.; Hamachi, I. Molecular Recognition and Fluorescence Sensing of Monophosphorylated Peptides in Aqueous Solution by Bis(zinc(II)-dipicolylamine)-Based Artificial Receptors. *J. Am. Chem. Soc.* **2004**, *126*, 2454-2463. (k) Buryak, A.; Severin, K. An Organometallic Chemosensor for the Sequence-Selective Detection of Histidine- and Methionine-Containing Peptides in Water at Neutral pH. *Angew. Chem. Int. Ed.* **2004**, *43*, 4771-4774. (l) Schmuck, C.; Geiger, L. Dipeptide Binding in Water by a de Novo Designed Guanidiniocarbonylpyrrole Receptor. *J. Am. Chem. Soc.* **2004**, *126*, 8898-8899. (m) Rzepecki, P.; Nagel-Steger, L.; Feuerstein, S.; Linne, U.; Molt, O.; Zadmard, R.; Aschermann, K.; Wehner, M.; Schrader, T.; Riesner, D. Prevention of Alzheimer's Disease-Associated Aβ Aggregation by Rationally Designed Nonpeptidic β-Sheet Ligands. *J. Biol. Chem.* **2004**, *279*, 47497-47505. (n) Mandl, C. P.; König, B. Luminescent Crown Ether Amino Acids: Selective Binding to N-Terminal Lysine in Peptides. *J. Org. Chem.* **2005**, *70*, 670-674. (o) Tashiro, S.; Tominaga, M.; Kawano, M.; Therrien, B.; Ozeki, T.; Fujita, M. Sequence-Selective Recognition of Peptides within the Single Binding Pocket of a Self-Assembled Coordination Cage. *J. Am. Chem. Soc.* **2005**, *127*, 4546-4547. (p) Wehner, M.; Janssen, D.; Schäfer, G.; Schrader, T. Sequence-Selective Peptide Recognition with Designed Molecules. *Eur. J. Org. Chem.* **2006**, 138-153.

9) Martell, A. E.; Smith, R. M. *Critical Stability Constants Volume 5: First Supplement*. Plenum Press: New York, 1982, p. 253.

10) (a) Irving, H.; Williams, R. J. P. Order of Stability of Metal Complexes. *Nature* **1948**, *162*, 746-747. (b) Irving, H. M.; Williams, R. J. P. Some Factors Controlling the Selectivity of Organic Reagents. *Analyst* **1952**, *77*, 813-829.

11) Irving, H.; Williams, R. J. P. The Stability of Transition-Metal Complexes. *J. Chem. Soc.* **1953**, 3192-3210.

12) Bonizzoni, M.; Fabbrizzi, L.; Piovani, G.; Taglietti, A. Fluorescent Detection of Glutamate with a Dicopper (II) Polyamine Cage. *Tetrahedron* **2004**, *60*, 11159-11162.

13) Hortala, M. A.; Fabbrizzi, L.; Marcotte, N.; Stomeo, F.; Taglietti, A. Designing the Selectivity of the Fluorescent Detection of Amino Acids: A Chemosensing Ensemble for Histidine. *J. Am. Chem. Soc.* **2003**, *125*, 20-21.

14) Kaim, W.; Rall, J. Copper – A "Modern" Element. *Angew. Chem. Int. Ed.* **1996**, *33*, 43-60.

15) Hasenknopf, B.; Lehn, J. –M.; Baum, G.; Fenske, D. Self-Assembly of a Heteroduplex Helicate From Two Different Ligand Strands and Cu(II) Cations. *Proc. Natl. Acad. Sci. USA.* **1996**, *93*, 1397-1400.

16) Patel, R. N.; Singh, N.; Shukla, K. K.; Gundla, V. L. N.; Chauhan, U. K. Synthesis, Characterization and Biological Activity of Ternary Copper (II) Complexes Containing Polypyridyl Ligands. *Spectrochemica Acta Part A* **2006**, *63*, 21-26.

17) Jia, L.; Fu, W.; Yin, Q., Yu, M.; Zhang, J.; Li, Z. Bis(2,2'-bipyridine-N,N')chlorocopper(II) Tetrafluoroborate Dichloromethane Solvate. *Acta. Cryst.* **2005**, *61*, 1039-1041.

18) Bejan, E.; Aït-Haddou, H.; Duran, J.; Balvoine, G. The Reaction of Enaminones with Carboxamidines: A Convenient Route for the Synthesis of Polyaza Heterocycles. *Synthesis* **1996**, 1012-1019.

19) Aït-Haddou, H.; Sumaoka, J.; Wiskur, S. L.; Folmer-Andersen, F.; Anslyn, E. V. Remarkable Cooperativity Between a ZnII Ion and Guanidinium/Ammonium Groups in the Hydrolysis of RNA. *Angew. Chem. Int. Ed.* **2002**, *41*, 4013-4016.

20) Folmer-Andersen, J. F.; Aït-Haddou, H.; Lynch, V. M.; Anslyn, E. V. 2,6-Di(pyrimidin-4-yl)pyridine Ligands with Nitrogen-Containing Auxiliaries: The Formation of Functionalized Molecular Clefts Upon Metal Coordination. *Inorg. Chem.* **2003**, *42*, 8674-8681.

21) Sundberg, R. J.; Martin, R. B. Interactions with Histidine and Other Imidazole Derivatives with Transition Metal Ions in Chemical and Biological Systems. *Chem. Rev.* **1974**, *74*, 471-517.

22) Sovago, I.; Farkas, E.; Gergely, A. Studies on Transition-Metal-Peptide Complexes. Part 7. Copper(II) Complexes of Dipeptides Containing L-Histidine. *J. Chem. Soc. Dalton Trans.* **1982**, 2159-2163.

23) Formation constants can be found in the following: Martell, A. E.; Smith, R. M. *Critical Stability Constants Volume 5: First Supplement*. Plenum Press: New York, 1982.

24) (a) Bailly, C.; Houssin, R.; Bernier, J. –L.; Henichart, J. –P. Depsipeptide Analogs of the Antitumor Drug Distamycin Containing Thiazole Amino Acid Residues. *Tetrahedron* **1988**, *44*, 5833-5843. (b) Lange, U. E. W.; Schäfer, B.; Baucke, D.; Buschmann, E.; Mack, H.; A New Mild Method for the Synthesis of Amidines. *Tetrahedron Lett.* **1999**, *40*, 7067-7071.

25) Bredereck, H.; Simchen, G.; Rebsdat, S.; Kantlehner, W.; Horn, P.; Wahl, R.; Hoffmann, H.; Grueshaber, P. *Chem. Ber.* **1968**, *101*, 41-50.

26) (a) Bejan, E.; Aït-Haddou, H.; Daran, J. –C.; Balavoine, G. G. A. Enaminones in the Synthesis of New Polyaza Heterocycles. *Eur. J. Org. Chem.* **1998**, 2907-2912.

27) Hudson, D. Methodoligical Implications of Simultaneous Solid-Phase Peptide Synthesis. 1. Comparison of Different Coupling Procedures. *J. Org. Chem.* **1988**, *53*, 617-624.

28) Song, A. I.; Rana, T. M. Synthesis of an Amino Acid Analogue to Incorporate *p*-Aminobenzyl-EDTA in Peptides. *Bioconjugate Chem*. **1997**, *8*, 249-252.

29) Murray, R. K. Jr.; Goff, D. L.; Raytch, R. E. Synthesis of 9,10-dehydrohomoadamantane. *Tetrahedron Lett*. **1975**, *16*, 763-764.

30) Ishii, A.; Hojo, H.; Kobayashi, A.; Nakamura, K.; Ito, Y.; Nakahara, Y. A Facile Linker Strategy for the Solid-Phase Synthesis of Protected Glycopeptide: Synthesis of an N-Terminal Fragment of IL-2 (1-10). *Tetrahedron* **2000**, *56*, 6235-6243.

31) Alauddin, M. M.; Fissekis, J. D.; Conti, P. S. α-Alkylation of Amino Acid Derivatives: Synthesis and Chiral Resolution of [^{11}C]β-Aminoisobutyric Acid. *Nuclear Med. Biol.* **1997**, *24*, 771-775.

32) Akaji, K.; Teruya, K.; Akaji, M.; Aimoto, S. Synthesis of Cyclic RGD Derivatives via Solid Phase Macrocyclization Using the Heck Reaction. *Tetrahedron* **2001**, *57*, 2293-2303.

33) Augeri, D. J.; O'Connor, S. J.; Janowick, D.; Szczepankiewicz, B.; Sullivan, G.; Larsen, J.; Kalvin, D.; Cohen, J.; Devine, E.; Zhang, E.; Cherian, S.; Saeed, B.; Ng, S. –C.; Rosenberg, S. Potent and Selective Non-Cysteine-Containing Inhibitors of Protein Farnesyltransferase. *J. Med. Chem*. **1998**, *41*, 4288-4300.

34) Connor, K. A. *Binding Constants, The Measurement of Molecular Complex Stability*. Wiley-Interscience: New York, 1987; pp. 147-149.

Chapter 3: A Functional Assay for Heparin in Serum

3.1 Introduction

The objectives when developing "lock-and-key" type synthetic receptors are high binding affinity and specificity for a single analyte.[1] These objectives are exponentially more difficult to achieve when targeting a complex and dynamic analyte in a competitive crude medium such as urine, saliva, or serum.[2] We have developed the fluorescent molecular sensor **3.1** for the high affinity, specific detection of the clinical anticoagulant heparin (**3.2**) in human and equine serum.[2f]

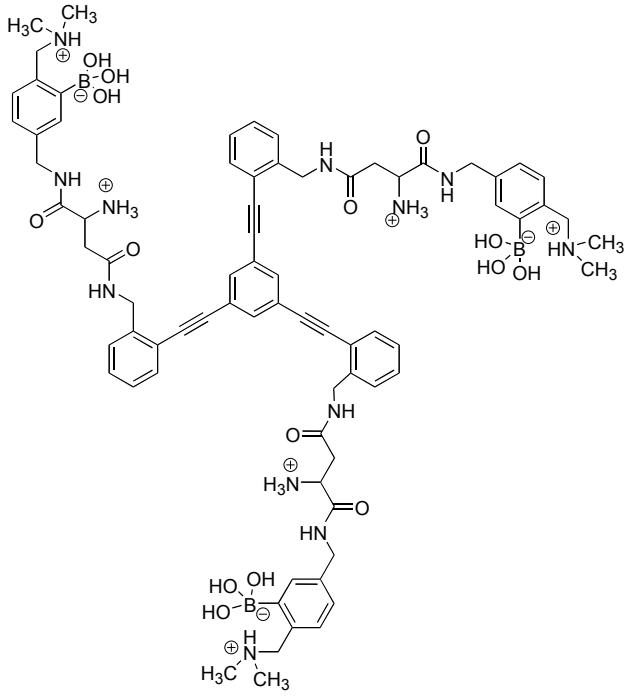

3.1

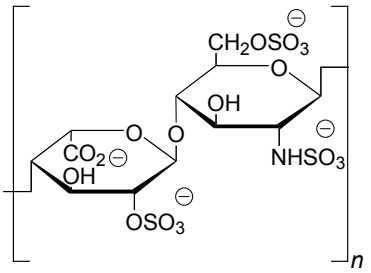

3.2
Heparin Biopolymer

Rivaling the affinity and selectivity of biological recognition processes has long been a goal of supramolecular chemists. Despite volumes of research that reflect this lofty pursuit, it has not been until the last two or three decades that significant advances have been made in artificial supramolecular systems. As discussed in the previous chapters, much research has been done to evaluate the binding of synthetic hosts to biological analytes such as amino acids and oligopeptides. As research progressed, the studies progressed from organic solvent studies to more competitive solvent systems, including aqueous systems buffered to biological pH. It has not been until the last few years that research with synthetic sensor systems has attempted to specifically bind to an analyte and quantify its concentration in crude solvent media such as urine, saliva, or serum.[2]

Chemosensor **3.1** was designed from lessons learned using a previously developed indicator-displacement assay in the Anslyn group for heparin.[3] The selectivity of the earlier receptor was not high enough to bind heparin in crude media. Our new sensor design incorporates a fluorescent core for sensitive signal transduction of binding and three pendant arms functionalized for selective heparin binding. The following chapter will discuss the importance of a selective and sensitive heparin sensor, and the development of and studies with **3.1** will be discussed.

3.2 Characteristics of Heparin

Heparin (**3.2**) can not be expressed exactly using a conventional chemical formula because it is a heterogenous polymeric sulphated glycosaminoglycan consisting predominantly of alternating $\alpha(1 \rightarrow 4)$-linked residues of D-iduronate-2-sulfate and *N*-sulfo-D-glucosamine-6-sulphate. Heparin has an average of 2.5 sulphates per residue

making it the strongest acid present in the human body. The highly anionic nature of heparin makes it an ideal target for synthetic sensors that can participate in ion-pairing or other anion-binding interactions.

Sulphated glycosaminoglycans are known to bind a number of proteins, and they have a role in several physiological processes including tumor growth, angiogenesis, nerve cell development, and metastasis.[4] While most glycosaminoglycans are a constituent of connective tissue, heparin occurs exclusively in the intracellular granules of mast cells that line arterial walls.[5] Heparin's primary function is the inhibition of blood clotting to prevent runaway clot formation upon injury. It is for this very reason that heparin is in wide use as a clinical therapeutic for surgical and postoperative therapy.

The drug heparin is recovered from porcine intestinal mucosa or bovine lung following tissue processing that includes treatment with alkali, proteases, and bleaching agents.[6] Over 33 metric tons of heparin are manufactured worldwide annually, representing approximately 500 million doses.[7] It is generally administered intravenously during extracorporeal procedures such as kidney dialysis and heart bypass procedures,[8] systemically when treating deep vein thrombosis, and subcutaneously as required.[9] Heparin has a low bioavailability, and thus is often administered in excess and must be neutralized using a cationic polypeptide drug called protamine, which is salmon sperm.[9] The major side effect of heparin treatment is hemorrhaging that can range from mild oozing of blood in mucus and stools to massive intracranial hemorrhaging.[6]

Two forms of heparin are in clinical use: unfractionated heparin (UFH) with a molecular weight range from 3000-30,000 Da, and low-molecular-weight heparin with a mean molecular weight of 5,000 Da.[10] UFH has a very low bioavailability; it must be administered intravenously or subcutaneously, and has been shown to be effective for operative treatment. Patients treated with UFH require hospitalization and close

monitoring. Irrespective of the route of administration, UFH concentration must be carefully monitored to prevent hemorrhaging. For this reason it is only used clinically under a doctor's supervision.

Low-molecular-weight heparins have been shown to be a safer anticoagulant for clinical use. The improved safety of LMWHs permits their use in an outpatient clinic rather than requiring hospitalization. The safety of LMWHs is due in part to a more predictable anticoagulant response than UFH due to their enhanced bioavailability, longer half-life, and dose-independent clearance. Furthermore, LMWHs bind less to platelets than UFH, and unlike UFH they do not increase microvascular permeability,[11] and they are less likely to interfere with interactions between platelets and vessel walls which is an effect of UFH treatment.[10] Low-molecular-weight heparins as clinical therapeutics with improved safety over UFH have been developed using a number of different methods. These include peroxidative depolymerization (Normiflo), nitrous acid depolymerization (Fragmin, Fraxiparene, and Clivarine), benzylation and alkaline depolymerization (Lovenox), and heparinase digestion (Innohep).[10]

The mechanism of anticoagulation activity for both UFH and LMWH involves the binding to and activation of antithrombin, which inhibits the coagulation enzyme factor Xa. Binding to antithrombin is mediated by a unique pentasaccharide sequence randomly distributed along both UFH and LMWH chains and involves significant ion-pairing interactions. Approximately 33% of the chains of UFH bear the unique pentasaccharide sequence, but only 15-25% of LMWH chains have the sequence.[12] Binding of antithrombin by the pentasaccharide sequence induces a conformational change to antithrombin resulting in a 1000-fold accelerated inhibition of factor Xa. Therefore, any heparin chain bearing the pentasaccharide sequence can inhibit factor Xa. However, a second coagulation enzyme, thrombin, can only be inactivated by the

formation of a ternary complex between heparin, antithrombin, and thrombin.[10] For this to occur the heparin chain must be a minimum of 18 saccharide units and possess the antithrombin binding pentasaccharide sequence. Nearly all UFH chains are at least 18 saccharide units long, but fewer than half of LMWH chains are long enough to bind thrombin.[13] Therefore, UFH is a more potent, but less bioavailable, clinical anticoagulant requiring greater care because of its enhanced activity. Scheme 3.1 illustrates the binding of UFH to coagulation enzymes factor Xa and thrombin.

Scheme 3.1 Inhibition of Coagulation Enzymes Factor Xa and Thrombin by UFH.

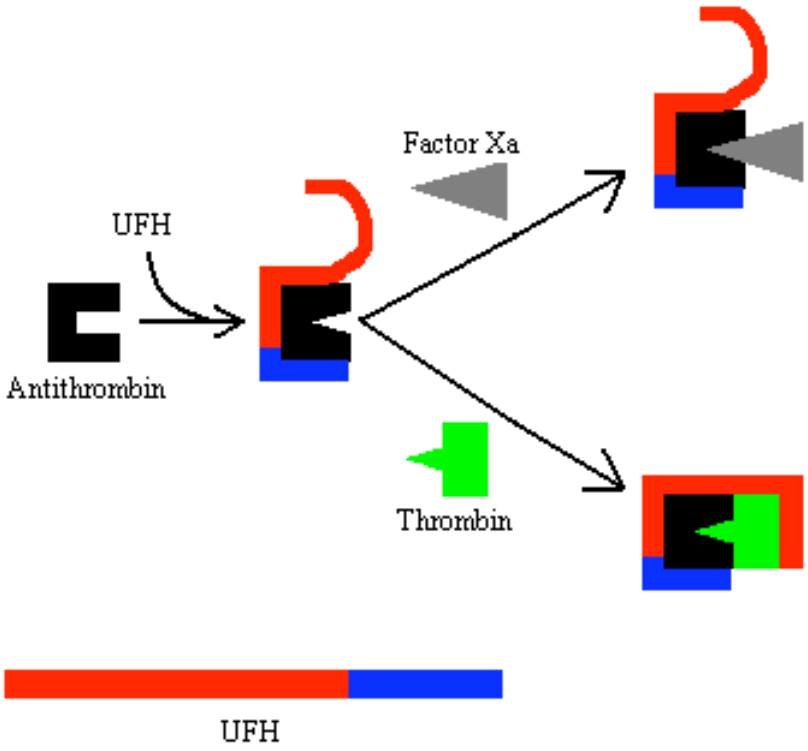

3.3 Methods for Quantifying Heparin Concentration

A number of issues muddy the waters when it comes to monitoring the concentration of either UFH or LMWH in plasma, serum, or urine. First, assays for monitoring the concentration of heparin in crude media are susceptible to strong interference from components of biological fluids, including other glycosaminoglycans such as chondroitin-4-sulfate (**3.3**) and hyaluronic acid (**3.4**). Second, clinically administered heparin (both UFH and LMWH) is a complex mixture that is difficult to chemically monitor in biological fluids with sensors not able to identify the heparin mixture as a whole. However, clinical administration of heparin is certainly not abated due to lack of sophisticated measuring techniques. While a number of current methods are clinically used for measuring the concentration of heparin, all methods are indirect and do not actually measure heparin concentration, and each method has its drawbacks.

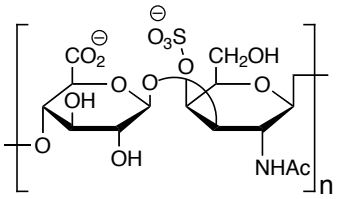

3.3

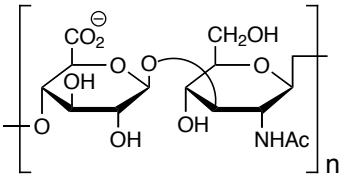

3.4

Current methods include the activated clotting time (ACT), activated partial thromboplastin time (aPTT), chromogenic antifactor Xa assay, electrochemical and piezoelectric assays, and complexation with protamine.[14] Although these are proven methods, only the first three are commonly employed, and they are often arduous, inaccurate, costly, and not necessarily all that amenable to clinical settings.[6,15] An

interesting recent method involves an engineered GST fusion protein containing three hyaluron binding domains from a heparin binding protein.[16] This engineered protein was able to accurately measure heparin in plasma at clinically relevant concentrations (0.08 μM – 3.2 μM), but it has not been employed as a clinical technique.

Of the clinical methods listed above the aPTT and antifactor Xa assay are the most routinely employed. Measurement of the ACT requires standardization of reagents within every clinical setting and is rather arduous, therefore it has a more limited use. Furthermore, as an indirect method of measurement it is not that accurate. Over the past 30 years the measurement of the aPTT has been the most widely used protocol for prescribing and monitoring the use of UFH and LMWH in patients. The aPTT is determined by comparing the aPTT of the patient to the aPTT of a standard. As a clinical assay aPTT is problematic because it correlates poorly with heparin concentration in several clinical settings.[15,16] Kitchen and Preston demonstrated that patients with the same aPTT ratios often had markedly different heparin concentrations in plasma, and samples with the same heparin concentration had myriad activated partial thromboplastin times.[17] The antifactor Xa assay is a more reliable method that measures the level of residual clotting activity due to enzyme Xa in the plasma after heparin administration (higher heparin concentrations lead to lower residual Xa activity and subsequently longer clotting times).[18] However, the antifactor Xa assay has not found widespread clinical use due to its considerably higher expense, despite its enhanced dependability over aPTT. Additionally, two different studies have compared protamine titrations with the antifactor Xa enzyme assay and have demonstrated inconsistencies.[19] In both cases the plasma heparin concentration was higher with the antifactor Xa assay than with the protamine titration. Clearly, a number of drawbacks exist for current methods of quantifying heparin concentration/activity in human patients. Our study resulted in the discovery of a

novel, sensitive detection assay for quantifying heparin, and it was one of the only cases of a synthetic sensor being specific for a target analyte in crude media.

3.4 Design of Heparin Chemosensor 3.1

3.4.1 Precedence for the Design of Heparin Chemosensor 3.1

The design of our heparin chemosensor builds upon the success of a previous Anslyn group glycosaminoglycan receptor, **3.5**. This receptor incorporated phenylboronic acids and ammonium groups for the complexation of the anionic polysaccharides UFH, hyaluronic acid, and chondroitin-4-sulfate.[3] Phenylboronic acids with an *o*-aminomethyl group are known to form boronate esters with alcohols in aqueous media and have been used extensively for the recognition of saccharides.[20] It has also been demonstrated that these boronate esters have high affinity for anions with closely appended hydroxy groups.[21] Additionally, it was found that the ammonium moieties of **3.5** enhanced ion-pairing interactions with the carboxylate and sulfate groups of glycosaminoglycans. Finally, the hexasubstituted benzene receptor scaffold of **3.5** is known to have groups alternating up and down[22] creating a preorganized cavity for binding as drawn.[23]

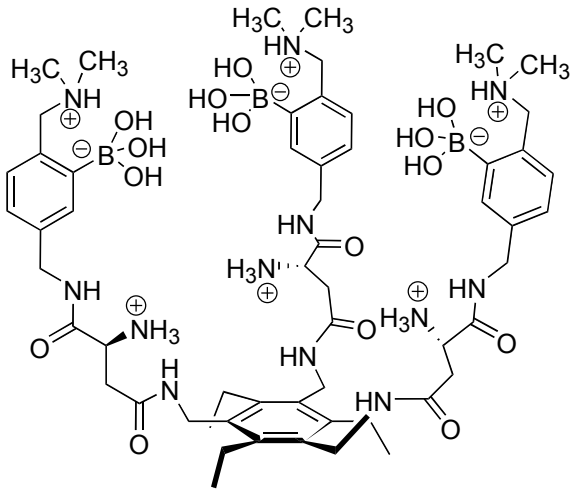

3.5

An indicator-displacement assay with pyrocatechol violet was employed to determine binding with UV/Vis spectroscopy (water/methanol, 1:1, 10 mM HEPES, pH 7.4) between **3.5** and UFH, chondroitin-4-sulfate, hyaluronic acid, and heparin disaccharide I-S (a two sugar mimic of heparin). Receptor **3.5** showed reasonable selectivity for heparin (3.8×10^4 M^{-1}) relative to the other polysaccharides. Because UFH is composed of multiple subunits the binding constant was calculated by using a UFH concentration defined by the concentration of each disaccharide unit. Despite a nice association, and a dramatic yellow-to-purple color shift upon binding UFH with the indicator-displacement assay, it was found that the indicator, and likely **3.5** as well, bound nonspecifically with proteins in crude serum skewing any attempt to quantify the UFH concentration in crude media.

3.4.2 Design and Synthesis of Heparin Chemosensor 3.1

Given the lessons gleaned from the studies using **3.5**, a second generation heparin receptor was designed with two goals in mind, both of which are embodied in the structure of **3.1**. First, the cavity was enlarged to allow the boronic acid and ammonium containing arms to encompass a larger surface of the oligosaccharide, which was predicted to raise the affinity by cooperatively increasing the number of interactions. Second, a fluorescent scaffold was incorporated into the design of the receptor, thereby avoiding the use of an indicator displacement assay. This new signaling technique also increased the overall sensitivity of the system. To satisfy both goals, a 1,3,5-triphenylethynylbenzene was employed as the fluorescent core unit. However, due to a number of synthetic difficulties to be discussed later, and the good selectivity previously determined for **3.5** with heparin, the boronic acid groups and ammonium containing side arms of **3.5** were retained in **3.1**.

A convergent synthesis was employed to develop the UFH and LMWH chemosensor **3.1**. In this manner the tris-acetylene core of **3.1** was developed separately from the arms and coupled to them in two latter steps. Therefore, the synthesis of the core commenced with a Sonogashira[24] coupling between 1,3,5-tribromobenzene (**3.6**) and trimethylsilylacetylene (**3.7**) to give 1,3,5-tris-trimethylsilanylethynyl-benzene (**3.8**).[25] The trimethylsilyl protecting groups were subsequently removed from **3.8** with cesium carbonate in methanol to give **3.9** in excellent yield. An alternate route of deprotection employing NaOH in methanol was unsuccessful prior to running the given deprotection. The successful synthesis of the fluorescent core is depicted in Scheme 3.2.

Scheme 3.2 Synthesis of the Fluorescent Core of **3.1**.

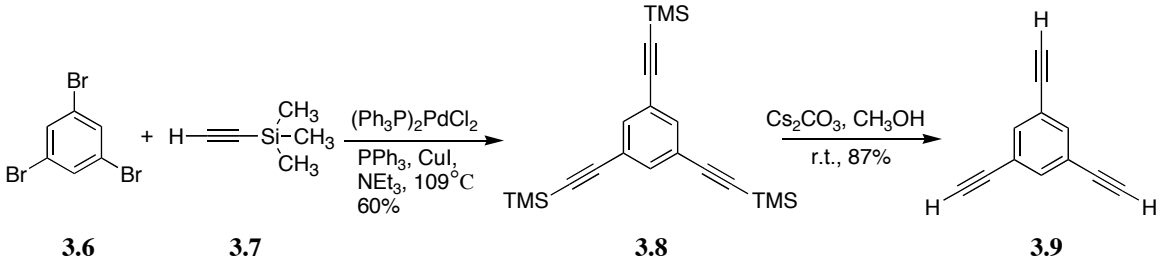

The second step of the convergent synthesis involved the formation of a halogenated benzylamine for Sonogashira coupling to the fluorescent core. 2-iodobenzylalcohol (**3.10**) was reacted with diphenylphosphorylazide and 1,8-diazabicyclo[5.4.0]undec-7-ene as base to form 2-iodobenzylazide (**3.11**) in modest yield.[26] The azide was reduced with triphenylphosphine followed by aqueous ammonia and sodium hydroxide to give 2-iodobenzylamine (**3.12**) which was used in the subsequent reaction without further workup or characterization.[26] Attempts at a Sonogashira reaction with amine **3.12** failed. Thus, di-*tert*-butyldicarbonate (Boc) was installed to protect **3.12**, giving the N-Boc-2-iodobenzylamine **3.13** in good overall yield. Synthesis of the preliminary element of the binding arms is illustrated in Scheme 3.3.

Scheme 3.3 Preliminary Formation of the Binding Arms of **3.1**.

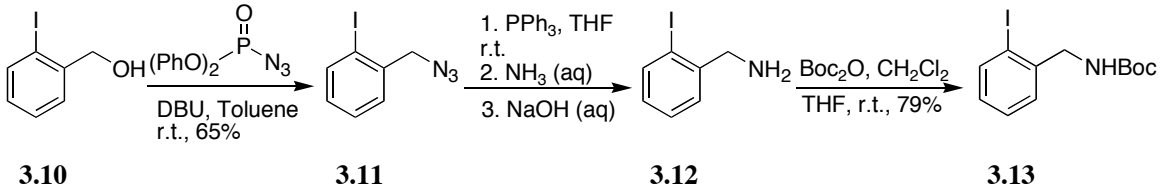

To bring the parts of **3.1** together a Sonogashira reaction was used to couple **3.9** and **3.13** to give (2-{3,5-bis[2-(*tert*-butoxycarbonylamino-methyl)-phenylethynyl]-phenylethynyl}-benzyl)-carbamic acid *tert*-butyl ester **3.14** in good yield. This reaction was attempted with the aryl-bromide derivative of **3.13** but yields were poor. The Boc groups were removed from all three arms of **3.14** using trifluoroacetic acid (TFA) in methylene chloride providing **3.15** in high yield. The reaction required cooling to prevent formation of the N-oxide, witnessed as a vibrant red color change in solution. As mentioned earlier the binding arms of **3.5** were incorporated into **3.1** due to synthetic difficulties and the reported selectivity of **3.5** for heparin. In a peptide coupling reaction the amine of **3.15** was coupled to **3.16**[3] using benzotriazole-1-yl-oxy-trispyrrolidinophosphonium (PyBOP) with hexafluorophosphate as the counter-ion and *N,N*-diisopropylethylamine as base to give **3.17**. Difficulties in purification provoked us to proceed without purifying the product. Thus, the 9-fluorenylmethyl carbamate (Fmoc) protecting group was removed using 20% piperidine in *N,N*-dimethylformamide (DMF) at elevated temperatures to give **3.1** in fantastic overall yield as shown in Scheme 3.4.

Scheme 3.4 Convergent Synthesis of UFH and LMWH Chemosensor **3.1**.

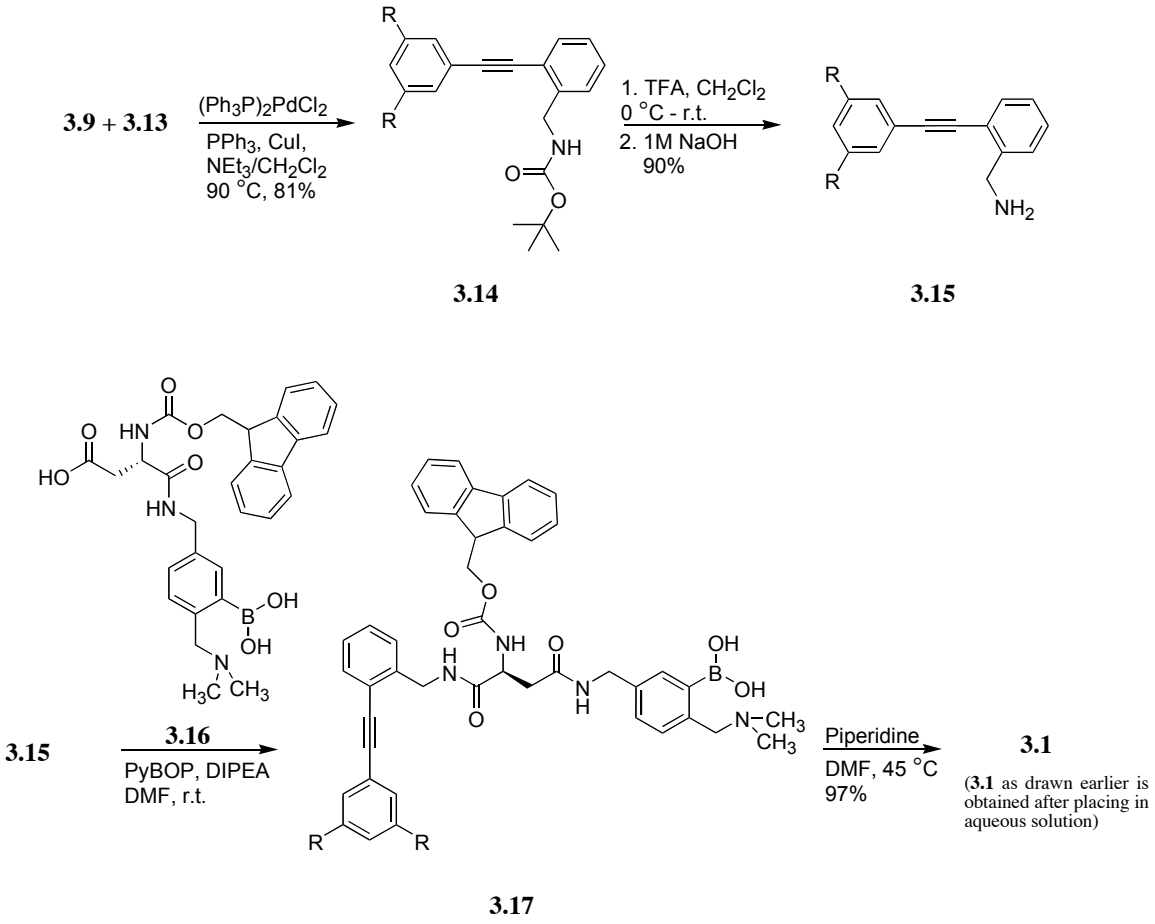

The "R" groups are identical to the single arm shown for each chemical structure.

3.4.3 Original Chemosensor Design and Synthetic Trials

Our initial synthetic aspiration was for a rather simple heparin sensor based solely on boronic acid moieties as in **3.18** and **3.19**, but it seemed that synthetic difficulties lay around every corner. The routes intended to obtain either of the two sensors is depicted

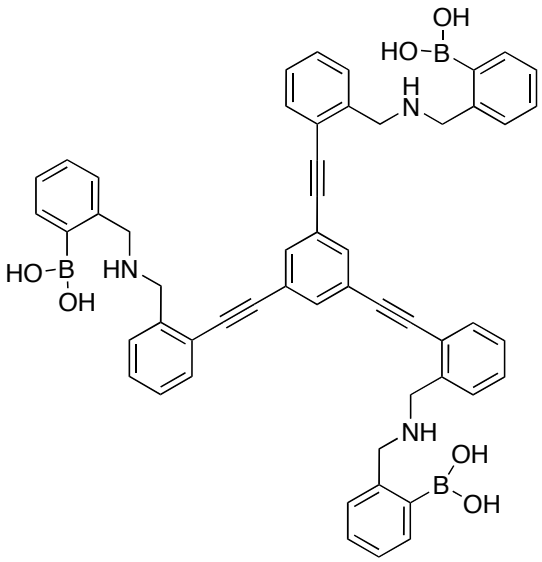

3.18

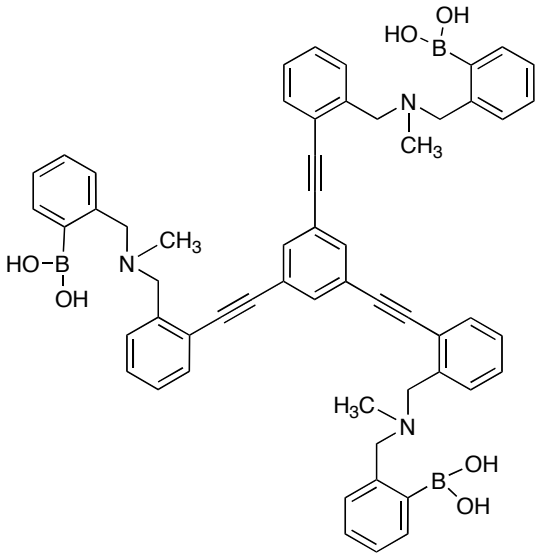

3.19

in Scheme 3.5. Formation of the tris-amino fluorescent core **3.15** was as shown in Scheme 3.4 (except when attempting to synthesize **3.19** the core was synthesized with identical reaction conditions using *N*-Boc-(2-iodobenzyl)-methyl amine rather than **3.13**). To derivatize **3.15** with the boronic acid moieties a reductive amination was employed in dry methanol with sodium borohydride and three to five equivalents *o*-formylphenyl boronic acid **3.20**.[20l,20m,27] The reaction was allowed to run 20 hours for formation of the iminium (**3.21**), followed by subsequent addition of the reducing agent with an overnight

run time. **3.18** or **3.19** were not isolated by TLC, crude NMR, or after running chromatographic columns on alumina. This reaction was repeated at various temperatures and with addition of catalytic acetic acid but no desired product was ever recovered. The reducing agent was changed to the less reactive sodium cyanoborohydride and the reductive amination was run in methanol at room temperature.[28] Again, after reaction workup, no desired product was isolated, but a large amount of starting material was recovered. Reaction conditions were modulated but to no avail.

Scheme 3.5 Attempted Synthesis of Sensor **3.18**.

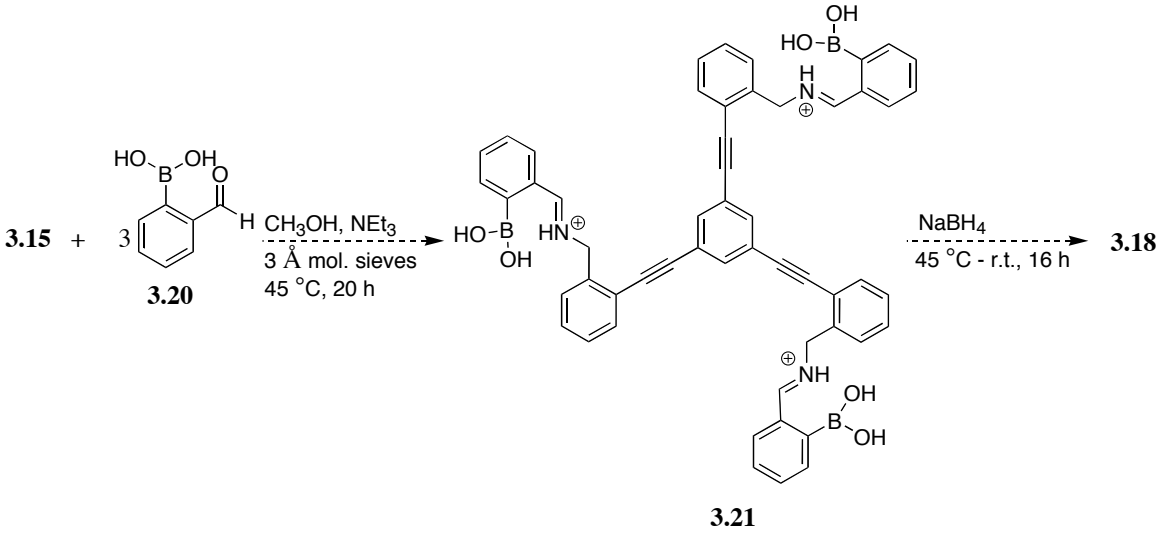

A second approach to the development of **3.18** or **3.19** is illustrated in Scheme 3.6. In this route a S_N2 substitution reaction was devised for the N-alkylation of **3.15**, and subsequent formation of **3.18**. This route commenced with protection of *o*-tolylboronic acid **3.22** with neopentylglycol **3.23** to form the boronic ester **3.24** in moderate yield.

The following radical reaction was inefficient without protection of the boronic acid. N-bromosuccinimide mediated radical addition of bromide to **3.24** was initiated by benzoyl peroxide to give **3.25** in high yield. The key reaction of this route followed, which was the N-alkylation step. Despite multiple attempts and reaction conditions the desired **3.26** was not obtained. Therefore, the subsequent deprotection of **3.26** with acid to yield **3.18** was not performed. What had become very clear to us is that reactions involving the fluorescent tris-amine core and boronic acid compounds were exceedingly more complicated then expected. It is well known that the workup and isolation of boronic acid derivatized compounds can be challenging, but we had not expected such rigors in the actual synthesis. Due to these challenges, we utilized the PyBOP coupling as discussed earlier to form UFH and LMWH chemosensor **3.1**.

Scheme 3.6 Attempted Synthesis of **3.18** Via *N*-Alkylation.

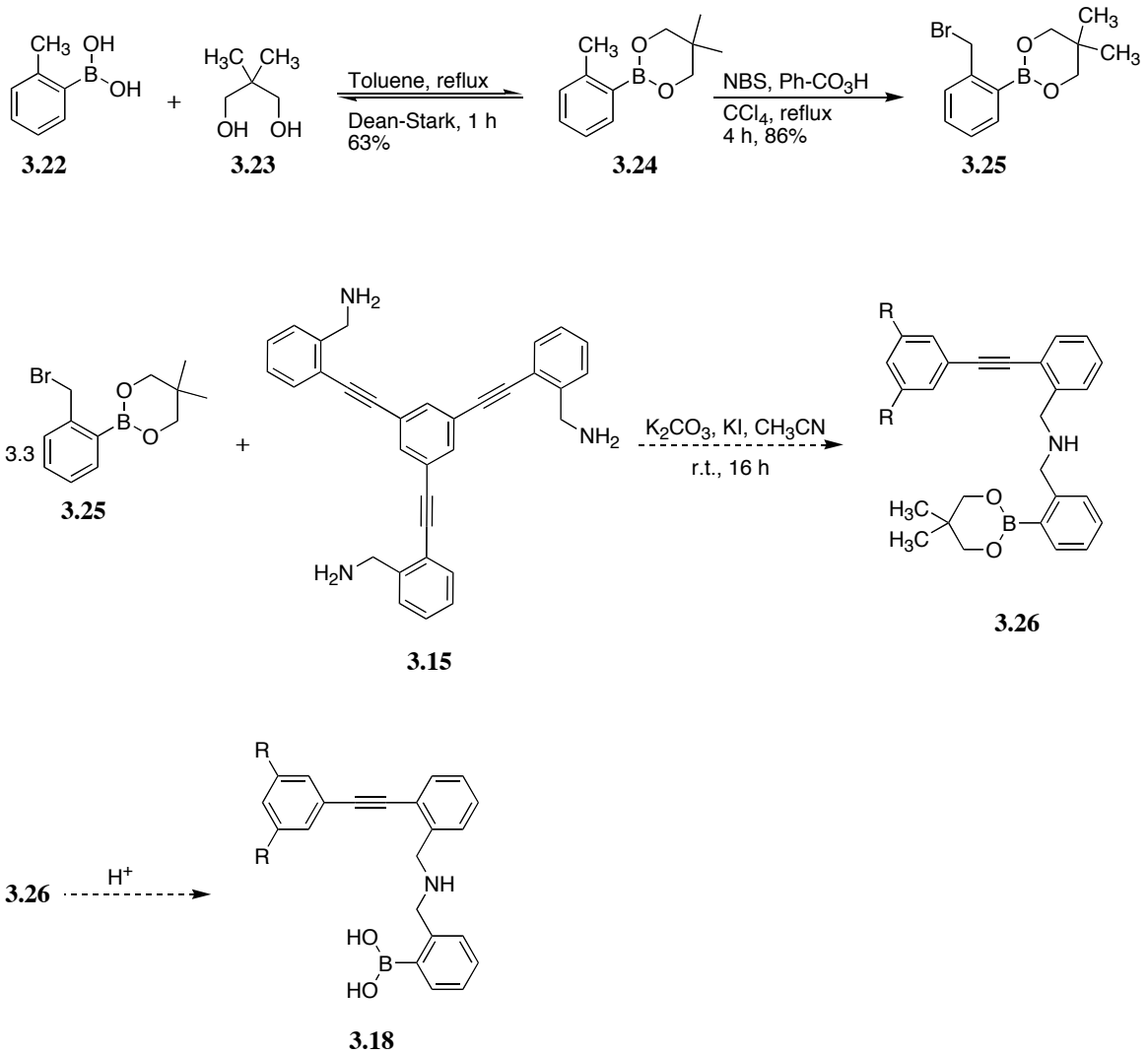

3.5 Binding Studies with Chemosensor 3.1 and LMWH and UFH

Prior to binding studies the UV/Vis absorbance and fluorescent emissions of **3.1** were evaluated. Figure 3.1a shows the absorbance spectrum of **3.1** (1.0×10^{-4} M), and Figure 3.1b shows the fluorescence spectrum (1.92×10^{-6} M). The absorbance spectrum

has a λ_{max} = 290 nm, and the fluorescent emission spectrum has a λ_{max} = 357 nm illustrating a clear Stokes shift, or red shift. The Stokes shift occurs because **3.1** releases a small amount of absorbed energy in its excited state prior to releasing the rest of the energy as fluorescence upon return to the electronic ground state.

Figure 3.1 (a) Absorbance and (b) Emission Profiles of **3.1** Demonstrating a Stokes Shift.

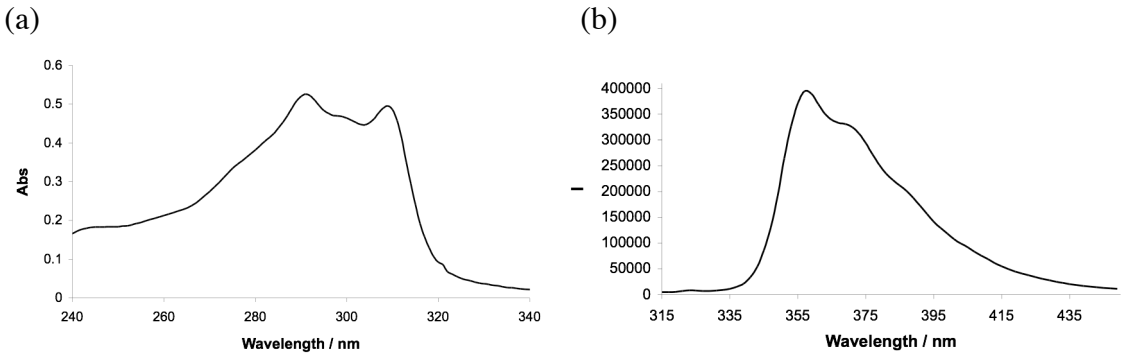

"I" represents fluorescent emission intensity.

To create an assay for UFH or LMWH in serum required a binding interaction between **3.1** and heparin in the nM range. To determine the affinity of **3.1** for UFH and LMWH, titrations of UFH and LMWH into **3.1** in water (1.92×10^{-6} M, buffered with 10 mM HEPES at pH 7.4) were monitored using fluorescence spectroscopy (Figure 3.2 – UFH shown). The binding of both UFH and LMWH with **3.1** caused a decrease in the emission spectra, resulting in a near complete quenching of the sensor's emission. Presumably, the interaction of heparin with **3.1** leads to conformational restriction of the receptor "arms," thereby modulating the fluorescence. This is a technique used routinely for creating chemosensors by Finney.[30] Titration data at 357 nm was used to generate a fluorescence binding isotherm (Figure 3.3), which was analyzed using a standard 1:1

binding algorithm.[31] Due to the heterogeneous structure of heparin, the repeating unit that sensor **3.1** interacts with had to be defined. The binding isotherm shown in Figure 3.3 was achieved by defining the concentration of UFH to be that of four saccharide units (though an integral number of saccharides is not required to fit the binding isotherm). The number four supports a stoichiometry where each **3.1** on average spans four saccharide units along the UFH biopolymer. The calculated association constant between **3.1** and UFH was 1.4×10^8 M^{-1}. This was an increase in affinity of near 10^4 for **3.1** over **3.5** gained by increasing the size and nature of the core. It should be noted that the glycosaminoglycans hyaluronic acid and chondroitin-4-sulfate did not bind **3.1** at low μM concentrations. The lack of binding to other glycosaminoglycans is further evidence for the high selectivity of **3.1** for UFH and LMWH.

Figure 3.2 Fluorescence Emission Spectra of Titration of UFH into **3.1** (1.92×10^{-6} M).

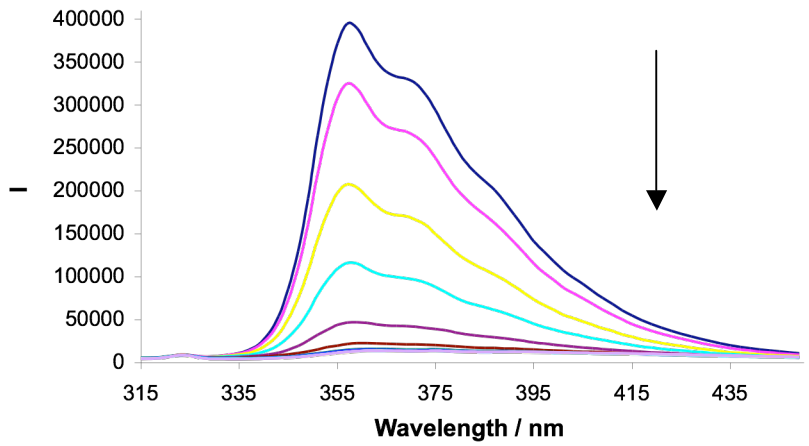

Figure 3.3 Binding Isotherm for Titration of UFH Into **3.1** (1.92×10^{-6} M). The orange line represents the calculated binding curve; a good fit is observed.

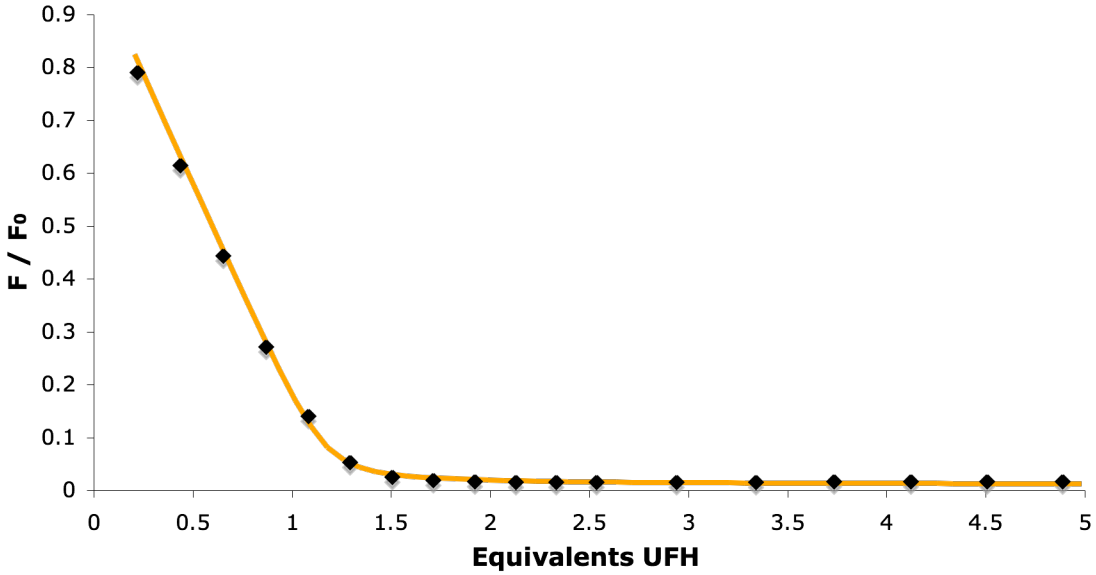

3.6 Protamine Titrations

As noted earlier, several clinical methods, such as aPTT, are calibrated by protamine titration. Protamine is a cationic biopolymer, and a natural substrate for heparin. Protamine sequesters heparin thereby lowering its bioavailability to bind antithrombin preventing the inhibition of clotting enzymes. Therefore, if there is a specific binding interaction between heparin and **3.1** as postulated, protamine should strip heparin from **3.1**, thereby restoring its fluorescence. Indeed, when analyzing either mixtures of **3.1** with UFH or LMWH, fluorescence was fully reestablished upon titration of the **3.1**:LMWH (UFH) complex with protamine (Figure 3.4). This illustrates that the binding between **3.1** and heparin is reversible, and acts analogous to that between heparin and antithrombin. When protamine was added to a solution of **3.1** (9.6×10^{-7} M, 10 mM HEPES, pH 7.4) there was no change in the emission spectrum of **3.1**, indicating that no binding interactions were occurring. Furthermore, if a LMWH:protamine (approximately 1:1) solution was titrated into **3.1** (9.6×10^{-7} M, 10 mM HEPES, pH 7.4) there was also no change in the emission spectrum indicating that the heparin and protamine biopolymers have an affinity for one another greater than the association between **3.1** and UFH.

Figure 3.4 Reversibility of LMWH:**3.1** Upon Titration with Protamine. Emission intensity at 357 nm; eleven 0.1 equivalent aliquots of LMWH (▲)were added followed by twelve aliquots of protamine (●) (approximately 1-2 equivalents total).

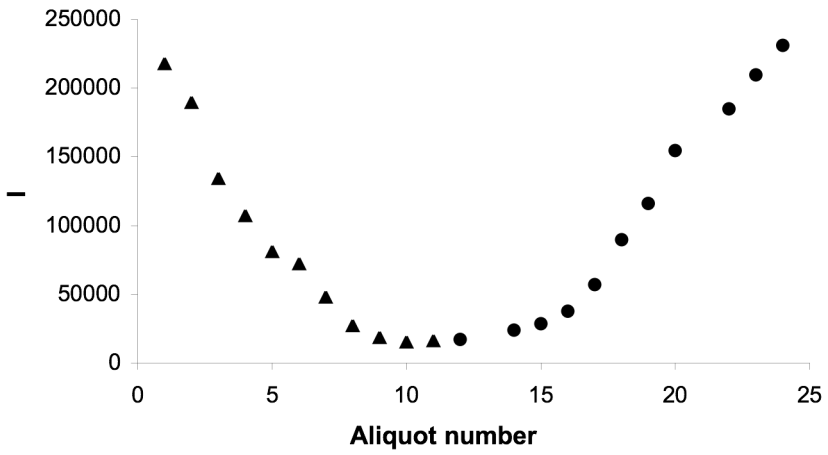

Interestingly, protamine stripping heparin from chemosensor **3.1** could be exploited as a way to regenerate a clinical sensing assay for heparin. Meaning, if **3.1** was attached to a solid support, be it a glass slide, fiber optic, etc., it could be used for determining the heparin concentration in serum, and then subsequently regenerated with a protamine solution for future reuse.

3.7 Dilution Studies

There were concerns that the observed emission of **3.1** was really that of an excimer - dimers consisting of one excited and one unexcited molecule with their fluorescence maximum red shifted to a longer wavelength in comparison with the

fluorescence maximum of monomeric **3.1**.[32] To address this concern a simple dilution experiment was employed. In this experiment **3.1** was diluted by addition of water (buffered with 10 mM HEPES, pH 7.4) as seen in Figure 3.5a. If the observed fluorescence emission of **3.1** was not an excimer it was believed that there would be a linear decrease in the emission spectrum. Upon dilution of **3.1** with 7 mL of buffered water a very peculiar increase in fluorescence was observed with a maximum emission after approximately 0.5 mL dilution. This fluorescent increase was followed by a nonlinear decrease with a near zero emission not occurring until 6 mL dilution. While this seemed a convincing argument for excimer formation, there was never a blue shift in the emission spectrum that would have been characteristic of the breakup of the excimer to the monomers (Figure 3.5c).

To have a standard by which to test our own system, the dilution of pyrene with n-hexanes was evaluated. Pyrene is known to form excimers, however we intentionally biased our system and started at a concentration at which the monomer exists. The monomer of pyrene is known to have a λ_{max} = 390 nm and red shifts to 470 nm upon excimer formation.[33] Our intention was to observe the characteristics of dilution of just the monomer form of pyrene and compare it to our system. As seen in Figure 3.5b dilution of pyrene had a near identical dilution chart as dilution of **3.1**! This was puzzling indeed because at no point did the λ_{max} of pyrene waver from 384 nm. It was postulated that this was a result of π-stacking forces in both cases. Therefore, dimers and higher order x-mers may exist that have an influence on the character of fluorescence emission, but we believe we can rule out excimer formation. Furthermore, it is not believed that higher order structures of **3.1** would necessarily adversely effect binding to **3.2** as is evident from the very high association constant. Therefore, we proceeded from this point without further concern of excimer formation.

Figure 3.5 Dilution of (a) **3.1** (9.6×10^{-7} M,) with Water and (b) Pyrene (2.99×10^{-6} M, 384 nm) with n-Hexanes, (c) Dilution of **3.1**, Note That the λ_{max} Does Not Shift.

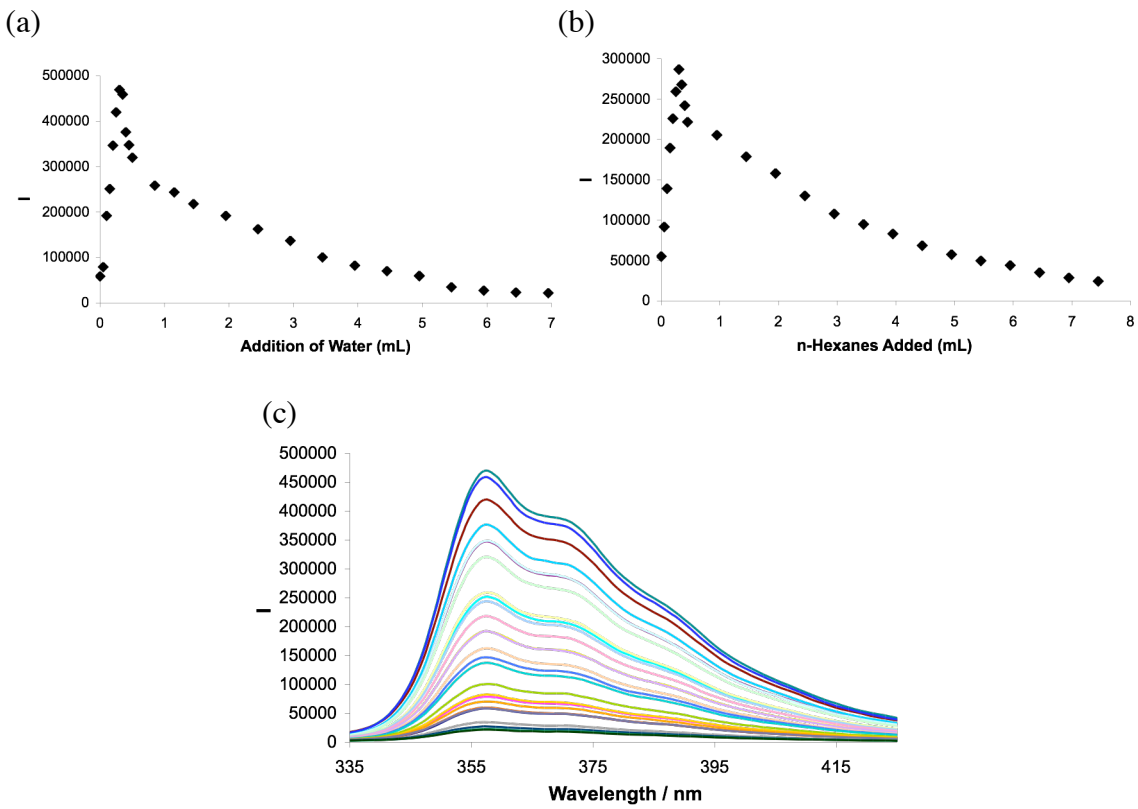

3.8 Calibration Curves – Heparin Concentration in Serum

The previous studies with **3.1** culminated in the creation of calibration curves for determining UFH and LMWH in human and equine serum. To prevent excessive clotting during cardiopulmonary surgery and emergency deep venous thrombosis (DVT)

conditions, heparin is administered intravenously or subcutaneously at therapeutic dosing levels of 2 U/mL – 8 U/mL (0.8 μM – 3.2 μM). However, in post-operative and long-term anticoagulant care of DVT, patients are treated at therapeutic dosing levels of 0.2 U/mL – 2 U/mL (0.08 μM - 0.8 μM) generally with LMWHs. To simulate monitoring conditions in a clinical setting, human and equine serums were doped with UFH and LMWH at these dosing levels. A serum sample (32 μL) doped with UFH or LMWH was added to a fluorimeter cell containing a total volume of 1.5 mL HEPES (10 mM) in deionized water. To the heparin/serum solution was added 2 μL of **3.1** (2.24×10^{-3} M^{-1}) (the fluorescence emission spectrum of **3.1** was modulated by the serum media as seen in Figure 3.6; however, this did not effect the sensor's activity). The fluorescence emission of the receptor stabilized over a period of 18 minutes, in contrast to the instantaneous response found in buffered water, indicating that forming the complex with heparin in serum was slow on the laboratory time scale. This is potentially due to the kinetics of release of heparin from natural receptors in the serum.

Figure 3.6 Emission Spectrum of **3.1** in Human Serum.

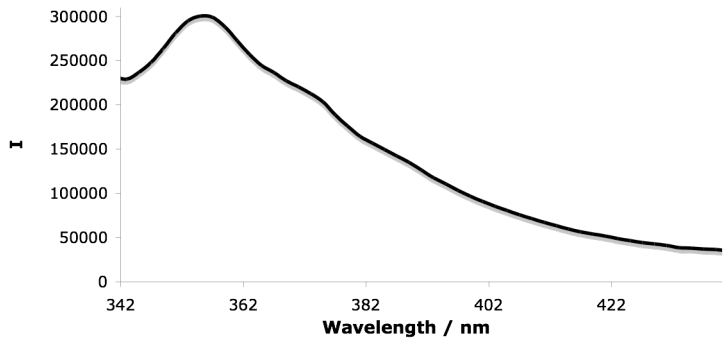

To generate calibration curves (355 nM), emission spectra were recorded after 18 minutes for each of nine samples with varying heparin concentration spanning clinical ranges. Increased levels of heparin in serum correlated linearly to lower emission responses from **3.1** for both UFH and LMWH within the range of clinically relevant concentrations, as was observed for the fluorimetric titrations using pure heparin in buffered water (Figure 3.7). Further, the method worked in both equine and human samples, illustrating that the affinity of the synthetic receptor for heparin is independent of the mammalian source, and could potentially be used for either human or veterinary applications.

Figure 3.7 Calibration Curves for (a) LMWH in Human Serum, (b) UFH in Human Serum, and (c) UFH in Equine Serum.

(a)

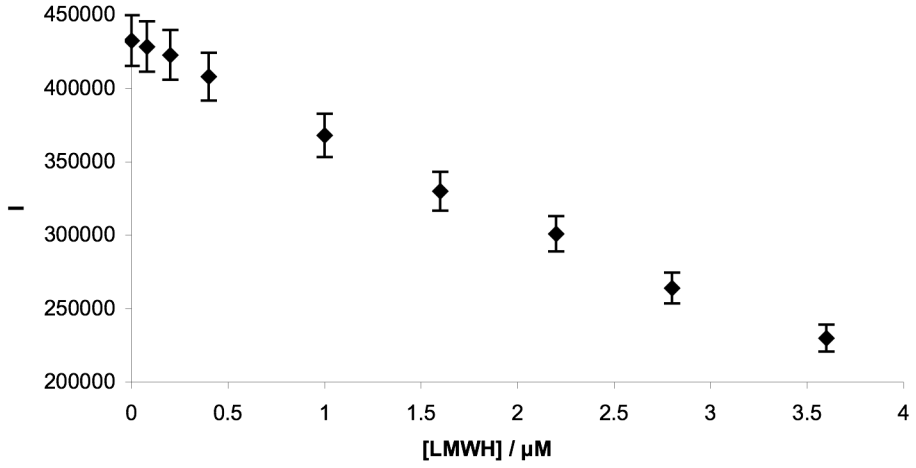

(b)

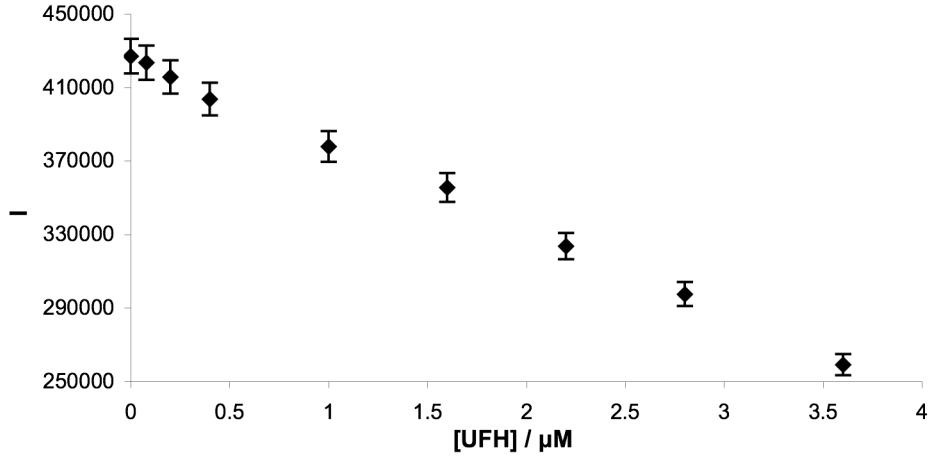

(c)

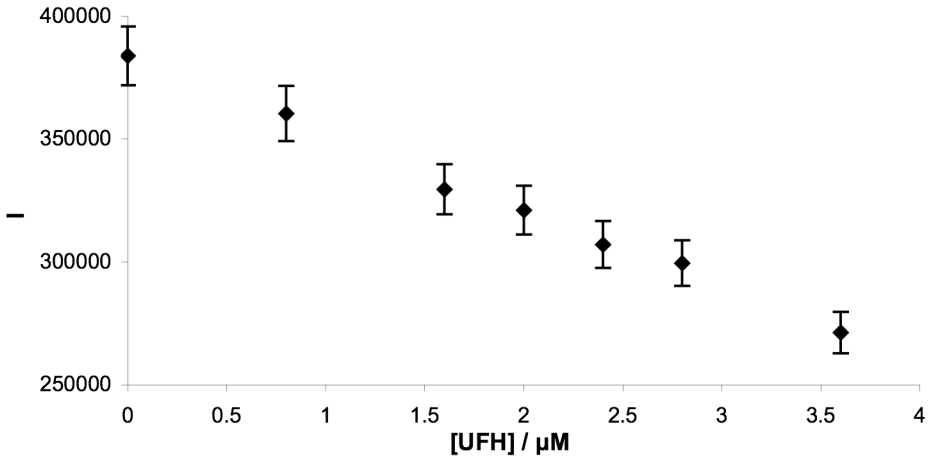

3.9 Summary

In summary, a functional synthetic fluorescent assay for the clinically administered anticoagulant heparin, both UFH and LMWH, has been demonstrated. The synthetic receptor highlighted herein showed remarkable selectivity and affinity for heparin, even in crude human and equine serum. The fluorescent emission of **3.1** was employed to generate calibration curves for UFH and LMWH in serum at clinically relevant dosing levels (0.2-8.0 U/mL). These calibration curves permit comparative analysis of the fluorescence emission of an unknown sample to determine its heparin concentration. The research presented in this chapter demonstrates that synthetic receptors can be created to target very complex bioanalytes, and function successfully in physiological settings.

3.10 Experimental

General. Reactions were run under an atmosphere of argon unless otherwise indicated. Anhydrous solvents were transferred by an oven-dried syringe. Flasks were flame dried under a stream of argon. Chemicals for synthesis were obtained from Acros Organics, Aldrich, and NovaBiochem and were used without further purification. Methlyene chloride and triethylamine were distilled over calcium hydride. Human and equine sera were purchased from Sigma-Aldrich and used without further purification. Low molecular weight heparin was prepared via oxidative depolymerization, pursuant to pharmaceutical procedures. The exact depolymerization method is proprietary to Sigma-Aldrich. UFH and LMWH were both employed as their sodium salts, as is common with pharmaceutical therapeutics. A Varian Gemini 400 MHz NMR was used to obtain ^{1}H and ^{13}C spectra. Finnigan TSQ70 and VG Analytical ZAB2-E mass spectrometers were used to obtain low and high resolution mass spectra respectively. Melting points were measured on a Thomas Hoover capillary melting point apparatus and are uncorrected. All products were dried for at least 6 hours prior to spectral analysis. Fluorescent measurements were performed on a Photon Technology International Fluorimeter (LPS-220B, MB-5020, PMT-814).

Procedures:

1,3,5-tris-trimethylsilanylethynyl-benzene (3.8)

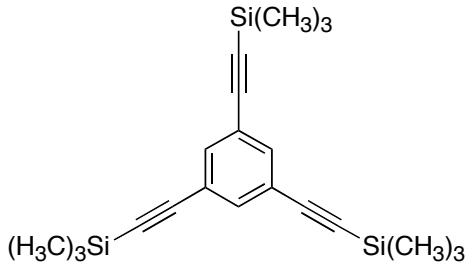

To a flame-dried, argon-purged flask with condenser was added 1,3,5-tribromobenzene (**3.6**) (5.08 mmol, 1 eq), $Pd(PPh)_3Cl_2$ (0.051 mmol, 0.01 eq), CuI (0.051 mmol, 0.01 eq), and triphenylphosphine (0.051 mmol, 0.01 eq) in distilled triethylamine (10 mL). This solution was mixed for 20 minutes at 109°C. To the solution was added trimethylsilylacetylene (**3.7**) (20.8 mmol, 4.1 eq). The reaction stirred for 4 h. Upon completion, the reaction was cooled to room temperature, diluted with hexanes, and filtered through Celite 545. The organic layer was removed *in vacuo*. The product was further purified on a SiO_2 column (petroleum ether). Obtained an off-white solid (3.03 mmol) in 60% yield. ^{1}H NMR (400 MHz, $CDCl_3$) δ 7.54 (s, 3H), 0.29 (s, 27H). ^{13}C NMR (100 MHz, CDC l_3) δ 135.1, 123.8, 103.3, 95.7, 0.0. MS (CI+) *m/z* 367 $[M]^+$. m.p. 78-80 °C.

1,3,5-trisethynyl-benzene (3.9)

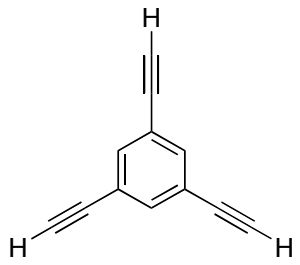

To a flame-dried flask under argon was added **3.8** (2.39 mmol, 1 eq), cesium carbonate (4.78 mmol, 2 eq), and methanol (10 mL). The reaction was stirred 16 h. The solution changed from opaque to translucent upon completion. The methanol was removed *in vacuo* and the solid was partitioned between water and methylene chloride. The water layer was extracted with methylene chloride (3 × 20 mL). The organic layer was washed with aqueous ammonium chloride (1.0 M, 2 × 20 mL), water (2 × 20 mL), and brine (2 × 20 mL). The organic layer was dried with sodium sulfate, filtered, and removed *in vacuo*. **3.9** was obtained as off-white soft crystals (2.09 mmol) in 87% yield. ^{1}H NMR (400 MHz, $CDCl_3$) δ 7.57 (s, 3H), 3.12 (s, 3H). ^{13}C NMR (100 MHz, CDC l_3) δ 135.6, 122.8, 81.6, 78.7. MS (CI+) *m/z* 151 $[M]^+$. m.p. 101-103 °C.

2-iodo-benzylazide (3.11)

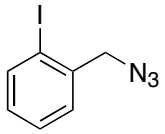

1,8-Diazabicyclo[5.4.0]undec-7-ene (5.55 mmol, 1.3 eq) was added to a solution of 2-iodobenzylalcohol **3.10** (4.27 mmol, 1.0 eq) and diphenylphosphoryl azide (5.13 mmol,

1.2 eq) in 9 mL toluene under argon. The reaction ran at room temperature for 1.25 h. At this time 3 N HCl (9 mL) was added and stirred briefly. The solution was extracted with ether, and the organic layer was washed successively with water (3 × 15 mL) and saturated NaCl (2 × 15 mL). The organic layer was dried with sodium sulfate, filtered, and removed *in vacuo*. Obtained **3.11** as a clear oil in 65% yield that was used without further purification. ^{1}H NMR (400 MHz, $CDCl_3$) δ 7.91 (d, 1H), 7.42 (d, 1H), 7.41 (t, 1H), 7.06 (t, 1H), 4.48 (s, 2H). ^{13}C NMR (100 MHz, CDC l_3) δ 139.4, 137.8, 129.7, 129.2, 128.4, 98.9, 58.7. MS (CI+) *m/z* 232 ($[M-N_2]^+$).

2-iodo-benzylamine (3.12)

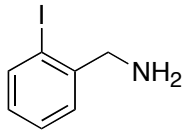

To a solution of **3.11** (2.75 mmol, 1 eq) in dry THF (5 mL) under argon was added triphenylphosphine (3.06 mmol, 1.11 eq) portionwise. This reaction stirred 16 h, upon completion aqueous ammonia was added. This stirred 3 h at which point 3 M NaOH (20 mL) was added and stirred 1 h. The solution was then neutralized with 2 M HCl (30 mL) and extracted with ether. The organic layer was washed with water (2 × 25 mL) and brine (2 × 25 mL). The organic layer was dried with sodium sulfate, filtered, and removed *in vacuo*. Obtained **3.12** as a yellow oil that was not purified and was immediately used in the subsequent step.

(2-iodo-benzyl)-carbamic acid *tert*-butyl ester (3.13)

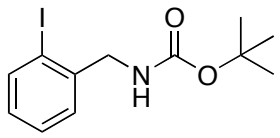

To crude **3.12** in THF (15 mL) was added di-*tert*-butyldicarbonate (3.66 mmol, 1.33 eq). This solution was stirred vigorously for 6 h. Upon completion ether was added (10 mL). The organic layer was washed with water (2 × 25 mL) and brine (2 × 25 mL), dried with sodium sulfate, filtered, and removed *in vacuo*. The product was further purified on a SiO_2 column (2% ethyl acetate in hexanes). The product was collected as an off-white powder (2.16 mmol) in 79% yield. ^{1}H NMR (400 MHz, $CDCl_3$) δ 7.79 (d, 1H), 7.34 (d, 1H), 7.31 (t, 1H), 6.94 (t, 1H), 4.31 (d, 2H), 1.44 (s, 9H). ^{13}C NMR (100 MHz, CDC l_3) δ 155.6, 140.8, 139.2, 128.9, 128.4, 98.6, 79.5, 49.2, 28.3. MS (CI+) *m/z* 233.8 $[M]^+$. m.p. 54-56 °C.

(2-{3,5-bis[2-(*tert*-butoxycarbonylamino-methyl)-phenylethynyl]-phenylethynyl}-benzyl)-carbamic acid *tert*-butyl ester (3.14)

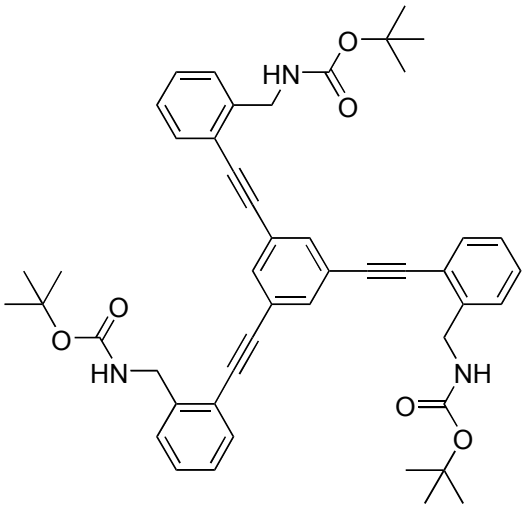

To a flame-dried, argon-purged flask with condenser was added **3.13** (1.24 mmol, 4.0 eq), $Pd(PPh)_3Cl_2$ (0.006 mmol, 0.02 eq), CuI (0.006 mmol, 0.02 eq), and triphenylphosphine (0.006 mmol, 0.02 eq) in distilled triethylamine (5 mL) and methylene chloride (5 mL). The reaction was set at 60 °C and the solution mixed 15 minutes. At this point **3.9** (0.309 mmol, 1.0 eq) was added and the reaction ran 16 h with constant stirring. Upon completion the solvent was removed *in vacuo*, and the product was purified on a SiO_2 column (22% ethyl acetate in hexanes). Product was recrystallized in hexanes with a minimal amount of methylene chloride to give a white solid (0.251 mmol) in 81% yield. ^{1}H NMR (400 MHz, $CDCl_3$) δ 7.66 (s, 3H), 7.52 (d, 3H), 7.38 (d, 3H), 7.32 (t, 3H), 7.25 (t, 3H), 5.08 (br, NH), 4.55 (d, 6H), 1.43 (s, 9H). ^{13}C NMR (100 MHz, CDC l_3) δ 155.8, 140.7, 134.1, 132.4, 129.0, 127.8, 127.2, 123.9, 121.5, 92.9, 88.3, 79.5, 43.3, 28.4. MS (CI+) *m/z* 766 $[M]^+$. m.p. 77-79 °C.

2-[3,5-bis(2-aminomethyl-phenylethynyl)-phenylethynyl]-benzylamine (3.15)

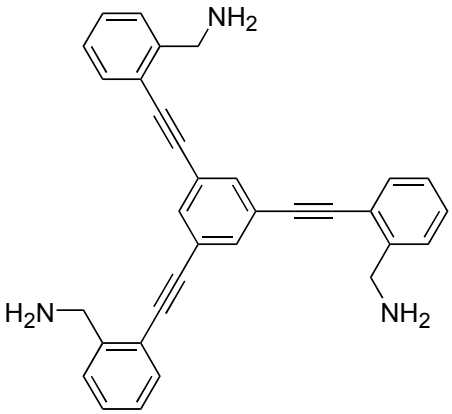

To a flame-dried, argon-purged flask was added **3.14** (0.092 mmol, 1 eq) and methylene chloride (5 mL). The solution was cooled to 0 °C and trifluoroacetic acid (1.35 mmol, 14.7 eq) was dripped into the reaction. The reaction was allowed to slowly warm to room temperature. After 10 h the solvents were removed *in vacuo*. The residue was dissolved in water, basified with 1 N NaOH, and extracted with methylene chloride (2 × 10 mL). The organic layer was washed with brine (10 mL), dried with sodium sulfate, filtered, and removed *in vacuo*. Obtained light yellow solid (0.082 mmol) in 90% yield. No further purification was necessary. ^{1}H NMR (400 MHz, CD_3OD) δ 7.79 (s, 3H), 7.60 (d, 3H), 7.59-7.41 (m, 9H), 4.33 (s, 6H). MS (CI+) *m/z* 466 $[M]^+$. Elemental composition, *m/z* 465.2 ($C_{33}H_{27}N_3$). m.p. decomposed, 117-121 °C.

Fmoc-protected Heparin Chemosensor (3.17)

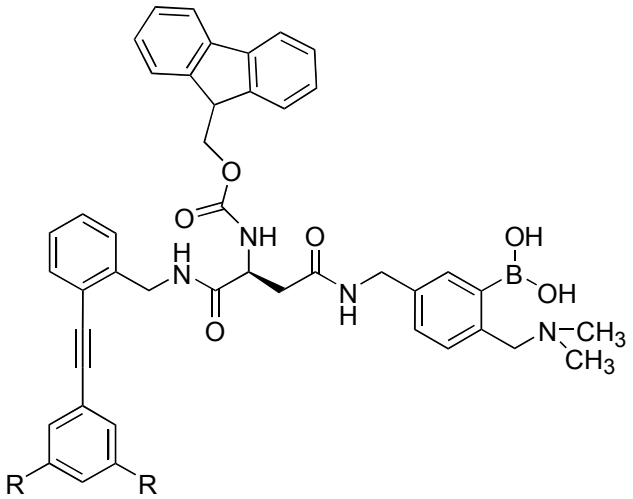

The "R" groups are identical to the single arm shown for each chemical structure.

To a solution of **3.15** (0.054 mmol, 1 eq), **3.16** (0.215 mmol, 4 eq), and diisopropylethylamine (0.556 mmol, 10 eq) in N,N-dimethylformamide (DMF) (3 mL) was added benzotriazole-1-yl-oxy-tris-pyrrolidino-phosphonium hexafluorophosphate (PyBOP) (0.215 mmol, 4 eq). The reaction stirred at room temperature for 3.5 h. Upon completion the product was precipitated with acetonitrile (15 mL). The product was filtered, redissolved in DMF (3 mL), and precipitated again with acetonitrile (15 mL). This process was repeated twice more. A slightly yellow residue was obtained and used without further purification or characterization in the next step.

Heparin Chemosensor (3.1)

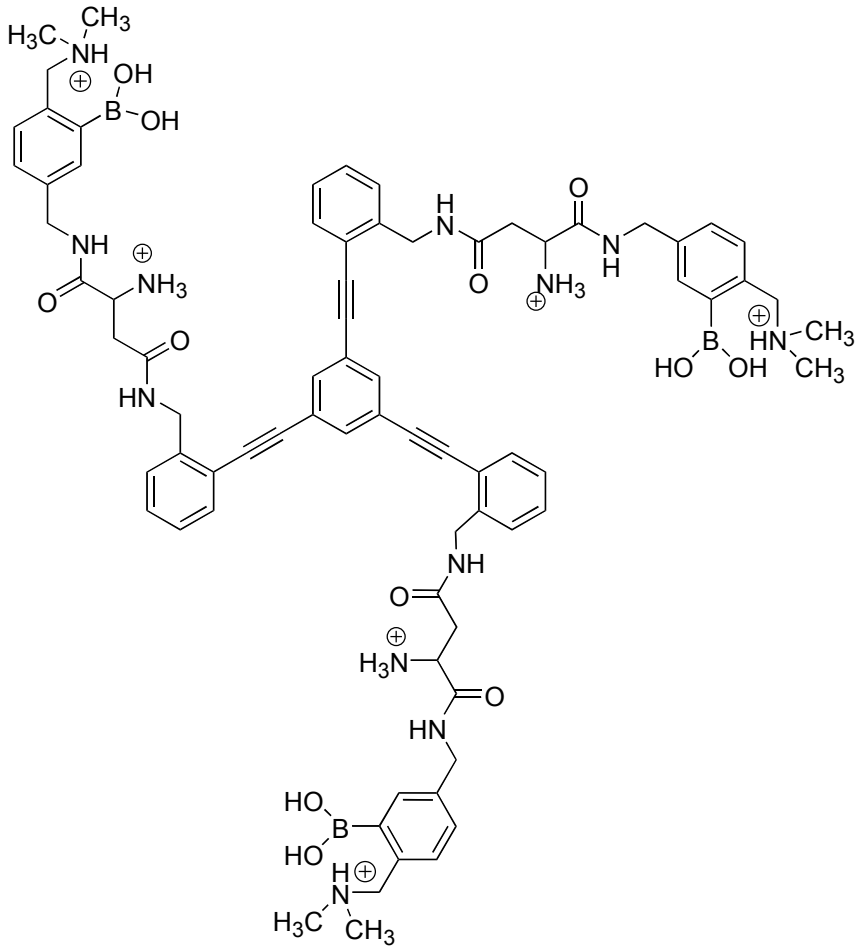

3.17 was dissolved in a solution of 20% piperidine in DMF (2 mL). The reaction was stirred at room temperature for 16 h. The solvent was removed *in vacuo* with azeotropic addition of toluene. Product was dried thoroughly on the hi-vac. The crude residue was dissolved in 0.2 M HCl (10 mL) and chloroform (6 mL). This solution stirred for 25 min. The precipitate was filtered and the aqueous layer collected. The aqueous layer was washed with methylene chloride (2 × 10 mL). The aqueous layer was removed *in vacuo*; the residue was redissolved in water (2 mL) and removed using a lyophilizer. A slightly

off-white solid (0.052 mmol) was collected in 96% yield. No further purification was necessary, however product contained minimal (3.7%) piperidine impurity. ^{1}H NMR (400 MHz, CD_3OD) δ 8.23 (d, NH), 7.77 (d, 3H), 7.64 (s, 3H), 7.47-7.21 (m, 18H), 4.31 (br, 12H), 3.31 (m, 3H), 3.02 (br, 6H), 2.94 (br, 6H), 2.79 (s, 18H). MS (ESI) *m/z* 1328 [M-3(OH), loss of one hydroxyl from each boronic acid induced by N-B bond formation]. MS (CI+) *m/z* 1328 [M-3(OH)]. m.p. decomposed, 144-148 °C.

5,5-Dimethyl-2-*o*-tolyl-[1,3,2]dioxaborinane (3.24)

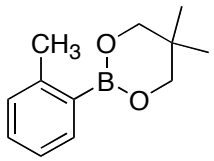

o-Tolylboronic acid **3.22** (1.92 mmol, 1 eq) was added concomitantly with neopentylglycol **3.23** (1.92 mmol, 1 eq) to toluene (25 mL) and the solution was heated to reflux with an attached Dean-Stark trap. After 1 h the reaction was removed from the heat and half of the solvent was removed *in vacuo*. The remaining solution was cooled in an ice bath, the precipitate was filtered off, and the remaining toluene was removed *in vacuo* to yield **3.24** (1.22 mmol, 63%) as a light yellow oil. This product was used in the next reaction without further workup. ^{1}H NMR (400 MHz, CD_3Cl) δ 7.85 (d, 1H), 7.39 (t, 1H), 7.24 (t, 2H), 3.84 (s, 4H), 2.62 (s, 3H), 1.10 (s, 6H). ^{13}C NMR (100 MHz, CDC l_3) δ 143.8, 134.8, 130.0, 124.6, 72.1, 31.5, 22.3, 21.8. MS (CI+) *m/z* 205 $[M]^+$.

2-(2-Bromomethyl-phenyl)-5,5-dimethyl-[1,3,2]dioxaborinane (3.25)

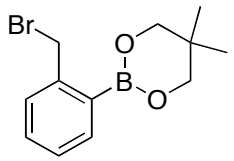

3.24 (1.22 mmol, 1 eq), N-bromosuccinimide (NBS) (1.34 mmol, 1.1 eq), and benzoyl peroxide (0.066 mmol, 0.054 eq) were dissolved in carbon tetrachloride (15 mL) and refluxed for 17 h. The reaction solution was then cooled to room temperature and the resultant precipitate was removed via vacuum filtration. The precipitate was washed with carbon tetrachloride and the combined filtrates were removed *in vacuo*. The yellow oil product (1.05 mmol, 85.8%) was obtained without further purification. ^{1}H NMR (400 MHz, $CDCl_3$) δ 7.83 (d, 1H), 7.38 (m, 2H), 7.29 (m, 1H), 4.96 (s, 2H), 3.82 (s, 4H), 1.07 (s, 6H). ^{13}C NMR (100 MHz, CDC l_3) δ 143.4, 135.5, 130.0, 127.5, 72.4, 31.6, 29.3, 21.8. MS (CI-) *m/z* 295 $[M]^1$.

Fluorescence Measurements and Heparin Charts

Binding Constants. In a 2 mL volumetric flask was prepared a HEPES (pH = 7.4) buffered solution of **3.1** (2.24×10^{-6} M). 1.50 mL of this solution was placed into a quartz cuvette. To the remaining 0.50 mL solution was added UFH or LMWH (6.66×10^{-5} M). At this concentration, each 5 μL titration of the heparin solution represents 0.1 equivalents to **3.1**. From the titration curves, emission data was extracted at 357 nm and plotted against heparin concentration as shown earlier. Using Microcal Origin software binding constants were determined to be in the range of 1.0×10^{8} M^{-1} to 2.0×10^{8} M^{-1}.

Protamine Titrations. As described in the determination of binding constants, a 1:1 heparin:**3.1** complex was formed prior to addition of protamine. In the 0.5 mL solution was added protamine (~3.33×10^{-5} M). However, the exact molecular weight of protamine was not known, so this was an approximate concentration. Titration of 10 μL aliquots of the protamine solution reversed the binding between heparin and **3.1**. Attempts to reverse heparin binding in serum did not work as addition of protamine elicited rapid precipitation of byproducts within the serum.

Dilution Studies with 3.1 and Pyrene. Chemosensor **3.1** (9.6×10^{-7} M) was added to water (1.348 mL) and HEPES (0.150 mL, 10 mM) and placed in a quartz fluorimeter cuvet. This solution was diluted with 0.050 mL aliquots of water, and after each aliquot a fluorescence spectrum was obtained. Eventually the aliquots were increased to 0.50 mL until the fluorescent emission of **3.1** approached zero.

A solution of pyrene (2.99×10^{-6} M) was prepared in n-heptanes (1.5 mL) in a fluorescence quartz cuvet. This solution was diluted with 0.050 mL aliquots of n-heptanes, and after each aliquot a fluorescence spectrum was obtained. Eventually the aliquots were increased to 0.50 mL until the fluorescent emission of **3.1** approached zero.

UFH and LMWH Standard Addition Curves. Human and equine serum samples were doped with UFH and LMWH. A 32 μL aliquot of each was added to HEPES buffer (148 uL, 10 mM) and water. **3.1** was added to the serum solution to obtain a concentration of 2.24×10^{-6} M. The total volume of the fluorimeter cuvette was 1.50 mL, and the UFH

and LMWH concentrations were varied to obtain therapeutic treatment concentrations (0.2 U/mL – 9.0 U/mL (0.08 μM – 3.6 μM) (Heparin MW was determined as the common repeating disaccharide = 644.2 g/mol)). Nine heparin doped serum solutions were prepared to span the therapeutic concentration range.

When **3.1** was initially added to the buffered aqueous serum solution binding was not immediately evident. It took approximately 18 minutes for binding to equilibrate. As a result the heparin charts illustrated in this chapter show measurements taken after 18 minutes. However, measurements could have been taken as early as 9-12 minutes, as the emission equilibration was nearly complete for all trials at this point. However, we chose to wait 18 minutes to ensure full equilibrium.

3.11 References

1) (a) Fischer, E. *Ber. Deutsch. Chem. Ges.* **1894**, *27*, 2985. (b) Behr, J. –P. *The Lock and Key Principle, The State of the Art – 100 Years On*. New York: John Wiley and Sons, 1994.

2) (a) Wiskur, S. L.; Anslyn, E. V. Using a Synthetic Receptor to Create an Optical-Sensing Ensemble for a Class of Analytes: A Colorimetric Assay for the Aging of Scotch. *J. Am. Chem. Soc.* **2001**, *123*, 10109-10110. (b) McCleskey, S. C.; Floriano, P. N.; Wiskur, S. L.; Anslyn, E. V.; McDevitt, J. T. Citrate and Calcium Determination in Flavored Vodkas Using Artificial Neural Networks. *Tetrahedron* **2003**, *59*, 10089-10092. (c) Tobey, S. L.; Anslyn, E. V. Determination of Inorganic Phosphate in Serum and Saliva Using a Synthetic Receptor. *Org. Lett.* **2003**, *5*, 2029-2031. (d) Zhong, Z.; Anslyn, E. V. Controlling the Oxygenation Level of Hemoglobin by Using a Synthetic Receptor for 2,3-Bisphosphoglycerate. *Angew. Chem. Int. Ed.* **2003**, *42*, 3005-3008. (e) Piatek, A. M.; Bomble, Y. J.; Wiskur, S. L.; Anslyn, E. V. Threshold Detection Using Indicator-Displacement Assays: An Application in the Analysis of Malate in Pinot Noir Grapes. *J. Am. Chem. Soc.* **2004**, *126*, 6072-6077. (f) Wright, A. T.; Zhong, Z.; Anslyn, E. V. A Functional Assay for Heparin in Serum Using a Designed Synthetic Receptor. *Angew. Chem. Int. Ed.* **2005**, *44*, 5679-5682.

3) Zhong, Z.; Anslyn, E. V. A Colorimetric Sensing Ensemble for Heparin. *J. Am. Chem. Soc.* **2002**, *124*, 9014-9015.

4) Lorentsen, R. H.; Graversen, J. H.; Caterer, N. R.; Thogersen, H. C.; Etzerodt, M. The Heparin-Binding Site in Tetranectin is Located in the N-Terminal Region and Binding Does Not Involve the Carbohydrate Recognition Domain. *Biochem. J.* **2000**, *347*, 83-87.

5) Hirsh, J.; Dalen, J. E.; Deykin, D.; Poller, L. Heparin: Mechanism of Action, Pharmacokinetics, Dosing Considerations, Monitoring, Efficacy, and Safety. *Chest* **1992**, *102*, 337S-352S.

6) Linhardt, R. J.; Toida, T. Heparin Oligosaccharides: New Analogues Development and Applications. *Carbohydrates in Drug Design*. Witczak, Z. J.; Nieforth, K. A.; Eds.; Marcel Dekker: New York, 1997, pp 277-341.

7) Linhardt, R. J.; Heparin: An Important Drug Enters its Seventh Decade. *Chem. & Indust*. **1991**, *2*, 45-50.

8) Langer, R.; Linhardt, R. J.; Cooney, C. L.; Klein, M.; Tapper, D.; Hoffberg, S. M.; Larsen, A. An Enzymatic System for Removing Heparin in Extracorporeal Therapy. *Science* **1982**, *217*, 261-263.

9) Freedman, M. D. Pharmacodynamics, Clinical Indications and Adverse Effects of Heparin. *J. Clin. Pharmacol*. **1992**, *32*, 584-596.

10) Weitz, J. I. Low-Molecular-Weight Heparins. *N. Engl. J. Med.* **1997**, *337*, 688-698.

11) Blajchman, M. A.; Young, E.; Ofosu, F. A. Effects of Unfractionated Heparin, Dermatan Sulfate, and Low Molecular Weight Heparin on Vessel Wall Permeability in Rabbits. *Ann. N. Y. Acad. Sci*. **1989**, *556*, 245-254.

12) Harenberg, J. Pharmacology of Low Molecular Weight Heparins. *Semin. Thromb. Haemost*. **1990**, *16*, Supplemental 12-18.

13) Jordan, R. E.; Oosta, G. M.; Gardner, W. T.; Rosenberg, R. D. The Kinetics of Hemostatic Enzyme-Antithrombin Interactions in the Presence of Low Molecular Weight Heparins. *J. Biol. Chem*. **1980**, *255*, 10081-10090.

14) (a) Mitchell, G. A.; Gargiulo, R. J.; Huseby, R. M.; Lawson, D. E.; Pochron, S. P.; Sehuanes, J. A. Assay for Plasma Heparin Using a Synthetic Peptide Substrate for Thrombin: Introduction of the Fluorophore Aminoisophthalic Acid, Dimethyl Ester. *Thromb. Res.* **1978**, *13*, 47-52. (b) *Blood Coagulation and Haemostasis*. Thomson, J. M., Ed.; Churchill Livingstone: Edinburgh, Scotland, 1989, pp. 301-339. (c) Ma, S. –C.; Yang, V. C.; Meyerhoff, M. E. Heparin-Responsive Electrochemical Sensor: A Preliminary Study. *Anal. Chem.* **1992**, *64*, 694-697. (d) Ma, S. –C.; Tang, V. C. Electrochemical Sensor for Heparin: Further Characterization and Bioanalytical Applications. *Anal. Chem.* **1993**, *65*, 2078-2084. (e) Mohri, H.; Katoh, K.; Motomura, S.; Okubo, T. Novel Synthetic Peptides from the C-Terminal Heparin Binding Domain of Fibronectin with Heparin Binding Activity. *Peptides* **1996**, *17*, 1079-1081. (f) Ramamurthy, N.; Baliga, N.; Wahr, J. A.; Schaller, U.; Yang, V. C.; Meyerhoff, M. E. Improved Protamine-Sensitive Membrane Electrode for Monitoring Heparin Concentrations in Whole Blood via Protamine Titration. *Clin. Chem.* **1998**, *44*, 606-613. (g) Mathison, S.; Bakker, E. Renewable pH Cross-Sensitive Potentiometric Heparin Sensors with Incorporated Electrically Charged H^+ Ionophores. *Anal. Chem.* **1999**, *71*, 4614-4621. (h) Ramamurthy, N.; Baliga, N.; Wakefield, T. W.; Andrews, P. C.; Yang, V. C.; Meyerhoff, M. E. Determination of Low-Molecular-Weight Heparins and Their Binding to Protamine and a Protamine Analog Using Polyion-Sensitive Membrane Electrodes. *Anal. Biochem.* **1999**, *266*, 116-124. (i) Cheng, T. –J.; Lin, T. –M.; Wu, T. –H.; Chang, H. –C. Determination of Heparin Levels in Blood with Activated Partial Thromboplastin Time by a Piezoelectric Quartz Crystal Sensor. *Anal. Chim. Acta* **2001**, *432*, 101-111.

15) Kitchen, S. Problems in Laboratory Monitoring of Heparin Dosage. *Br. J. Haematol.* **2000**, *111*, 397-406.

16) Cai, S.; Dufner-Beattie, J. L.; Prestwich, G. D. A Selective Protein Sensor for Heparin Detection. *Anal. Biochem.* **2004**, *326*, 33-41.

17) Kitchen, S.; Preston, F. E. The Therapeutic Range for Heparin Therapy: Relationship Between Six APTT Reagents and Two Heparin Assays. *Thrombosis & Haemostasis* **1996**, *75*, 734-739.

18) Denson, K. W. E.; Bonnar, J. The Measurement of Heparin: a Method Based on the Potentiation of Anti Factor Xa. *Thromb. Diath. Haem.* **1973**, *30*, 471-479.

19) (a) Levine, M. N.; Hirsh, J.; Gent, M.; Turpie, A. G.; Cruikshank, M.; Weitz, J.; Anderson, D.; Johnson, M. A Randomized Trial Comparing APTT with Heparin Assay in Patients with Acute Venous Thromboembolism Requiring Large Daily Doses of Heparin. *Arch. Intern. Med.* **1994**, *154*, 49-56. (b) Kitchen, S.; Theaker, J.; Philips, J. K.; Preston, F. E. Monitoring Unfractionated Heparin Therapy: Relationship Between Anti Xa Assays and the Protamine Titration Assay. *Blood Coagul. Fibrinolysis* **2000**, *11*, 137-144.

20) (a) Mohler, L. K.; Czarnik, A. W. Ribonucleoside Membrane Transport by a New Class of Synthetic Carrier. *J. Am. Chem. Soc.* **1993**, *115*, 2998-2999. (b) James, T. D.; Sandanayake, K. R. A. S.; Iguchi, R.; Shinkai, S. Novel Saccharide-Induced Photoinduced Electron Transfer Sensors Based on the Interaction of Boronic Acid and Amine. *J. Am. Chem. Soc.* **1995**, *117*, 8982-8987. (c) James, T. D.; Linnane, P.; Shinkai, S. Fluorescent Saccharide Receptors: A Sweet Solution to the Design, Assembly, and Evaluation of Boronic Acid Derived PET Sensors. *Chem. Comm.* **1996**, 281-288. (d) James, T. D.; Sandanayake, K. R. A. S.; Shinkai, S. Saccharide Sensing with Molecular Receptors Based on Boronic Acid. *Angew. Chem. Int. Ed.* **1996**, *35*, 1910-1922. (e) Davis, D. J.; Lewis, P. T.; McCarroll, M. E.; Read, M. W.; Cueto, R.; Strongin, R. M. Simple and rapid Visual Sensing of Saccharides. *Org. Lett.* **1999**, *1*, 331-334. (f) Wang, W.; Gao, S.; Wang, B. Building Fluorescent Sensors by Template Polymerization: The Preparation of a Fluorescent Sensor for D-Fructose. *Org. Lett.* **1999**, *1*, 1209-1212. (g) Cabell, L. A.; Monahan, M. –K.; Anslyn, E. V. A Competition Assay for Determining Glucose-6-Phosphate Concentration with a *tris*-Boronic Acid Receptor. *Tetrahedron Lett.* **1999**, *40*, 7753-7756. (h) Ward, C. J.; Patel, P.; Ashton, P. R.; James, T. D. A Molecular Color Sensor for Monosaccharides. *Chem. Comm.* **2000**, 229-230. (i) DiCesare, N.; Lakowicz, J. R. Fluorescent Probe for Monosaccharides Based on a Functionalized Boron-Dipyrromethane with a Boronic Acid Group. *Tetrahedron Lett.* **2001**, *42*, 9105-9108. (j) Arimori, S.; Bosch, L. I.; Ward, C. J.; James, T. D. A D-Glucose Selective Fluorescent Internal Charge Transfer (ITC) Sensor. *Tetrahedron Lett.* **2002**, *43*, 911-913. (k) Camara, J. N.; Suri, J. T.; Cappuccio, F. E.; Wessling, R. A.; Singaram, B. Boronic Acid Substituted Viologen Based Optical Sugar Sensors: Modulated Quenching with Viologen as a Method for Monosaccharide Detection. *Tetrahedron Lett.* **2002**, *43*, 1139-1141. (l) Zhu, L.; Zhong, Z.; Anslyn, E. V. Guidelines in Implementing Enantioselective Indicator-Displacement Assays for α-Hydroxycarboxylates and

Diols. *J. Am. Chem. Soc.* **2005**, *127*, 4260-4269. (m) Zhu, L.; Shabir, S. H.; Gray, M.; Lynch, V. M.; Sorey, S.; Anslyn, E. V. A Structural Investigation of the N-B Interaction in an *o*-(*N,N*-Dialkylaminomethyl)arylboronate System. *J. Am. Chem. Soc.* **2006**, *128*, 1222-1232.

21) (a) Burgess, K.; Porte, A. M. A Reagent for Determining Optical Purities of Diols by Formation of Diastereomeric Arylboronate Esters. *Angew. Chem. Int. Ed.* **1994**, *33*, 1182-1184. (b) Lavigne, J. J.; Anslyn, E. V. Teaching Old Indicators New Tricks: A Colorimetric Sensing Ensemble for Tartrate/Malate in Beverages. *Angew. Chem. Int. Ed.* **1999**, *38*, 3666-3669. (c) Wiskur, S. L.; Lavigne, J. J.; Metzger, A.; Tobey, S. L.; Lynch, V.; Anslyn, E. V. Thermodynamic Analysis of Receptors Based on Guanidinium/Boronic Acid Groups for the Complexation of Carboxylates, α-Hydroxycarboxylates, and Diols: Driving Force for Binding and Cooperativity. *Chem. Eur. J.* **2004**, *10*, 3792-3804.

22) (a) Iverson, D. J.; Hunter, G.; Blount, J. F.; Damewood, J. R.; Mislow, K. Static and Dynamic Stereochemistry of Hexaethylbenzene and of its Tricarbonylchromium, Tricarbonylmolybdenum, and Dicarbonyl(triphenylphosphine)chromium Complexes. *J. Am. Chem. Soc.* **1981**, *103*, 6073-6083. (b) Kilway, K. V.; Siegel, J. S. Effect of Transition-Metal Complexation on the Stereodynamics of Persubstituted Arenes. Evidence for Steric Complementarity Between Arene and Metal Tripod. *J. Am. Chem. Soc.* **1992**, *114*, 255-261. (c) Gottlieb, H. E.; Ben-Ari, C.; Hassner, A.; Marks, V. *Tetrahedron* **1999**, *55*, 4003-4014.

23) (a) Stack, T. D. P.; Hou, Z.; Raymond, K. N. Rational Reduction of the Conformational Space of a Siderophore Analog Through Nonbonded Interactions: the Role of Entropy in Enterobactin. *J. Am. Chem. Soc.* **1993**, *115*, 6466-6467. (b) Szabo, T.; O'Leary, B. M.; Rebek, J. Self-Assembling Sieves *Angew. Chem. Int. Ed.* **1998**, *37*, 3410-3413. (c) Jon, S. Y.; Kim, J.; Kim, M.; Park, S. –H.; Jeon, W. S.; Heo, J.; Kim, K. A Rationally Designed NH4+ Receptor Based on Cation-π Interaction and Hydrogen Bonding. *Angew. Chem. Int. Ed.* **2001**, *40*, 2116-2119.

24) (a) Takahashi, S.; Kuroyama, Y.; Sonogashira, K.; Hagihara, N. A Convenient Synthesis of Ethynylarenes and Diethynylarenes. *Synthesis* **1980**, 627-630. (b) Mongin, O.; Papamicaël, C.; Hoyler, N.; Gossauer, A. Modular Synthesis of

Benzene-Centered Porphyrin Trimers and a Dendritic Porphyrin Hexamer. *J. Org. Chem.* **1998**, *63*, 5568-5580.

25) Weber, E.; Hecker, M.; Koepp, E.; Orlia, W.; Czugler, M.; Csoregh, I.; New Trigonal Lattice Hosts: Stoichiometric Crystal Inclusions of Laterally Trisubstituted Benzenes – X-ray Crystal Structure of 1,3,5-tris-(4-carboxyphenyl)benzene Dimethylformamide. *J. Chem. Soc., Perkin Trans. 2* **1988**, 1251-1258.

26) Hiroya, K.; Jouka, R.; Kameda, M.; Yasuhara, A.; Sakamoto, T. Cyclization Reactions of 2-Alkynylbenzyl Alcohol and 2-Alkynylbenzylamine Derivatives Promoted by Tetrabutylammonium Fluoride. *Tetrahedron* **2001**, *57*, 9697-9710.

27) Gray, C. W.; Houston, T. A. Boronic Acid Receptors for α-Hydroxycarboxylates: High Affinity of Shinkai's Glucose Receptor for Tartrate. *J. Org. Chem.* **2002**, *67*, 5426-5428.

28) (a) Abdel-Magid, A. F.; Maryanoff, C. A. Reductive Amination of Aldehydes and Ketones with Weakly Basic Anilines Using Sodium Triacetoxyborohydride. *Synlett* **1990**, 537-538. (b) Abdel-Magid, A. F.; Maryanoff, C. A.; Carson, K. G. Reductive Amination of Aldehydes and Ketones by Using Sodium Triacetoxyborohydride. *Tetrahedron Lett.* **1990**, *31*, 5595-5598.

29) Karnati, V. V.; Gao, X.; Gao, S.; Yang, W.; Ni, W.; Sankar, S.; Wang, B. A Glucose-Selective Fluorescence Sensor Based on Boronic acid-Diol Recognition. *Bioorg. Med. Chem. Lett.* **2002**, *12*, 3373-3377.

30) (a) McFarland, S. A.; Finney, N. S. Fluorescent Chemosensors Based on Conformational Restriction of a Biaryl Fluorophore. *J. Am. Chem. Soc.* **2001**, *123*, 1260-1261. (b) Mello, J. V.; Finney, N. S. Dual-Signaling Fluorescent Chemosensors Based on Conformational Restriction and Induced Charge Transfer. *Angew. Chem. Int. Ed.* **2001**, *40*, 1536-1538. (c) McFarland, S. A.;

Finney, S. A. Fluorescent Signaling Based on Control of Excited State Dynamics. Biarylacetylene Fluorescent Chemosensors. *J. Am. Chem. Soc.* **2002**, *124*, 1178-1179.

31) Connor, K. A. *Binding Constants, The Measurement of Molecular Complex Stability*. Wiley-Interscience: New York, 1987.

32) (a) Berlmann, I. *Handbook of Fluorescence Spectra of Aromatic Molecules*. Academic Press: New York, 1971. (b) Lakowicz, J. R. *Principles of Fluorescence Spectroscopy*. Kluwer Academic Press: New York, 1999.

33) Krishnan, K. S.; Balaram, P. Perturbation of Lipid Structures by Fluorescent Probes. *FEBS Letters* **1975**, *60*, 419-422.

Chapter 4: Differential Recognition

4.1 Introduction

The last two chapters focused on research with substrate-selective synthetic sensors. Despite our success with these sensors, it is synthetically prohibitive to design and synthesize receptors for the myriad dynamic and complex potential substrates that exist for applications in environmental monitoring, medical diagnostics, and chemical warfare agent detection.

An alternative to highly substrate-specific synthetic receptors are arrays of combinatorially developed "differential" receptors used in an electronic array format.[1] These receptor arrays are inspired by mammalian olfaction and gustation. In these assays each receptor in an array provides an individual signal response to a substrate that is collected and analyzed as part of a cumulative whole-array response. To analyze the cumulative array responses, chemometric pattern recognition tools are employed to decrease the overwhelming dimensionality of the array response to simple pattern responses that are comprised of all the individual responses.[2] These dimension-reduced responses are termed "patterns" and are diagnostic for each substrate analyzed by the array. Electronic arrays do not have requirements for substrate-specific or even substrate-selective host-guest interactions provided each receptor in the array elicits a response that is unique from the other arrayed receptors. Thus, the power of electronic arrays of differential receptors lies within the inherent capability of the array to recognize multiple analytes and even mixtures of analytes via pattern recognition. For complex and

dynamic analytes such as proteins, electronic arrays offer a rather facile assay for their detection without the synthetic complexity required of substrate-specific receptors.

Progress in the field of differential recognition with synthetic combinatorially derived receptors has been made in large part by the Anslyn group.[3] This chapter will focus on the use of synthetic combinatorial libraries **4.1** and **4.2**. Library **4.1** was employed for the recognition and substrate differentiation of both intra- and interanalyte classes of proteins and glycoproteins.[3b] This work was followed by the recognition and discrimination of tripeptides and tripeptide mixtures by a **4.2:Cu(II)** complex library.[3c] In both research cases, chemometric tools were applied to analyze the complex multisignal responses of the array to provide patterns that differentiated complex and dynamic biosubstrates.

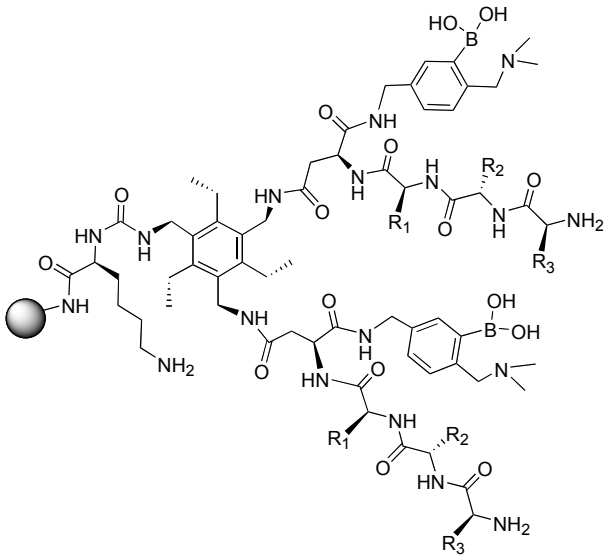

4.1
R_n are amino acids

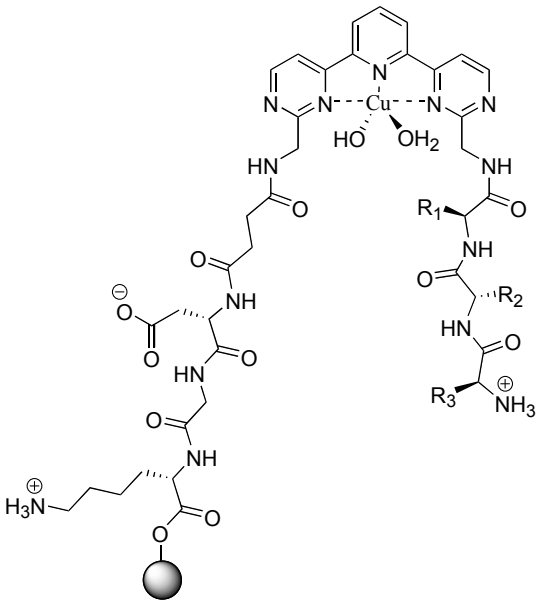

4.2:Cu(II)

4.2 Electronic Array Setup

A united effort was formed in the late 1990s at the University of Texas toward the development of an "electronic tongue;" a solution-based array of differential receptors that provides pattern responses to various analytes.[4] The earliest electronic array model was composed of one specific and three nonspecific (differential) resin-bound sensors responding to pH, di- and trivalent metal cations, and simple sugars. The sensors were arrayed in micromachined wells on a silicon wafer, and because there is one resin bead per well, each bead is individually addressable by the user. The silicon wafer was held within a microfluidic flow cell for analyte solution delivery and excretion. The flow cell was affixed to a stereoscope for close analysis of binding events occurring on the beads. Simultaneous detection of analytes at various pH values was accomplished by integration of a commercially available charge-coupled device (CCD) for concurrent access of spectral data from the arrayed sensors. The CCD permits access to red, green, and blue color transduction from each sensor in the array to form unique diagnostic patterns for each analyte. Though the differential recognition approach has amplified in complexity, and the number of arrayed receptors has increased, the general format of our electronic array has not changed significantly. The mechanics and setup of the array system will be addressed further shortly.

The array system we use is formally a microfluidic lab-on-a-chip. The development of these devices has led to significant advances for both chemical and biological applications.[5] McDevitt, Anslyn, Shear, and Neikirk have made a number of significant contributions to the lab-on-a-chip field. A full examination of the multianalyte sensor array was reported in 2001[6] followed by the use of an enzyme-based sensor array for the analysis of multicomponent monosaccharide solutions.[7] Later,

antibody-derivatized sensors were developed for use in the array for the simultaneous detection of two serum cardiac risk factors, C-reactive protein and interleukin-6.[8] A later follow-up study employed antibody-derivatized resin beads for detection of C-reactive protein in human saliva.[9] Novel capillary sample introduction[10] and chromatographic[11] sensor arrays have also been developed. Subsequent research has evaluated the incorporation of various biotinylated DNA capture agents on agarose resin beads for the rapid recognition of DNA oligonucleotides.[12] As mentioned earlier, a number of synthetic, combinatorially developed resin-bound sensors have been used for the recognition of bioanalytes such as nucleotides, proteins, and tripeptides.[3]

4.2.1 Flow Cell Arrangement

We have developed synthetic combinatorial libraries of receptors for proteins, glycoproteins, tripeptides, and tripeptide mixtures. These libraries were built on NovaSyn tentagel amino resin beads that are composites of low cross-linked polystyrene and polyethylene glycol (MW: 3,000-4,000). The polyethylene glycol chains are terminally functionalized with amino groups from which the libraries are built using standard split-and-pool solid phase chemistry. The beads have a diameter of 130 μM with a narrow size distribution from one to the next. Furthermore, these resin beads have good swelling properties across a myriad of solvents, which is important to the water based studies we have conducted. The resin swells to ~200 μM in aqueous buffered solutions which is ideal for filling the space of the microcavity. The bead matrix of the tentagel amino resin is also optically transparent permitting transduction of optical signals that are used for pattern recognition.

Figure 4.1 Tentagel Amino Resin Beads Arrayed in a Micromachined Silicon Wafer.

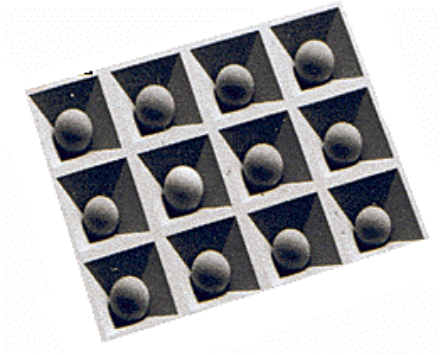

Resin beads from library **4.1** or **4.2** were randomly selected and placed within pyramidal microcavities of the array wafer (Figure 4.2). These wafers are micromachined in-house by Professor Neikirk's chemical engineering laboratory. The microcavities are prepared using a 40% KOH anisotropic etching of the silicon wafer. During the KOH process the wafer was masked with a silicon nitride layer. After completion of the pyramidal pits, the masking layer was removed entirely from the cavities and the wafer was soaked in a 30% H_2O_2 solution for 15-20 minutes to form a thin SiO_2 layer that improves the wetting characteristics.[6] After this etching procedure the wafer has a 7 × 5 array of identical pyramidal microcavities. The cavities have sides angled inward at 54.7° forming a pyramidal pit with a top opening of ~500 μM across, and a bottom opening that is ~90 μM across as seen in Figure 4.1. The distance from the top to the bottom of the pyramidal pit is ~220 μM. This is an appropriate size for holding the 110 μM tentagel resin beads.

Figure 4.2 A Cross-Section Diagram of the Pyramidal Microcavities with a Resin Bead Held in the Cavity.

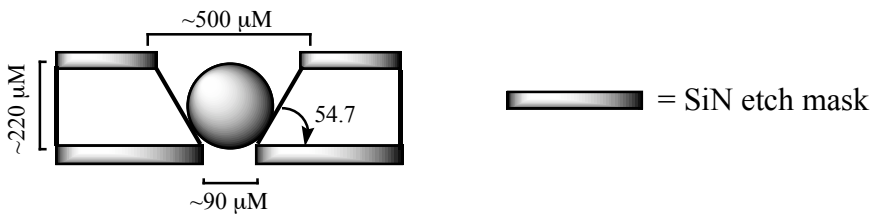

The development of an analytical microfluidic device for differential recognition requires more than a Si wafer to hold the tentagel library members. The Si wafer is sandwiched within two transparent machined circular Teflon frame discs from which the substrate solution is delivered and extricated via PEEK tubing. Because the tubing is inserted deep into the disc the solution only enters and exits through the array. A hydrophobic adhesive is fixed to the surfaces of the discs to promote solution flow through the microcavities, but the adhesive is not placed in the region of the wafer where it could interfere with the optical signal. The adhesive also forms a depression for the wafer array to lay in. The array and Teflon discs are held firmly within an aluminum housing that compresses the wafer array between the Teflon framing (Figure 4.3). This compression forces all solvent to enter through the top disc, cover the array, and flow through the microcavities and thus through the arrayed receptors. This resulting microfluidics flow cell can handle flow rates as high as 10 mL/min and permits optical measurements to be made.[6]

Figure 4.3 Solvent Flow (arrows) and Arrangement of Wafer Within Teflon Discs and Aluminum Housing.

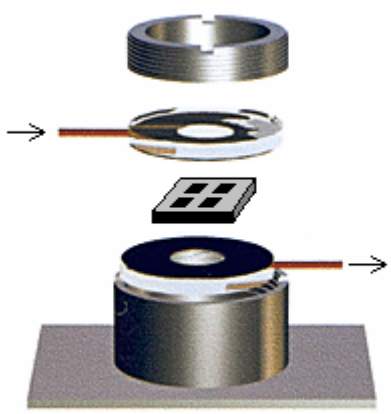

Substrate, buffer, and wash solutions were introduced to the array by an Amersham Pharmacia Biotech AKTA Fast Protein Liquid Chromatograph (FPLC) controlled by Unicorn 3.0 Software. This instrumentation acts as a readily controllable, precise, and versatile solution pump. The solvent delivery tubing of the FPLC is readily attached to the flow cell via male/female luer-lock connection joints to the PEEK tubing of the Teflon framing. PEEK tubing is linked to a waste container on the excretion side of the flow cell. The FPLC unit employed for differential recognition array studies is capable of drawing from two solutions (e.g. buffer and acidic wash solution) and is also fitted with a syringe injection port and a 5 mL sample loop that permit delivery of other necessary reagents and washes.

4.2.2 Data Acquisition

The developed microfluidic flow cell was fixed with common lab tape to the stage of an Olympus SZX 12 stereoscope that illuminated the resin beads from below the wafer array. Illumination of the beads in the array was done using a General Electric Quartzline lamp with which illumination intensity could be controlled. The array was observed and analyzed through the stereoscope optics using a three-chip 12-bit CCD (DVC 1312C) directly attached to the stereoscope. The CCD, in conjunction with video capture cards and integrated Image Pro 4.0 software, was used to analyze spectral changes resulting from substrate binding to the differential receptors in the array. Image capture can occur at rates up to 30 images/second, but for our analysis rates never exceeded 1 image/2 seconds. A computer controller permits parallel operation of image capture and solution flow. Figure 4.4 illustrates the full electronic array setup.

Figure 4.4 Electronic Array Setup – the CCD is attached directly to the top of the stereoscope. The array is fixed to the scope stage. On the left hand side of the image is the FPLC for solution delivery.

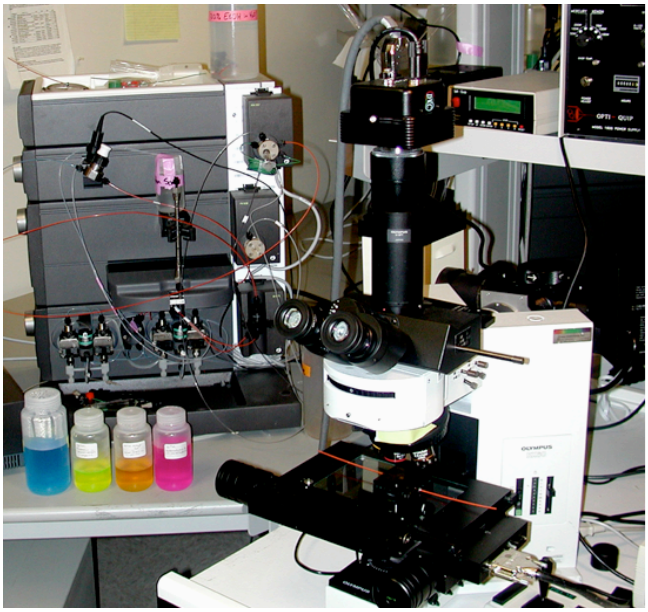

Numerical red, green, and blue (RGB) intensity data can be extracted from the captured CCD images and used to form diagnostic substrate patterns (Figure 4.5). To obtain RGB data an area of interest (AOI) is defined for each bead in the array. This commands the computer to extract RGB data from each bead in the array, but only from within a certain portion of each bead. However, AOIs are drawn to maximize bead coverage. The RGB data from each bead is exported to Excel worksheets for further analysis. For our colorimetric assays the RGB intensity values were converted to "effective absorbance" values. These values are calculated using Beer's Law (A_{RGB} = -Log (I_{RGB}/I_N)), where A_{RGB} is the effective absorbance of either the red, green, or blue intensity, I_N is the average pixel intensity of a blank N-acetylated bead, and I_{RGB} is the

experimental pixel intensity of either the red, green, or blue channel. The effective absorbance is a correction factor that removes the residual background noise due to lamp fluctuations during the assay.

Figure 4.5 RGB Data is Collected From Each Bead in the Array From Video Card Captured Images. As seen the purple color of the bead actually relates to various levels of RGB pixel intensity.

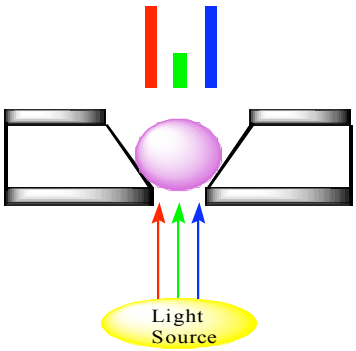

4.2.3 Pattern Recognition

Discrimination of patterns by humans starts at a very young age. Toddlers are taught to recognize differences between squares, circles, cylinders, and other shapes. Older children are given matrices of numbers and asked to determine the pattern such as evens and odds, etc. Adults recognize patterns daily from the clothes they wear to the art they enjoy. However, human visual pattern recognition is trumped by gustatory and olfactory pattern recognition of complex flavors and aromas. As demonstrated in Figure 4.6, the gustatory response to either a lemon or apple is really a combination of multiple

differential interactions. An apple signals higher levels of sweet sensation, but lemons are far more bitter and sour. However, the human brain takes all of the composite signals and recognizes these various sensations as a unique pattern for a single tastant. The gustatory system has provided much inspiration for our research, and we have developed an array assay akin to taste sensation.

Figure 4.6 Mammalian Gustatory "Pattern" Recognition of Tastants.

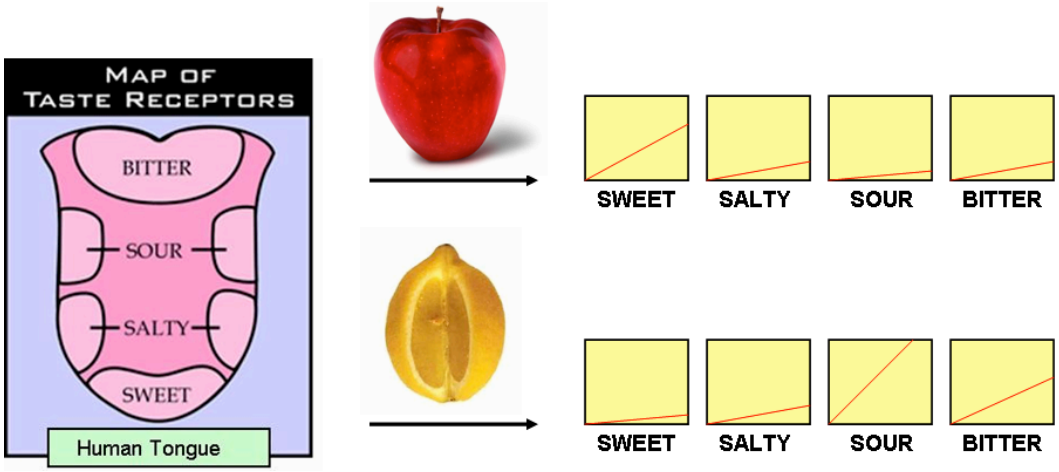

Our array assay is designed such that analyte recognition by each differential receptor in the array induces a different signal. The combined response of all the receptors in the array is the diagnostic pattern for a particular analyte. However, this is where a human's visual detection of patterns is limited. Simple patterns in relatively small data matrices can be identified, but as the complexity increases it becomes more difficult, or impossible. Figure 4.7 illustrates an example of this. A 4 × 5 array of responses to two analytes is illustrated. The pattern for either analyte is the combination of all the responses. If responses from a third, fourth, or fifth analyte were added to the

image visual pattern detection would be nearly impossible. In our own recognition of tripeptides, proteins, and glycoproteins similar matrices of kinetic responses were used to formulate diagnostic patterns. Our patterns were generated using the chemometric tool of principal component analysis (PCA), which reduces the overall dimensionality of the data set, and develops a new graph that provides clear visualization of patterns. In the next section the concept of PCA will be further expanded.

Figure 4.7 Kinetic Responses from Two Analytes Represent the Difficulty in Visual Detection of Patterns.

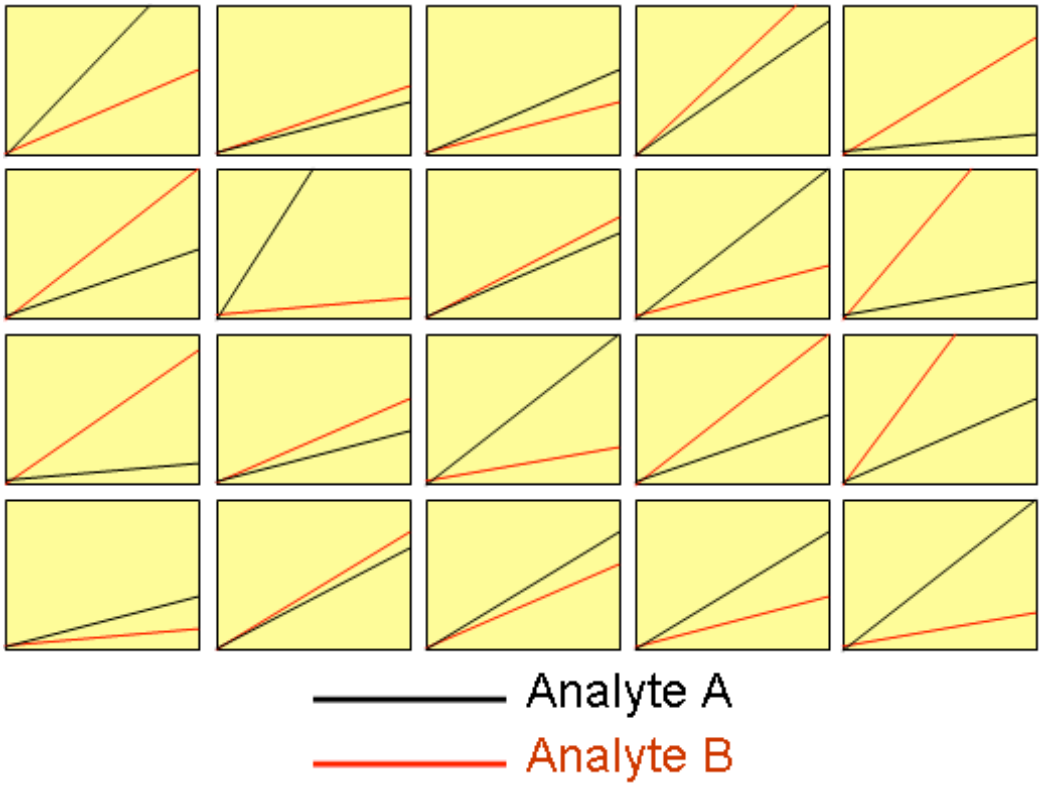

4.2.3.1 Indicator-Uptake Assay

So far the electronic array has been discussed and pattern recognition formally introduced. It was mentioned that the CCD attached to stereoscope can analyze RGB pixel intensities at each resin-bound receptor in the array. However, tentagel amino resin covalently linked through an amide bond to receptors of library **4.1** or **4.2** have no intrinsic color. Additionally, the targeted substrates of proteins, glycoproteins,

tripeptides, and tripeptide mixtures have no intrinsic colorimetric properties. Therefore, to probe binding events occurring at each arrayed receptor a signal-modulating event was incorporated into the array. Previously, an indicator-displacement assay was employed with the array.[3a,14] In an indicator-displacement assay, an indicator is initially added to the array followed by subsequent addition of substrates and displacement of indicators. The greater the indicator-displacement the more effective the binding. However, during the course of our array research it was determined that a staining, or indicator-uptake, signaling assay significantly increased the sensitivity of the analysis in bead-based arrays. A number of refinements of the indicator-uptake protocol were made throughout our research resulting in high sensitivity recognition and discrimination of substrates. The original substrate concentration used for the indicator-displacement assay array was 20 mM.[3a] In our studies the sensitivity was enhanced with an indicator-uptake assay to substrate concentrations as low as 14 μM.[3b,3c]

In an indicator-uptake analysis an analyte is first delivered to the array at a slow rate to maximize adsorption of the analyte to the arrayed differential receptors. At the low concentrations of analytes employed, it is believed that several binding sites on each bead in the array remain empty following the initial analyte delivery. Following analyte delivery and a brief buffer wash to remove unbound analyte, the indicator is delivered at a fast rate through the flow cell. The indicator occupies binding sites that remain open. If an analyte interacts strongly with a receptor and thus binds to more sites, less indicator-uptake will occur. On the other hand, if an analyte:receptor interaction is weak a larger indicator-uptake occurs. Therefore, the colorimetric event correlates indicator-uptake to substrate binding at each receptor within the array. At the end of an analysis, acidic and basic wash solutions are delivered to the array to remove all bound analyte and indicator. The entire indicator-uptake assay within the electronic array is illustrated in Scheme 4.1.

Scheme 4.1 Electronic Array Indicator-Uptake Assay. Note: the adsorption of analyte is shown as a purple color for emphasis, but the substrates used did not have any intrinsic colorimetric properties.

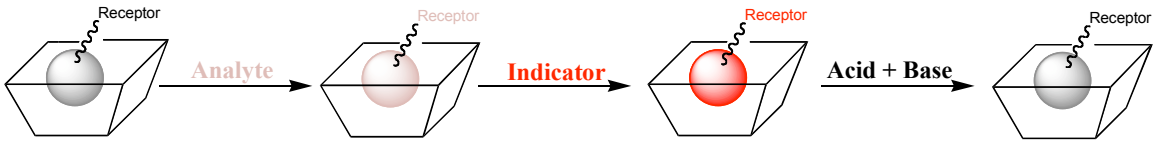

It is now established that the colorimetric properties measured result from indicator-uptake following substrate adsorption to the arrayed receptors. However, this does not yet answer the question of how the colorimetric response is measured and correlated to substrate binding to the receptor, or how patterns were obtained for an analyte.

During indicator-uptake analysis, 215 12-bit CCD images were captured for each tentagel-bound differential receptor in the array. These images were analyzed by drawing an AOI covering a maximum portion of each bead. From within the AOI, red, green, and blue pixel intensity values were obtained from each CCD image. For analysis, only the red, green, or blue channel intensity that had the greatest signal to noise ratio was used for data acquisition. The color channel intensity values used for analysis were converted to an "effective absorbance" value. For each substrate trial a slope of indicator-uptake was obtained for each receptor by snapping one image every two seconds. These slopes describe the kinetics of indicator-uptake for each differential receptor as a function of substrate binding.

Figure 4.8 shows three indicator-uptake slopes taken from three different receptors from the array in response to a single analyte. As observed in Figure 4.8, each receptor responds in a unique fashion to the analyte. Multiple trials from our research

have demonstrated that these kinetic slopes are reproducible, a key factor for assays that require multiple trials. It is also required that each receptor responds differently from one substrate or mixture to the next. The kinetic slopes defined for each of the receptors in the array are combined to provide an overall response. This cumulative response is defined as the pattern for an individual substrate or mixture. This is similar to multiple receptors on the tongue giving differential responses to an analyte that leads to a single unique flavor response. For a complete analysis of multiple analytes and mixtures, it is required that each receptor also responds differently from one another in response to a single analyte. If each receptor responded identically to a single analyte it would not illustrate a differential response, but rather that the primary mode of association between receptors and analytes was identical across the array regardless of the composition of the peptidic arms (the differential element of the receptors in both library **4.1** and **4.2**). Therefore, we have now established how the kinetic signal is obtained and analyzed, and how it pertains to the unique diagnostic pattern of an analyte.

Figure 4.8 Kinetic Indicator-Uptake Responses From Three Arrayed Receptors to a Single Analyte.

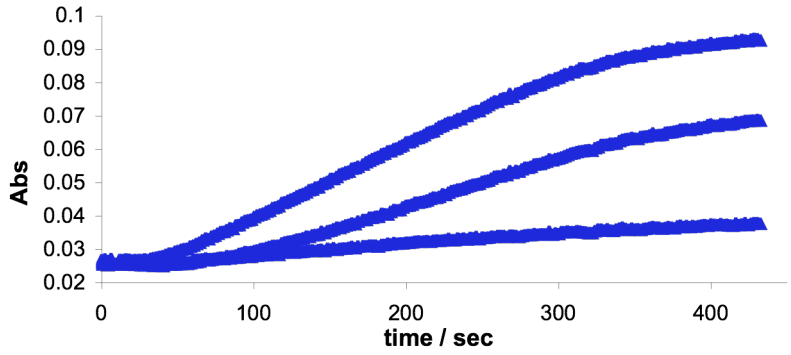

4.2.3.2 Principal Component Analysis

Principal component analysis (PCA) is a chemometric tool used for pattern recognition.[15] For the array, a good experiment leads to discrimination (graphical separation) of various analytes on a principal component chart. If multiple trials are run with the same analyte, a good experiment is determined by close clustering of the same analyte, and spatial discrimination from any other analyte(s) tested. PCA is best understood using an example from the array. If four substrates are run through an array four times each that would be 16 experiments, and each experiment, or trial, is known as a *case*. If the array is composed of 35 differential receptors each providing a response to an analyte, then each receptor in the array is termed a *variable*. Each analyte leads to 35 distinct responses, one for each variable. This is akin to a 35 dimension graphical response for each analyte. Because it is not feasible to graphically determine analyte correlations in 35 dimensions, PCA is used to reduce the dimensionality of the data set and provide visually detectable patterns. PCA attempts to "represent the variation present in many variables using a small number of 'factors'."[16] Therefore, a new plot of the cases is made by redefining the axes as factors, also known as *principal components* (PCs), rather than the original variables. The PC axes are always orthogonal to one another, and the maximum number of PCs calculated is the smaller of the number of cases or variables. The new PCs permit visual analysis of measurements made with many variables in a small number of dimensions.

On the new PCA chart, the first principal component explains the maximum amount of variation present in the data set. Subsequent PCs describe diminishing levels of variation. The cases (analytes) have new coordinates as well on the PCA chart that are termed *scores*. Each PC axis is constructed from combinations of the original 35

measurement variables. The contribution from a variable to the formation of a PC axis depends on the orientation in space between the original variable axes to the new PC. If the cosine of the angle between them is near 1 or -1 (so the variable axis is nearly parallel to the PC axis) then measurements from that variable are very important to the formation of the PC. The value of the cosine of the angle between the original variable axis and the PC is termed a *loading value*. Figure 4.9 shows a sample experiment. The measurement data from the 35 original variables has been reduced to two PC axes with PC1 describing 79% of the variance and PC2 13% of the variance. The remaining variance is described by four PC axes that describe more noise than signal so they are excluded. Clustering of multiple trials of a single analyte, and separation of differing analytes is important to the array analysis.

Figure 4.9 PCA Chart Describing the Relationship of Analytes (Cases) on PC Axes Determined from Measurements from 35 Arrayed Variables.

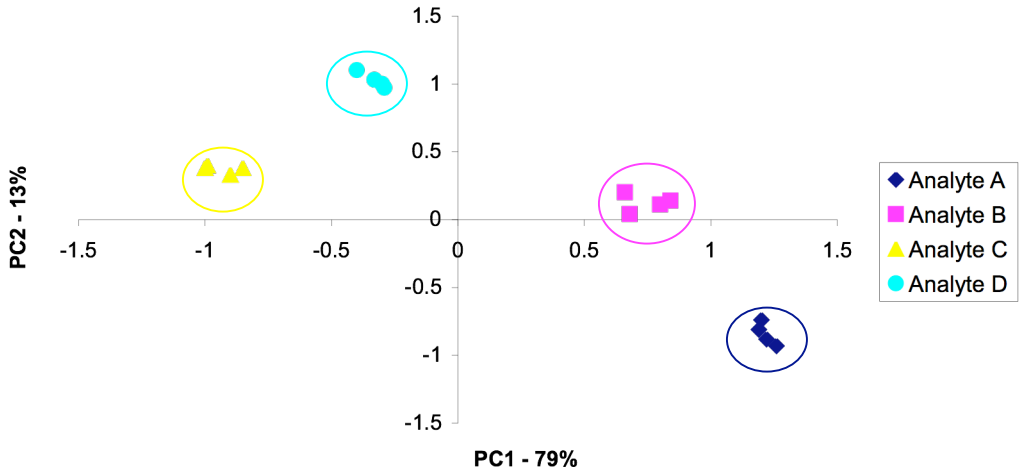

4.3 Differential Recognition of Proteins and Glycoproteins

4.3.1 Design and Synthesis of Receptor Library 4.1

To differentiate various proteins and glycoproteins, library **4.1** was designed and synthesized incorporating one of 19 natural amino acids (cysteine excluded) at each of three sites on two different binding arms using combinatorial chemistry. This created a library with 19^3 (6,859) unique members. The peptide arms provide sites for molecular recognition of proteins via ion-pairing, hydrogen bonding, and the hydrophobic effect. The boronic acids provide effective sugar binding sites because these groups rapidly and reversibly form cyclic esters with diols in aqueous media.[17] The hexasubstituted benzene scaffold acts as a spacer and assists in the creation of a binding cavity.[18] The expectation was that each receptor would display differential binding with proteins based on the variance in the peptide arms, and the boronic acids would assist in differentiation of proteins from glycoproteins.

Commencing with NovaSyn Tentagel Amino Resin **4.3**, an Fmoc-Lys(Boc)-OH group was added via a peptide bond forming reaction with PyBOP, HOBt, and TBTU. To ensure that the amino groups of **4.3** had been fully reacted acetic anhydride and 2,6-dimethylamino pyridine (DMAP) were added to cap any remaining amino functional groups. The Fmoc protecting group of Lys was subsequently removed with a solution of 20% piperidine in DMF to give **4.4**. The urea linkage between the receptor core **4.7** and **4.4** was formed by addition of 4-nitrophenylchloroformate (**4.5**) with N,N-diisopropylethylamine as base to give **4.6**. The core **4.7** was added to a THF/methylene chloride (DCM)/DMF solution containing resin **4.6** and mixed overnight to give the urea linked core to the resin **4.8**. The boronic acid containing side arms (**4.9**) of receptor **4.1**

were coupled to **4.8** using a PyBOP mediated peptide bond forming reaction. Subsequent removal of the Fmoc protecting groups of the two side arms using a solution of 20% piperidine in DMF yielded **4.10**. With the free amine groups of **4.10** we were suitably prepared to develop the peptide arms of **4.1** using split-and-pool combinatorial chemistry. In this method the resin was split into 19 equal portions by weight. Each portion was reacted with a single Fmoc protected amino acid in a PyBOP mediated coupling reaction. If amino acids contained reactive side chains then they were protected with an acid-labile protecting group in addition to the Fmoc protection of the amino functional group. Following amino acid coupling, all resin portions were mixed together and reacted with acetic anhydride and DMAP to cap any unreacted amino groups of **4.10**. The Fmoc groups were then removed using a solution of 20% piperidine in DMF. The resin was then split into 19 equal portions by weight once again and the coupling, capping, and deprotection steps were repeated. The split-and-pool procedure was carried out three times to give the tripeptide binding arms on receptor **4.1**. The split-and-pool procedure of combinatorial chemistry for library development results in the synthesis of resin beads covered with only one distinct receptor per bead. Thus, it is a one-bead-one-compound synthetic approach. To obtain library **4.1** in a fully deprotected state, a solution of trifluoroacetic acid (TFA)/water/1,2-ethanedithiol/triisopropylsilane (94:2.5:2.5:1) was reacted with the library. Prior to use in the array, library **4.1** was rinsed multiply with TFA and then washed several times with DMF, methanol, DCM, and water.

Scheme 4.2 Resin-Based Synthesis of Library **4.1**.

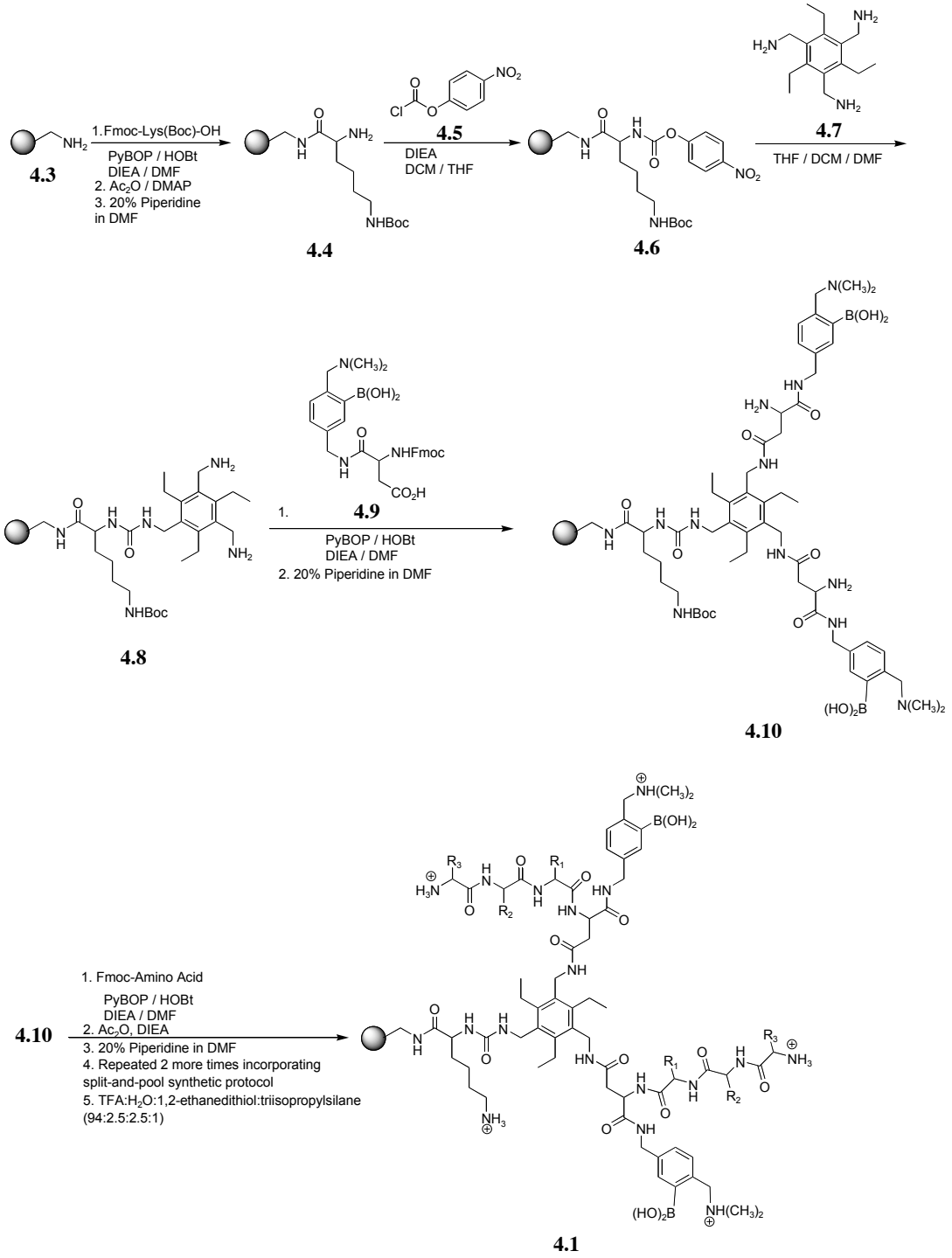

4.3.2 Optimization of Array Studies

After reviewing previous Anslyn array research with nucleotide phosphates,[3a] as well as a few of our own test cases, it was evident that an indicator-displacement assay would have to be replaced with an indicator-uptake assay if guest substrates were to ever be bound at reasonably low micromolar concentrations. In our own displacement studies using the glycoproteins ovalbumin and fetuin (355 μM) and the indicator ethyl orange (125 μM) little to no displacement of the indicator was achieved. The high indicator concentration was required to see any changes at all, but it was also counterproductive. It was very difficult to extricate the indicator from the beads following a substrate trial because the indicator at the high concentrations used bound tightly to the resin-bound receptors. Therefore, the attention of the research was turned toward an indicator-uptake assay.

To identify an indicator for a full binding study with proteins and glycoproteins, a screening approach was taken. It was necessary to identify an indicator that would give a good signal via the CCD, be stable to the buffer conditions, and readily wash out following each substrate trial. Several indicators were tested as shown in Figure 4.10. The indicators chosen contained diols or α-hydroxy acids to enhance binding between the boronic acid moieties of library **4.1** and the indicators. It was believed that this would facilitate reproducible indicator-uptake from trial to trial. In small vials ~5 mg of resin was added to buffered water (1 mL, HEPES 50 mM, pH 7.4) and one of the nine indicators from Figure 4.10 was added (solution concentration = 100 μM). The vials were mixed for 20 min. and the resin beads were filtered from the solution. The beads were washed several times with the buffer solution to remove unbound indicator and then were dried.

Figure 4.10 Indicator Screening for Use in Electronic Array Studies with Library **4.1**.

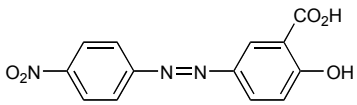

Mordant Orange 1

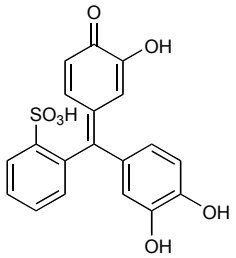

Pyrocatechol Violet

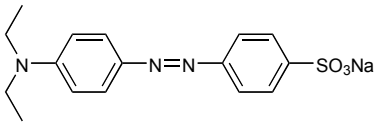

Ethyl Orange

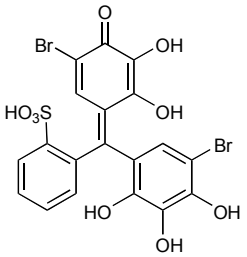

Bromopyrogallol Red

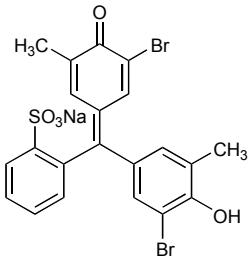

Bromocresol Purple

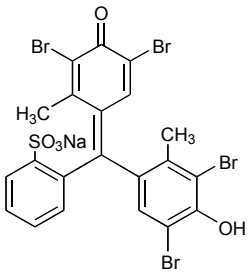

Bromocresol Green

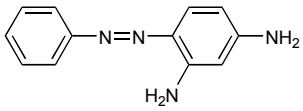

Chrysoidin

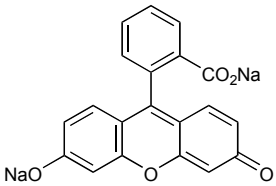

Fluorescein

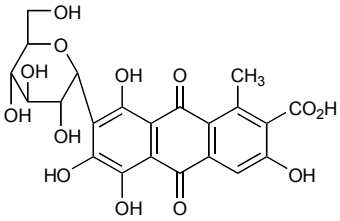

Carminic Acid

The first study with the indicator-bound receptors was to test the effectiveness of extricating the indicators from the receptors using acid and base washes. Three or four of each indicator-bound receptor were loaded into a 7 × 5 array and used in purging studies. Using HCl (0.6 M) and NaOH (0.6M) it was found that carminic acid, bromopyrogallol red, mordant orange, and fluorescein were all completely, or nearly completely, washed

from their respective receptors in the array. Further studies using 26 carminic acid (50 μM) bound receptors and 9 N-acylated blank beads determined that repeated loading of carminic acid followed by acid and base washes did not effectively remove all the carminic acid. Therefore, carminic acid was eliminated as a possible indicator for array binding studies. A subsequent study with bromopyrogallol red determined that an effective concentration for working with it was 15 μM. Therefore, a mini-array study was completed in which library members and blank beads were loaded in an array and tested for indicator-uptake (15 μM, 5 mL injection) following addition of the glycoprotein ovalbumin (0.533 mM, 5 mL injection). Ovalbumin was added, followed by indicator, and then HCl and NaOH (both 0.6 M) were used to renew the array for a subsequent trial. Three trials with ovalbumin were run, but a problem arose concerning the removal of protein from the receptors. Following acid and base washes the indicator was rinsed out, but a dull grey color was left behind. As multiple trials were tested the grey color increased indicating that we were likely not removing all the protein between trials.

It was determined that removal of both proteins and glycoproteins could be effected by using multiple NaOH injections (0.6 M, 5 mL injection, 1.5 mL/min flow rate) followed by a prolonged HCl wash (0.3 M, 25 min. constant flow at 2 mL/min). Other studies were conducted to determine the appropriate flow rate for protein injection, (0.25 mL/min) and lowest possible protein concentrations (355 μM) for a full array analysis. Additionally, it was found that indicator-uptake studies at a relatively rapid flow rate (1.0 mL/min) resulted in more reproducible results.

4.3.3 Full Array Studies with Proteins and Glycoproteins

A 7 × 5 array was used that contained 29 randomly selected resin-bound receptors from library **4.1** and six N-acylated blank beads. The indicator used for indicator-uptake analysis was bromopyrogallol red because of its excellent colorimetric response and facile removal from the array. The proteins utilized for our differential recognition study were ovalbumin, fetuin, lysozyme, bovine serum albumin (BSA), and elastin. These choices were made to challenge our design principles by grouping proteins of similar properties. The characteristics of the proteins span a variety of molecular weights, glycosidic properties, and isoelectric points (pI). The molecular weights of ovalbumin and fetuin are similar, as are elastin and BSA. The pI of ovalbumin, BSA, and fetuin are similar, as are lysozyme and elastin (Table 4.1).

Table 4.1 Characteristics of Proteins and Glycoproteins Discriminated by Library **4.1**.

Protein	Molecular Weight [kDa]	pI	Glycoprotein?
Ovalbumin	44-45	4.6	Yes
Fetuin	48.4	4.5-4.9	Yes
Lysozyme	14	9.6-11	No
BSA	66	4.7-5.2	No
Elastin	60	9.3-10.2	No

Our experimental protocol commenced with a relatively prolonged delivery of a protein solution (0.25 mL/min, 355 μM in HEPES buffer, 25 mM, pH 7.4). This was

followed by a three minute buffer (25 mM HEPES, pH 7.4, 1.0 mL/min) wash, and then a rapid delivery of bromopyrogallol red (3.0 μM in HEPES buffer, 1.0 mL/min). After each analysis, the protein and indicator were washed from the array with NaOH (150 mM) and HCl (300 mM) rinses. This allowed for repeated use of the array. 215 12-bit images were captured every 2 seconds during the indicator uptake from which a slope was garnered from a graph of time versus green channel absorbance for each receptor bead in the array (see Figure 4.8). Effective absorbance values were obtained by calculating the negative log of the ratio of the green channel intensity of each bead to the green channel intensity of a blank bead.

Four trials were performed for each protein.[21] The indicator-uptake slopes were calculated for each receptor bead over the time period at which the dye was passing through the array (49 to 403 s). For each trial, a slope was measured for the indicator-uptake for each resin-bound receptor (blanks not included). The slopes acquired from the graphs for each resin-bound receptor represent the diagnostic fingerprint for a particular protein/glycoprotein. Because of the large number of slopes calculated from each trial, the dimensionality of the data set was reduced using PCA.

In this study, the first four PC axes effectively satisfied the Kaiser criterion, which states that as many factors could be extracted as variables that have eigenvalues greater than one.[22] Figure 4.11 is a two dimensional PCA plot which effectively separates proteins from glycoproteins. As illustrated there is nice differentiation between proteins and glycoproteins, which was a primary goal of this study. But, it is clear that there is significant overlap between lysozyme and elastin, and relative close spatial orientation between the two glycoproteins. Clearly BSA was well differentiated by the array of differential receptors. The weights along the axes should also be noted. The horizontal axis has a 75.2% weighting, whereas the vertical PC2 axis has only a 10.6% weighting.

Therefore, separation between scores along the horizontal PC1 axis is far more significant than separations along the PC2 axis. However, because four PC axes satisfied the Kaiser criterion it was possible to generate a three dimensional PCA plot that further separated the proteins.

Figure 4.11 PCA Plot Illustrating the Recognition and Discrimination of Proteins and Glycoproteins by an Array of Library **4.1**. (● Lysozyme, ● Elastin, ● Ovalbumin, ● Fetuin, ● BSA).

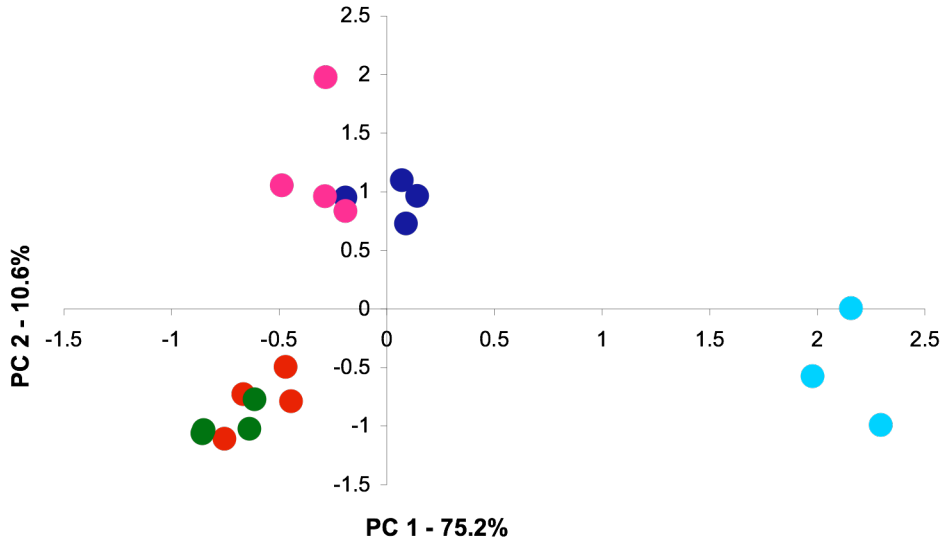

Figure 4.12 shows an expanded PCA plot using PC axes 1-3. This demonstrates that the array of receptors adequately separated proteins from glycoproteins, and to a lesser extent even separated proteins within the classes. The major separation that occurs upon addition of PC3 is lysozyme from elastin. This is a key factor as there is now very little score overlap in the PCA plot. This demonstrates that the array of receptors bound and recognized a series of proteins and glycoproteins using pattern recognition. The fact that we used a random selection of receptors to achieve these results illustrates the power

of our method. More than likely any one of these 29 receptors would not have been a good receptor for a particular protein, however, when functioning in tandem, the array worked well. Further, any 29 receptors could presumably be used to obtain analogous patterns for the proteins. PC axis 4 (4.7%) could have also been used for further discrimination in a separate three-dimensional plot.

Figure 4.12 Expanded PCA Plot Demonstrating the Discrimination Capability of an Electronic Array of Library **4.1**. (● Lysozyme, ● Elastin, ● Ovalbumin, ● Fetuin, ● BSA).

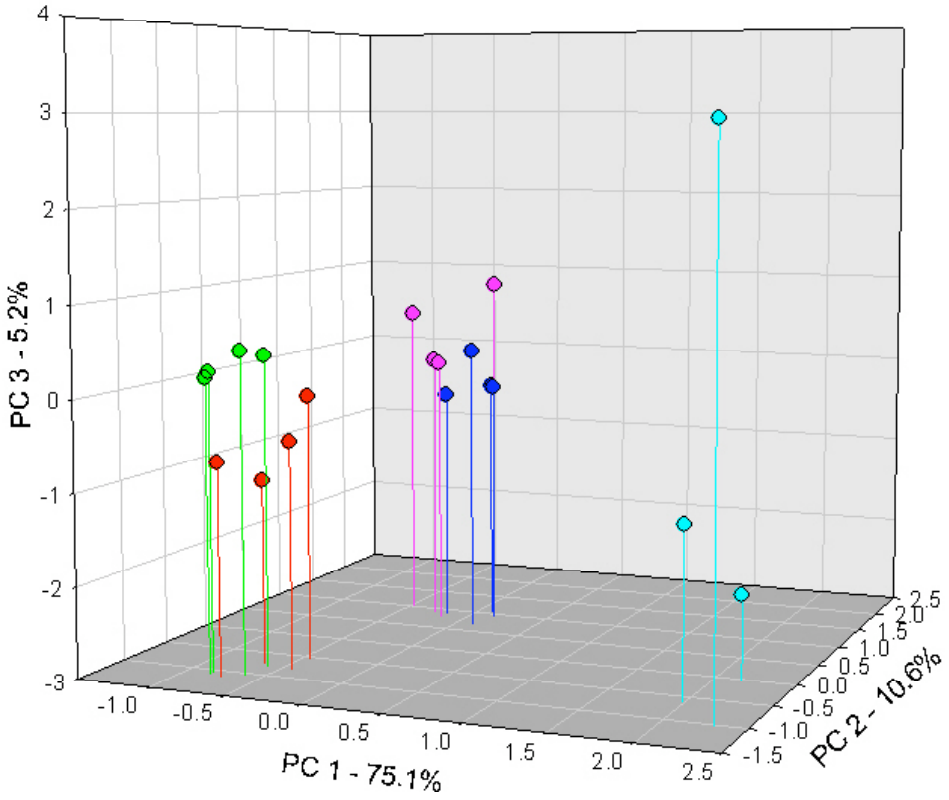

A control was performed using a 7 × 5 array with six blanks and 29 resin beads derivatized only with tripeptides that were obtained from a combinatorial library synthesized with 19 natural amino acids (cysteine excluded).[23] Using this array of tripeptide beads, no separation of analytes occurred. This control illustrated that some element of design must be incorporated into the receptors to bind certain analyte classes, and that simple random receptors are inefficient. These results do not strictly demonstrate that the boronic acids bind to glycoproteins and not standard proteins. More likely the boronic acids interact with surface epitopes on both protein classes, but to varying extents. Yet, if differential covalent bond formation to the boronic acids was the only factor in discrimination between protein classes, then because they are the only binding moiety present in every receptor, no differences within each protein class would have been expected. Therefore, both the boronic acids and the variable peptide arms of the receptors are critical in identification and discrimination of proteins and glycoproteins.

Though the analyte concentrations were significantly reduced from the previous report with nucleotide phosphates, the protein concentrations (355 μM) were still relatively high for practical analysis. Reduction to practical concentrations (nM) could be accomplished with higher affinity differential receptors or further alterations to the array methodology.

The PCA plots demonstrated similarities between ovalbumin and fetuin, and similarities between elastin and lysozyme. Yet, even the proteins in similar groups were separated. The proximity of ovalbumin and fetuin is reasonable as both are glycoproteins with similar pI values, and both likely interacted with the boronic acid moieties. Further, elastin and lysozyme have similar pI values. Therefore, the separation defined by the differential receptor array analysis was not simply a facet of charge. Interestingly,

molecular weight was not a key factor to the patterns exhibited for the proteins/glycoproteins. BSA is likely separated from the others because it has a different pI than elastin and lysozyme and is not a glycoprotein. The differentiation between similar proteins is likely due to specific contacts between the receptors and proteins that are cross-reactive and subtly discriminatory.

As mentioned earlier in this chapter, factor loading values are calculated in PCA to determine the magnitude of contribution of an original variable to the formation of a PC axis. Variables with loading values approaching -1 or 1 have a dominant role in the formation of a PC axis. Because PC axis 1 described the most variance, five beads with high loading values on PC 1 and two beads with low loading values were selected for receptor characterization (Table 4.2) using Edman degradation. Edman degradation in combination with GC/MS permits identification of the amino acids that make up the differential binding arms of the seven receptors selected from the array for sequencing. Figure 4.13 illustrates the 35 member array with bead positions numbered. The bead positions can be related to Table 4.2. The sequencing results did not reveal any obvious homologies for either the significant or insignificant receptors of the array. Yet, the lack of any homology is a lesson in itself: differential sensing schemes can be successful and may even benefit from a wide variety of structurally diverse receptors.

In summary, the ability of an array of differential receptors to differentiate between classes of proteins, and even between very structurally similar proteins, has been demonstrated. This separation was not due solely to charge differences nor molecular weight differences, but rather specific contacts between receptors and proteins that gave discriminatory patterns.

Table 4.2 Sequencing Results from Edman Degradation of 7 Resin-Bound Receptors from Library **4.1** Either Significant or Insignificant to the Formation of PC Axis 1.

Tripeptide Sequence	Factor Loadings (PC1)	Bead Position
Ala-Ser-Asp	0.984	12
Ser-Lys-Gly	0.963	9
Arg-Lys-Lys	0.951	15
Gly-Asp-Ser	0.932	2
Asp-Leu-Val	0.928	22
Lys-Arg-Met	0.774	23
Gly-Gln-Gln	0.722	6

Figure 4.13 Numbering of Receptor Positions Within the Electronic Array.

1	2	3	4	5	6	7
8	9	10	11	12	13	14
15	16	17	18	19	20	21
22	23	24	25	26	27	28
29	30	31	32	33	34	35

4.4 Differential Recognition of Tripeptides and Tripeptide Mixtures

4.4.1 Design and Synthesis of Library 4.2

In chapter two the synthesis of a chemosensor for the tripeptide His-Lys-Lys was detailed. Library **4.2** was built using the same synthetic reactions, however **4.2** was affixed to NovaSyn Tentagel amino resin as was the case with library **4.1**. As was described in chapter two, the metal ligand core readily chelates Cu(II), and the complex is an excellent ligand for peptides with N-terminal His or Cys. Furthermore, the peptide arms provide key interactions that permit discrimination of various analytes. As was demonstrated in chapter two, the tripeptide binding arms can significantly enhance the affinity of the receptor for a tripeptide guest. With our previous research experiences at hand, **4.2:Cu(II)** seemed well suited for differential recognition of tripeptides and tripeptide mixtures.

In addition to size and dynamic complications in the analysis of biomolecules, most real-world applications involve the analysis of multi-component fluids containing multiple analytes of potential interest. Several potential applications exist for solution-based analysis using differential synthetic receptor arrays. These include environmental testing for pollutants, on-line process monitoring, and medical diagnostics for identification of disease states and risk markers. Additionally, differential arrays may be useful in the fields of proteomics and metabolomics, which are essentially mixture analyses. Prior to tackling these challenging applications, the progression must be made from fundamental analyses of simple analytes, to complex bioanalytes, and ultimately to complicated mixtures in biological media.

The challenge of developing an array for diagnostic sample analysis lies within identifying an analyte in a complex clinical or field sample. A first step is to determine how a differential receptor array responds to both single analytes and complex mixtures. Ideally, unique patterns would be obtained for both the mixtures and single analytes. It is expected that patterns for mixtures should be composites of the individual component responses. To date there has been very little use of differential recognition assays for the evaluation of analyte mixtures. These have included the analysis of urine doped with steroids,[25] mixtures of metal cations,[26] and various sodas.[27] The use of **4.2:Cu(II)** for the analysis of tripeptides and tripeptide mixtures is a first approach at observing the patterns of solutions composed of multiple analytes for which the individual analyte pattern is known.

The design of library **4.2** involved the synthesis of the first tripeptide arm (that which is affixed directly to the resin) comprised of Asp-Gly-Lys. It was important to make this arm the same for all library members because it would not be possible to use Edman degradation to sequence this arm due to the incorporation of the core. Therefore, for characterization purposes, the first peptide arm is identical across the library. As with the studies in chapter two, succinic acid was used as a spacer to attach the first peptide arm to the core. Because a diamino core is incorporated, it was necessary to "turn" the direction of the synthesis using the diacid spacer. In other words, the core is coupled to the acid of the succinic acid spacer on the peptide affixed to the resin and to the carboxyl group of the first amino acid of the second peptide arm.

The details for the synthesis of the core of library **4.2** and the synthesis of a peptide arm incorporating the succinic acid linker have been described previously.[24] As with library **4.1**, solid-phase synthesis with a tentagel amino resin and 1-hydroxybenzotriazole (HOBt), TBTU, and N-methylmorpholine (NMM) were used for

the peptide forming reactions. In lieu of PyBOP, TBTU was used as a coupling reagent. As depicted in Scheme 4.3, addition of Fmoc-Lys(Boc)-OH to the Tentagel amino resin afforded **4.11**. Deprotection of the Fmoc group with a solution of 20% piperidine in DMF gave **4.12**. Coupling of Fmoc-Gly-OH and Fmoc-Asp(O*t*Bu)-OH and subsequent deprotection gave **4.13**. The Fm-protected succinic acid **4.14** was coupled to the resin in the same manner as the Fmoc-protected amino acids and subsequently deprotected to give **4.15**. The mono-Fmoc-protected core **4.16** was coupled to the core using HOBt, TBTU, and NMM and then deprotected to afford **4.17**. After attaching the core to the Resin-Lys-Gly-Asp-Succinic acid arm, library **4.2** was developed with split-and-pool Fmoc-protecting group synthetic protocols.[20,28]

The variable tripeptide arm of **4.2** was synthesized by incorporating one of 19 natural amino acids (cysteine was not used to eliminate the potential for disulfide linkages) at each of three sites on the peptide arm. This resulted in a library of 19^3 (6,859) unique members. The combinatorial development of library **4.1** was conducted in simple shaker vials. The development of library **4.2** involved the use of a Quest automated synthesizer, but the general reaction scheme is equivalent to using simple vials as with library **4.1**. The resin is relatively fragile and the automated synthesizer does not require a stir bar, so the resin is less likely to be damaged. The protecting groups on the side chains of the amino acids making up the peptide arms were removed using a TFA/water/1,2-ethanedithiol/triisopropylsilane solution (94.5:2:2:1.5). Following the deprotection reaction, the resin was washed multiply with the deprotection solution followed by several washes with DMF, methylene chloride, methanol, and water.

Scheme 4.3 Simplified Synthesis of Library **4.2**.

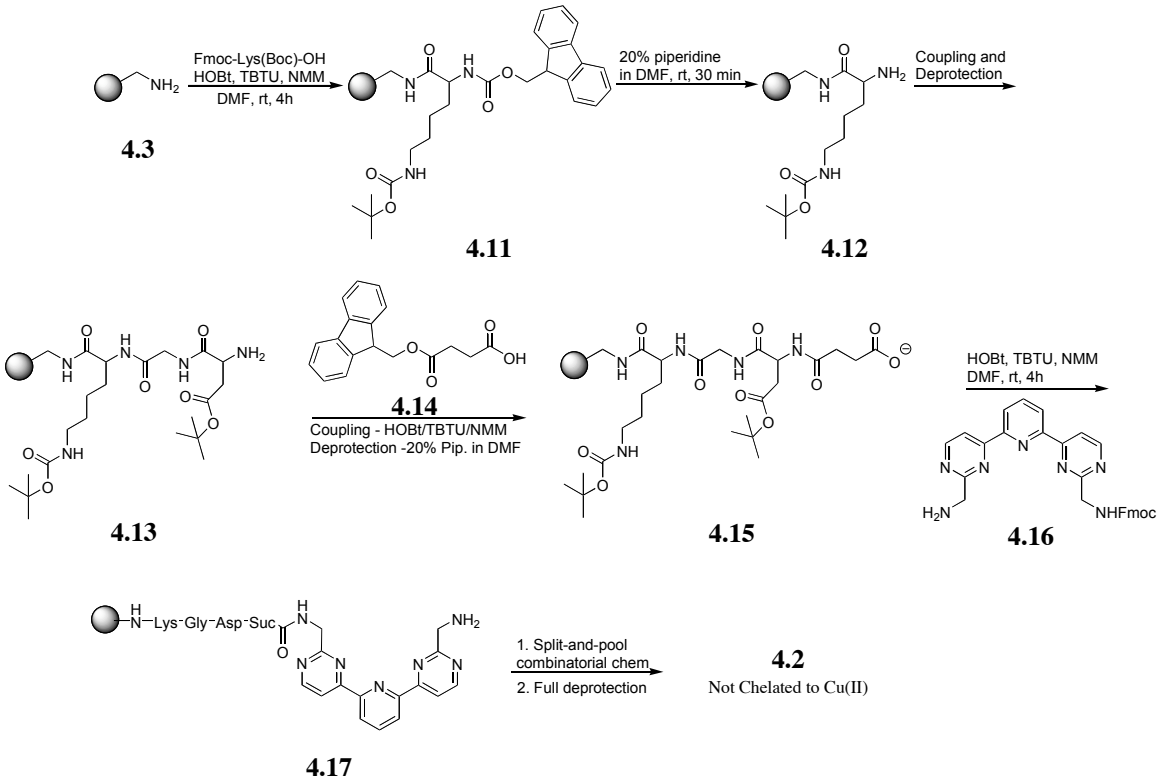

4.4.2 Tripeptide Analytes

Tripeptides **4.18-4.21** were prepared using the acid labile resin 2-chlorotrityl chloride resin purchased from NovaBiochem. Three tripeptides terminated at the N-terminus with histidine (**4.18-4.20**), a known Cu(II) ligand, and the fourth tripeptide terminated with glycine at the N-terminus (**4.21**). These tripeptides were prepared to test the ability of our library to recognize four tripeptides (13 μM each) that differ only in the middle or *N*-terminal residue. The tripeptides included one acidic (**4.19**), two basic (**4.18**, **4.21**), and one nonpolar (**4.20**) residue at the middle position. These differences were

reflected in the differential responses obtained from the receptor array. In all cases, the third residue was threonine. Threonine increased the overall polarity of the tripeptides subsequently increasing the solubility in buffered aqueous solutions. Tripeptides **4.18** and **4.19**, **4.19** and **4.20**, and **4.20** and **4.21** (13 μM in water buffered with HEPES at pH = 7.4) were mixed. It was expected that mixing the analytes would result in pattern responses that are composites of the two individual tripeptide pattern responses.

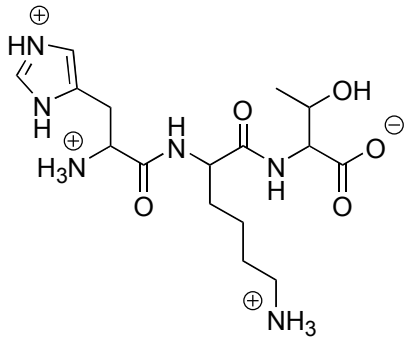

4.18
His-Lys-Thr

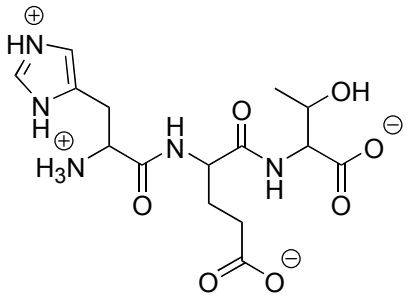

4.19
His-Glu-Thr

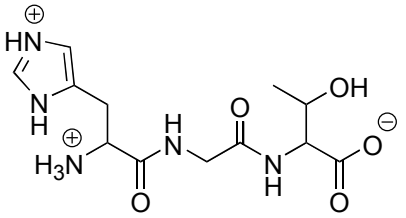

4.20
His-Gly-Thr

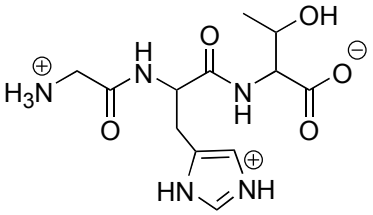

4.21
Gly-His-Thr

4.4.3 Optimization of Array Conditions

As with library **4.1**, an indicator for the indicator-uptake analysis was needed. Therefore, the first optimization experiment involved determining an indicator best suited for array studies. Resin beads (~5 mg) from library **4.2** were added to 1.5 mL Eppendorf tubes fitted with a frit on bottom and a solvent evacuation hole cut into the bottom tip of the tube. The receptors were initially incubated with an aqueous $Cu(II)Cl_2$ (50 mM, 1 mL) solution for 16 hours to ensure that all receptors on each resin bead were fully saturated with Cu(II). Ligation to the divalent metal is very important to both tripeptide binding and the horseshoe conformation of **4.2**. Following saturation with Cu(II), a number of indicators were tested. We intended to identify an indicator with good signal transduction (if too dark, e.g. blue or black, the CCD can not capture quality RGB values), stability to the buffer system (HEPES, 50 mM, pH 7.4), and minimal leaching. If resin beads pretreated with indicator readily leach the indicator back into an aqueous solution than the association between indicator and receptor:metal complex is too weak for array purposes. The indicators illustrated in Figure 4.14 were chosen for their likelihood to both complex the metal center of members of library **4.2** and interact with the differential peptide binding arms. The indicators (0.6 M, except gallocyanine and Celestine blue = 0.3 M, buffered with HEPES, 50 mM, pH 7.4) in Figure 4.14 were added to the metal-bound resin portions (~5 mg) in the Eppendorf tubes and mixed for 1 hour. The indicator solution was evacuated, and the resin was washed multiple times with the buffer solution. This initial test confirmed five of the indicators in Figure 4.14 as reasonable possibilities: Evans blue, bromocresol green, light green SF yellowish, orange G, and Palatine Fast Yellow BLN. The next test was to identify the properties of

the selected indicators within the array; how would they respond to acid and base washes?

Figure 4.14 Indicators Tested for the Optimization of Array Studies with Library **4.2**.

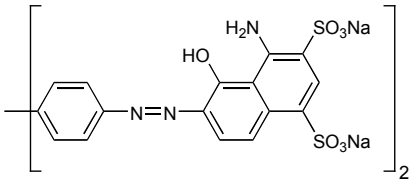

Evans Blue

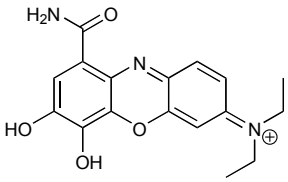

Celestine Blue

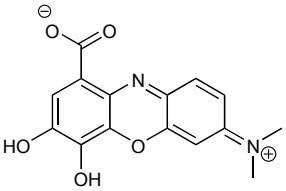

Gallocyanine

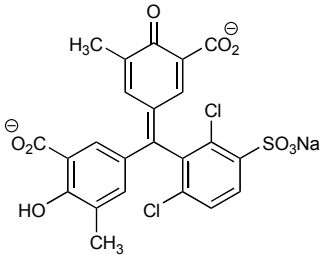

Chromoxane Cyanine R

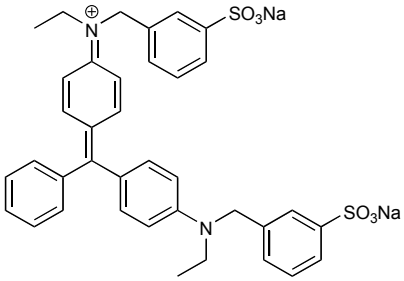

Light Green SF Yellowish

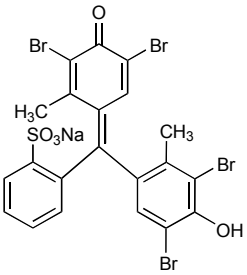

Bromocresol Green

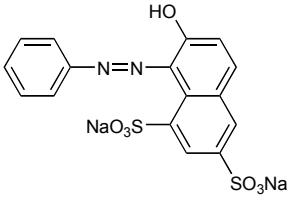

Orange G

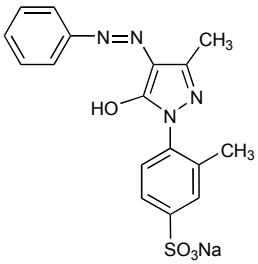

Palatine Fast Yellow BLN

Seven resin beads of each of the selected indicator-bound receptor:metal complexes were added to a 7 × 5 array. First a buffer rinse (HEPES, 50 mM, pH 7.41, 12.5 min, 3 mL/min flow rate) was used to test the leaching of indicators at a high flow rate within the array. This was followed by a HCl (0.3 M, 20 min, 2 mL/min) rinse and NaOH (0.15 M, 5 mL injection, 1.5 mL/min) rinse. These rinses were repeated and the results reviewed. It was found that Evans blue and bromocresol green were incompatible with the array of library **4.2:Cu(II)** receptor complexes, leaving orange G, palatine fast yellow BLN, and light green SF yellowish for further optimization experiments.

To test the remaining indicators arrays of 31 members of library **4.2** were prepared without any prior treatment of the resin beads. In these array experiments a single trial was as follows: (a) Cu(II) added (10 mM in 100 mM acetate buffer, pH 4.55, 5 mL injection, 0.5 mL/min), (b) indicator added (0.3 M in 50 mM HEPES, pH 7.41, 5 mL injection, 0.5 mL/min), (c) buffer rinse (HEPES, 50 mM, pH 7.41), (d) acid rinse (0.3 M HCl, 22.5 min, 2.5-3.0 mL/min), (e) and a final base rinse (0.15 M NaOH, 5 mL injection, 1.2 mL/min). Light green SF yellowish displayed undesirable results and was immediately thrown out as a possible indicator. Palatine fast yellow BLN was very difficult to remove from the beads without extra acid and base rinses. Because a full array study involves several trials it is undesirable to employ long rinse times. This can result in a single trial requiring several hours to complete. Much lower concentrations of palatine fast yellow BLN were attempted later but still the indicator did not perform as needed. Orange G performed very well. Two base washes and a shorter acid wash thoroughly rinsed the indicator from all beads in the array.

Following a number of array studies to identify proper conditions for a full analysis, an attempt was made to separate **4.18**-**4.21**, Gly-Gly-His, His-Glu-Ser, and His-Asp-Thr using differential library **4.2** as a Cu(II) complex. A full analysis was run

including four trials for each analyte, and full extrication of orange G following each trial. The conditions for a single trial were as follows: 1) Cu(II) (14 mM in 100 mM acetate buffer, pH 5.16; 6.25 min, 1.0 mL/min flow rate), 2) HEPES buffer rinse (50 mM, pH 7.41; 6.25 min, 1.0 mL/min), 3) tripeptide or mixture (0.02 mM, 50 mM HEPES, pH 7.41; 25 min, 0.25 mL/min), 4) orange G (0.016 mM, 50 mM HEPES, pH 7.41; 215 12-bit images captured at 2 sec/image, 1.0 mL/min), and 5) acid rinse (0.3 M HCl; 17.5 min, 3.0 mL/min). From the images captured during the orange G uptake, slopes were generated for each bead in the array and used to generate patterns on a PCA plot for the analytes (Figure 4.15).

Figure 4.15 PCA Plot for the First Full Array Analysis with Library **4.2**.

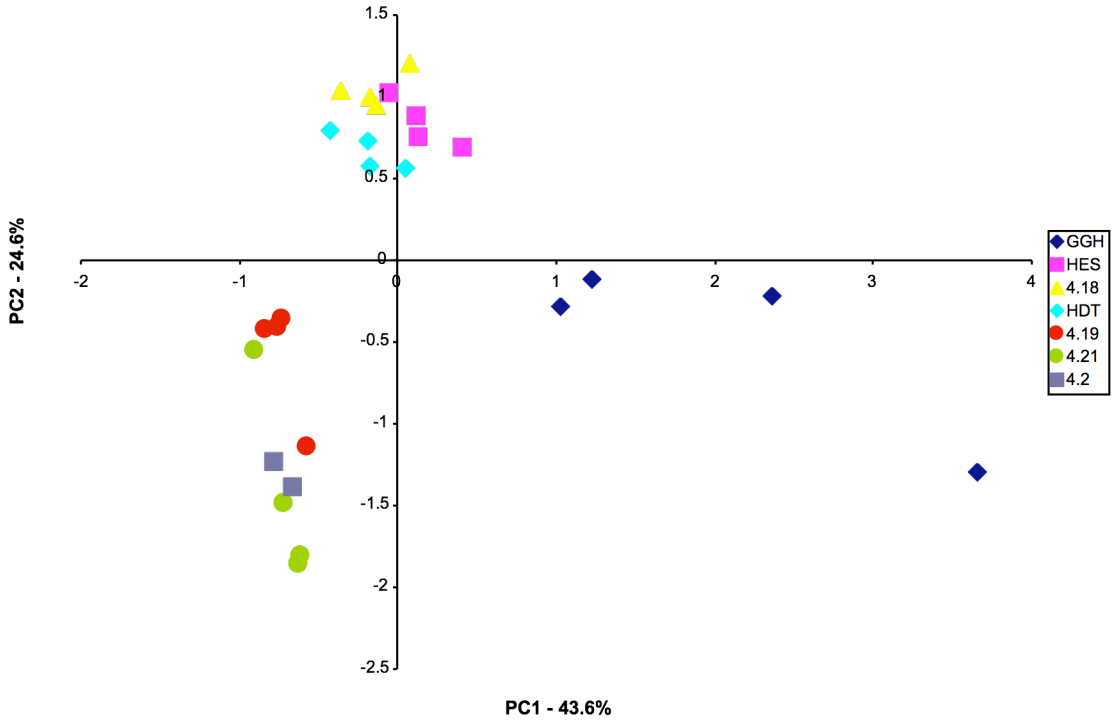

Figure 4.15 is clearly not a great PCA chart. Separation was weak at best with many analytes overlapping, but looking at the slopes from the various indicator-uptake events throughout the analysis shed a great deal of light on our dilemma. As the analysis proceeded from trial to trial, the slopes reduced in a nearly linear fashion. This indicated that the resin-bound receptors were not being properly rinsed out from trial to trial. Further inspection led us to believe that the Cu(II) was the primary problem, with residual effects from leftover tripeptides. Subsequent studies illustrated that NaOH and HCl rinses are important to clearing the metal and analyte from the resin. It was also realized that the Cu(II) concentration needed to be as high as 100 mM, with orange G concentration kept to a minimum.

4.4.4 Full Array Study with Differential Receptor Library 4.2

Thirty members of library **4.2** were randomly selected and placed in a 7 × 5 array. The remaining five sites of the array were occupied by N-acetylated resin blanks. The indicator used for this study was the acidic dye Orange G (**14**, 60 μM in HEPES, pH 7.41). It was believed that this indicator interacts with the peptide arms via Cu(II) ligation. The analyte delivery flow rate was changed to 0.5 mL/min from 0.25 mL/min as used with library **4.1**. This simple modification likely changed the extent of binding occurring between the tripeptides and differential receptors. The indicator concentrations were also increased twenty fold from the previous study from 3.0 μM to 60 μM. These two minor changes resulted in a significant decrease in the analyte concentration required, from 355 μM using library **4.1** with proteins and glycoproteins, to only 13 μM for tripeptides and mixtures using library **4.2**.

During the indicator-uptake analysis, 215 12-bit CCD images were obtained for each resin bead in the array. These images were analyzed by drawing a circular area of interest (AOI) that covered a maximum area of each bead. From within the AOI, blue pixel intensity ($\lambda \sim 420$ - 500 nm) values were obtained from each 12-bit CCD image. For analysis, only the blue channel intensities were used because they had the greatest signal-to-noise ratio. The blue channel intensity values were converted to "effective blue absorbance" values, A_B, using Beer's Law ($A_B = -\text{Log}\ (I_B/I_N)$), where I_N was the average blue pixel intensity of a blank N-acetylated bead. For each trial, a slope of indicator uptake was obtained for each receptor by snapping one image every two seconds. These slopes described the kinetics of indicator-uptake for each differential receptor.

Figure 4.16 Indicator Uptake Slopes for Four Members of Library **4.2** in Response to a Single Tripeptide.

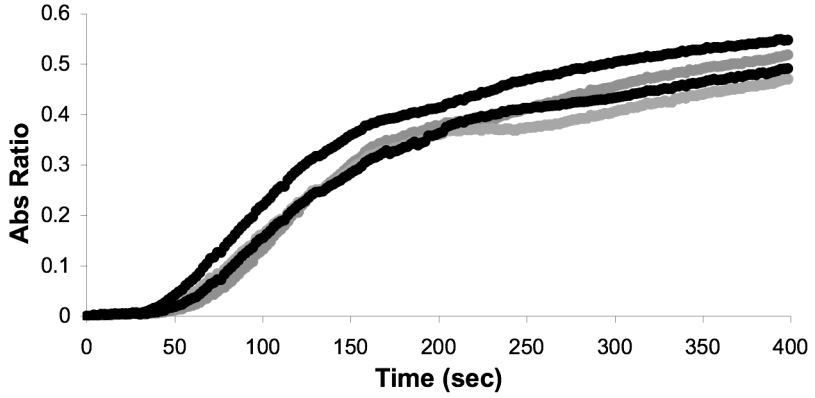

Figure 4.16 shows four indicator-uptake slopes taken from four different receptors from the array in response to His-Glu-Thr (**4.19**). As observed in Figure 4.16, each receptor responds uniquely to **4.19**. Multiple trials demonstrated that these kinetic slopes

were reproducible. It is also required that each receptor responds differently from one tripeptide or mixture to the next. The kinetic slopes defined for each of the 30 receptors in the array were combined to provide an overall response. This cumulative response was defined as the pattern for an individual tripeptide or mixture as discussed earlier with library **4.1**. For a complete analysis of multiple analytes and mixtures, it is required that each receptor responds differently from one another in response to a single analyte. If each receptor responded identically to a single tripeptide, it would not illustrate a differential response, but rather that the primary mode of association between receptors and analytes was identical across the array regardless of the composition of the peptidic arms. If this had occurred in this case it could have been attributed to the metal-ligating core, because that is the common structural feature between receptors in library **4.2**. However, as previously noted, all the receptors in the array responded uniquely.

In the analysis with library **4.2**, the resin was initially saturated with Cu(II) (100 mM in 200 mM acetate buffer, pH 4.55; 6 min, 1.2 mL/min). The tripeptide or tripeptide mixture (13 μM in HEPES buffer, pH 7.41; 12.5 min, 0.5 mL/min) was then added through the array, followed by the indicator Orange G (60 μM in HEPES buffer; 215 12-bit CCD images captured at 2 sec/image, 1.0 mL/min). Twelve-bit images were captured during the indicator-uptake, and data was extracted to obtain the indicator-uptake slopes for each receptor. The copper, analytes, and indicator were rinsed from the array using acid (HCl, 0.3 M; 48 min, 3.0 mL/min) and base (NaOH, 0.15M; 6 min, 1.2 mL/min) washes. Four trials were completed for each tripeptide or tripeptide mixture, and patterns were determined with PCA.

The indicator-uptake rates display a complicated behavior involving a combination of fluid mixing, analyte transport and complex binding dynamics. Thus, the uptake curves deviated from linear behavior (Figure 4.16). As described, the patterns are

obtained from the cumulative slopes from all the receptors within the array. Since the array uptake responses were not linear, it was necessary to determine if the PCA plots were different depending on the time increments from which the slope was obtained. Thus, the curves of Figure 4.16 were split into three sections: 1) the entire area from 50-400 sec., 2) the steep slope region from 50-175 sec., and 3) the gentle slope from 175-400 sec. A PCA plot was generated for each slope region, and the graphs were consistent in all slope areas indicating that the differential array responses were consistent throughout the indicator-uptake.

4.4.4.1 PCA Analysis of Pattern Responses Exhibited by a 30-Member Array of Library 4.2 to Tripeptides and Tripeptide Mixtures.

The PCA plots for an array of differential receptors from library **4.2** were generated from the full indicator-uptake slope region from 50-400 seconds (see Figure 4.16). As a first analysis, a PCA was generated for the tripeptides alone. As illustrated in Figure 4.17, individual tripeptides clustered, and different tripeptides were spatially separated with PCA. The two PC axes describe 95% of the variance in the original data set, with PC1 describing 91%.

Figure 4.17 PCA Chart for Library **4.2** in Response to Tripeptides **4.18-4.21**. (His-Glu-Thr ◆, His-Lys-Thr ◆, Gly-His-Thr ◆, His-Gly-Thr ◆).

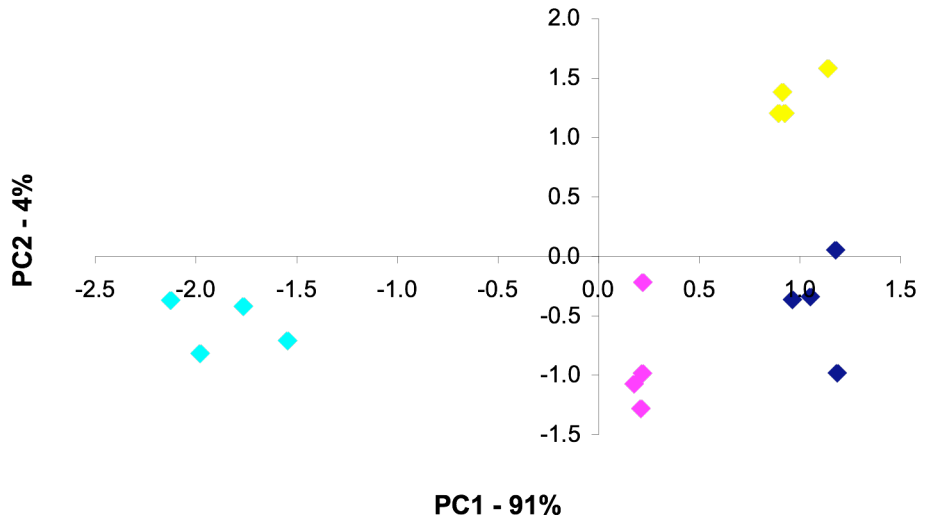

The observed PCA separation of analytes was not due solely to the interaction between the N-terminal amino acid and the copper core of the receptor. If three tripeptides with His in the N-terminus would have clustered together, the graph would not have shown distinct separation. This suggests that the peptide arms were important for discriminating between the individual tripeptides. This was to be expected considering our previous explorations with a synthetic selective receptor for His-Lys-Lys.[24] Therefore, specific interactions occurring between the peptides of the receptors and the tripeptide analytes elicit different modes of binding that were reflected in the PCA plot. Evaluating the slope responses, those analytes on the far right side of the PCA had cumulatively higher slope responses than those on the left. As described earlier, higher slope values with indicator uptake assays correlate to weaker binding interactions between receptors and analytes. Therefore, as illustrated in Figure 4.17 His-Gly-Thr

(**4.20**) had the strongest interaction because the majority of the receptors had lower indicator-uptake slopes than the other analytes. Conversely, Gly-His-Thr (**4.21**) had the weakest interaction so several of the receptors within the array had large indicator-uptake slopes. The nature of these receptors was still differential, as several receptors did not respond in this fashion; the responses were not identical, but there were some consistencies.

A full application of the array required a mixture analysis. To our knowledge mixtures of bioanalytes have not been explored with library-derived differential analysis. The responsiveness of the differential receptor array to mixtures was tested by attempting to discriminate single tripeptides from composite mixtures. Three tripeptide mixtures were evaluated at concentrations identical to the single tripeptides (13 μM, 6.5 μM for each tripeptide in the mixture). As shown in Figure 4.18, the mixtures separated from one another, and from the single tripeptides. All of the mixtures have scores on the PCA plot that lie between the scores of their individual components. This implies that in all cases the interactions of the mixtures are governed by both tripeptides in the mixtures. This initial analysis of mixtures demonstrates that differential arrays are sensitive to mixtures and are capable of discriminating between mixtures and individual analytes.

Figure 4.18 PCA Chart for an Electronic Array of Library **4.2** in Response to Tripeptides and Tripeptide Mixtures. (His-Glu-Thr ◆, His-Lys-Thr ◆, Gly-His-Thr ◆, His-Gly-Thr ◆, His-Lys-Thr & His-Glu-Thr ◆, His-Gly-Thr & Gly-His-Thr ◆, His-Lys-Thr & His-Gly-Thr ◆).

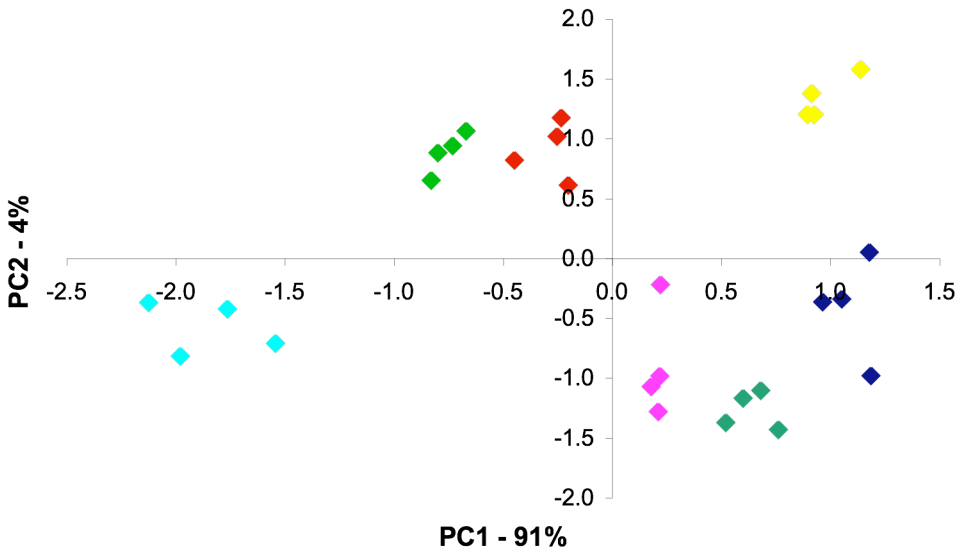

4.4.4.2 Characterization of Receptors in the Array

Factor loading values were again used to identify the receptors in the array that were most significant to the formation of the first PC axis in both PCA plots. Once the significance of each bead was identified, Edman degradation was employed to determine the specific amino acid residues on several beads. This provided full characterization of several receptors within the array.

The analysis of the factor loading values provided interesting insight into the operation and functionality of the array response. Indeed, nearly all of the 30 receptors were found to be important to the formation of PC1, meaning their values were close to -1 or 1. This is intuitively sensible as PC1 describes such a large portion of the original

variance. Therefore, a common interaction likely exists between the tripeptides/mixtures and the Cu(II) center of the receptor for all analytes. However, the strength of association between the variable peptide arms of the receptor and the analytes is the discriminating factor resulting in the separation and clustering of analytes on the new principal component charts.

Four receptors from the array with the largest loading values and two with the least were chosen for Edman degradation (Table 4.3). However, the receptors with lesser loading values were still relatively significant. The two receptors with smaller loading values both contained a proline and arginine, but in different positions. This may indicate that one or both of these residues caused either a charged or steric interference with the analytes, thereby limiting association. The receptors with the largest loading values had basic amino acids conserved, lysine and histidine, as well as a number of different aliphatic residues: glycine, leucine, isoleucine, valine, and alanine. However, it would be errant to draw any large conclusions from this information, as the factor loading values across the array were relatively similar.

Table 4.3 Sequencing Results and Factor Loading Values for the First Principal Component (PC1).

Tripeptide Sequence	Factor Loading (PC1)	Bead Number
Lys-Ala-Asp	0.989	26
Gln-Val-Gly	0.985	2
Leu-Lys-Ile	0.981	7
His-Ala-Ile	0.954	31
Phe-Pro-Arg	0.901	35
Arg-Gly-Pro	0.844	22

4.5 Summary

The current approach to differential sensing represents a powerful tool for the analysis of dynamic analytes and complex mixtures. We have shown the use of two separate differential libraries for the differential array analysis of complex bioanalytes. Using an indicator-uptake analysis, significant enhancement to the sensitivity of the arrays has been gained. We have demonstrated two examples of targeting complex bioanalytes with differential (or cross-reactive) arrays that would have required highly labor-intensive design and synthesis to develop multiple selective receptors. It is likely that in the future large gains will be made toward the development of a functional tool for medical or environmental diagnostics with differential arrays of synthetic receptors.

4.6 Experimental

General. Chemicals for the synthesis of libraries **4.1** and **4.2** and the tripeptide analytes were purchased from Novabiochem, Sigma-Aldrich, and Acros and used without further purification. All solvents used were obtained from dry stills. Solvents used for the solid phase synthesis were obtained from dry stills and kept in argon purged containers with molecular sieves. Buffer components were of reagent grade. The proteins used in the array assay with library **4.1** were obtained from Sigma-Aldrich and ICN and were used without further purification. NovaSyn TG amino resin LL was purchased from Novabiochem and used for the synthesis of libraries **4.1** and **4.2**. Normal amine loading levels for these beads were between 0.2-0.3 mmol/g. The resin size (130 μM) and swelling characteristics make this resin suitable for use within the array platform. Synthesis of library 9 was carried out using an Argonaut Technologies Quest 210 automated peptide synthesizer with an automated solvent delivery system. 2-Chlorotrityl chloride resin (200-400 mesh) was purchased from Novabiochem and used for the synthesis of the tripeptides 10-13. Normal loading levels for these beads were between 0.8-1.6 mmol/g. This resin is ideal for His containing peptides, and is exceedingly labile under mildly acidic conditions.

General Synthesis. For all solid phase synthesis, regardless of resin used, the resin was placed into a reaction vessel fabricated with a frit and waste extension for coupling to a vacuum hose to rapidly extricate reagent and wash solutions. The reaction vessel was clamped to a converted rotary motor, and tumbled end-over-end for a specified amount of time depending on the reaction or wash.

Procedures:

Library 4.1 Synthesis. The Novasyn TG amino resin purchased from Novabiochem with a loading value of 0.26 mmol/g was used for the solid phase synthesis. All common amino acids except cysteine were used in the synthesis. Each was Fmoc-protected and side chains were appropriately protected with t-butyl, Pbf, trityl, or Boc.

(4.4)

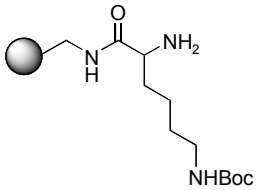

Novasyn TG amino resin **4.3** (1.2 g, 0.31 mmol) was added to a solid-phase reaction vessel (50 mL reaction vessel with a frit for evacuating reaction solutions and wash solutions) and allowed to swell for 30 min. A solution of Fmoc-Lys(Boc)-OH (0.292 g, 0.62 mmol), 1-hydroxybenzotriazole (HOBt) (0.084 g, 0.62 mmol), benzotriazole-1-yl-oxy-tris-pyrrolidino-phosphonium hexafluorophosphate (PyBOP) (0.322 g, 0.62 mmol), and diisopropylethylamine (DIEA) (0.216 mL, 1.24 mmol) were prepared in DMF (5 mL). This was mixed at room temperature for 4 h. The reaction solution was evacuated, and the resin was rinsed with DMF, methanol, methylene chloride (DCM), and hexanes. DMF (5 mL) was added to the resin along with acetic anhydride (0.1 g, 1 mmol) and dimethylaminopyridine (DMAP) (1 mg). This mixed for 30 minutes to cap all unreacted amines. Again the resin was washed as before, and then 20% piperidine in DMF (5 mL) was added to deprotect the Fmoc protecting groups. This mixed for 5 min. Again 20%

piperidine in DMF (10 mL) was added and mixed for 5 min. The resin was washed twice with DMF, DCM, methanol, and hexanes.

(4.6)

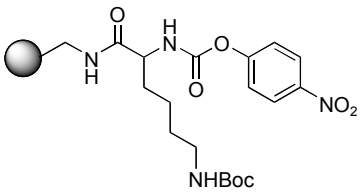

4.4 was initially swelled in THF/DCM (1:1, 5 mL) for 30 min. A solution of 4-nitrophenylchloroformate **4.5** (0.312 g, 1.55 mmol) in THF/DCM (1:1, 5 mL) and DIEA (0.27 mL, 1.55 mmol) was added to the resin. This mixed for one hour and the solution was evacuated. The resin was rinsed several times with 1:1 THF/DCM, and then dried on the hi-vac.

(4.8)

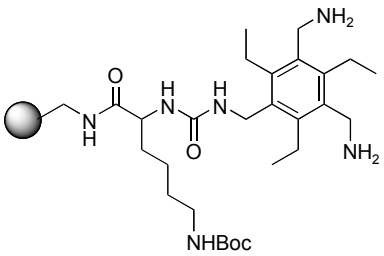

4.6 was added to a solution of 1,3,5-tris-aminomethyl-2,4,6-triethyl benzene **4.7** (0.62 g, 2.5 mmol) in THF/DCM (6 mL, 1:1) and DMF (4 mL). This mixed overnight and was evacuated. The resin was then washed with DMF followed by 5% butylamine in DMF until the solution remained colorless. The resin was then washed twice with methanol, DCM, and hexanes. The resin was dried on the hi-vac.

(4.10)

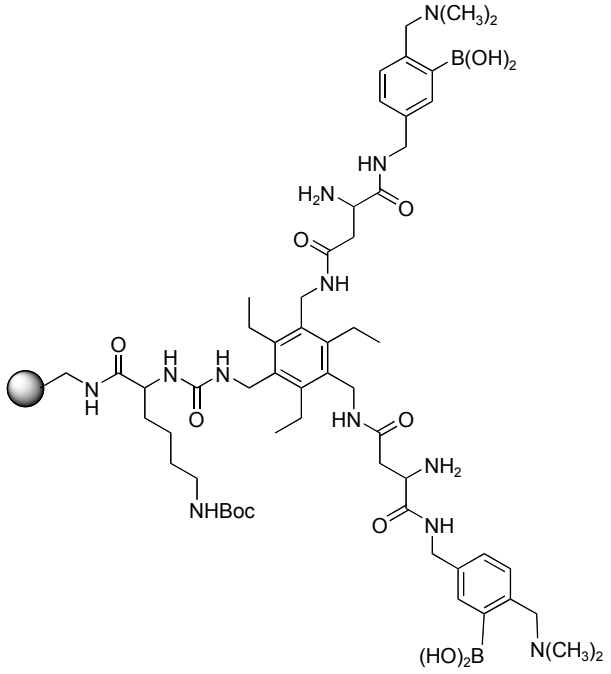

4.8 was swollen in dry DMF (5 mL) for 30 min. A solution of **4.9** (1.45 g, 2.2 mmol), PyBOP (1.14 g, 2.2 mmol), HOBt (0.30 g, 2.2 mmol), and DIEA (0.76 mL, 4.4 mmol) was prepared at 0° C in DMF (5 mL) as the solution tends to warm upon addition of DIEA. After the solution cooled to room temperature, it was added to the swollen resin. It was spun for 4 h. and the solution was evacuated. A Kaiser test was performed and was negative. The resin was washed with methanol, DCM, DMF, and hexanes. The Fmoc groups were removed with 20% piperidine in DMF (10 mL). The resin was washed twice with methanol, DCM, DMF, and hexanes. A Kaiser test was performed and was positive. The resin was dried on the hi-vac.

(4.1)

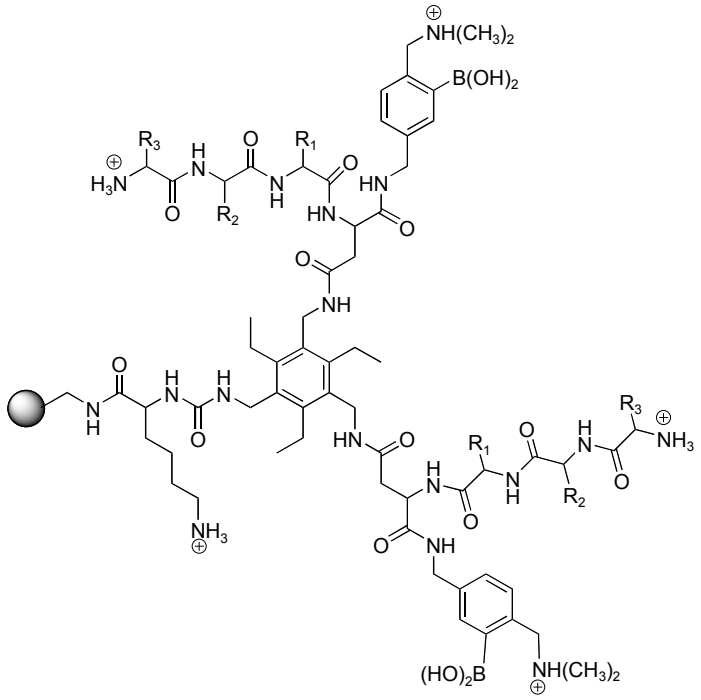

The library was synthesized using standard split-and-pool combinatorial chemistry. Resin **4.10** was split into 19 equal portions. One of the 19 amino acids (0.47 M), HOBt (0.47 M), DIEA (0.47 M), and PyBOP (0.47 M) solutions were added to each of the resin portions and mixed overnight in DMF. The reaction solution was evacuated and the resin washed with methanol, DCM, DMF, and hexanes. DMF (5 mL) was then added to the resin along with acetic anhydride (0.1 g, 1 mmol) and DIEA (0.47 M). Following evacuation and rinses, 20% piperidine in DMF (5 mL) was added and mixed for 10 minutes. This was evacuated, and the resin was rinsed with methanol, DCM, DMF, and hexanes. All 19 portions of the resin were mixed together once again and then split again into 19 equal portions. The synthetic split-and-pool procedure was performed until three amino acids were added to both arms of the receptor. The acid-labile protecting groups on the amino acid side chains were removed using a TFA/water/1,2-

ethanediol/triisopropylsilane (94:2.5:2.5:1, 12 mL) solution. The resin was washed twice with DCM, methanol, and hexanes, thoroughly dried on the hi-vac, and subsequently used in the array.

Library 4.2 Synthesis.

(4.11)

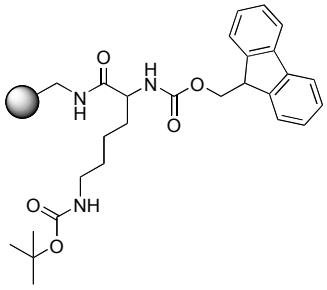

Prior to addition of the first amino acid the NovaSyn TG amino resin (**4.3**) (3.0 g, 0.26 mmol/g, 0.78 mmol) was washed with methylene chloride (1 × 10 mL × 2 min), methanol (2 × 10 mL × 2 min), N,N-dimethylformamide (2 × 10 mL × 2 min), and methylene chloride (1 × 10 mL × 2 min). Fmoc-Lys(Boc)-OH (0.731 g, 1.56 mmol) was added to a separate dried flask with HOBt (0.422 g, 3.12 mmol), TBTU (1.00 g, 3.12 mmol), and NMM (0.78 mL, 7.02 mmol). This was dissolved in N,N-dimethylformamide (12 mL) and mixed until formation of the activated ester (~5 min). This solution was then transferred to the reaction vessel and tumbled for 4 h. Upon completion the reagent solution was evacuated, and the resin with Lys (**2**) was washed with methylene chloride (2 × 10 mL × 2 min), methanol (2 × 10 mL × 2 min), N,N-dimethylformamide (2 × 10 mL × 2 min), and methylene chloride (2 × 10 mL × 2 min). The resin gave a negative Kaiser test result.

(4.12)

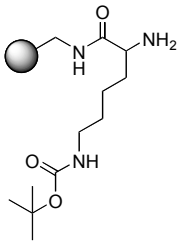

To remove the Fmoc protecting group, a solution of 20% piperidine in N,N-dimethylformamide (12 mL) was added to **4.11**. The reaction vessel was tumbled for 30 min and the reagents evacuated. Again the deprotected resin was washed with methylene chloride (2 × 10 mL × 2 min), methanol (2 × 10 mL × 2 min), N,N-dimethylformamide (2 × 10 mL × 2 min), and methylene chloride (2 × 10 mL × 2 min). The resin produced a positive Kaiser test indicative of a free primary amine on the Lys.

(4.13)

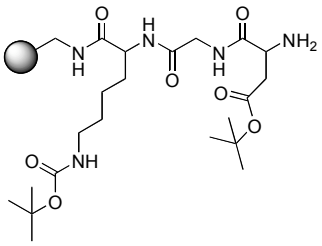

Addition of the next two amino acids, Fmoc-Gly-OH and Fmoc-Asp(OBu^t)-OH, and their subsequent Fmoc deprotections were carried out exactly as with the first amino acid.

(4.15)

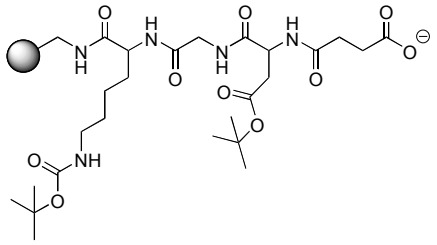

To add the core to the resin a diacid linker was incorporated onto the resin following Asp. To a separate dried flask was added monoflourenylmethylsuccinic acid (0.462 g, 1.56 mmol), HOBt (0.422 g, 3.12 mmol), TBTU (1.00 g, 3.12 mmol), and NMM (0.78 mL, 7.02 mmol). This was dissolved in N,N-dimethylformamide (12 mL) and mixed until formation of the activated ester (~5 min). This solution was then transferred to the reaction vessel and tumbled for 4 h. Upon completion, the reagent solution was evacuated, and the resin was washed in the same fashion as before. The resin gave a negative Kaiser test result. The fluorenylmethyl protecting group was removed using a solution of 20% piperidine in N,N-dimethylformamide (12 mL). The reaction vessel was tumbled for 12 min, and the reagents were evacuated. Again the deprotected resin was washed as before.

(4.17)

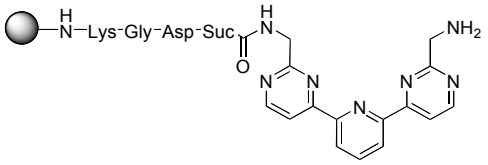

The mono-Fmoc protected core (**4.16**) was coupled to the resin by adding HOBt (0.422 g, 3.12 mmol), TBTU (1.00 g, 3.12 mmol), and NMM (0.78 mL, 7.02 mmol) directly to the

reaction vessel with N,N-dimethylformamide (12 mL). The reaction vessel was tumbled (15 min), and then the core was added (0.650 g, 1.26 mmol) directly to the reaction and tumbled for 4 h. Washing proceeded as before. A Kaiser test was negative. The Fmoc group was removed with the same solution as above, but the run time was 90 min. Again, the wash sequence was the same. A Kaiser test was positive for the resin.

(4.2)

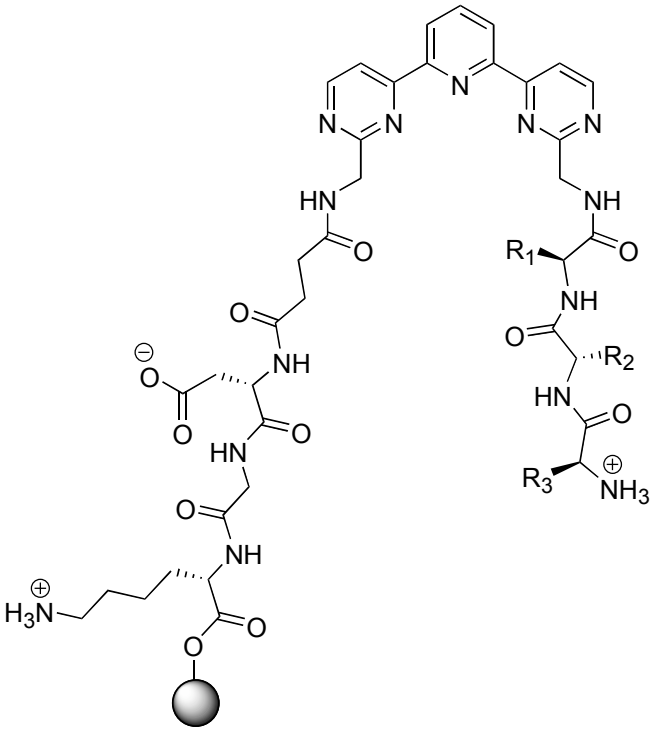

To develop library **4.2**, the resin was split into 19 portions (each 0.167 g, 0.0434 mmol) and placed in reaction vessels fitted into the Quest 210 synthesizer. To each vessel was added a Fmoc-protected amino acid (0.174 mmol), HOBt (0.217 mmol), TBTU (0.217 mmol), and NMM (0.391 mmol). N,N-dimethylformamide (4.0 mL) was added to each vessel and the reactions were run for 4 h. Upon completion the reagents were evacuated, and the resin was washed with methylene chloride (2 × 10 mL × 2 min), methanol (2 × 10

mL × 2 min), N,N-dimethylformamide (2 × 10 mL × 2 min), and methylene chloride (2 × 10 mL × 2 min). Kaiser tests were negative for all resin portions.

The Fmoc groups were removed by adding a solution of 20% piperidine in N,N-dimethylformamide (4 mL). This reaction ran for 45 min. Upon completion, Kaiser tests for all portions were positive. Again the reagents were evacuated, and the resin was washed in the same fashion as above. All resin portions were then pooled together and dried under high vacuum for 12 h. The resin was then split again into 19 portions and the exact same coupling, deprotection, and pooling steps were repeated. After the third amino acid was added to the peptide arm, the Fmoc was removed, and the resin washed. To fully deprotect the acid labile protecting groups on the side chains of the amino acids, a solution of trifluoroacetic acid:water:ethanedithiol:triisopropylsilane (94.5:2:2:1.5) (4 mL) was added to each portion and mixed for 1 h. The resin was washed with methylene chloride (2 × 10 mL × 2 min), methanol (2 × 10 mL × 2 min), N,N-dimethylformamide (2 × 10 mL × 2 min), and methylene chloride (2 × 10 mL × 2 min). The deprotection and washing steps were repeated, and the completed library resin was pooled and dried 24 h. under high vacuum.

Tripeptide Synthesis. For the development of **4.18-4.21**, the syntheses commenced with the attachment of the C-terminal amino acid to the 2-chlorotrityl chloride resin. Prior to reaction the resin (0.6 g, 1.4 mmol/g, 0.84 mmol) was washed with methylene chloride (1 × 10 mL × 2 min (this format shows the number of times × amount × duration of each solvent wash)), methanol (2 × 10 mL × 2 min), N,N-dimethylformamide (2 × 10 mL × 2 min), and methylene chloride (1 × 10 mL × 2 min). In a separate oven-dried flask was added Fmoc-Thr(OBu^t)-OH (0.401 g, 1.01 mmol) and N-methylmorpholine (0.37 mL,

3.36 mmol) to methylene chloride (8 mL) and stirred 3 min. This solution was then added to the washed resin and tumbled for 1 h. The reagent solution was evacuated from the vessel, and a solution of methylene chloride:methanol:diisopropylamine (45:4:1, 12 mL) was added to quench unreacted resin sites. The quenching solution was added once more. The resin was then washed with methylene chloride (2 × 10 mL × 2 min), methanol (2 × 10 mL × 2 min), N,N-dimethylformamide (2 × 10 mL × 2 min), and methylene chloride (2 × 10 mL × 2 min). The resin produced a negative Kaiser (ninhydrin) test.

To remove the Fmoc group from the resin-bound Thr, a solution of 20% piperidine in N,N-dimethylformamide (10 mL) was added. The reaction vessel was tumbled for 30 min, and the reagents were evacuated. Again the resin was washed with methylene chloride (2 × 10 mL × 2 min), methanol (2 × 10 mL × 2 min), N,N-dimethylformamide (2 × 10 mL × 2 min), and methylene chloride (2 × 10 mL × 2 min). The resin produced a positive Kaiser test indicative of a free primary amine on the Thr.

Tripeptides **4.18-4.21** all share a common C-terminal amino acid. They differ at the middle and N-terminal positions. The conditions for the completion of **4.18-4.21** are subsequently generalized from this point. To an oven-dried flask was added the middle Fmoc-protected amino acid (3.36 mmol, 4 eq) with appropriate side-chain protection (Bu^t, Boc, or Trt), HOBt (4.20 mmol, 5 eq), TBTU (4.20 mmol, 5 eq), and N-methylmorpholine (7.56 mmol, 9 eq). These reactants were dissolved in DMF (10 mL) and mixed until the activated ester formed (~10 min). This solution was added to the reaction vessel containing the resin and tumbled for 3 h. Upon completion, the excess reactants were evacuated from the reaction vessel, and the resin was washed with

methylene chloride (2 × 10 mL × 2 min), methanol (2 × 10 mL × 2 min), N,N-dimethylformamide (3 × 10 mL × 2 min), and methylene chloride (2 × 10 mL × 2 min). The resin produced a negative Kaiser test. The Fmoc group was removed in the same fashion as described above, and the resin was washed in the same manner as before. The resin produced a positive Kaiser test indicative of a free amine on the middle amino acid. The third amino acid was added to the washed resin following Fmoc deprotection. To an oven-dried flask was added the Fmoc-protected amino acid (3.36 mmol, 4 eq) with appropriate side-chain protection (Bu^t, Boc, or Trt), N-hydroxybenzotriazole (HOBt) (4.20 mmol, 5 eq), 2-(1H-benzotriazole-1-yl)-1,1,3,3-tetramethyluronium tetrafluoroborate (TBTU) (4.20 mmol, 5 eq), and N-methylmorpholine (NMM) (7.56 mmol, 9 eq). These reactants were dissolved in N,N-dimethylformamide (10 mL) and mixed until the activated ester formed (~10 min). This solution was added to the reaction vessel containing the resin and tumbled for 3 h. Upon completion, the excess reactants were evacuated from the reaction vessel, and the resin was washed as before. The resin produced a negative Kaiser test. The Fmoc group was removed in the same fashion as described above, and the resin was washed as before. The resin produced a positive Kaiser test indicative of a free amine on the N-terminal amino acid.

To remove the side-chain protecting groups and to cleave the tripeptides from the resin, a solution of trifluoroacetic acid:methylene chloride:triethylsilane (95:4:1) (15 mL) was added to the reaction vessel containing the resin and tumbled 1 h. The product was collected by evacuating the solution from the reaction vessel. The resin was subsequently washed with methylene chloride (3 × 10 mL × 2 min). The combined solutions, including the washes, were placed in a dry flask and reduced to ~5 mL on a rotary evaporator. Cold diethyl ether (10 mL) was added to the concentrated solution and the

products readily precipitated. These were filtered by vacuum filtration, washed with diethyl ether (2 × 10 mL), and dried under high vacuum for 12 h. The tripeptides were then dissolved in water and lyophilized twice.

Characterization of Tripeptides 4.18-4.21.

(4.18) His-Lys-Thr. ^{1}H NMR (CD_3OD): 8.83 (s, 1H), 4.51 (d, 1H), 4.46 (t, 1H), 4.36 (m, 1H), 3.95 (t, 1H), 3.48 (t, 1H), 3.49 (d, 2H), 2.94 (t, 2H), 1.80 (q, 2H), 1.71 (m, 2H), 1.57 (m, 2H), 1.21 (d, 3H). LRMS (CI^+) calcd for $C_{16}H_{29}N_6O_5$: 385 (M^+), found 385 (M^+).

(4.19) His-Glu-Thr. ^{1}H NMR (CD_3OD): 8.88 (s, 1H), 7.47 (s, 1H), 4.53 (t, 1H), 4.50 (d, 1H), 4.36 (m, 1H), 4.29 (t, 1H), 3.46 (d, 2H), 2.19 (t, 2H), 2.05 (q, 2H), 1.21 (d, 3H). LRMS (CI^+) calcd for $C_{15}H_{23}N_5O_7$: 386 (M^+), found 386 (M^+).

(4.20) His-Gly-Thr. ^{1}H NMR (CD_3OD): 8.85 (s, 1H), 7.51 (s, 1H), 4.52 (d, 1H), 4.35 (m, 1 H), 4.29 (s, 2H), 3.94 (t, 1H), 3.47 (d, 2H), 1.21 (d, 3H). LRMS (CI^+) calcd for $C_{12}H_{19}N_5O_5$: 314 (M^+), found 314 (M^+).

(4.21) Gly-His-Thr. ^{1}H NMR (CD_3OD): 8.77 (s, 1H), 7.38 (s, 1H), 4.92 (t, 1H), 4.37 (d, 1H), 3.75 (s, 2H), 3.47 (t, 1H), 3.29 (d, 2H), 1.17 (d, 3H). LRMS (CI^+) calcd for $C_{12}H_{19}N_5O_5$: 314 (M^+), found 314 (M^+).

Acetylated (Blank) Resin. The NovaSyn TG amino resin **4.3** (1.0 g, 0.26 mmol/g, 0.26 mmol) was washed with methylene chloride (2 × 10 mL × 2 min), methanol (2 × 10 mL × 2 min), DMF (2 × 10 mL × 2 min), and methylene chloride (2 × 10 mL × 2 min). To the resin was added acetic anhydride (5 mL, 53.3 mmol) and triethylamine (2.6 mL, 18.5 mmol). Methylene chloride (5 mL) was added and the reaction tumbled 1 h. The reaction solution was evacuated, and the resin was washed as described previously. A Kaiser test was negative for the resin.

Assay Conditions for Array Studies with Library 4.1. Each trial was performed at room temperature under continuous flow conditions. All protein and indicator solutions were buffered with HEPES (25 mM, pH 7.4). Each protein (0.355 μM, buffered with HEPES, 25 mM, pH 7.4; 5 mL injection; 0.25 mL/min) sample was loaded into the flow cell through the sample injection port. To ensure complete removal of non-specifically bound proteins, a three minute HEPES (25 mM, pH 7.4; 1.0 mL/min) wash was employed. Following this rinse, bromopyrogallol red (3.0 μM, buffered with HEPES, 25 mM, pH 7.4; 1.0 mL/min, 215 12-bit images captured at 2 sec/image) was immediately injected. To repeat the experiment, the array was regenerated by washing with base (NaOH, 0.15 M; 2 × 5 mL injections, 1.5 mL/min, total 13.5 min), acid (HCl, 0.3 M; 22 min, 3.0 mL/min), and finally with more concentrated base (NaOH, 0.40 M; 4.5 min, 1.5 mL/min). A buffer rinse (2 min, 2.0 mL/min) followed to rinse any excess base from the array before beginning the next trial.

Assay Conditions for Array Studies with Library 4.2. Cu(II) (100 mM in acetate buffer (200 mM, pH 5.5); 5 mL injection, 5 min, 1.2 mL/min) was added via the injection port. Unbound Cu(II) was removed during a HEPES buffer rinse (50 mM, pH 7.41; 3 min, 1.2 mL/min). The buffer was drawn directly by the FPLC, not through the injection port. Following the rinse, the tripeptide or mixture (13 μM in HEPES (pH 7.41, 50 mM); 5 mL injection, 12.5 min, 0.5 mL/min) was added to the injection port and then through the array. Unbound analyte was removed by a HEPES buffer wash (3 min, 1.2 mL/min). This wash was followed by Orange G (60 μM in HEPES (pH 7.41, 50 mM); 5 mL injection, 7.2 min, 1.0 mL/min) added through the injection port. Twelve-bit CCD images (215) were captured during the Orange G uptake, and data was extracted to obtain the indicator-uptake slopes for each receptor in the array. The copper, analytes, and

indicator were rinsed from the array using HCl (300 mM, 48 min, 3.0 mL/min) that was drawn directly by the FPLC. The acid rinse was followed by a NaOH (150 mM; 5 mL injection, 6 min, 1.2 mL/min) rinse through the injection port.

4.7 References

1) (a) Lavigne, J. J.; Anslyn, E. V. Sensing a Paradigm Shift in the Field of Molecular Recognition: From Selective to Differential Receptors. *Angew. Chem. Int. Ed.* **2001**, *40*, 3118-3130. (b) Wright, A. T.; Anslyn, E. V. Differential Receptor Arrays and Assays for Solution-Based Molecular Recognition. *Chem. Soc. Rev.* **2006**, *35*, 14-28.

2) Jurs, P. C.; Bakken, G. A.; McClelland, H. E. Computational Methods for the Analysis of Chemical Sensor Array Data from Volatile Analytes. *Chem. Rev.* **2000**, *100*, 2649-2678.

3) (a) McCleskey, S. C.; Griffin, M. J.; Schneider, S. E.; McDevitt, J. T.; Anslyn, E. V. Differential Receptors Create Patterns Diagnostic for ATP and GTP. *J. Am. Chem. Soc.* **2003**, *125*, 1114-1115. (b) Wright, A. T.; Griffin, M. J.; Zhong, Z.; McCleskey, S. C.; Anslyn, E. V.; McDevitt, J. T. Differential Receptors Create Patterns That Distinguish Various Proteins. *Angew. Chem. Int. Ed.* **2005**, *44*, 6375-6378. (c) Wright, A. T.; Anslyn, E. V.; McDevitt, J. T. A Differential Array of Metallated Synthetic Receptors for the Analysis of Tripeptide Mixtures. *J. Am. Chem. Soc.* **2005**, *127*, 17405-17411.

4) Lavigne, J. J.; Savoy, S.; Clevenger, M. B.; Ritchie, J. E.; McDoniel, B.; Yoo, S. –J.; Anslyn, E. V.; McDevitt, J. T.; Shear, J. B.; Neikirk, D. Solution-Based Analysis of Multiple Analytes by a Sensor Array: Toward the Development of an "Electronic Tongue." *J. Am. Chem. Soc.* **1998**, *120*, 6429-6430.

5) (a) Tudos, A. J.; Besselink, G. A. J.; Schasfoort, R. B. M. Trends in Miniaturized Total Analysis Systems for Point-of-Care Testing in Clinical Chemistry. *Lab Chip* **2001**, *1*, 83-95. (b) Lagally, E. T.; Emrich, C. A.; Mathies, R. A. Fully Integrated PCR-Capillary Electrophoresis Microsystem for DNA Analysis. *Lab Chip* **2001**, *1*, 102-107. (c) Reyes, D. R.; Iossifidis, D.; Auroux, P. –A.; Manz, A. Micro Total Analysis Systems. 1. Introduction, Theory, and Technology. *Anal. Chem.* **2002**, *74*, 2623-2636. (d) de Mello, A. J.; Beard, N. Dealing with 'Real' Samples:

Sample Pre-Treatment in Microfluidic Systems. *Lab Chip*, **2003**, *3*, 11N-19N. (e) Verpoorte, E. Beads and Chips: New Recipes for Analysis. *Lab Chip*, **2003**, *3*, 60N-68N. (f) Pamme, N.; Koyama, R.; Manz, A. Counting and Sizing of Particles and Particle Agglomerates in a Microfluidic Device Using Laser Light Scattering: Application to a Particle-Enhanced Immunoassay. *Lab Chip* **2003**, *3*, 187-192. (g) Kricka, L. J.; Wilding, P. Microchip PCR. *Anal. Bioanal. Chem.* **2003**, *377*, 820-825. (h) Landers, J. P. Molecular Diagnostics on Electrophoretic Microchips. *Anal. Chem.* **2003**, *75*, 2919-2927. (i) Srinivasan, V.; Pamula, V. K.; Fair, R. B. An Integrated Digital Microfluidic Lab-on-a-Chip for Clinical Diagnostics on Human Physiological Fluids. *Lab Chip*, **2004**, *4*, 310-315. (j) Vilkner, T.; Janasek, D.; Manz, A. Micro Total Analysis Systems. Recent Developments. *Anal. Chem.* **2004**, *76*, 3373-3385.

6) Goodey, A.; Lavigne, J. J.; Savoy, S. S.; Rodriguez, M. D.; Curey, T.; Tsao, A.; Simmons, G.; Wright, J.; Yoo, S. –J.; Sohn, Y.; Anslyn, E. V.; Shear, J. B.; Neikirk, D. P.; McDevitt, J. T. Development of Multianalyte Sensor Arrays Composed of Chemically Derivatized Polymeric Microspheres Localized in Micromachined Cavities. *J. Am. Chem. Soc.* **2001**, *123*, 2559-2570.

7) Curey, T. E.; Goodey, A.; Tsao, A.; Lavigne, J.; Sohn, Y.; McDevitt, J. T.; Anslyn, E. V.; Neikirk, D.; Shear, J. B. Characterization of Multicomponent Monosaccharide Solutions Using an Enzyme-Based Sensor Array. *Anal. Biochem.* **2001**, *293*, 178-184.

8) Christodoulides, N.; Tran, M.; Floriano, P. N.; Rodriguez, M.; Goodey, A.; Ali, M.; Neikirk, D.; McDevitt, J. T. A Microchip-Based Multianalyte Assay System for the Assessment of Cardiac Risk. *Anal. Chem.* **2002**, *74*, 3030-3036.

9) Christodoulides, N.; Mohanty, S.; Miller, C. S.; Langub, M. C.; Floriano, P. N.; Dharshan, P.; Ali, M. F.; Bernard, B.; Romanovicz, D.; Anslyn, E.; Fox, P. C.; McDevitt, J. T. Application of Microchip Assay System for the Measurement of C-Reactive Protein in Human Saliva. *Lab Chip*, **2005**, *5*, 261-269.

10) Sohn, Y. –S.; Goodey, A.; Anslyn, E. V.; McDevitt, J. T.; Shear, J. B.; Neikirk, D. P. A Microbead Array Chemical Sensor Using a Capillary-Based Sample Introduction: Toward the Development of an "Electronic Tongue." *Biosens. Bioelec.* **2005**, *21*, 303-312.

11) Goodey, A. P.; McDevitt, J. T. Multishell Microspheres with Integrated Chromatographic and Detection Layers for Use in Array Sensors. *J. Am. Chem. Soc.* **2003**, *125*, 2870-2871.

12) Ali, M. F.; Kirby, R.; Goodey, A. P.; Rodriguez, M. D.; Ellington, A. D.; Neikirk, D. P.; McDevitt, J. T. DNA Hybridization and Discrimination of Single-Nucleotide Mismatches Using Chip-Based Microbead Arrays. *Anal. Chem.* **2003**, *125*, 4732-4739.

13) Bayer, E. Towards the Chemical Synthesis of Proteins. *Angew. Chem. Int. Ed.* **1991**, *30*, 113-129.

14) Wiskur, S. L.; Ait-Haddou, H.; Anslyn, E. V.; Lavigne, J. J. Teaching Old Indicators New Tricks. *Acc. Chem. Res.* **2001**, *34*, 963-972.

15) (a) Brereton, R. G. *Chemometrics Applications of Mathematics and Statistics to Laboratory Systems*. Ellis Horwood: New York, 1990. (b) Beebe, K. R.; Pell, R. J.; Seasholtz, M. B. *Chemometrics A Practical Guide*. John Wiley & Sons: New York, 1998. (c) Brereton, R. G. *Chemometrics Data Analysis for the Laboratory and Chemical Plant*. Wiley: San Francisco, 2003.

16) Beebe, K. R.; Pell, R. J.; Seasholtz, M. B. *Chemometrics A Practical Guide*. John Wiley & Sons: New York, 1998, p.81.

17) (a) Mohler, L. K.; Czarnik, A. W. Ribonucleoside Membrane Transport by a New Class of Synthetic Carrier. *J. Am. Chem. Soc.* **1993**, *115*, 2998-2999. (b) James, T.

D.; Sandanayake, K. R. A. S.; Iguchi, R.; Shinkai, S. Novel Saccharide-Induced Photoinduced Electron Transfer Sensors Based on the Interaction of Boronic Acid and Amine. *J. Am. Chem. Soc.* **1995**, *117*, 8982-8987. (c) James, T. D.; Linnane, P.; Shinkai, S. Fluorescent Saccharide Receptors: A Sweet Solution to the Design, Assembly, and Evaluation of Boronic Acid Derived PET Sensors. *Chem. Comm.* **1996**, 281-288. (d) James, T. D.; Sandanayake, K. R. A. S.; Shinkai, S. Saccharide Sensing with Molecular Receptors Based on Boronic Acid. *Angew. Chem. Int. Ed.* **1996**, *35*, 1910-1922. (e) Davis, D. J.; Lewis, P. T.; McCarroll, M. E.; Read, M. W.; Cueto, R.; Strongin, R. M. Simple and rapid Visual Sensing of Saccharides. *Org. Lett.* **1999**, *1*, 331-334. (f) Wang, W.; Gao, S.; Wang, B. Building Fluorescent Sensors by Template Polymerization: The Preparation of a Fluorescent Sensor for D-Fructose. *Org. Lett.* **1999**, *1*, 1209-1212. (g) Cabell, L. A.; Monahan, M. –K.; Anslyn, E. V. A Competition Assay for Determining Glucose-6-Phosphate Concentration with a *tris*-Boronic Acid Receptor. *Tetrahedron Lett.* **1999**, *40*, 7753-7756. (h) Ward, C. J.; Patel, P.; Ashton, P. R.; James, T. D. A Molecular Color Sensor for Monosaccharides. *Chem. Comm.* **2000**, 229-230. (i) DiCesare, N.; Lakowicz, J. R. Fluorescent Probe for Monosaccharides Based on a Functionalized Boron-Dipyrromethane with a Boronic Acid Group. *Tetrahedron Lett.* **2001**, *42*, 9105-9108. (j) Arimori, S.; Bosch, L. I.; Ward, C. J.; James, T. D. A D-Glucose Selective Fluorescent Internal Charge Transfer (ITC) Sensor. *Tetrahedron Lett.* **2002**, *43*, 911-913. (k) Camara, J. N.; Suri, J. T.; Cappuccio, F. E.; Wessling, R. A.; Singaram, B. Boronic Acid Substituted Viologen Based Optical Sugar Sensors: Modulated Quenching with Viologen as a Method for Monosaccharide Detection. *Tetrahedron Lett.* **2002**, *43*, 1139-1141. (l) Zhu, L.; Zhong, Z.; Anslyn, E. V. Guidelines in Implementing Enantioselective Indicator-Displacement Assays for α-Hydroxycarboxylates and Diols. *J. Am. Chem. Soc.* **2005**, *127*, 4260-4269. (m) Zhu, L.; Shabir, S. H.; Gray, M.; Lynch, V. M.; Sorey, S.; Anslyn, E. V. A Structural Investigation of the N-B Interaction in an *o*-(*N,N*-Dialkylaminomethyl)arylboronate System. *J. Am. Chem. Soc.* **2006**, *128*, 1222-1232.

18) (a) Iverson, D. J.; Hunter, G.; Blount, J. F.; Damewood, J. R.; Mislow, K. Static and Dynamic Stereochemistry of Hexaethylbenzene and of its Tricarbonylchromium, Tricarbonylmolybdenum, and Dicarbonyl(triphenylphosphine)chromium Complexes. *J. Am. Chem. Soc.* **1981**, *103*, 6073-6083. (b) Kilway, K. V.; Siegel, J. S. Effect of Transition-Metal Complexation on the Stereodynamics of Persubstituted Arenes. Evidence for Steric Complementarity Between Arene and Metal Tripod. *J. Am. Chem. Soc.* **1992**, *114*, 255-261. (c) Gottlieb, H. E.; Ben-Ari, C.; Hassner, A.; Marks, V. *Tetrahedron* **1999**, *55*, 4003-4014.

19) (a) Stack, T. D. P.; Hou, Z.; Raymond, K. N. Rational Reduction of the Conformational Space of a Siderophore Analog Through Nonbonded Interactions: the Role of Entropy in Enterobactin. *J. Am. Chem. Soc.* **1993**, *115*, 6466-6467. (b) Szabo, T.; O'Leary, B. M.; Rebek, J. Self-Assembling Sieves *Angew. Chem. Int. Ed.* **1998**, *37*, 3410-3413. (c) Jon, S. Y.; Kim, J.; Kim, M.; Park, S. –H.; Jeon, W. S.; Heo, J.; Kim, K. A Rationally Designed NH4+ Receptor Based on Cation-π Interaction and Hydrogen Bonding. *Angew. Chem. Int. Ed.* **2001**, *40*, 2116-2119.

20) (a) Lam, K. S.; Salmon, S. E.; Hersch, E. M.; Hruby, V. J.; Kazmierski, W. M.; Knapp, R. J. A New Type of Synthetic Peptide Library for Identifying Ligand-Binding Activity. *Nature* **1991**, *354*, 82-84. (b) Lam, K. S.; Lebl, M.; Krchnák, V. The "One-Bead-One-Compound" Combinatorial Library Method. *Chem. Rev.* **1997**, *97*, 411-448.

21) Only three trials were evaluated for BSA. The fourth BSA trial developed a large air bubble in the array and skewed the captured CCD images.

22) Kaiser, H. F. The Application of Electronic Computers to Factor Analysis. *Educ. Psychol. Meas.* **1960**, *20*, 141-150.

23) This control library was prepared by Dr. Shawn C. McCleskey, a former graduate student of Professor Eric Anslyn.

24) Wright, A. T.; Anslyn, E. V. Cooperative Metal-Coordination and Ion Pairing in Tripeptide Recognition. *Org. Lett.* **2004**, *6*, 1341-1344.

25) Stojanovic, M. N.; Green, E. G.; Semova, S.; Nikic, D.; Landry, D. W. Cross-Reactive Arrays Based on Three-Way Junctions. *J. Am. Chem. Soc.* **2003**, *125*, 6085-6089.

26) (a) Mayr, T.; Liebsch, G.; Klimant, I.; Wolfbeis, O. S. Multi-ion Imaging Using Fluorescent Sensors in a Microtiterplate Array Format. *Analyst* **2002**, *127*, 201-203. (b) Mayr, T.; Igel, C.; Liebsch, G.; Klimant, I.; Wolfbeis, O. S. Cross-Reactive Metal Ion Sensor Array in a Micro Titer Plate Format. *Anal. Chem.* **2003**, *75*, 4389-4396.

27) Zhang, C.; Suslick, K. S. A Colorimetric Sensor Array for Organics in Water. *J. Am. Chem. Soc.* **2005**, *127*, 11548-11549.

28) (a) Furka, A.; Sebestyen, F.; Asgedom, M.; Dibo, G. *Int. J. Pept. Protein Res.* **1991**, *37*, 487-493. (b) Chan, W. C.; White, P. D. *Fmoc Solid Phase Peptide Synthesis: A Practical Approach*. Oxford University Press: New York, 2000.

Chapter 5: Library Screening

5.1 Introduction

Molecular recognition has evolved from selective, lock-and-key,[1] recognition of substrates to novel sensing methods including differential recognition,[2] and screening of receptor/sensor libraries for substrate binding.[3] Complex biological analytes such as oligopeptides, hormones, and proteins represent substrates for any type of sensing assays. However, these are dynamic analytes for which the synthesis of a specific receptor is arduous and synthetically prohibitive. Screening methods involve the combinatorial[4] development of a library of resin-bound receptors, and subsequent binding studies to a labeled (colorimetric or fluorescent) target analyte. Those library members that are labeled upon binding the colorimetric or fluorescent analyte are selected and their respective chemical architecture determined. Therefore, selective substrate binders are determined from a receptor library in a rapid and facile manner.

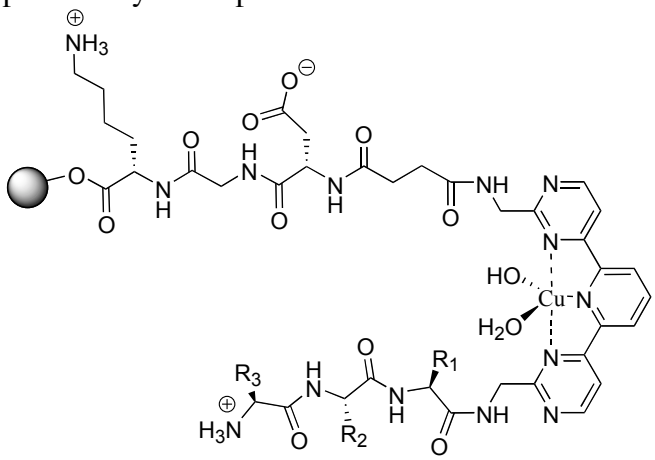

5.1:Cu(II)

Library **5.1** has been synthesized and used for differential array studies as discussed in chapter four,[5] and the common receptor architecture was used for selective recognition of His-Lys-Lys as discussed in chapter two.[6] In this chapter the screening on solid phase, and binding studies in solution, of library **5.1** with α-neurokinin will be described. α-Neurokinin (**5.2**) is a decapeptide hormone and a member of the tachykinin hormone family. Tachykinins have diverse pharmacological actions in the central nervous system and the cardiovascular, genitourinary, respiratory, and gastrointestinal systems, as well as in glandular tissues.[7] Screening and subsequent sequencing of α-neurokinin selective receptors identified receptor characteristics important to the recognition of tachykinins, specifically α-neurokinin.

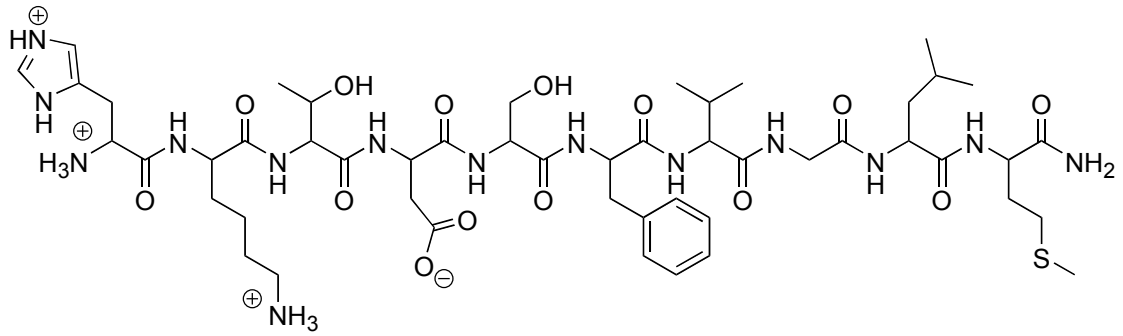

5.2
α-Neurokinin

5.2 Tachykinins

Mammalian tachykinins are a family of peptides (10-11 amino acid residues) traditionally classified as neurotransmitters. All tachykinins share a conserved hydrophobic C-terminal region, Phe-X-Gly-Leu-Met-NH_2, where X is a hydrophobic β-branched or aromatic amino acid.[8] Each tachykinin is bound by a specific tachykinin

receptor that upon activation implicates the diverse biological actions of the tachykinins. Previously, it was believed that tachykinins were only found in neuronal cells, however they have now been found in inflammatory, vascular endothelial, somatotroph, and thyrotroph cells.[8] The three primary tachykinins are Substance P, α-neurokinin, and β-neurokinin, all of which are encoded by the preprotachykinin-A gene.[9] The structures of the three common tachykinins are displayed in Figure 5.1.

Figure 5.1 Substance P, α-Neurokinin, and β-Neurokinin: Common Tachykinins.

Substance P: Arg-Pro-Lys-Pro-Gln-Gln-Phe-Phe-Gly-Leu-Met-C(O)-NH2

α-Neurokinin: His-Lys-Thr-Asp-Ser-Phe-Val-Gly-Leu-Met-C(O)-NH2

β-Neurokinin: Asp-Met-His-Asp-Phe-Phe-Val-Gly-Leu-Met-C(O)-NH2

5.3 Library Design and Screening

In chapter two the synthesis of a chemosensor for the tripeptide His-Lys-Lys was detailed. In Chapter four the chemosensor scaffold was expanded to a combinatorial library of 6,859 members, each bearing one identical and one unique combinatorially developed tripeptide arm. As was described the metal ligand core readily chelates Cu(II), and the complex (**5.1:Cu(II)**) is an excellent ligand for peptides with N-terminal His or Cys. Furthermore, the peptide arms provide key binding interactions that permit discrimination of various analytes. As was demonstrated in chapter two the tripeptide binding arms enhance the affinity of the receptor complex for a tripeptide guest. In this chapter we will discuss the screening of the **5.1**:**Cu(II)** complex with a colorimetric mimic of α-neurokinin to identify strong binding receptor complexes. It was expected

that the N-terminal His of α-neurokinin would bind well to the metal center of the receptor complex, and the peptide arms would add affinity for the tachykinin substrate. Strong binding receptors were identified and subsequently resynthesized, and binding studies were conducted with a mimic of α-neurokinin in a buffered aqueous solution.

5.3.1 Synthesis of α-Neurokinin Mimic

The C-terminal region of tachykinins is conserved, so it was determined that a colorimetric variant of α-neurokinin would be synthesized incorporating key residues of the N-terminus as this is discriminating between the three primary tachykinins. Because neither the complexes of library **5.1**, or α-neurokinin, have any inherent color it was necessary to covalently append a dye directly to the tachykinin substrate to identify binding events. Therefore, α-neurokinin mimic **5.3** was developed for screening studies.

Fmoc-Asp(O*t*Bu)-OH (**5.4**) was coupled to the dye disperse red 1 using diethylazodicarboxylate and triphenylphosphine to give **5.5** in good yield. The Fmoc/*t*Bu protection scheme on **5.4** was employed for appropriate coupling to the carboxylic acid and for later incorporation onto solid phase. The *t*Bu group was removed using trifluoroacetic acid (TFA) and triethylsilane as a cation scavenger to give **5.6**. To complete the synthesis of the mimic solid phase chemistry was employed. **5.6** was added to the 2-chlorotrityl chloride resin using N-methylmorpholine (NMM) as base yielding **5.7**. The Fmoc group was subsequently removed using 20% piperidine in DMF to provide **5.8**. The second amino acid, Fmoc-Asp(O*t*Bu)-OH, was coupled to the free amine on the resin using HOBt, TBTU, and NMM in DMF. This was followed by deprotection of the Fmoc group to give **5.9**. The other amino acids, with appropriate side

chain protection, were added to the resin and deprotected as with the previous amino acid. The connection between the growing peptide chain and the resin is highly labile

Scheme 5.1 Synthesis of the α-Neurokinin Mimic for Screening Studies.

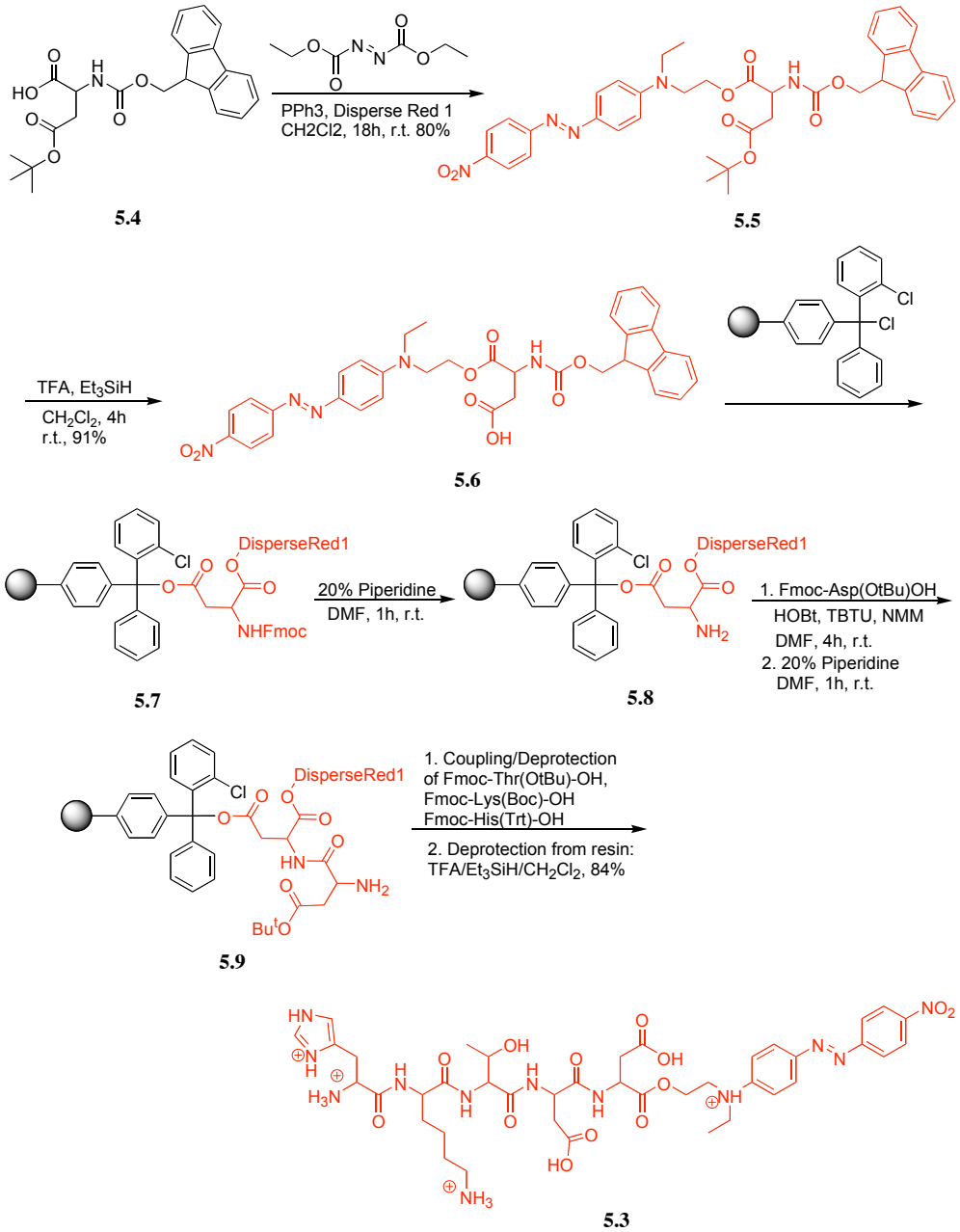

when subjected to acid. Therefore, to cleave the mimic from the resin, and remove the acid-sensitive protecting groups, TFA and triethylsilane in methylene chloride were added to the resin. Cold ether was added and **5.3** was collected upon precipitation. The product was dissolved in water and washed repeatedly with ether. The water was removed with lyophilization to give the α-neurokinin mimic in good yield. The synthesis of **5.3** is illustrated in Scheme 5.1.

5.3.2 Library Screening

To identify strong α-neurokinin binding the **5.1**:Cu(II) complex library was mixed with **5.3**, and the strongest binding complexes were selected and sequenced to obtain full characterization. A number of concentrations of **5.3** (70, 90, and 110 μM) were used for screening the receptor library. Portions of the receptor library (5 mg) were added to modified Eppendorf vials containing a frit and opening on the bottom to extricate solutions. The first step involved incubation of the library resin with Cu(II)Cl_2 (1 mM, 200 μL) overnight. The copper solution was extricated and the resin was rinsed multiply with HEPES (10 mM, pH 7.4). Following rinsing, mimic **5.3** was added at the three different concentrations in a buffered solution (HEPES, 10 mM, pH 7.4). These solutions were mixed overnight. The beads were rinsed several times with the buffer solution to remove any unbound mimic from the resin-bound receptor complexes. The beads were placed on cover slips and images were obtained using an Olympus stereoscope equipped with a charge-coupled device and a video capture card. Figure 5.2 shows the close angle images captured of the **5.3**-incubated **5.1:Cu(II)** complex library.

Figure 5.2 Images of Metalated Library **5.1** Following Incubation with Multiple Concentrations of α-Neurokinin Mimic **5.3**. Brightly colored beads indicate strong binding between the receptor:metal complex and **5.3**. These are close-up images that illustrate the relative binding (coloration) to the mimic.

a) 70 uM

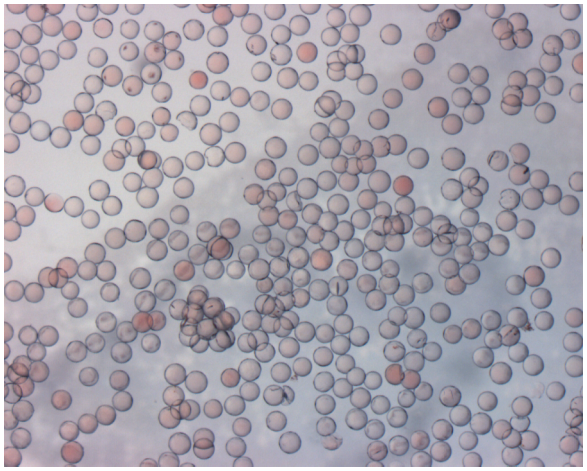

b) 90 uM

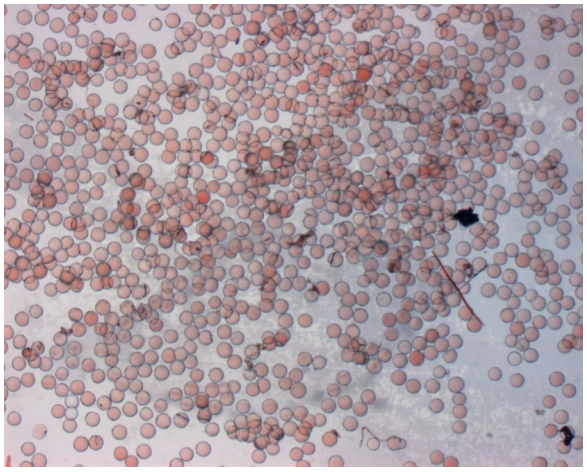

c) 110 uM

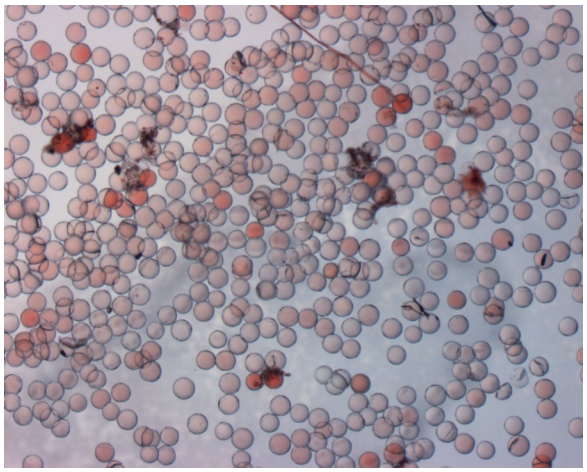

At 70 μM concentrations of **5.3**, 0.1-0.2% of the resin-bound receptors (5 mg) were deep red in color. At 90 μM, approximately 1.7% were deep red, and approximately 4% were darkly stained at 110 μM. Concentrations greater than 110 μM gave widespread deep coloration, and were not worthwhile for detecting the most selective receptors for the α-neurokinin mimic (130 μM = ~20%, 150 μM = ~40%).

To determine the selectivity of metalated library **5.1** for the α-neurokinin mimic a control was run. In the control a tripeptide library was developed on NovaSyn tentagel amino resin.[12] This tripeptide library was incubated with **5.3** at the same concentrations as library **5.1**. An interesting result ensued, approximately 1-2% of the tripeptide library, regardless of the concentration, were darkly colored as seen in Figure 5.3. It must be noted that the effective molarity of the tripeptides on the resin is very high, therefore tripeptides that are specifically complementary to **5.3** are likely colored darkly. Notice that the rest of the resin is nearly colorless. However, with **5.1** most of the resin-bound receptors had some color indicating association with **5.3**. This is likely due to the conserved metal ligand core of all the receptors in the library.

Figure 5.3 Images of a Tripeptide Control Library Following Incubation with Multiple Concentrations of α-Neurokinin Mimic **5.3**. Brightly colored beads indicate strong binding between the tripeptides and **5.3**. These are wide images that illustrate the relative binding (coloration) to the mimic.

a) 70 uM

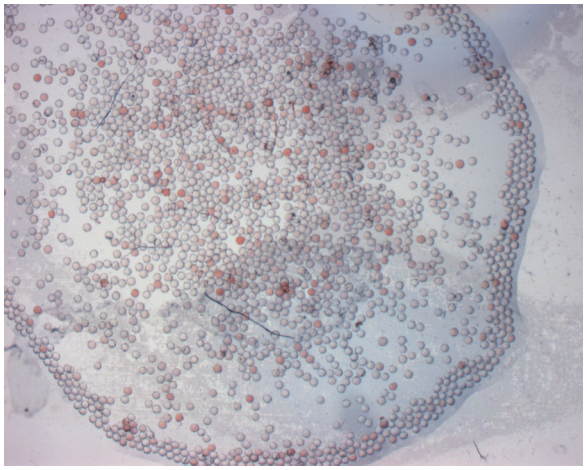

b) 90 uM

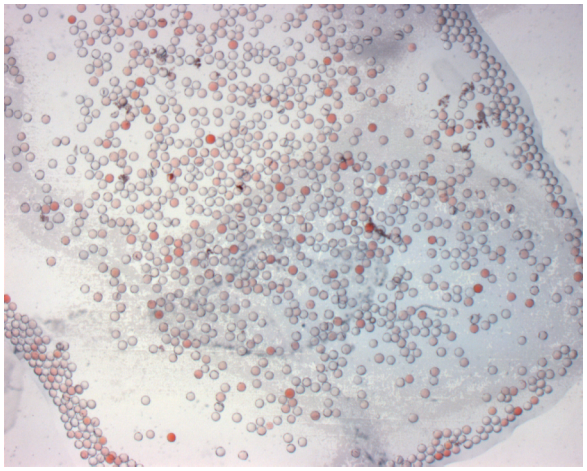

c) 110 uM

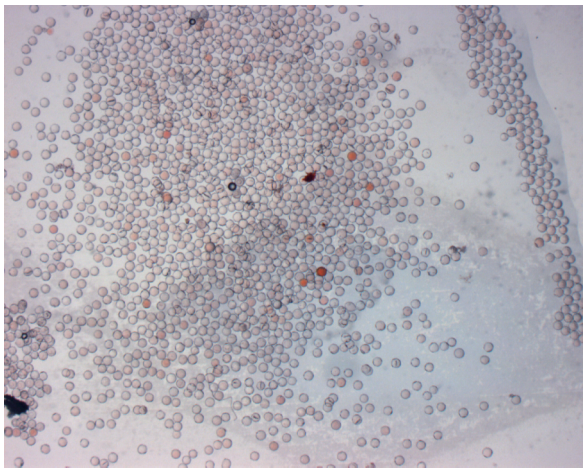

The results from the studies with the tripeptide control library illustrated the importance of complementary interactions between **5.3** and peptides. It can be assumed that the highly colored beads from library **5.1** involve both complexation of the N-terminal His, and specific binding interactions between the peptide arms. However, the contribution to binding of the disperse red 1 portion of **5.3** was not known. It was hypothesized that strong binding interactions may be due to interactions between the dye portion of **5.3** and receptors from **5.1**. A control was set up by incubating metalated library **5.1** (5 mg) with an acylated derivative of disperse red 1 (**5.10**). The control **5.10** was added to metalated **5.1** and mixed overnight. As is evident from Figure 5.4 there were no specific interactions between any of the receptors in the library and **5.10**.

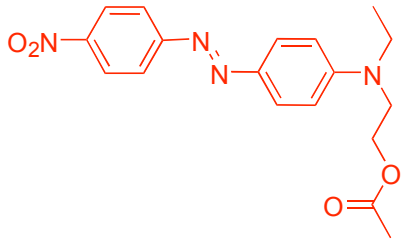

5.10

Figure 5.4 Images of Metalated Library **5.1** Following Incubation with 70 μM α-Neurokinin Mimic **5.3**.

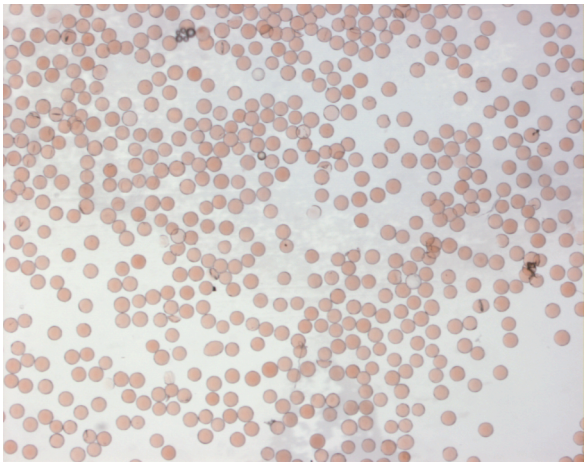

To learn more about the nature of selective binding interactions between metalated receptors of **5.1** and **5.3**, as well as selective binding interactions between tripeptides in the control library and **5.3**, a number of the strong binders were selected for sequencing characterization. Seven of the darkly colored beads of metalated library **5.1** from the 70 μM incubation with **5.3** were obtained and sequenced using Edman degradation, and three darkly colored tripeptides from the control library were sequenced. The results from the sequencing are shown in Figure 5.5.

The three tripeptides sequenced from the tripeptide control library all have high charge density. Interestingly, both cationic and anionic tripeptides were found. This is interesting because **5.3** likely has a +2 charge at pH 7.4 (the pH of the screening studies).

The tripeptide Glu-Glu-Glu likely bound through strong electrostatic interactions. However, the two cationic peptides likely associated via cation-π interactions with the disperse red 1 portion of **5.3**.

Figure 5.5 Sequencing Results for Selective Binders of **5.3** from Library **5.1** and the Tripeptide Control Library (Blue).

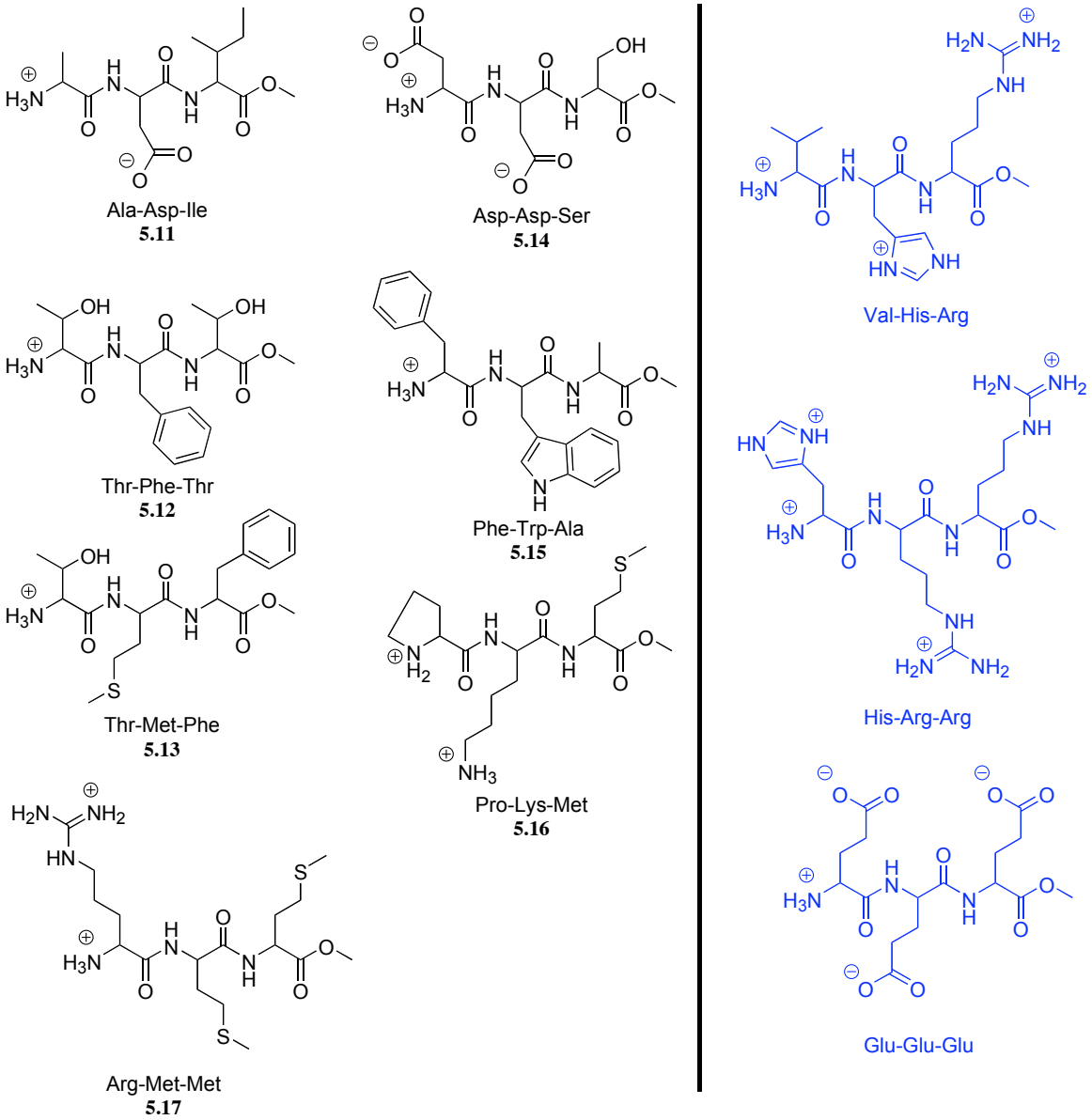

Library **5.1** was designed with the first peptide arm being set for every receptor in the library as Lys-Gly-Asp followed by the spacer succinic acid. The metal-ligand core was incorporated next followed by combinatorial development of the second tripeptide arm using split-and-pool combinatorial methodology. When seeking trends in the sequencing results in Figure 5.5 it is immediately evident that a number of hydrophobic groups were important for binding including Met, Trp, Phe, Ala, and Ile. A second trend was acidic Asp residues, and polar Ser and Thr residues. One must remember when considering the results that the first peptide arm was also important to binding, likely via electrostatic interactions. With these sequencing results in hand we sought to determine the strength of association between the sequenced receptors and α-neurokinin in solution.

5.4 UV/Vis Solution Studies with Resynthesized Receptor:Metal Complexes

The seven sequenced receptors from library **5.1** were resynthesized using 2-chlorotrityl chloride resin. Peptide bond forming reactions, cleavage from the resin, and workup are akin to those used in chapter two, chapter four, and earlier in this chapter for the synthesis of **5.3**. For this reason the synthesis of the receptors will not be discussed again. However, the synthesis of **5.15** was attempted twice without good yield, and with very poor purity; for this reason it was removed from further studies.

In chapter two a receptor:metal complex designed for binding His-Lys-Lys was discussed. Prior to binding the tripeptide an association constant for $Cu(II)Cl_2$ was determined as approximately 85,000 M^{-1} (water/methanol (1:1), HEPES buffer (100 mM, pH 7.4).[6] Using the six remaining receptors binding studies with $Cu(II)Cl_2$ and Cu(II)trifluoromethanesulfonate were conducted in buffered water (HEPES, 10 mM, pH

7.41). Keeping the receptor concentration constant (80 μM) Cu(II) in either form was titrated into the solution, and the absorbance of the receptor was monitored. Absorbance values from 334 nm were used to develop binding graphs, and association constants were calculated using 1:1 binding isotherm equations. Figure 5.6a shows the binding isotherm for the receptor **5.14:Cu(II)** complex that was calculated as ~75,000 M^{-1}.[13] This value was consistent for the other five receptors as well. However, binding studies with the weaker counter ion resulted in two receptor **5.14** molecules binding one Cu(II) ion. The 2:1 binding constant was not calculated, but by looking at the isotherm it is clear that it is significantly stronger than Cu(II) with chloride as the counter ion. These results were also consistent for the other five resynthesized receptors.

Figure 5.6 (a) 1:1 Binding Isotherm for **5.14** and $Cu(II)Cl_2$, (b) 2:1 Binding Isotherm for **5.14** Cu(II)trifluoromethanesulfonate.

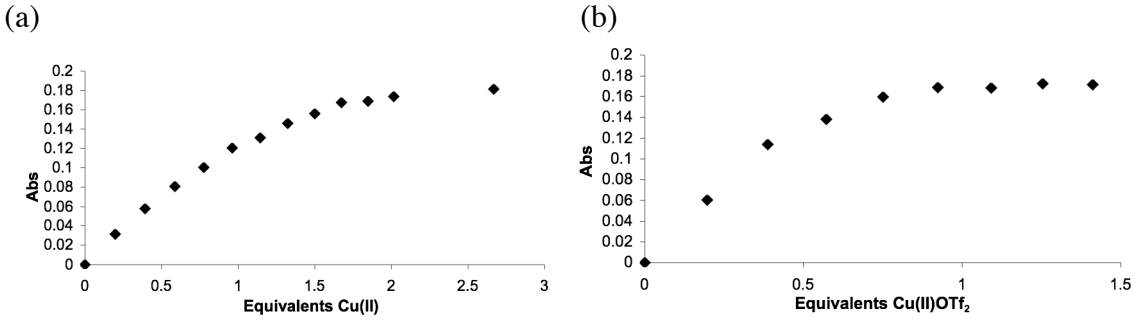

As discussed in chapter two, spectral modulations of the His-Lys-Lys selective receptor were rather minimal when binding the substrate. In this research we sought to enhance spectral modulations by incorporating an indicator-displacement assay. In this type of assay an indicator is initially bound to the receptor:metal complex giving a discreet color. When an analyte is added to the solution the indicator is displaced by the

analyte into solution, and a change in color is observed. Indicators can provide the large spectral modulations in UV/Vis binding studies that we were seeking. Therefore, a number of indicators were tested for their binding to a complex of one of the six resynthesized receptors and either Cu(II)Cl_2 or Cu(II)trifluoromethanesulfonate. These indicators included pyrocatechol violet, chrome azurol S, mordant orange 1, gallocyanine, and methylthymol blue. In all cases titration of a metal:receptor complex to an indicator solution (constant indicator concentration maintained) resulted in spectral modulations to the indicator absorbance spectrum. However, in no case was a clean isosbestic point found. The lack of an isosbestic point is indicative of multiple binding equilibria occurring in solution. It is possible that in some cases the indicator was stripping the metal from the metal:receptor complex, and in some cases the appropriate metal:receptor:indicator complex likely formed in addition to other binding events. Unfortunately, the inability to find a suitable indicator to participate in 1:1 binding with the metal:receptor complex stopped this direction of the research. Figure 5.7 shows a titration of **5.14**:Cu(II) into pyrocatechol violet (60 μM – constant concentration maintained, buffered with HEPES, 10 mM, pH 7.41). Drifting of the isosbestic point is readily apparent.

Figure 5.7 Titration of **5.14**:Cu(II) Into Pyrocatechol Violet (60 μM). Note the drifting isosbestic point.

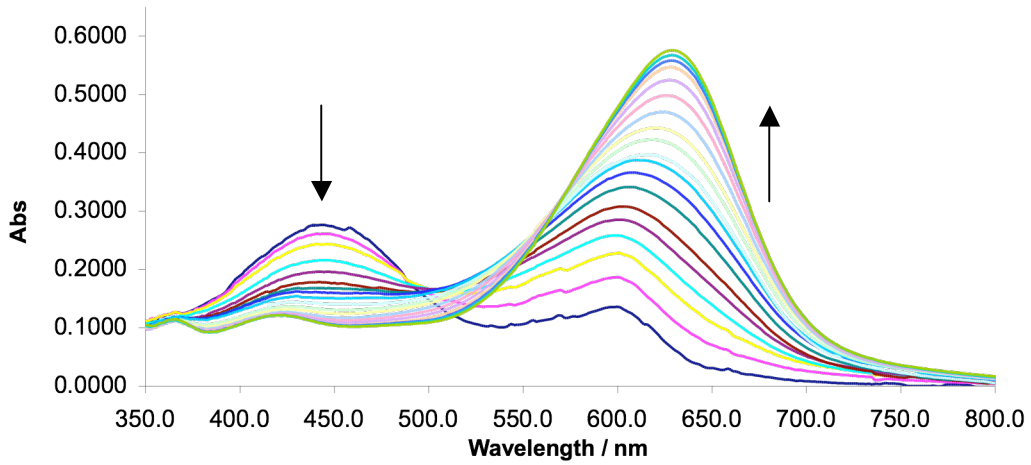

With the above results we were somewhat stymied on how to approach our goal of screening a receptor library, identifying strong receptors, resynthesizing the receptors and testing them for binding to tachykinins. We chose to synthesize **5.18**, which is a short analog of α-neurokinin for binding studies with receptor:Cu(II) (**5.11** – **5.17**, no **5.15**) complexes. As with the binding studies in chapter two the inherent absorbance of the receptor:metal complex was monitored. But, the results of the current binding studies were not akin to our prior studies. The UV/Vis spectra of a titration of **5.18** into a solution of **5.12:**Cu(II) (120 μM) is shown in Figure 5.8a. The first equivalent of **5.18** added had no effect on the absorbance of the **5.12:**Cu(II) complex, but the addition from 1-3 equivalents had an isosbestic point. This is characteristic of multiple equilibria binding, and stoichiometries greater than 1:1. A binding isotherm is shown in Figure 5.8b generated from the absorbance spectrum at 321 nm.

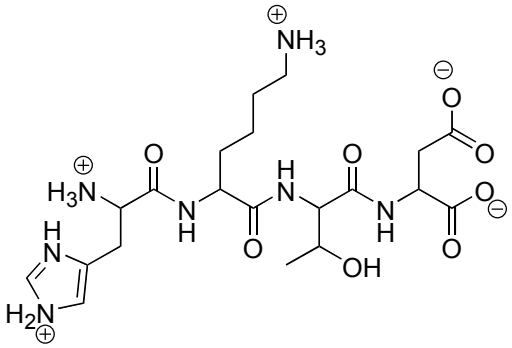

5.18

Figure 5.8 (a) UV/Vis Spectra of a Titration of 5.18 Into a Solution of Cu(II):5.12 (120 μM), (b) Binding Isotherm Generated from the Absorbance Spectrum at 321 nm.

(a)

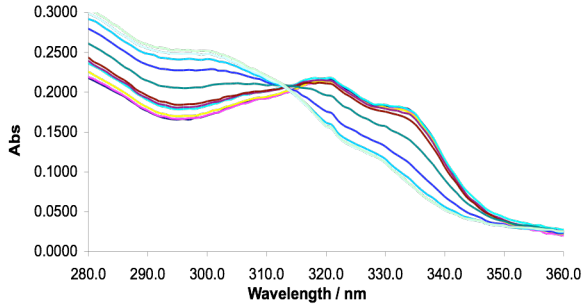

(b)

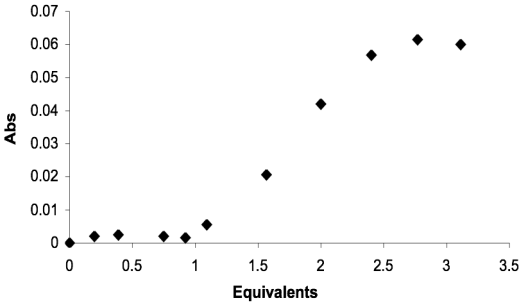

5.5 Multianalyte Approach

Knowing that binding does indeed occur between various peptides, including tachykinins, with the receptor complexes the attention was turned to using a multianalyte sensing approach akin to those in Chapter 4.[15] In this case receptors **5.12-5.14** and **5.16-5.17** (267 μM) were placed in a Costar 96-well flat-bottomed plate. Complexes of each receptor were formed with $CuCl_2$ (2 equivalents), Cu(II)trifluoromethanesulfonate (1 equivalent), and Cd(II)acetate (1 equivalent). HEPES (pH 7.4) was added to each well to give solutions with 50 mM buffer. The absorbances of the receptor complexes were evaluated (from 300-355 nm) before and after the addition of various analytes: α-neurokinin, Substance P, His-Asp-Thr, His-Lys-Thr, and α-neurokinin mimic (His-Lys-Thr-Asp) (all analytes added at 1 equivalent). A Biotrak 96-well plate reader was used for the analysis. Three absorbance measurements were monitored for each analyte with each metal-receptor complex at 315, 321, and 333 nm. The initial absorbance of each metal-receptor complex was subtracted from the final absorbance of the metal-receptor complex bound to the analyte.

A principal component analysis (PCA) plot was developed using Statistica software as outlined in Chapter 4. The patterns for the analytes are seen below in Figure 5.9. Interestingly, PCA plots developed only from results from one metal-receptor complex (e.g. all the receptors with $CuCl_2$) did not provide as nice of separation as seen with all the metal-receptor complexes used simultaneously. This demonstrates the advantage of having multiple receptor types. Furthermore, different Cu(II) counter-ions gave large enough effects to provide totally different receptor types. As seen in Figure 5.9 excellent separations were made with the multianalyte receptor array. Interestingly

the tachykinins (α-neurokinin and Substance P) were in a similar quadrant; they are by far the largest peptides and share a conserved C-terminal region. Additionally, the tetrapeptide and tripeptides are very similar in structure, but they were readily discriminated by the receptor array. Additionally, it should be noted that a third axis containing 14% of the variance could have been included to further separate the data. A fourth axis containing 8% of the variance also could have been used to further the distances between analytes. This work demonstrates the utility of a differential sensor array. Though good results were not obtained using UV/Vis and indicator-displacement assays, a differential sensor array suitably differentiated the complex and similar analytes.

Figure 5.9 A PCA Plot Demonstrates the Discrimination Capability of the Resynthesized Receptor Array.

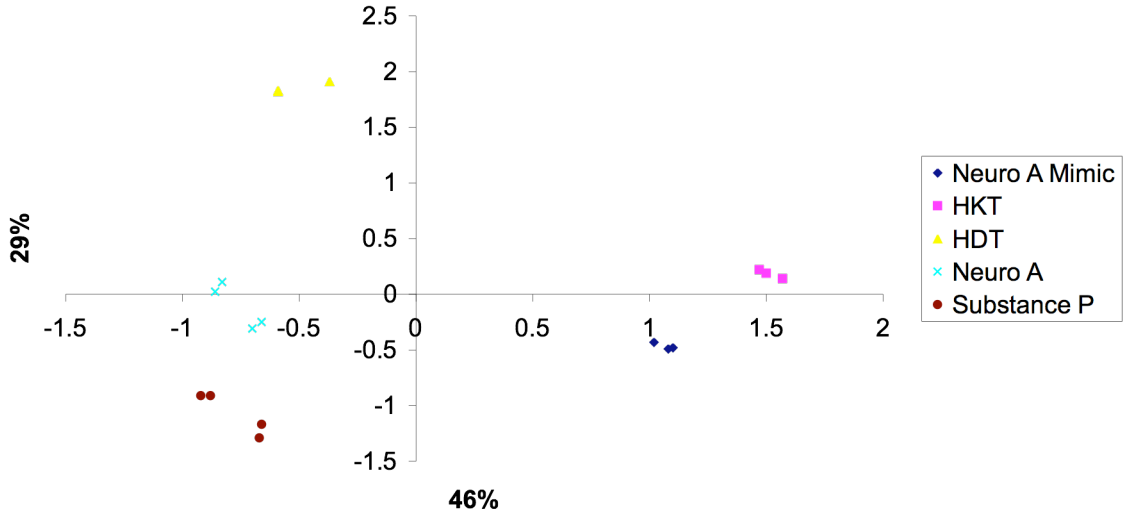

5.6 Experimental

General. Reactions were run under an atmosphere of argon unless otherwise indicated. Anhydrous solvents were transferred by an oven-dried syringe. Flasks were flame dried under a stream of argon. The chemicals were obtained from Acros Organics, Aldrich, Alfa Aesar, and NovaBiochem and were used without further purification unless otherwise noted. NovaSyn Tentagel Amino resin and 2-chlorotrityl chloride resin were both purchased from NovaBiochem. Methlyene chloride and triethylamine were distilled over calcium hydride. A Varian Gemini 400 MHz NMR was used to obtain ^{1}H and ^{13}C spectra. A Finnigan MAT-VSQ 700 spectrometer was used to obtain low-resolution mass spectra. HPLCs were run on a Gemini Chromasil C18 reverse phase column. The UV-visible absorption measurements were recorded on a Beckman DU640 spectrometer. All products were dried for at least 6 hours prior to spectral analysis.

Procedures:

The synthesis of Library **5.1** was described in chapter four (see Library **4.2**).

2-(9H-Fluoren-9-ylmethoxycarbonylamino)-succinic acid 4-tert-butyl ester 1-(2-{ethyl-[4-(4-nitro-phenylazo)-phenyl]-amino}-ethyl) ester (5.5)

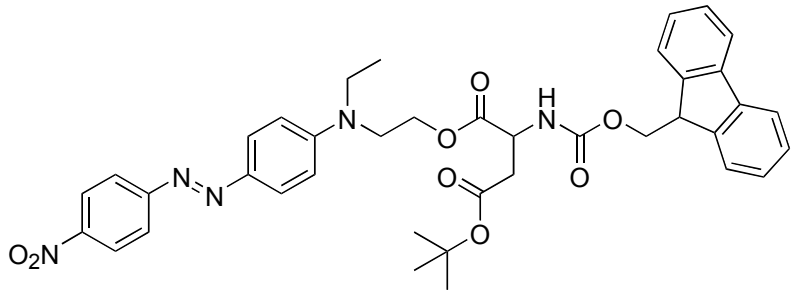

To an argon purged dry flask was added Fmoc-Asp(O*t*Bu)-OH (0.562 g, 1.37 mmol), disperse red 1 (0.515 g, 1.64 mmol), triphenylphosphine (0.358 g, 1.37 mmol), and methylene chloride (20 mL). This solution mixed at room temperature for 30 min at which point diethylazodicarboxylate (0.216 mL, 1.37 mmol) was added dropwise to the reaction mixture. The reaction was left to stir overnight (16 h) at room temperature. The solvent was removed *in vacuo*, and the dried residue was redissolved in methylene chloride (2 mL) and purified on a SiO_2 column (eluent: progressed from 20% ethyl acetate to 30% ethyl acetate in hexanes). The product was collected as a red solid (0.77 g, 0.992 mmol, 80%). ^{1}H NMR ($CDCl_3$): 8.28 (d, 2H), 7.87 (d, 2H), 7.85 (d, 2H), 7.73 (d, 2H), 7.57 (d, 2H), 7.37 (t, 2H), 7.28 (t, 2H), 6.75 (d, 2H), 5.80 (d, NH), 4.55 (t, 1H), 4.41 (t, 1H), 4.34 (d, 2H), 4.21 (t, 2H), 3.66 (t, 2H), 3.49 (q, 2H), 2.92 (d, 2H), 1.46 (s, 9H), 1.22 (t, 3H). ^{13}C NMR ($CDCl_3$): 170.6, 169.4, 156.5, 155.8, 150.9, 147.2, 143.7,

143.5, 141.1, 127.6, 126.9, 126.1, 125, 124.9, 124.5, 122.5, 119.9, 111.2, 67.1, 61.6, 60.2, 56.9, 50.8, 48.4, 41.1, 38.0, 27.7, 12.1. MS (CI^+) *m/z* 708 $[M]^+$.

2-(9H-Fluoren-9-ylmethoxycarbonylamino)-succinic acid 1-(2-{ethyl-[4-(4-nitro-phenylazo)-phenyl]-amino}-ethyl) ester (5.6)

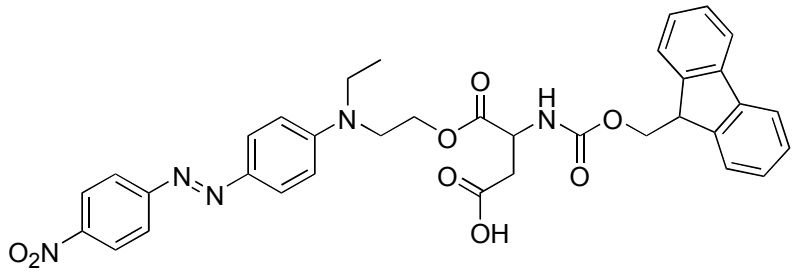

5.5 (0.70 g, 0.992 mmol) was added to a dry flask and dissolved in methylene chloride (8 mL). Trifluoroacetic acid (1.1 mL, 14.9 mmol) and triethylsilane (0.48 mL, 2.98 mmol) were then slowly dripped into the solution. The reaction was stirred for 4 h at room temperature. The solvent was removed and the product was redissolved in methylene chloride (1.5 mL) and purified on a SiO_2 column (eluent: 1:1 ethyl acetate:hexanes). The product was collected as a red solid (0.638 g, 0.979 mmol, 91%) from the column. ^1H NMR ($CDCl_3$): 8.28 (d, 2H), 7.87 (d, 2H), 7.85 (d, 2H), 7.73 (d, 2H), 7.57 (d, 2H), 7.37 (t, 2H), 7.28 (t, 2H), 6.75 (d, 2H), 5.80 (d, NH), 4.55 (t, 1H), 4.41 (t, 1H), 4.34 (d, 2H), 4.21 (t, 2H), 3.66 (t, 2H), 3.49 (q, 2H), 2.92 (d, 2H), 1.22 (t, 3H). ^{13}C NMR ($CDCl_3$): 170.6, 169.4, 156.5, 155.8, 150.9, 147.2, 143.7, 143.5, 141.1, 127.6, 126.9, 126.1, 125, 124.9, 124.5, 122.5, 119.9, 111.2, 67.1, 61.6, 60.2, 56.9, 50.8, 48.4, 41.1, 38.0, 12.1. MS (CI^+) *m/z* 652 $[M]^+$.

(5.7)

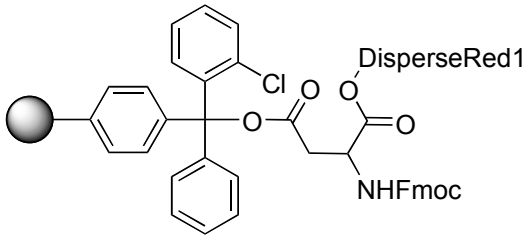

5.6 (0.266 g, 0.408 mmol) was dissolved in methylene chloride (9 mL) in a dried flask. N-methylmorpholine (0.15 mL, 1.36 mmol) was added to the flask followed immediately by the 2-chlorotrityl chloride resin (1.4 mmol/g, 0.244 g, 0.34 mmol). The mixture stirred for 1 h at room temperature. At this point a solution of methylene chloride/methanol/*N,N*-diisopropylethyl amine (17:5:2, 8 mL) was added to quench unreacted resin, and the solution stirred for 10 min. The solvents were filtered from the resin, and the resin was washed with DMF, methylene chloride (2x), methanol (2x), and DMF once again. MS (CI^+) *m/z* 652 $[M]^+$.

(5.8)

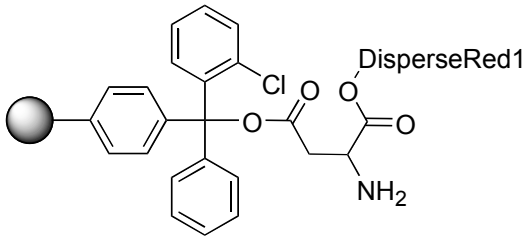

5.8

A solution of 20% piperidine in DMF (5 mL) was added to **5.7** (0.244 g, 0.34 mmol) in a dry reaction flask. The reaction was mixed for 30 min, and the solvents were filtered from the resin. The resin was washed with DMF, methylene chloride (2x), methanol

(2x), and DMF once again. A Kaiser test was positive indicating the presence of free primary amines.

(5.9)

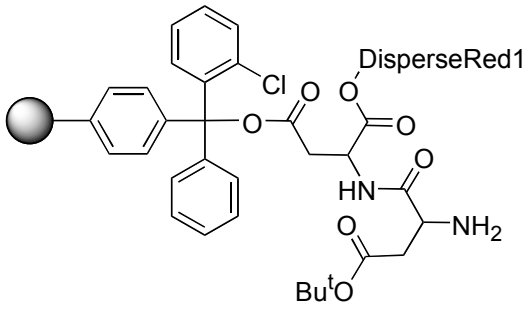

Fmoc-Asp(O*t*Bu)-OH (0.53 g, 1.29 mmol), 1-hydroxybenzotriazole (0.23 g, 1.7 mmol), TBTU (0.55 g, 1.7 mmol), and N-methylmorpholine (0.34 mL, 3.06 mmol) were dissolved in DMF (5 mL) in a dry flask. This solution mixed for 10 min; during this time the color changed from clear to yellow. The color change is indicative of formation of the active ester. At this point **5.8** (0.244 g, 0.34 mmol) was added, and the reaction mixed for 4 h. The solution was filtered from the resin, and the resin was washed with DMF, methylene chloride (2x), methanol (2x), and DMF once again. A Kaiser test was negative, indicating the absence of free primary amines. A solution of 20% piperidine in DMF (5 mL) was added to the resin (0.244 g, 0.34 mmol) in a dry reaction flask. The reaction was mixed for 30 min, and the solvents were filtered from the resin. The resin was washed with DMF, methylene chloride (2x), methanol (2x), and DMF once again. A Kaiser test was positive indicating the presence of free primary amines.

(5.3)

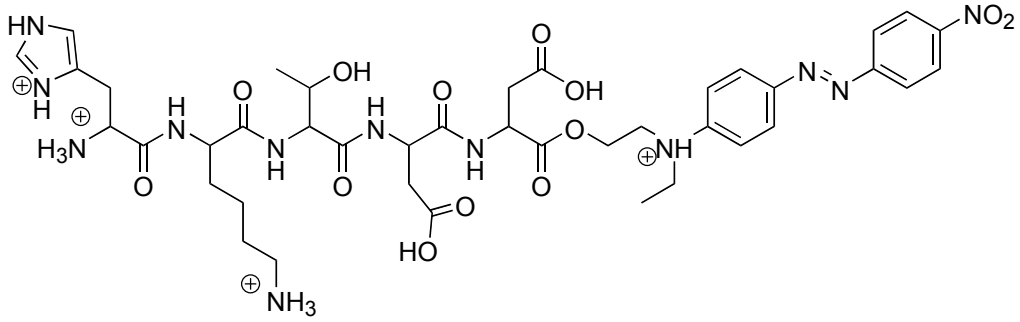

Beginning with **5.9** (0.244 g, 0.34 mmol) three additional amino acids were coupled to the resin. Fmoc-Thr(O*t*Bu)-OH (0.513 g, 1.29 mmol), Fmoc-Lys(Boc)-OH (0.6 g, 1.29 mmol), and Fmoc-His(Trt)-OH were coupled to the resin using 1-hydroxybenzotriazole (0.23 g, 1.7 mmol), TBTU (0.55 g, 1.7 mmol), and N-methylmorpholine (0.34 mL, 3.06 mmol) in DMF (5 mL). Between additions of each amino acid the Fmoc group was removed using 20% piperidine in DMF (5 mL). Kaiser tests were used to determine effective coupling and Fmoc deprotection. Upon completion of the solid phase synthesis the compound was cleaved from the resin using a TFA/CH_2Cl_2/triethylsilane (45/4/1, 15 mL) solution. The deprotection solution was filtered and collected, and the resin was washed twice more with the deprotection solution. The deprotection solution was then concentrated *in vacuo*. The product was obtained by precipitation with ether, and was subsequently dissolved in water and lyophilized multiple times to obtain a solid red powder (0.261 g, 0.286 mmol, 84%). MALDI-MS, *m/z* 911.4 [M]. HPLC retention time: 17.8 minutes, single peak on spectrum from 0-30 minutes (eluent = water).

Acetic acid 2-{ethyl-[4-(4-nitro-phenylazo)-phenyl]-amino}-ethyl ester (5.10)

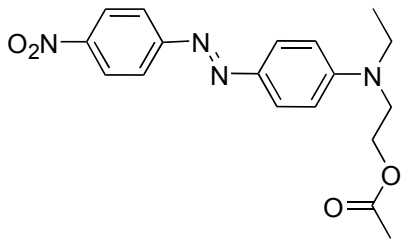

Disperse red 1 (0.2 g, 0.636 mmol) was dissolved in methylene chloride (10 mL) in a dry flask. To the solution was added acetic anhydride (120 μL, 1.27 mmol) and dimethylaminopyridine (.016 g, 0.131 mmol). The reaction was mixed for 4 h and then concentrated *in vacuo*. The product was purified on a SiO_2 column (eluent: 99:1 methylene chloride/methanol) to yield a red solid (0.09 g, 0.252 mmol). ^{1}H NMR ($CDCl_3$): 8.33 (d, 2H), 7.89 (q, 4H), 6.80 (d, 2H), 4.29 (t, 2H), 3.67 (t, 2H), 3.54 (q, 2H), 2.06 (s, 3H), 1.24 (t, 3H).

Synthesis of 5.11 – 5.17:

Synthesis of the receptors **5.11 – 5.17** on 2-chlorotrityl chloride resin (0.161 g, 0.221 mmol) paralleled syntheses described in the previous chapters so only a rough description will be given here. The first three amino acids: Lys(Boc)-OH (0.47 g, 0.995 mmol), Fmoc-Gly (0.296 g, 0.995 mmol), and Fmoc-Asp(O*t*Bu)-OH (0.409 g, 0.995 mmol) were coupled on the resin. This was followed by addition of mono-fluorenylmethylsuccinic acid (0.294 g, 0.995 mmol) and the mono-Fmoc protected core (0.512 g, 0.995 mmol). The coupling agents used were HOBt (0.122 g, 1.22 mmol), TBTU (0.36 g, 1.22 mmol) and N-methylmorpholine (0.30 mL, 1.63 mmol). Between coupling steps the Fmoc and

Fm protecting groups were removed using 20% piperidine in DMF (5 mL). The additional amino acids coupled to develop **5.11 – 5.17** were: Fmoc-Ile (0.35 g, 0.995 mmol), Fmoc-Thr(O*t*Bu)-OH (0.39 g, 0.995 mmol), Fmoc-Phe (0.37 g, 0.995 mmol), Fmoc-Ser(O*t*Bu)-OH (0.38 g, 0.995 mmol), Fmoc-Trp(Boc)-OH (0.52 g, 0.995 mmol), Fmoc-Met (0.37 g, 0.995 mmol), Fmoc-Glu(O*t*Bu)-OH (0.42 g, 0.995 mmol), Fmoc-Ala (0.31 g, 0.995 mmol), Fmoc-Arg(Pbf)-OH (0.65 g, 0.995 mmol), and Fmoc-Pro (0.33 g, 0.995 mmol). The receptors were cleaved from the resin using trifluoroacetic acid/triisopropylsilane/ethane dithiol/water (90/2.5/2.5/5, 20 mL). The cleavage reactions were run for 5 h, and the cleavage solution was filtered and collected. The resin was rinsed with the cleavage solution two additional times. The combined cleavage solutions were reduced *in vacuo*, and the products were precipitated with cold ether. The receptors were redissolved in water and rinsed multiple times with methylene chloride and ether. The water was removed using lyophilization. The products were once again dissolved in water and washed with methylene chloride and ether, and the water was removed with lyophilization. The products were characterized using low resolution MS, ESI, MALDI, and HPLC (1.0 mL/min, 30 min, ran from 100% water to methanol/water (95:5)).

(5.11) MS (CI^+) *m/z* 1008 $[M]^+$. MALDI-MS, 1008.58 [M]. HPLC retention time = 1.683 min.

(5.12) MS (CI^+) *m/z* 1045 $[M]^+$. ESI (+C) 1044. HPLC retention time = 2.067 min.

(5.13) MS (CI^+) *m/z* 1074 $[M]^+$. HPLC retention time = 1.700 min.

(5.14) ESI (+C) 1040. HPLC retention time = 1.983 min.

(5.15) MS (CI^+) *m/z* 1100 $[M]^+$. ESI (+C) 1099. HPLC retention time = 1.533 min.

(5.16) MALDI-MS, 1051.6 [M]. HPLC retention time = 2.750 min.

(5.17) MALDI-MS, 1114.7 [M]. HPLC retention time = 2.017 min.

Screening of Library 5.1:Cu(II) with 5.10:

Library **5.1** (5 mg) was added to an Eppendorf vial prefitted with a frit, and with a hole cut into the tip for extricating any solutions from the vial. To this solution was added Cu(II)Cl_2 (200 μL, 1 mM), and the resin and solution were mixed for 16 h. The Cu(II) solution was removed and the resin was washed multiple times with HEPES buffer (10 mM, pH 7.40). **5.10** (200 μL, 70-130 μM, buffered with HEPES, pH 7.40, 10 mM) was added to the resin and mixed for 16 h. The **5.10** solution was removed, and the resin was washed multiple times with HEPES buffer. Images of the "stained" beads were captured using an Olympus stereoscope fitted with a charge-coupled device and video capture card.

Screening of Tripeptide Control Library with 5.10:

The tripeptide control library (5 mg) was added to an Eppendorf vial prefitted with a frit, and with a hole cut into the tip for extricating any solutions from the vial. **5.10** (200 μL, 70-130 μM, buffered with HEPES, pH 7.40, 10 mM) was added to the resin and mixed for 16 h. The **5.10** solution was removed, and the resin was washed multiple times with HEPES buffer. Images of the "stained" beads were captured using an Olympus stereoscope fitted with a charge-coupled device and video capture card.

Screening of Library 5.1:Cu(II) with 5.18:

Library **5.1** (5 mg) was added to an Eppendorf vial prefitted with a frit, and with a hole cut into the tip for extricating any solutions from the vial. To this solution was added Cu(II)Cl_2 (200 μL, 1 mM), and the resin and solution were mixed for 16 h. The Cu(II) solution was removed and the resin was washed multiple times with HEPES buffer (10 mM, pH 7.40). **5.18** (200 μL, 70-130 μM, buffered with HEPES, pH 7.40, 10 mM) was added to the resin and mixed for 16 h. The **5.18** solution was removed, and the resin was washed multiple times with HEPES buffer. Images of the "stained" beads were captured using an Olympus stereoscope fitted with a charge-coupled device and video capture card.

UV/Vis titrations of Cu(II)Cl_2 (or Cu(II)trifluoromethanesulfonate) into 5.1:

All solutions were buffered with HEPES (pH 7.40, 10 mM) in water. A solution of **5.1** (80 μM, 1.2 mL) was prepared in a quartz cuvette and into this was titrated a solution of Cu(II) (0.00192 M in 0.8 mL; each 10 μL titration was 0.2 equivalents) keeping the buffer and host concentration constant. The data was collected at 322 nm to determine the association constant.

UV/Vis Titrations of 5.1 into Indicator (Pyrocatechol Violet):

All solutions were buffered with HEPES (pH 7.40, 10 mM) in water. A 1:1 complex of **5.1**:Cu(II) (0.48 mM) was prepared (total volume 0.8 mL), and this was titrated (each 10 μL titration was 0.2 equivalents) into a solution of pyrocatechol violet (20 μM) keeping

the buffer and pyrocatechol violet concentration constant. The data was collected at 600 nm when attempting to determine association constants.

UV/Vis titrations of 5.18 into 5.1:

All solutions were buffered with HEPES (pH 7.40, 10 mM) in water. A solution of **5.1:Cu(II)Cl_2** (1:1, 80 μM, 1.2 mL) was prepared in a quartz cuvette, and into this was titrated **5.18** (0.00192 M in 0.8 mL; each 10 μL titration was 0.2 equivalents) keeping the buffer and host concentration constant. The data was collected at 314 nm when attempting to determine the association constant.

5.7 References

1) (a) Fischer, E. *Ber. Deutsch. Chem. Ges.* **1894**, *27*, 2985. (b) Behr, J. –P. *The Lock and Key Principle, The State of the Art – 100 Years On*. New York: John Wiley and Sons, 1994.

2) Wright, A. T.; Anslyn, E. V. Differential Receptor Arrays and Assays for Solution-Based Molecular Recognition. *Chem. Soc. Rev.* **2006**, *35*, 14-28.

3) (a) Lam, K. S.; Salmon, S. E.; Hersch, E. M.; Hruby, V. J.; Kazmierski, W. M.; Knapp, R. J. A New Type of Synthetic Peptide Library for Identifying Ligand-Binding Activity. *Nature* **1991**, *354*, 82-84. (b) Still, W. C. Discovery of Sequence-Selective Peptide Binding by Synthetic Receptors Using Encoded Combinatorial Libraries. *Acc. Chem. Res.* **1996**, *29*, 155-163. (c) Still, W. C. Combinatorial Chemistry Searching for a Winning Combination. *Curr. Opin. Chem. Biol.* **1997**, *1*, 3-4. (c) De Miguel, Y. R.; Sanders, J. K. M. Generation and Screening of Synthetic Receptor Libraries. *Curr. Opin. Chem. Biol.* **1998**, *2*, 417-421. (d) Linton, B.; Hamilton, A. D. Host-Guest Chemistry: Combinatorial Receptors. *Curr. Opin. Chem. Biol.* **1999**, *3*, 307-312. (e) Lavigne, J. J.; Anslyn, E. V. Sensing a Paradigm Shift in the Field of Molecular Recognition: From Selective to Differential Receptors. *Angew. Chem. Int. Ed.* **2001**, *40*, 3118-3130. (f) Srinivasan, N.; Kilburn, J. D. Combinatorial Approaches to Synthetic Receptors. *Curr. Opin. Chem. Biol.* **2004**, *8*, 305-310.

4) Lam, K. S.; Lebl, M.; Krchnák, V. The "One-Bead-One-Compound" Combinatorial Library Method. *Chem. Rev.* **1997**, *97*, 411-448.

5) Wright, A. T.; Anslyn, E. V.; McDevitt, J. T. A Differential Array of Metalated Synthetic Receptors for the Analysis of Tripeptide Mixtures**.** *J. Am. Chem. Soc.* **2005**, *127*, 17405-17411.

6) Wright, A. T.; Anslyn, E. V. Cooperative Metal-Coordination and Ion Pairing in Tripeptide Recognition. *Org. Lett.* **2004**, *6*, 1341-1344.

7) (a) O'Connor, T. M.; O'Connell, J.; O'Brien, D. I.; Goode, T.; Bredin, C. P.; Shanahan, F. The Role of Substance P in Inflammatory Disease. *J. Cell. Physiol.* **2004**, *201*, 167-180. (b) Almeida, T. A.; Rojo, J.; Nieto, P. M.; Pinto, F. M.; Hernandez, M.; Martin, J. D.; Candenas, M. L. Tachykinins and Tachykinin Receptors: Structure and Activity Relationships. *Curr. Med. Chem.* **2004**, *11*, 2045-2081. (c) Candenas, L.; Lecci, A.; Pinto, F. M.; Patak, E.; Maggi, C. A.; Pennefather, J. N. Tachykinins and Tachykinin Receptors: Effects in the Genitourinary Tract. *Life Sciences* **2005**, *76*, 835-862.

8) Severini, C.; Improta, G.; Falconieri-Erspamer, G.; Salvadori, S.; Erspamer, G.; Salvadori, S.; Erspamer, V. The Tachykinin Peptide Family. *Pharm. Rev.* **2002**, *54*, 285-322.

9) Page, N. M. New Challenges in the Study of the Mammalian Tachykinins. *Peptides* **2005**, *26*, 1356-1368.

10) Pennefather, J. N.; Lecci, A.; Candenas, M. L.; Patak, E.; Pinto, F. M.; Maggi, C. A. Tachykinins and Tachykinin Receptors: A Growing Family. *Life Sciences* **2004**, *74*, 1445-1463.

11) (a) Braxmeier, T.; Demarcus, M.; Fessmann, T.; McAteer, S.; Kilburn, J. D. Identification of Sequence Selective Receptors for Peptides with a Carboxylic Acid Terminus. *Chem. Eur. J.* **2001**, *7*, 1889-1898. (b) Wennemers, H.; Conza, M.; Nold, M.; Krattiger, P. Diketopiperazine Receptors: A Novel Class of Highly Selective Receptors for Binding Small Peptides. *Chem. Eur. J.* **2001**, *7*, 3342-3347.

12) The library was developed using combinatorial split-and-pool chemistry with all natural amino acids except cysteine. This library was prepared by former graduate student Shawn McCleskey.

13) Connors, K. A. *Binding Constants, The Measurement of Molecular Stability*. John Wiley & Sons: New York, 1987.

14) Wiskur, S. L.; Ait-Haddou, H.; Anslyn, E. V.; Lavigne, J. J. Teaching Old Indicators New Tricks. *Acc. Chem. Res.* **2001**, *34*, 963-972.

15) Folmer-Andersen, J. F.; Kitamura, M.; Anslyn, E. V. Pattern-Based Discrimination of Enantiomeric and Structurally Similar Amino Acids: An Optical Mimic of the Mammalian Taste Response. *J. Am. Chem. Soc.* **2006**, *ASAP*.

Vita

Aaron Todd Wright was born in Kirkland, Washington on September 26, 1978, the son of Nelson and Helen Wright. Prior to moving to Austin, Texas for graduate school he was a lifelong resident of Kirkland. Aaron attended school in the Lake Washington School District, followed by undergraduate studies at George Fox University in Newberg, Oregon. He completed his B.S. in chemistry in May 2001 with honors. During his undergraduate studies he met, and following graduation married, Janet DeYoung. In August 2001, Aaron entered the University of Texas at Austin chemistry graduate program.

Permanent address: 6547 125th Ave NE, Kirkland, Washington 98033

This dissertation was typed by Aaron Todd Wright.